

RECONSTRUCTING LARGE HERBIVORE ABUNDANCE AND ENVIRONMENTAL
INTERACTIONS IN POSTGLACIAL NORTH AMERICA

by

John Arthur Frederic Wendt IV

A dissertation submitted in partial fulfillment
of the requirements for the degree

of

Doctor of Philosophy

in

Ecology and Environmental Sciences

MONTANA STATE UNIVERSITY
Bozeman, Montana

December 2023

©COPYRIGHT

by

John Arthur Frederic Wendt IV

2023

All Rights Reserved

ACKNOWLEDGEMENTS

My family has been a source of inspiration and encouragement throughout my journey. My thanks to my parents, Eric Sr., and Susan; my siblings, Eric Jr., Kathleen, and Caroline; my parents-in-law, Doug and Mioko; and my brothers-in-law, Carl and Edward. To my best friend, my wife, and my son's mother, Julie. You are my joy. Thank you for these years of love and support.

My sincere gratitude to my advisor Dave McWethy for providing the conditions to promote my intellectual growth. As I go forth, I will strive to emulate your patience, generosity, creativity, and love of learning. I am proud to have been your student.

My thanks to my committee, Cathy Whitlock, Jack Brookshire, and Dario Battistel. Your mentorship, intellectual contributions, and support have made a mark on this dissertation and my development as a scientist.

I am grateful for the camaraderie of my lab mates in the Paleoecology Lab, especially Mio "Pico" Alt, Christopher Schiller, and William "Buzz" Nanavati. *Grazie mille* to Elena Argiriadis and Mara Bortolini for your friendship, hospitality, and patience. I thank Kari LaPierre, Alex Mausshardt, Georgy Fischer, Tennison Big Day, Massimiliano Pavan, Clarissa Salvalaio, and Giorgia Montecchio for field and laboratory assistance.

My research activities were supported by the MSU PhD Dissertation Completion Award, the MSU PhD Enhancement Award, the MSU Institute on Ecosystems Yellowstone Doctoral Scholars Fellowship, the Joint Fire Science Program Graduate Research Innovation Award (19-1-01-30), and the American Museum of Natural History Theodore Roosevelt Memorial Grant.

TABLE OF CONTENTS

1. INTRODUCTION TO DISSERTATION	1
The Ecological Significance of Large Herbivores	1
Paleoherbivore Proxies	3
Palynological indicators	3
Fossils	5
aDNA	5
sedaDNA	5
Molecular Biomarkers	6
Bison: North America’s Dominant Herbivore	7
Wallowing, Trailing, and Rubbing	8
Changes in Biotic Interactions	9
Nutrient Cycling and Biomass Turnover	10
Fire and Fuel Interactions	11
Overview	11
Structure and Attribution of Contents	13
2. LARGE-SCALE CLIMATIC DRIVERS OF BISON DISTRIBUTION AND ABUNDANCE IN NORTH AMERICA SINCE THE LAST GLACIAL MAXIMUM	17
Contributions of Authors and Co-Authors	17
Manuscript Information	18
Abstract	19
Introduction	20
Coevolution of North American Herbivores and Grasslands and Controls on Large-Herbivore Populations	21
Climate-Driven Stress and Large Herbivore Adaptation	22
Heat Stress	23
Cold Stress	23
Predicting Bison Response to Broad-Scale Climate Changes	24
Methods	24
Documenting Millennial-Scale Changes in Bison Distribution and Abundance	24
Bison Site Dataset	25
Bison Abundance	26
Modeling Bison Distribution with MaxEnt	28
Climate Data	28
Model Description	29
Variable Selection	29
Model Evaluation	30
Temporal Changes in Variable Importance	30

TABLE OF CONTENTS CONTINUED

Defining Bison Distribution.....	31
Results	32
Climate and Patterns of Bison Distribution and Abundance.....	32
Last Glacial Maximum (LGM): 20.0-14.7 ka	38
Bølling–Allerød Interstadial (BA): 14.7-12.9 ka	38
Younger Dryas (YD): 12.9-11.7 ka.....	39
Early Holocene (EH): 11.7-8.0 ka.....	39
Mid-Holocene (MH): 8.0-4.0 ka	40
Late Holocene (LH): 4.0-0.0 ka	40
Discussion.....	43
Key Intervals of Change for Bison Populations.....	43
Pleistocene-Holocene Transition	43
Younger Dryas.....	45
Early and Mid-Holocene.....	46
Late Holocene	47
Regional Bison Abundance and Distribution Patterns	48
Northward Migration into the Ice-Free Corridor	48
Bison Persistence in the Intermountain West	49
Bison in Midcontinent North America	51
Bison Adaptation: Evolution of the Bison Climate “Niche”	54
Conclusions	57
Acknowledgements	58
3. PAST AND PRESENT BIOMASS CONSUMPTION BY HERBIVORES AND FIRE ACROSS PRODUCTIVITY GRADIENTS IN NORTH AMERICA	60
Contributions of Authors and Co-Authors	60
Manuscript Information.....	61
Abstract.....	62
Introduction	63
Methods	68
Reconstructing Modes of Herbivory and Fire.....	68
Bison Abundance	69
Charcoal	69
Pollen.....	69
Study Regions	70
Regional Composites.....	71
Holocene Hydroclimatic Phases of Midcontinent North America.....	71
Spatial Analyses of Modern Fire and Herbivory.....	72
Results and Discussion	74
Acknowledgements	84

TABLE OF CONTENTS CONTINUED

4. FECAL BIOMARKERS REVEAL UNPRECEDENTED 20TH CENTURY HERBIVORE DENSITIES AND IMPACTS IN THE YELLOWSTONE NORTHERN RANGE	86
Contributions of Authors and Co-Authors	86
Manuscript Information.....	87
Abstract.....	88
Introduction	89
Site Description	93
Vegetation	93
Climate	95
Materials and Methods	95
Sediment Core Collection	95
Sediment Core Chronology.....	95
Biomarker Sample Preparation	97
Extraction of Dung Samples	97
Biomarker Extraction of Lake-Sediment Samples.....	98
GC-MS Analysis	99
Fecal Steroid Nomenclature	99
Statistical Analysis of Biomarker Profiles	100
Herbivore Population and Biomass.....	100
Pollen Analysis.....	101
Statistical Charcoal Analysis.....	102
Results	102
Chronology.....	102
Lithology	103
Fecal Steroids	103
Pollen.....	107
Charcoal	108
Discussion.....	108
Conclusions	115
5. CONCLUSION TO DISSERTATION.....	117
Summary.....	117
Significance	118
6. REFERENCES CITED.....	121
7. APPENDICES	154
SUPPLEMENTARY INFORMATION FOR CHAPTER TWO.....	155
SUPPLEMENTARY INFORMATION FOR CHAPTER THREE	187

TABLE OF CONTENTS CONTINUED

SUPPLEMENTARY INFORMATION FOR CHAPTER FOUR 195

LIST OF TABLES

Table	Page
1. Table 1.1. Summary of proxies for past herbivore abundance and identity.	4
2. Table 2.1. Summary of area under the curve (AUC), threshold value (sensitivity = specificity), count of observations used for model training, and count of background points for evaluation across all time intervals modeled.	34
3. Table 4.1 Calendar ages, AMS radiocarbon dates, and ²¹⁰ Pb dates from Buffalo Ford Lake, WY, US.	96
4. Table 4.2. Timeline of significant events relating to elk and bison in Yellowstone National Park, adapted from (National Research Council et al., 2002)	113
5. Supplementary Table 3.1. Moisture availability site metadata. Sites listed from west to east.	188
6. Supplementary Table 3.2. Charcoal site metadata. Sites ordered from driest to wettest.	189
7. Supplementary Table 3.3. Pollen site metadata. Sites ordered from driest to wettest.	190
8. Supplementary Table 3.4. Herbivore mass estimates, based on average values from scientific publications.	191
9. Supplementary Table 4.1. Recent population estimates for ungulates in Yellowstone's Northern Range.	198
10. Supplementary Table 4.2. Concentrations (µg/g) of fecal steroids from dung samples. <LOD = Below limit of detection.	199
11. Supplementary Table 4.3. Concentrations (ng/g) of fecal steroids from Buffalo Ford Lake, Yellowstone National Park, WY, USA. <LOD = below limit of detection.	201
12. Supplementary Table 4.4. Compound information for analyzed fecal steroids.	203

LIST OF FIGURES

Figure	Page
1. Figure 1.1 Temporal and spatial scales covered in the dissertation chapters. Also portrayed are each chapter's geographic focus (upper left quadrant), temporal extent (lower left quadrant), study species (upper right quadrant), and paleoherbivore proxy used (lower right quadrant).....	13
2. Figure. 2.2. Relative change in bison abundance based on raw bison site counts. The color of each 2.5° x 2.5° grid cell indicates whether the number of bison sites (black dots) within the cell decreased (purple), did not change (light blue), or increased (green) relative to the preceding 1000-year interval. Ice sheet extent shown in gray (Gowan et al., 2016). Signs indicate directionality of agreement (positive: + or negative: -) between raw and corrected frequency datasets within each 1000-year interval.	36
3. Figure. 2.4. Geographic representation of modeled bison distributions at key intervals between 20-0 ka. The middle number on each scale identifies the interval-specific predicted probability threshold for defining bison presences (blue) and absences (green and white). Observations (bison sites) shown as points (black). Ice sheet extent shown in gray (Gowan et al., 2016). All maps are available in the supplementary material.....	41
4. Figure. 2.5. Simulated evolution of climate conditions and variable rank for each 1000-year interval since 20 ka. The distributions of climate variables within the model-defined distribution of bison (blue) and North America minus ice-covered areas (green) are summarized with the median (line) and 1st and 3rd quartiles (IQR; shading). Variable rank (dots) reflects the ranking of the percent contribution score relative to the other climate variables (right axis) within a given interval.	42
5. Figure. 2.6. Elevation (top) and latitude (bottom) of bison observations (small dots) across 1000-year intervals between 20-0 ka. Summarized by mean (large black dots) and standard deviation (gray shading).	44

LIST OF FIGURES CONTINUED

Figure	Page
6. Figure. 2.7. Comparison of independent records of large herbivore abundance 5-0 ka. The abundance of <i>S. densa</i> -type spores (top) is expressed as a percentage relative to the terrestrial pollen sum of a given pollen subsample from Kettle Lake, ND (Grimm et al., 2011). The large artiodactyl index (center) represents the abundance of large artiodactyl fossils (elk or bison size) versus medium artiodactyls (deer, sheep, or pronghorn size) across archaeological surveys of Wyoming Basin oil & gas fields (Byers and Smith, 2007). Frequency of dated strata with bison fossils and directly dated fossils (bottom) from archaeological and paleontological studies throughout North America with raw (black) and transformed frequencies (gray).....	53
7. Figure 3.1. Map of study region and sites, with charcoal, pollen, and moisture records (panel A), distribution of study regions and paleoenvironmental sites across the midcontinent moisture gradient in North America (panel B), and conceptual diagram of predicted proportion of biomass consumed by herbivores (black line) or fire (red line) across a precipitation gradient (panel C). Panel B shows the current density distribution of area at a given moisture value for the northern grasslands (NG; yellow) and the grassland-forest transition (GFT; green), with pollen and charcoal sites labeled. Dominant consumer modes are expected to vary across the moisture gradient (panel C). Herbivore density (black line), area burned (red line) curves in panel C represent hypothesized consumer dominance patterns in North America based on empirical data for Sub-Saharan Africa from Archibald and Hempson (2016).....	65
8. Figure 3.2. Regional comparison of reconstructed bison abundance (black line), biomass burning (red line), and woody plant dominance (green line) between 10-0.5k Cal yr BP in the northern grasslands and grassland-forest transition regions. Bootstrapped means (thick colored lines), 95% confidence intervals (dark gray lines), and unsmoothed composite means (light gray lines) are shown. Units for mean charcoal influx are particles cm ⁻² yr ⁻¹ . AP:NAP is the ratio of arboreal pollen to non-arboreal pollen; higher values reflect greater arboreal pollen abundance.....	76

LIST OF FIGURES CONTINUED

Figure	Page
9. Figure 3.3. Fire and herbivory dynamics across moisture gradients in modern North America (left column), modern Sub-Saharan Africa (right column), and Holocene midcontinent North America (bottom panel). For modern data, points represent median values within each 25 mm mean annual precipitation band. Panels A & B compare herbivore biomass to area burned, and panels C & D compare dry matter consumed. Panel E shows regional consumer dominance in Holocene midcontinent North America, points represent the mean of bison abundance or charcoal influx at a given level of woody plant dominance (arboreal pollen:non-arboreal pollen) for every 50 year interval between 10,000-250 Cal yr BP (bison abundance and charcoal influx were standardized at the population level). Lines are based on loess regressions through the points. Data for Sub-Saharan Africa are from Archibald and Hempson (2016).....	78
10. Figure 3.4. Map of relative proportion biomass consumed by herbivores and fire in contemporary North America (panel A); and annual total dry matter consumed by both livestock and fire in contemporary NA (panel B); and predicted relative proportion of dry matter consumed by herbivores and fire (panel C) are based on the observed precipitation-consumer dominance relationship for Sub-Saharan Africa (Archibald and Hempson 2016; Appendix B Sup. Fig. 3.3 B).....	82
11. Figure 4.1. Maps of (panel A) Yellowstone National Park showing extent of the Yellowstone Northern Range (gray shading), location of Buffalo Ford Lake (red X), and extent indicator for panel B (black dashed line); (panel B) the Yellowstone Northern Range (gray shading) with the Buffalo Ford Lake catchment area (white outline), roads (red), rivers and streams (blue), and extent indicator for panel C (dashed black line); (panel C) the Lower Lamar Valley showing Buffalo Ford Lake and its catchment (hatched area); and (panel D) Buffalo Ford Lake showing location of BF19 core (red X).....	94

LIST OF FIGURES CONTINUED

Figure	Page
12. Figure 4.2. Characterization of fecal steroid profiles bison (red), elk (blue), moose (green), mule deer (purple), and pronghorn (orange) based on the relative abundances of sterols, stanols, and stanones and bile acids in individual dung samples. Distributions of (A) sterols, stanols, and stanones and (B) bile acids (mean \pm SE). (C) Score plot and (D) biplot showing the first two principal components of the fecal steroid profile PCA. Chenodeoxycholic acid, and ursodeoxycholic acid were excluded from principal components analysis. Number of individuals: bison: 17, elk: 7, moose: 7, mule deer: 2, pronghorn: 6. See Appendix C Sup. Table 4.4 for compound information. See Appendix C Sup. Table 4.2 for individual sample information and fecal steroid distributions.	104
13. Figure 4.3. Characterization of 5β -stanol profiles of sediments from Buffalo Ford Lake, YNP, Wyoming in relation to the dung profiles of local ungulates. (A) PCA score plot of 5β -stanols in dung, with lake sediment samples as supplementary observations. Clusters are defined by HCPC (panel C). (B) PCA correlation circle depicting correlation between the first two principal components the relative abundance of 5β -stanols. (C) HCPC dendrogram of 5β -stanol distributions for individual ungulate dung samples. (D) Euclidean distance of lake-sediment samples to cluster centroids (from panel A). Shorter distance indicates greater similarity (note the y-axis reversal).	106
14. Figure 4.4. Evolution of (A) relative elk/bison dominance at Buffalo Ford Lake, (B) ungulate fossil presence at Lamar Cave, (C) local ungulate use/density at Buffalo Ford Lake, (D) pollen-inferred vegetation dominance, (E) sediment accumulation rate, and (F) charcoal accumulation rates and long-term CHAR trends (red line; loess smoother; window = 500). Significant (+) and insignificant (●) charcoal peaks throughout the last 2300 years identify past fire-episodes.	107

LIST OF FIGURES CONTINUED

Figure	Page
15. Figure 4.5. Summary of historical Yellowstone Northern Range (YNR) bison and elk management regimes and biomass trends in relation to fecal steroids and associated records of environmental change at Buffalo Ford Lake, YNP, WY. (A) YNR elk (red) and bison (black) biomass trends, based on survey records, with key events noted below. Elk counts before aerial surveys began in 1952 are considered less reliable (dashed line). (B) Influx of total zoostanols (sum of 24-ethylcoprostanol, 24-ethylepicoprostanol, coprostanol, and epicoprostanol). (C) Influx of lithocholic acid. Horizontal gray lines in panels B and C indicate age uncertainty (95% confidence range) associated with sample depths. (D) Biogenic silica concentration from BF87 (Engstrom et al., 1991) show changes in algal production. (E) Sediment accumulation rates based on BF19 & BF87 composite age-depth model (gray line), with loess smoother (light brown), marking periods of increased lake productivity and/or sediment redeposition. (F) Ratio of pollen percentage of locally dominant trees (<i>Pinus</i> & <i>Pseudotsuga</i>) to sagebrush and grasses (<i>Artemisia</i> & <i>Poaceae</i>). (G) <i>Salix</i> pollen percentage. The dashed horizontal lines in all plots indicate long-term means from 340 BCE to 1850 CE.	111
16. Supplementary Figure 2.1. Area of modeled bison distribution across 1000-year intervals between 20-0 ka.	156
17. Supplementary Figure 2.2. Response curves for Temperature Seasonality (bio4) in 1000-year intervals between 20-0 ka.	157
18. Supplementary Figure 2.3. Response curves for Mean Temperature of the Wettest Quarter (bio8) in 1000-year intervals between 20-0 ka.	158
19. Supplementary Figure 2.4. Response curves for Mean Temperature of the Warmest Quarter (bio10) in 1000-year intervals between 20-0 ka.	159
20. Supplementary Figure 2.5. Response curves for Mean Temperature of the Coldest Quarter (bio11) in 1000-year intervals between 20-0 ka.	160
21. Supplementary Figure 2.6. Response curves for Precipitation of the Driest Month (bio14) in 1000-year intervals between 20-0 ka.	161
22. Supplementary Figure 2.7. Response curves for Precipitation Seasonality (bio15) in 1000-year intervals between 20-0 ka.	162

LIST OF FIGURES CONTINUED

Figure	Page
23. Supplementary Figure 2.8. Response curves for Precipitation of the Wettest Quarter (bio16) in 1000-year intervals between 20-0 ka.....	163
24. Supplementary Figure 2.9. Response curves for Precipitation of the Warmest Quarter (bio18) in 1000-year intervals between 20-0 ka.....	164
25. Supplementary Figure 2.10. Response curves for Precipitation of the Coldest Quarter (bio19) in 1000-year intervals between 20-0 ka.....	165
26. Supplementary Figure 2.11. Bison distribution map 20-19 ka.	166
27. Supplementary Figure 2.12. Bison distribution map 19-19 ka.	167
28. Supplementary Figure 2.13. Bison distribution map 18-17 ka.	168
29. Supplementary Figure 2.14. Bison distribution map 17-16 ka.	169
30. Supplementary Figure 2.15. Bison distribution map 16-15 ka.	170
31. Supplementary Figure 2.16. Bison distribution map 15-14 ka.	171
32. Supplementary Figure 2.17. Bison distribution map 14-13 ka.	172
33. Supplementary Figure 2.18. Bison distribution map 13-12 ka.	173
34. Supplementary Figure 2.19. Bison distribution map 12-11 ka.	174
35. Supplementary Figure 2.20. Bison distribution map 11-10 ka.	175
36. Supplementary Figure 2.21. Bison distribution map 10-9 ka.	176
37. Supplementary Figure 2.22. Bison distribution map 9-8 ka.	177
38. Supplementary Figure 2.23. Bison distribution map 8-7 ka.	178
39. Supplementary Figure 2.24. Bison distribution map 7-6 ka.	179
40. Supplementary Figure 2.25. Bison distribution map 6-5 ka.	180
41. Supplementary Figure 2.26. Bison distribution map 5-4 ka.	181

LIST OF FIGURES CONTINUED

Figure	Page
42. Supplementary Figure 2.27. Bison distribution map 4-3 ka.	182
43. Supplementary Figure 2.28. Bison distribution map 3-2 ka.	183
44. Supplementary Figure 2.29. Bison distribution map 2-1 ka.	184
45. Supplementary Figure 2.28. Bison distribution map 1-0 ka.	185
46. Supplementary Table 2.1. Fossil bison observations used in this study (file available at https://doi.org/10.1016/j.quascirev.2022.107472).....	186
47. Supplementary Figure 3.1. Fossil bison observations in North America 10,000-0 Cal yr BP. Observations the grassland-forest transition (green) and northern grasslands (tan) ecoregions were used to create regional bison abundance curves. Data from Wendt et al. (2022).....	192
48. Supplementary Figure 3.2. Moisture availability proxy records of midcontinent North America 10-0k Cal yr BP, with summarized hydroclimate phases (top). See Supplementary Table 3.1 for site and record metadata.	193
49. Supplementary Figure 3.3. Comparison of proportion of biomass consumed by herbivores and fire across precipitation gradients in modern North America (panel A) and Sub-Saharan Africa (panel B). Lines are based on loess regressions through the points. Data for Sub-Saharan Africa are from Archibald and Hempson (2016).....	194
50. Supplementary Figure 4.1. Composite age-depth model and sediment accumulation rate for BF19 & BF87. (A) Composite age-depth model for Buffalo Ford Lake based on ¹⁴ C dates from BF19 (blue density curves), ²¹⁰ Pb dates from BF87 (green density curves), and the charcoal lens from the 1988 Yellowstone fires using rbacon version 2.5.7 (Blaauw and Christen, 2011). (B) Sediment accumulation rate over core depth. The dotted red line represents the weighted mean age at a given depth, gray shading and the dotted gray lines represent the distribution of the most likely age-depth model and 95% posterior density intervals.	196

LIST OF FIGURES CONTINUED

Figure	Page
51. Supplementary Figure 4.2. Percentage diagrams of major pollen types and spores, total sum of terrestrial pollen, the ratio <i>Pinus</i> and <i>Pseudotsuga</i> to <i>Artemisia</i> and <i>Poaceae</i> pollen, local density of ungulates based on fecal steroid biomarkers (total zoostanols: sum of 24-ethylcoprostanol, 24-ethylepicoprostanol, coprostanol, and epicoprostanol), and charcoal data (CHAR and BCHAR) with significant and insignificant peaks from Buffalo Ford Lake 2019 sediment core. Curve exaggeration is represented by light shading.	197

NOMENCLATURE

AUC	Area Under the Curve
BA	Bølling–Allerød Interstadial
BCE/CE	Before Common Era/Common Era
BCHAR	Background charcoal accumulation rate
Cal yr BP	Calendar Years Before Present (1950)
CARD	Canadian Archaeological Radiocarbon Database
CCSM3	Community Climate System Model Version 3
CHAR	Charcoal Accumulation Rate
EH	Early Holocene
GFT	Grassland-Forest Transition
HCPC	Hierarchical Clustering on Principal Components
IQR	Interquartile Range
LGM	Last Glacial Maximum
LH	Late Holocene
MAP	Mean Annual Precipitation
MH	Mid-Holocene
MNI	Minimum Number of Individuals
NG	Northern Grasslands
NISP	Number of Identifiable Specimens
PCA	Principal Components Analysis
PDSI	Palmer Drought Severity Index

NOMENCLATURE CONTINUED

TraCE-21ka Transient Climate Evolution Simulation Dataset

YD Younger Dryas

YNP Yellowstone National Park

YNR Yellowstone Northern Range

ABSTRACT

Large herbivores drive critical ecological processes, yet their long-term dynamics and effects are poorly understood due to the limitations of existing paleoherbivore proxies. To address these shortcomings, long-term records of paleoherbivores were constructed by (i) applying new analytical techniques to existing bison fossil datasets; and (ii) examining fecal steroid data that characterize temporal changes in ungulate abundance and community composition. These paleoherbivore reconstructions were analyzed in relation to their environmental contexts to better understand herbivore-ecosystem interactions through time in three separate studies: First, spatiotemporal changes in postglacial bison distribution and abundance in North America were examined by summarizing fossil bison observations. Bison observations were compared with simulated climate variables in a distribution modeling framework to project probable bison distributions in 1000-year intervals from the Last Glacial Maximum to present in light of changing climatic drivers over time. Since the Bølling–Allerød Interstadial (14.7–12.9 ka) the geographic distribution of bison is primarily explained by seasonal temperature patterns. Second, Holocene records of bison abundance were compared to paleofire reconstructions spanning the midcontinental moisture gradient to determine the relative dominance of herbivores and fire as biomass consumers. Bison dominated biomass consumption in dry settings whereas fire dominated consumption in wetter environments. Historical distributions of herbivory and burning resemble those of Sub-Saharan Africa, suggesting a degree of generality in the feedbacks and interactions that regulate long-term consumer dynamics. Third, the utility of fecal steroids in lake sediments for reconstructing past herbivore abundance and identity was tested by (i) characterizing the fecal steroid signatures of key North American ungulates, (ii) comparing these signatures with multiproxy data preserved in lake sediments from the Yellowstone Northern Range, and (iii) comparing influxes of fecal steroids over time to historical records of ungulate biomass and use. Bison and/or elk were abundant at Buffalo Ford Lake over the past *c.* 2300 years. Ungulate densities in the watershed were highest in the early 20th century and likely contributed to decreases in forage taxa and possibly increased lake production. These results demonstrate long-term ecological impacts of herbivores and highlight opportunities for continued development of paleoherbivore proxies.

CHAPTER ONE

INTRODUCTION TO DISSERTATION

The Ecological Significance of Large Herbivores

My dissertation was motivated by a desire to improve scientific understanding of herbivore ecology. Large herbivores influence plant trait evolution (Charles-Dominique et al., 2016), the relative dominance of vegetation (Staver et al., 2021), and fuel loads and fire patterns (Rouet-Leduc et al., 2021), and thereby play a role in governing vegetation structure, composition, and the distribution of biomes globally. In contrast to vegetation and fire paleoecology, methods for characterizing spatial and temporal variability in paleoherbivore populations and communities are poorly developed. The lack of reliable methods and datasets has left herbivores somewhat overlooked in paleoecological reconstructions and limited our ability to evaluate hypotheses involving their ecological impacts.

For example, the hypothesis that herbivores determine vegetation patterns across large portions of Earth's terrestrial surface (Bond, 2005; Hairston et al., 1960) is difficult to test because even the longest long-term observational scientific records of relevant variables (e.g., vegetation structure, herbivore populations and community composition, and fire activity) are short relative to timescales at which plant communities develop and turn over. Observations from the paleo record have produced some insights into this question. Paleorecords show that Late Quaternary megafaunal extinctions were associated with increased fire activity and rapid transformation of plant communities (Gill et al., 2009; Karp et al., 2021; O'Keefe et al., 2023;

Perrotti et al., 2022). However, the proxies used by these studies to infer paleoherbivore impacts have serious limitations that prevent further insights.

Herbivore effects are contingent upon foraging strategy (Holdo et al., 2009a; Rouet-Leduc et al., 2021), which is related to body size, digestive plan, diet quality, and metabolism (Clauss et al., 2013). Yet, common palynological proxies for herbivores (e.g., dung fungal spores) do not provide information about the relative dominance or composition of herbivore communities. Development of proxies that can provide highly resolved records of herbivore identity and impacts will greatly improve understanding of paleoherbivore ecology. Given the limitations of existing methods, it is necessary to develop new datasets and analytical techniques for paleoherbivores. Chapters 2-4 of this dissertation represent my efforts to integrate new paleoherbivore data and methods with new and/or previously published environmental data to address unanswered questions:

What are the long-term drivers of bison distribution and abundance in late Quaternary North America? (Chapter 2)

How did consumer dominance and prevalence respond to spatial and temporal moisture gradients in Holocene North America? And how do past and present consumer dominance patterns in North America compare to less altered consumer regimes in modern Sub-Saharan Africa? (Chapter 3)

Are fecal steroids in lake sediments reliable indicators of past herbivore abundance and community composition? (Chapter 4)

Paleoherbivore Proxies

Herbivore community composition and abundance are known to influence vegetation composition and other important ecosystem properties, yet evaluations of the impacts of large herbivores in the past have been largely based upon methods that cannot reliably characterize community composition and abundance (Table 1.1).

Palynological indicators

Palynological indicators are among the most frequently used proxies for past herbivore presence in continuous sediment records (Baker et al., 2013). Coprophilous fungal spores are especially popular because they primarily originate from dung and are easily quantified using pollen analysis protocols. Yet taxonomic investigation has shown that ‘coprophilous fungal spores’ is a misnomer, as many of these spores, including widely-used *Sporormiella*-type spores, are also produced by fungi with affinity for alternative, non-dung substrates (Kruys and Wedin, 2009). Therefore, it is often impossible to ascertain whether a given spore originated from dung of a large herbivore or if it grew from soil or decaying vegetation. Even if it is assumed that most coprophilous fungal spores originate from dung, they still cannot provide information about source-animal identity. Furthermore, absence of coprophilous fungal spores cannot be interpreted as absence of large herbivores because of complications arising from dung fungus ecology (Perrotti and van Asperen, 2019). Even when dung fungi occur locally in association with large herbivores, lake sediment records still may not yield spores due to dispersal or preservation issues (Ulrich, 2020; van Asperen et al., 2020).

Table 1.1. Summary of proxies for past herbivore abundance and identity.

Proxy	Description	Example	Identity?	Abundance?
Palynological indicators	Coprophilous fungal spores and other microscopic indicators of herbivores or herbivory	<i>Sporormiella</i> spores in Galapagos sediments reflects tortoise extirpation and livestock introduction (Bush et al., 2022).	No	Maybe (low sensitivity at low herbivore densities)
Fossils	Preserved animal bone and other tissues	Late Holocene bison fossils at Big Bone Lick, KY demonstrate local adaptation of bison to eastern forests (Widga, 2006).	Yes	Yes (depends on context and scale)
aDNA	DNA from preserved fossil specimens	Genetic analysis of Beringian bison identifies millennial-scale population trends and timing of bison decline (Shapiro et al., 2004).	Yes	Yes (large spatiotemporal scales)
sedaDNA	Fossil DNA in sedimentary records	DNA metabarcoding of alpine lake sediments shows presence of domestic herbivore species and vegetation (Giguet-Covex et al., 2014).	Yes	Maybe (pseudo-abundance with replicates)
Molecular biomarkers	Fossil molecules from organic tissues	Bile acids in Greenland lake sediments correspond to Norse and Danish settlements (Guillemot et al., 2015).	Yes	Yes

Fossils

Fossils including bones and preserved soft tissues provide strong evidence of animal presence and identity. Unlike lake sediments and tree rings which typically provide continuous records, fossil bone deposits usually capture a single event or a sequence of discrete events. However, recent methodological developments in analysis of radiocarbon dates now allow fossil assemblages to be analyzed for continuous population trends when fossil observations are aggregated at large spatial scales (e.g., Chaput and Gajewski 2016) or when unique local conditions produce especially rich fossil deposits (e.g., O’Keefe *et al* 2023). Chapters 2 and 3 feature analyses of new fossil bison occurrence datasets to understand how long-term changes in bison abundance and geographic distribution are influenced by climate change at continental (Chapter 2) and regional scales (Chapter 3).

aDNA

Ancient DNA (aDNA) refers to DNA isolated from fossil specimens. Due to the degradation from abiotic and biotic processes, ancient remains usually contain only a small fraction of an organism’s original DNA. However, even fragmented DNA can provide critical information about ancestral relations (Karpinski et al., 2020), breeding population sizes and trends (Shapiro et al., 2004), time since last common ancestor (Groenen, 2016), genetic diversity (Campos et al., 2010), and pathogens (Rasmussen et al., 2015).

sedaDNA

Sedimentary ancient DNA (sedaDNA) enables detection of traces of ancient life from DNA fragments preserved in sedimentary archives. Because all living organisms contain and produce DNA, this approach can be applied to any branch of the tree of life, including large

herbivores. A small packet of sediment can reveal the genetic composition of entire ecosystems with high precision. In general, sedaDNA is limited to presence/absence determinations as it does not provide good evidence for abundance changes. However, the number of positive replicates for a given taxon may be used as a pseudo-abundance measure (e.g., Giguet-Covex et al., 2019).

Absences are more difficult to interpret than presences because dispersal pathways and degradation processes are not well understood. SedaDNA applications are limited by preservation issues because DNA degrades rapidly in warm, moist, and/or high-UV conditions. To date, successful studies have been focused on colder polar and alpine environments (Giguet-Covex et al., 2019; Pedersen et al., 2013). However, a recent study of Hall's Cave in Texas demonstrates that DNA can be well-preserved in and recovered from temperate settings as well (Seersholm et al., 2020).

SedaDNA is highly susceptible to contamination and thus requires specialized equipment, facilities, and procedures. Additionally, genomic analysis for source identification is computationally intensive. Correct source identification is limited by the quality and completeness of reference databases. Misidentifications are common but relatively easy to detect if analysts possess prior knowledge about likely inhabitants.

Molecular Biomarkers

In paleoenvironmental contexts, molecular biomarkers refer to thermodynamically stable molecules that originate from organism tissues and thus provide some information about the conditions under which the molecules formed (Eglinton and Eglinton, 2008; Gaines et al., 2008). The most widely used molecular biomarkers for herbivores are 5-beta stanols and bile acids, both

of which are fecal steroids that are synthesized and modified in the digestive tracts of higher animals. Because molecular biomarkers are found in lake sediments, they can produce continuous records and be compared directly to other paleoenvironmental proxies such as charcoal and pollen.

Methods for fecal steroid analysis have been used in other studies to detect and differentiate among animal and human sources of environmental pollution (Sánchez et al., 2017; Tyagi et al., 2008) and to identify and quantify animals in archaeological contexts (Prost et al., 2017; Zocatelli et al., 2017). Recently, researchers have extended the use of fecal steroid biomarkers to develop continuous reconstructions that quantify shifts in the abundance of humans and/or herbivores over time (Argiriadis et al., 2018; Guillemot et al., 2015; McWethy et al., 2020). In Chapter 4 I build upon recent advances in fecal steroid analysis (Harrault et al., 2019) to differentiate wild ungulates of the Greater Yellowstone Ecosystem based on their fecal steroid profiles and characterize changes in relative herbivore dominance through time.

Bison: North America's Dominant Herbivore

Bison (*Bison*) first arrived in North America via the Bering Land Bridge during the Penultimate Glacial Period between ~195-135 thousand years ago (Froese et al., 2017). Until the late Pleistocene extinctions ~14-11 thousand years ago, bison were one large herbivore among many others including mammoths, mastodons, equids, and giant ground sloths. The decline of other North American megafauna was an opportunity for bison, which became more abundant and more widespread into the Holocene. Over the past 12 thousand years, bison were the dominant herbivore throughout North America.

The near extermination of bison in the 19th century and their subsequent replacement by cattle is one of the most dramatic cases of biological turnover ever witnessed by humans. This continent-scale event permanently altered the course of natural and human history, but the ecological consequences have hardly been explored. As the largest native land animal on the continent, and once one of the most numerous, bison undoubtedly had substantial impacts on biomass turnover, vegetation structure, and nutrient cycling.

Bison are widely recognized by scientists and the public as ecologically influential creatures. Their keystone status refers to their critical role in determining community structure via trophic interactions (Knapp et al., 1999). As the term implies, removal of the ‘keystone’ is likely to result in significant changes in community composition and other ecosystem attributes (Paine, 1969). By virtue of their sheer size and historical abundance, North American bison have long served a keystone function in trophic dynamics and community structures of ecosystems. Their importance to Great Plains ecosystems has been outlined in many studies (e.g., Anderson, 2006; Knapp et al., 1999; Ratajczak et al., 2022).

Wallowing, Trailing, and Rubbing

In addition to consuming large quantities of forage (a trophic interaction), bison physically modify materials through non-consumptive behaviors such as wallowing, trailing, and rubbing. Wallows are patches of bare soil that are created and maintained by pawing and rolling. Wallows contribute to heterogeneous prairie patch dynamics. Disturbance-adapted plant species (e.g., *Ambrosia psilostachya*, *Coreopsis tinctoria*, and *Hordeum pusillum*) that would otherwise be outcompeted by grassland dominants are able to persist in wallows (Polley and Wallace, 1986). Compacted soil in wallows also hold open pools of rainwater that host ephemeral wetland

species, akin to a vernal pool. Wallowing increases arthropod community diversity (Nickell et al., 2018) and amphibians have been observed breeding in old wallows (Busby and Brecheisen, 1997)

Bison trailing is also an important ecological process that alters the physical state of abiotic materials. Trail formation reduces the amount of energy that bison and other animals expend to traverse landscapes. Trails facilitate propagule dispersal and create habitat for disturbance-adapted species. Late Holocene bison trails were so impactful that many remain visible today. Some of these extensive and visually striking trails were originally interpreted by geologists as joints and faults or glacial disintegration trenches (Clayton, 1975).

Bison horning and rubbing impacts on vegetation structure have also been observed. At a tallgrass prairie site in Oklahoma, Coppedge and Shaw (1997) found that bison killed or severely damaged 4% of woody plants within the study area. Over the 2-year study period, bison killed or severely damaged 17% of willow saplings and shrubs. Evidence from Lamar Valley in Yellowstone National Park suggests that horning and rubbing damage from the resident bison population contributes to tree decline in stands of aspen, cottonwood, and lodgepole pine (Beschta et al., 2020).

Changes in Biotic Interactions

Large herbivores such as bison can influence the outcome of plant competition via effects of herbivory, trampling, and nutrient removal/delivery. Herbivores promote plant diversity by removing foliage of dominant plants and promoting increased light penetration (Eskelinen et al., 2022). At the Konza Prairie Biological Station in the Flint Hills of Kansas, bison grazing has progressively reduced grass cover and increased native species richness relative to no-grazing

and domestic cattle treatments (Ratajczak et al., 2022). Under high herbivore pressure, vegetation communities often begin to resemble lawns dominated by low-stature, grazing-adapted plants.

Nutrient Cycling and Biomass Turnover

As the largest and one of the most numerous herbivores in Holocene North America, bison had substantial impacts on biomass turnover and nutrient cycling. High gut capacities, long digestive tracts, and large ranges allow large herbivores to disperse organic matter and nutrients across greater distances than their smaller-bodied counterparts. Large herbivores thus counteract nutrient entropy by redistributing P and other nutrients from river basins to uplands (Wolf et al., 2013).

Grazing lawns are patches of locally stable, short, grazing-adapted vegetation that are created and maintained by concentrated herbivore use. Continuous herbivory keeps vegetation in a state of constant regrowth, which is maintained by an influx of nutrients from animal dung and urine (Cromsigt and Olf, 2008). In these heavily grazed systems, plants adapted to grazing pressure benefit from nutrient delivery and release from competition, while herbivores consume high-quality regrowth (Agrawal, 2000). Bison regularly demonstrate a preference for prairie dog towns with closely cropped vegetation and low standing biomass (Coppock et al., 1983; Whicker and Detling, 1988). Similarly, by consuming large quantities of fresh growth during spring green-up, bison effectively maintain their own ‘green wave’ of high quality forage (Geremia et al., 2019).

Fire and Fuel Interactions

Grazing, browsing, and trampling by large herbivores can reduce fire activity via reduced fuel continuity (Archibald et al., 2005; Rouet-Leduc et al., 2021) and fuel loads (Bruegger et al., 2016; Rouet-Leduc et al., 2021). The low palatability of fire-adapted plants may limit large herbivore influence over fire patterns in more pyrogenic systems (Archibald et al., 2019; Hempson et al., 2019). Although dietary preferences of herbivores vary with body size, digestive system, and oral/dental morphology, large herbivores, including bison, tend to prefer post-burn vegetation because it is easier to physically access and has higher nutritional value than unburned forage (Augustine et al., 2010; Fuhlendorf and Engle, 2004; Hobbs et al., 1991; Knapp et al., 1999; Vermeire et al., 2004). This preference produces pyric herbivory, wherein herbivores select recently burned areas, leading to temporarily reduced fuel loads. Positive and negative feedbacks associated with fire-driven grazing promote landscape heterogeneity across multiple spatial and temporal scales (Allred et al., 2011).

Overview

Each chapter of my dissertation investigates Quaternary paleoherbivore ecology in North America at different spatial and temporal scales (Fig. 1.1). Figure 1.1 provides a visual overview of the structure of my dissertation. As North America's dominant herbivore, bison feature prominently throughout.

Chapter 2 explores how bison distribution and abundance responded to changing climate conditions from the Last Glacial Maximum (20k cal yr BP) to present. As their environments changed during this period, bison underwent remarkable physiological, behavioral, and ecological transformations. As the climate warmed and the Laurentide and Cordilleran ice sheets

receded, bison body mass and horn spans shrunk, and they become more numerous and more widely distributed. As all larger megaherbivores succumbed to extinction at the Pleistocene-Holocene transition, bison thrived and spread throughout North America.

Chapter 3 explores patterns of biomass consumption by herbivores and fire in Holocene midcontinent North America. Throughout the Holocene the relative dominance of bison and fire shifted along spatial and temporal moisture gradients, with herbivores consuming a greater share of plant biomass in drier regions with more open vegetation, while fire dominated biomass consumption in wetter, more closed environments. Today, domestic livestock is responsible for the vast majority of biomass consumption in North America, and agricultural practices have disrupted historic biomass consumption patterns. Fire and bison are now functionally absent from many regions where they were once key ecological drivers.

Chapter 4 investigates the application of fecal steroid biomarkers to develop continuous lake sediment records of dominant herbivore identity and local density. This is achieved by characterizing fecal stanol signatures of bison, elk, moose, mule deer, and pronghorn and then comparing these to the signatures of sediments from Buffalo Ford Lake in the Northern Range of Yellowstone National Park. The fecal steroid signatures of the lake sediment resemble those of elk and bison, indicating that one or both species were dominant during the past *c.* 2300 years. Following the establishment of Yellowstone National Park in 1872, predator suppression and hunting bans led to explosive elk population growth in the early 20th century. High local elk use is evidenced by high fecal steroid influxes and resulted in significant environmental impacts in the Buffalo Ford Lake area, including declines in forage species dominance and increased lake production.

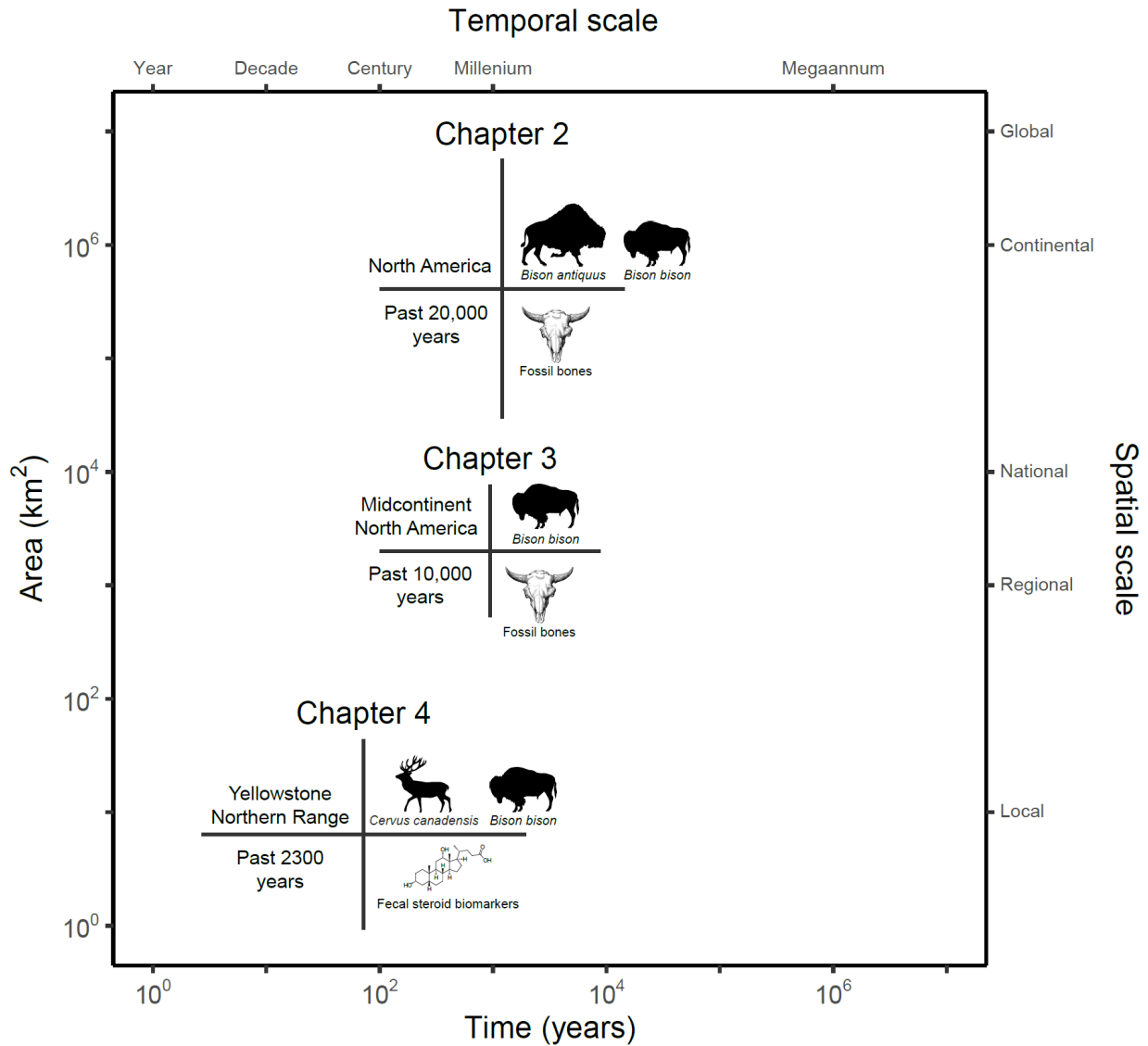


Figure 1.1 Temporal and spatial scales covered in the dissertation chapters. Also portrayed are each chapter’s geographic focus (upper left quadrant), temporal extent (lower left quadrant), study species (upper right quadrant), and paleoherbivore proxy used (lower right quadrant).

Structure and Attribution of Contents

In addition to this introduction (Chapter 1) and a conclusion (Chapter 5), this dissertation is composed of three stand-alone articles, with contributions from co-authors:

- Chapter 2 – “Large-scale climatic drivers of bison distribution and abundance in North America since the Last Glacial Maximum” was published in *Quaternary Science Reviews* (Wendt et al., 2022).
 - Author contributions
 - J.A.F. Wendt (me): Conceptualization, data curation, formal analysis, funding acquisition, investigation, methodology, software, visualization, writing – original draft, and writing – review & editing.
 - D.B. McWethy: Conceptualization, funding acquisition, project administration, supervision, writing – original draft, and writing – review & editing.
 - C. Widga: Conceptualization, data curation, and writing – review & editing.
 - B.N. Shuman: Conceptualization and writing – review & editing.
 - Funding
 - NSF grant BCS-1832486 awarded to D.B. McWethy.
 - Joint Fire Science Program grant 19-1-01-30 awarded to me and D.B. McWethy.
- Chapter 3 – “Past and present biomass consumption by herbivores and fire across productivity gradients in North America” was published in *Environmental Research Letters* (Wendt et al., 2023).
 - Author contributions

- J.A.F. Wendt (me): Conceptualization, data curation, formal analysis, funding acquisition, investigation, methodology, visualization, writing – original draft, and writing – review and editing.
- D.B. McWethy: Conceptualization, funding acquisition, supervision, investigation, writing – original draft, and writing – review and editing.
- G.P. Hempson: Investigation, methodology, visualization, writing – original draft, and writing – review and editing.
- E.N.J. Brookshire: Investigation and writing – review and editing.
- S.D. Fuhlendorf: Investigation and writing – review and editing.
- Funding
 - Joint Fire Science Program grant 19-1-01-30 awarded to me and D.B. McWethy.
- Chapter 4 – “Molecular biomarkers reveal unprecedented 20th century herbivore densities and impacts in the Northern Range of Yellowstone National Park” is in preparation for submission to *Ecology Letters*.
 - Author contributions
 - J.A.F. Wendt (me): Conceptualization, data curation, formal analysis, funding acquisition, investigation, methodology, visualization, writing – original draft, and writing – review and editing.
 - E. Argiriadis: Data curation, formal analysis, supervision, investigation, methodology, writing – original draft, and writing – review and editing.

- C. Whitlock: Conceptualization, supervision, project administration, pollen analysis, investigation, and writing – review and editing.
 - M. Bortolini: Data curation, methodology, writing – original draft, and writing – review and editing.
 - D. Battistel: Methodology, project administration, supervision, and writing – review and editing.
 - D.B. McWethy: Conceptualization, supervision, funding acquisition, writing – original draft, and writing – review and editing.
- Funding
 - NSF grant EAR-2149482 to C. Whitlock and D.B. McWethy.
 - American Museum of Natural History Theodore Roosevelt Memorial Grant to me
 - MSU Institute on Ecosystems Yellowstone Doctoral Scholars Fellowship to me

CHAPTER TWO

LARGE-SCALE CLIMATIC DRIVERS OF BISON DISTRIBUTION AND ABUNDANCE IN
NORTH AMERICA SINCE THE LAST GLACIAL MAXIMUM

Contributions of Authors and Co-Authors

Manuscript in Chapter 2

Author: John A.F. Wendt

Contribution: Conceptualization, data curation, formal analysis, funding acquisition, investigation, methodology, software, visualization, writing – original draft, and writing – review & editing.

Co-Author: David B. McWethy

Contribution: Conceptualization, funding acquisition, project administration, supervision, writing – original draft, and writing – review & editing.

Co-Author: Chris Widga

Contribution: Conceptualization, data curation, and writing – review & editing.

Co-Author: Bryan N. Shuman

Contribution: Conceptualization and writing – review & editing.

Manuscript Information

John A.F. Wendt, David B. McWethy, Chris Widga, Bryan N. Shuman

Quaternary Science Reviews

Status of Manuscript

- Prepared for submission to a peer-reviewed journal
- Officially submitted to a peer-reviewed journal
- Accepted by a peer-reviewed journal
- Published in a peer-reviewed journal

Volume 284, Elsevier BV

<https://doi.org/10.1016/j.quascirev.2022.107472>

CHAPTER TWO

LARGE-SCALE CLIMATIC DRIVERS OF BISON DISTRIBUTION AND ABUNDANCE IN
NORTH AMERICA SINCE THE LAST GLACIAL MAXIMUMAbstract

As the dominant large herbivore in midcontinent North America since the terminal Pleistocene, bison (*Bison* spp.) have been a fundamental component of ecosystems and economies. Despite the importance of bison in late Quaternary North America, large-scale (regional to continental) patterns of bison biogeography are not well understood. Here we integrate archaeological and paleontological bison occurrence data with simulated climate data to better understand long-term drivers of bison distribution and abundance in North America. We used these records to model bison distribution and abundance over the past 20 thousand years at 1-thousand-year intervals. Our results show that late Quaternary changes in the distribution and abundance of bison were influenced by large-scale trends in temperature and precipitation. The distribution of bison since the Bølling–Allerød Interstadial (ca. 14 ka) is primarily explained by seasonal temperature patterns (mean temperature of the coldest quarter is the most important variable for 12 of 14 1-thousand-year intervals). The modeled climate of bison distributions progressively narrowed since the Last Glacial Maximum (ca. 20 ka) as bison populations retracted from disjunct Pleistocene refugia and congregated in midcontinent rangelands. Through the Pleistocene-Holocene transition, bison experienced rapidly warming summer temperatures that increased faster in midcontinent North America than other regions and the continent as a whole. Model results suggest that Holocene bison abundance was influenced by hydroclimatic

shifts that affected the quality and availability of forage. Bison abundances decreased through the dry early and mid-Holocene and increased when moisture availability improved in the late Holocene. We infer that bison have thrived under a broad range of environmental conditions since the Last Glacial Maximum and that the climatic and biogeographic space occupied by bison narrowed in recent millennia.

Introduction

As the largest survivors of the late Pleistocene extinctions in North America (NA), bison (*Bison* spp.) have demonstrated remarkable capacity to persist and thrive despite periods of rapid and severe climatic changes and pressures from shifting predator guilds. From the Pleistocene-Holocene transition to the introduction of Old World livestock ca. 500 years ago, bison were the dominant herbivores throughout mid-latitude NA with population estimates ranging from 30-60 million individuals (Flores, 1991; McHugh, 1979; Seton, 1929; Shaw, 1995). Prior to their near extinction in the early 20th century, the geographic range and density of bison were on par with the world's largest ungulate populations. Despite the historical significance of bison for the evolution of North American ecosystems and Indigenous cultures, there has been little research that examines long-term changes in the distribution and abundance of bison across the continent and the underlying drivers. Additionally, our understanding of large herbivore responses to changing climatic and environmental conditions during the Late Pleistocene and Holocene is limited (Meltzer, 2020).

Previous research examining trends in bison distribution and abundance and the drivers of these trends is mostly restricted to individual sites or subregional studies and/or shorter decadal to millennial time scales (e.g., Byers and Smith, 2007; Cooper, 2008; Lohse et al., 2014;

Lupo and Schmitt, 1997; Lyman, 2004; Martin et al., 2017; Scott, 2010; Shapiro et al., 2004). As recent efforts to reintroduce large bison herds in NA accelerate (Martin et al., 2021; Pejchar et al., 2021; Sanderson et al., 2008; Shamon et al., 2022; Steenweg et al., 2016; Torbit and LaRose, 2001; Wilkins et al., 2019), and concerns over the fate of large herbivores increase across the globe, there is a critical need to evaluate bison responses to changing climate. Here we set out to: 1) document changes in the distribution and abundance of North American bison populations since the Last Glacial Maximum (LGM) using archaeological and paleontological datasets of bison occurrences, 2) identify the primary controls on bison distribution and abundance by evaluating changes in these phenomena in relation to modeled and empirical climate data, 3) use a distribution modeling framework to characterize bison responses to shifting environmental gradients during the late Quaternary, and 4) discuss results in the context of current efforts to conserve and restore bison across NA.

Coevolution of North American Herbivores and Grasslands and Controls on Large-Herbivore Populations

While recent work has advanced our understanding of climate controls on herbivores in contemporary ecosystems (Pachzelt et al., 2015; Payne and Bro-Jørgensen, 2016; Veldhuis et al., 2019), the short duration of the observational record limits our understanding of how herbivores respond to climate change on longer, millennial time scales. In a multi-proxy synthesis of paleoecological records, Strömberg (2011) reports that the first grassy ecosystems in NA appeared in the late Oligocene and early Miocene, followed by the evolution of grassland-adapted fauna in the early to middle Miocene. Open, grass-dominated ecosystems continued to expand through the middle to late Miocene (Janis et al., 2002). The progressive development and evolution of grassland ecosystems was likely driven by long-term regional aridification

(Strömberg, 2011). The importance of moisture availability for grassland expansion and persistence is supported by observations of modern grasslands and savannas, where maximum woody cover is primarily constrained by moisture availability, and further reduced by edaphic controls and disturbance from fire, herbivores, and pathogens (Sankaran et al., 2005; Scholtz et al., 2018). The Miocene proliferation of herbivores adapted to open habitats would have introduced novel disturbance processes including the destruction of woody plant species by proboscideans and other large ungulates (Morrison et al., 2016; Rivals et al., 2007) and altered fire regimes (Davies et al., 2015; Donaldson et al., 2018; Starns et al., 2019). Large mammal species richness peaked during the middle Miocene and subsequently declined (Jardine et al., 2012). As taxonomic richness of large mammals decreased into the Pleistocene, the proportion of taxa adapted to open habitats increased (Janis et al., 2002; Jardine et al., 2012). Concomitantly, the median body mass of artiodactyl and perissodactyl species increased substantially through the late Miocene (Huang et al., 2017). In short, aridification was a primary climatic factor of the expansion of grasslands and subsequent herbivore populations that radiated to fill new open-habitat niches. Bison successfully exploited these open landscapes after crossing the Bering Land Bridge ca. 195-135 ka (Froese et al., 2017).

Climate-Driven Stress and Large Herbivore Adaptation

Climatic conditions impact large herbivores via multiple pathways. Because precipitation and temperature govern primary production, and large herbivores have substantial forage and water intake requirements, climate indirectly affects herbivore fitness, production (Coe et al., 1976; Raynor et al., 2020) and diversity (Olf et al., 2002; Veldhuis et al., 2019). Climate also

acts as a direct control on individuals and populations by influencing physiological functioning and behavior.

Heat Stress Exposure to temperatures above or below an animal's capacity to thermoregulate can result in thermal stress and, under extreme conditions, mortality (Martin and Barboza, 2020a). In general, large-bodied animals such as bison, are more susceptible to heat stress than their smaller-bodied counterparts. Elevated ambient temperatures limit the capacity of endotherms to dissipate heat, resulting in heat stress (Martin and Barboza, 2020a, 2020b; Speakman and Król, 2010). Larger-bodied animals generally do not dissipate heat in warm conditions as effectively as smaller animals because larger animals have greater volumes per unit of surface area. To mitigate heat stress in the short-term, large herbivores may employ behavioral and physiological strategies including wallowing (Marai and Haezeb, 2010), limiting activity to cooler hours of the day, panting, sweating, seeking thermal cover (McCann et al., 2013), and reducing forage intake (Spiers et al., 2004). Increased frequency of extreme temperatures over millennial timescales can exert pressure on large herbivores to migrate, adapt, or decrease populations in response to thermal stress.

Cold Stress Winter and early spring are the most physiologically stressful seasons for large herbivores at mid- to high latitudes. Harsh conditions including cold temperatures, deep snow, predator pressure, and a lack of high-energy forage coincides seasonally with high energy demands from gestation and lactation. The convergence of these stressors exerts a strong influence on mortality (Gaillard et al., 2000; Horne et al., 2019; Jackson et al., 2021; Singer et al., 1997; Smith and Anderson, 1998). To sustain energy reserves through winter and early spring, large herbivores consume quality forage during warmer months to build energy reserves

(Bårdsen and Tveraa, 2012), reduce movement when snow is deep and temperatures are low (Sheppard et al., 2021), and allocate more time to resting and less time to foraging during winter (Beumer et al., 2020).

Predicting Bison Response to Broad-Scale Climate Changes

Based on known physiological constraints and foraging behavior of bison and other large herbivores, we hypothesize that, (H1) in open habitats, bison abundance will be positively correlated with moisture availability that indirectly influences the abundance and availability of grassland forage, and (H2) changes in the geographic distribution of bison will respond to long-term changes in temperatures and associated hydrothermal stress.

Methods

Documenting Millennial-Scale Changes in Bison Distribution and Abundance

Reconstructing long-term trends in bison abundance is limited by the quality and availability of fossil occurrence records, which are temporally discontinuous and can be spatially biased by the distribution of appropriate depositional settings, adequate preservation of identifiable remains, and other taphonomic processes. The rich late Quaternary fossil record in NA, however, provides a unique opportunity to investigate the relationships between climate change, bison range dynamics, and demographic patterns. Past research has employed a variety of metrics to quantify changes in the relative abundance of fossil taxa including the number of identifiable specimens (NISP; e.g., Byers and Smith, 2007; Hill, 2007) and minimum number of individuals (MNI) within an assemblage. In order to examine bison response to environmental and climatic changes, we compared dated occurrences of bison in the fossil record with empirical

and modeled paleoclimate data. Instead of relying on traditional abundance estimates from skeletal element counts, we considered individual archaeological and paleontological sites containing bison fossils as evidence for the presence of bison at a given time and place. We infer that large-scale, spatiotemporal changes in bison abundance are reflected in changes in the presence or absence of bison in fossil assemblages within a subregion. We acknowledge the coarse spatiotemporal resolution of the fossil record. Therefore, we evaluate changes in abundance at millennial time scales (between adjacent 1000-year intervals).

Bison Site Dataset

We compiled a dataset of *Bison* spp. fossil occurrences in NA (Appendix A Sup. Table 2.1). Records of direct-dated bones and age-constrained stratigraphic units containing bison were acquired from the Neotoma Paleoecology Database in December 2021 (Goring et al., 2015; Williams et al., 2018). This dataset was supplemented with records accessed from the Canadian Archaeological Radiocarbon Database (CARD; Martindale et al., 2015) in January 2022 and primary source publications. Using the criteria detailed below, only high-quality observations were retained in our analysis. Observations were removed if they were identified as duplicates, non-bison observations, imprecisely dated (radiocarbon date sigma > 250 years), stratigraphically dated with overly-broad time periods (e.g., “Pleistocene”), dated outside of the study period (youngest age > 20 ka), or dated with material known to be unreliable (e.g., apatite). After removing low-quality observations, the dataset consisted of 2700 observations (Appendix A Sup. Table 2.1; CARD: n=1828; Neotoma: n=731; primary sources: n=141).

Data processing and analysis were performed with R version 4.1.2 (R Core Team, 2022) in RStudio (Posit team, 2023). Radiocarbon (^{14}C) dates reported by original publications were

calibrated to calendar years before present (cal yr BP) with the Intcal20 curve (Reimer et al., 2020), using the rcarbon package (Bevan and Crema, 2018). Observations were grouped by median calibrated ages into 20 equal 1000-year intervals spanning 20-0 ka. Observations with dates spanning interval boundaries were classified as present in overlapping intervals.

Bison Abundance

The presence of bison at a dated fossil locality is a necessary precondition for a positive determination from the fossil record. It is reasonable to expect that the abundance of living bison at a given time will be related to the abundance of bison fossils that are subsequently discovered. However, the fossil record does not perfectly represent bison populations in the past because multiple post-depositional processes can influence the frequency of bison observations. Processes contributing to information loss from the fossil record include site destruction from weathering and erosion, poor preservation of fossil materials, gaps in the spatial and temporal focus of research efforts, and taxonomic misidentification.

To correct for the influence of taphonomic bias (i.e., overrepresentation of younger fossils), the frequency distribution of bison occurrences over time was adjusted with a transformation function following the methods of Surovell et al. (2009). The transformed and untransformed (raw) frequency distributions were then binned into 1000-year intervals, the mean frequency within each interval was calculated, and it was determined whether means increased or decreased relative to the prior interval (Fig. 2.1). Taphonomic bias will cause a time series of untransformed frequencies to overestimate increases and underestimate decreases in occurrences, whereas a taphonomic correction will adjust observation frequencies such that the probability of site survival decreases over time (Surovell et al., 2009). Because the biases of the untransformed

and transformed data are opposed, we interpret directional agreement in the raw and transformed datasets as an indicator of an increase or decrease in bison abundance.

Spatial patterns of relative bison abundance through time were also examined. Time-binned, spatially explicit data on bison occurrences were used to create gridded datasets representing the count of bison sites within each $2.5^\circ \times 2.5^\circ$ grid cell for each 1000-year interval between 20-0 ka. Bison sites are defined as localities where bison remains have been positively identified, documented, and dated. Bison site counts were used to derive a second series of gridded datasets that indicate the directionality of change in the number of bison sites between a given time interval and the preceding interval. The resulting raster datasets contained cell values indicating either: 1) increased number of bison sites, 2) decreased number of bison sites, or 3) no change relative to the preceding time interval. Continental-scale trends and spatial patterns in bison abundance were visualized by mapping each gridded dataset at 1000-year intervals (Figs. 2.2 and 2.3). This approach indicates the directionality of changes in bison site abundance and does not measure magnitude of change. It is assumed that times and places with high bison populations yield more remains, and therefore, more sites. Conversely, declining populations will yield fewer remains and sites as time progresses. This approach shows the directionality of sub-regional population changes and quantifies the extent of range contractions and expansions.

Our spatial approach also reduces taphonomic bias by comparing the number of bison sites within a given time interval directly to the preceding time interval, instead of relating the number of older sites to a baseline of modern/recent sites that are far more likely to be preserved and discovered (Surovell et al., 2009). This approach is not intended to identify population

increases or decreases operating at finer spatiotemporal scales (e.g., population crashes following a harsh winter, or disturbance event, etc.).

Modeling Bison Distribution with MaxEnt

Climate Data Climate data for the last 20,000 years were derived from the Transient Climate Evolution (TraCE-21ka) simulation dataset, run with the Community Climate System Model version 3 (CCSM3) from the US National Center for Atmospheric Research (NCAR). Previous model-proxy comparisons have shown that TraCE-21ka adequately represents key features of late Quaternary climate evolution (He et al., 2013; Liu et al., 2014; Lora et al., 2016; Shakun et al., 2012). Absolute monthly minimum temperature, maximum temperature, and mean precipitation were extracted from the TraCE-21ka climate simulation at 2.5° resolution for the period 20,000-0 yr BP at 80-year intervals taken in 100-year steps with PaleoView software (Fordham et al., 2017). The resulting gridded datasets were averaged to yield 1000-year means. The monthly climate data were used to generate 17 bioclimatic variables that are commonly used predictors in species distribution models (Hijmans et al., 2017). The bioclimatic data were then resampled without interpolation to a 0.25° resolution to increase the number of background points available for model validation. Climate data were masked with ice sheet extent layers based on modeled data from Gowan et al. (2016).

To our knowledge, the TraCE-21ka is the most appropriate climate dataset for the spatial and temporal scale of this study. This simulation has a unique combination of monthly temporal resolution through the past 21,000 years, including abrupt change events such as the Younger Dryas (YD), while also having sufficient spatial resolution to facilitate geographic comparisons with North American bison sites. The TraCE-21ka simulations using the CCSM3 model,

however, appear to underrepresent early to mid-Holocene aridity followed by a trend towards wetter conditions across much of NA, outside the southwestern United States, indicated by multiple empirical paleoclimate datasets (Liefert and Shuman, 2020; Shuman and Marsicek, 2016). This discrepancy between the TraCE-21ka simulation and empirical data is common to most paleoclimate model simulations, including up-to-date models with more complete ocean and sea-ice dynamics, atmospheric dust loading, and other relevant processes (e.g., Morrill et al., 2019; Sun et al., 2019). We consider this bias in the discussion and interpretation of results.

Model Description Analysis of the climate drivers of bison distribution was performed with MaxEnt, a software program that employs a machine-learning algorithm to estimate relationships between environmental variables and species occurrences (Elith et al., 2011; Phillips et al., 2016, 2006). MaxEnt uses spatially explicit environmental variables and species occurrence data to predict habitat suitability, which is expressed as predicted probability of occurrence on a scale of 0 to 1 (lowest to highest).

Variable Selection Initial models used to predict the distribution of bison data included 17 bioclimatic variables. Variable importance rankings were determined by counting how frequently a variable was assigned a given importance ranking (based on percent contribution) across all time intervals. When Pearson correlations between variables exceeded 0.8, the variable with more high rankings across time intervals was retained and the variable with lower rankings was dropped. The resulting 9 bioclimatic variables were selected for subsequent modeling and analysis. Variables used in final model selection are: mean temperature of the coldest quarter, temperature seasonality, mean temperature of the wettest quarter, mean temperature of the

warmest quarter, precipitation of the coldest quarter, precipitation seasonality, precipitation of the wettest quarter, precipitation of the warmest quarter, and precipitation of the driest month.

Model Evaluation To evaluate model performance, a random sample of 20% of bison observations was withheld and the remaining 80% of observations were retained for model training. 1000 background points were randomly selected from the climate data for cross-validation of the trained model against the withheld observations. Model performance of each MaxEnt run was evaluated with the area under the curve (AUC) statistic (Table 2.1). AUC is derived by plotting sensitivity (the proportion of positives that are correctly identified) versus 1 minus specificity (the proportion of negatives that are correctly identified) and quantifying the area under the curve. In other words, AUC is a measure of a model's success in predicting presences and absences. Models with an AUC of 1.0 perfectly differentiate between presences and absences, whereas an AUC of 0.5 indicates that a model performs no better than random chance.

Temporal Changes in Variable Importance The MaxEnt maximum entropy algorithm quantifies the relative contribution of an environmental predictor variable with a 'percent contribution' score. Percent contribution reflects how much a given variable improves regularized gain (model fit relative to a uniform distribution). To understand how the relative importance of variables changed over time, each predictor variable was assigned a rank corresponding to its percent contribution score (1: highest contribution; 7: lowest contribution) for each time interval. Changes in variable rank over time are interpreted as shifts in the fundamental climatological drivers of bison distribution.

Defining Bison Distribution The boundaries of the geographic distribution of bison were defined by imposing a threshold to convert predicted probabilities to binary presence/absence data (Fig. 2.4). The threshold is defined as the predicted probability value where model sensitivity and model specificity are equal. As such, threshold values varied across time intervals. Grid cells with predicted probabilities that exceeded the threshold were classified as presences and cells with values below were classified as absences. To characterize climatic conditions experienced by bison, changes in climate variables throughout the threshold-defined ranges of bison were summarized by medians and 25% and 75% quantiles (interquartile range: IQR). The distribution of climate variables throughout the ice-free landmass of North America were similarly summarized. Climate within the model-defined bison distribution was contrasted with the medians and IQRs of the continental North American climate (Fig. 2.5). Because IQRs do not span the entire range of each independent variable, it is possible for the IQR of the predicted bison distribution to fall entirely outside of the NA IQR.

Because bison distribution was modeled at the genus level, observations from late Pleistocene and early Holocene intervals included specimens originally ascribed to multiple bison taxa. In our analysis, we consider bison as part of a large, geographically variable meta-population on the basis of genetic and morphological evidence (Heintzman et al., 2016; Martin et al., 2018; Shapiro et al., 2004; Zver et al., 2021). While we do not attempt to define subpopulations and characterize niche variability between them, our results may be useful for identifying ecologically distinct subpopulations for future investigation.

Results

Climate and Patterns of Bison Distribution and Abundance

Analysis of the bison fossil record shows that the spatial distribution and density of bison populations have varied considerably since the LGM (Figs. 2.2 and 2.3). Millennial-scale changes in the distribution and abundance of bison were linked to climatic and environmental variability. During the LGM ca. 20-17 ka, the distribution of bison was widely scattered across NA into regional clusters, suggesting subpopulations were isolated into disjunct glacial refugia (Fig. 2.4). As post-glacial ecosystems developed, some regionally isolated subpopulations migrated and/or became extinct. By the late Holocene, the distribution of bison was largely spatially contiguous throughout the Great Plains and Intermountain West.

Based on the simulated climates of the last 20 ka, bison consistently inhabited places with warmer winters, summers, and wet seasons relative to the overall climate of the ice-free North American landmass. Within the climatic envelope where bison occurrences were most dense, Holocene temperature was slightly less seasonal, and precipitation was slightly more seasonal than the continent-wide climate. The geographic areas inhabited by bison experienced less seasonal variation in precipitation during the Holocene relative to the late Pleistocene due to declining winter precipitation and increasing summer precipitation during the Pleistocene-Holocene transition.

The simulated climatic envelope occupied by bison progressively narrowed since the LGM (Fig. 2.5). Interquartile ranges contracted for eight of the nine climate variables (mean temperature of the coldest quarter, temperature seasonality, mean temperature of the wettest quarter, mean temperature of the warmest quarter, precipitation of the coldest quarter,

precipitation seasonality, precipitation of the wettest quarter, and precipitation of the warmest quarter). For example, the bison distribution IQR for mean temperature of the coldest quarter was 10°C (16-6°C) at 20-19 ka, but it narrowed to 6.5°C (14.25-7.75°C) by 1-0 ka. Similarly, the precipitation of the coldest quarter IQR decreased from 8 cm (11-3 cm) to 2 cm (4-2 cm).

Variable importance for defining the distribution of bison varied over time. During the Bølling–Allerød Interstadial (BA) ca. 14.7-12.9 ka, as the range of temperatures encountered across NA increased, the distribution of bison shifted from primarily precipitation-limited to primarily temperature-limited (Fig. 2.5). Precipitation seasonality was the most important variable between 18-16 ka and mean temperature of the coldest quarter ranked first or second in relative importance between 14-0 ka. The predicted distributions of bison largely correspond to observed presences across all time intervals. The AUC evaluation metric suggests that the model achieved good differentiation ($AUC > 0.70$) between bison presences and absences across all time intervals, except 20-19 ka (AUC: 0.65), which only had 11 observations (Table 2.1). Model performance improved with more recent time intervals, partially due to a greater number of more recent bison observations and increasing spatial cohesion of bison sites over time.

During most thousand-year intervals, the distribution models show moderate predicted probabilities in Beringia despite the presence of multiple bison sites in the region. This is related to the strong influence of midcontinent bison sites on the model fit. As such, the models best represent the potential range of bison originating from south of the continental ice sheets. This result indicates that there are likely meaningful ecological differences between Beringian and southern bison populations that may explain limited north-to-south dispersal (Heintzman et al., 2016), a topic warranting further investigation.

Table 2.1. Summary of area under the curve (AUC), threshold value (sensitivity = specificity), count of observations used for model training, and count of background points for evaluation across all time intervals modeled.

Interval (ka)	AUC	Threshold (sensitivity = specificity)	Observations
20-19	0.65	0.63	11
19-18	0.81	0.47	18
18-17	0.76	0.55	20
17-16	0.76	0.61	24
16-15	0.79	0.57	23
15-14	0.74	0.58	27
14-13	0.73	0.56	58
13-12	0.84	0.54	85
12-11	0.79	0.65	70
11-10	0.80	0.54	73
10-9	0.82	0.59	55
9-8	0.86	0.57	64
8-7	0.87	0.54	78
7-6	0.87	0.54	69
6-5	0.86	0.54	78
5-4	0.91	0.39	93
4-3	0.88	0.47	160
3-2	0.89	0.55	208
2-1	0.88	0.62	360
1-0	0.87	0.63	722

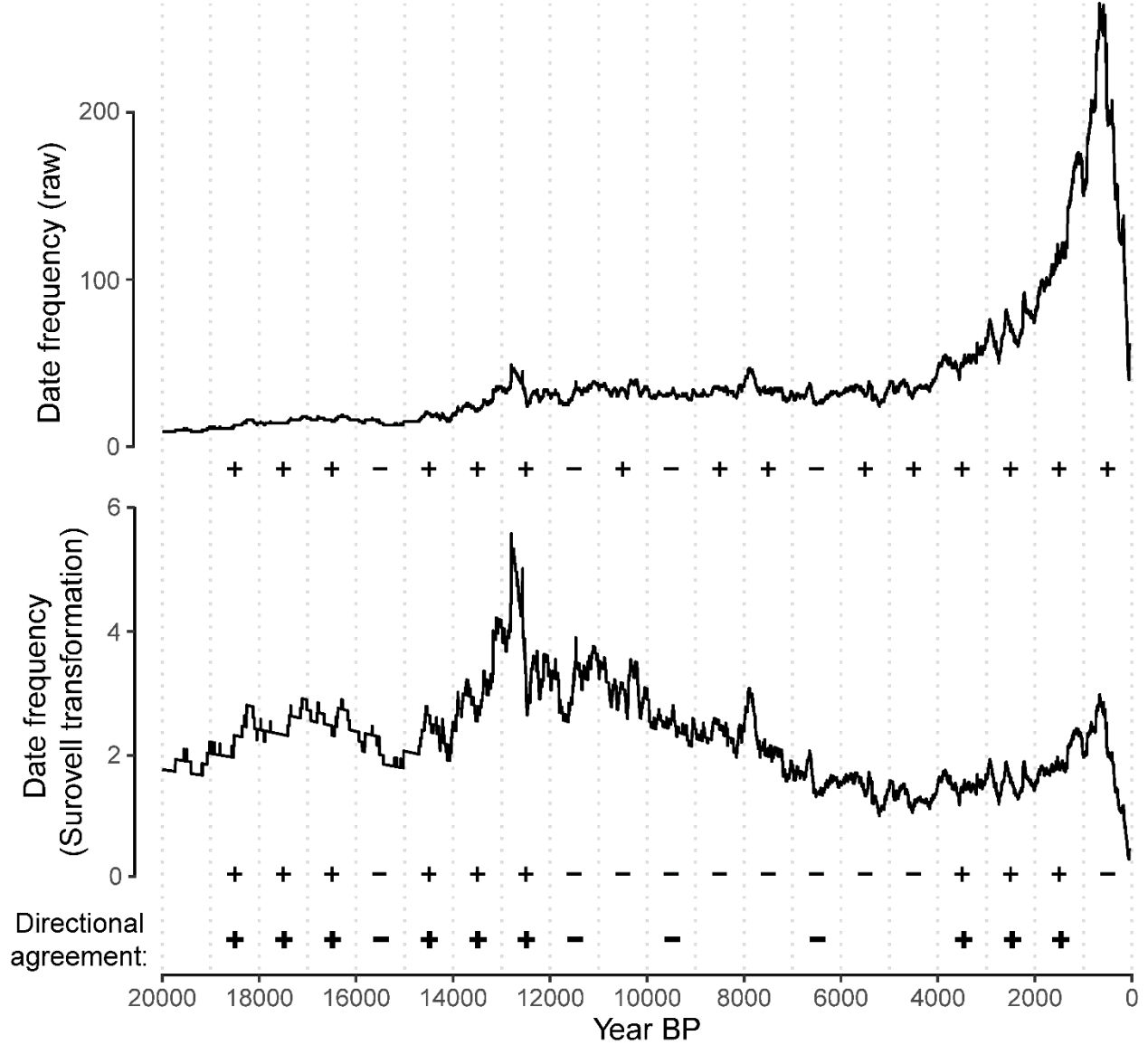


Figure 2.1. Raw (top) and transformed (middle, via Surovell et al. method) frequency distributions of bison observations in North America 20-0 ka. Signs indicate whether mean frequencies increased (+) or decreased (-) relative to the prior 1000 year interval (top and middle) and whether there is directional agreement between raw and corrected frequency datasets (bottom).

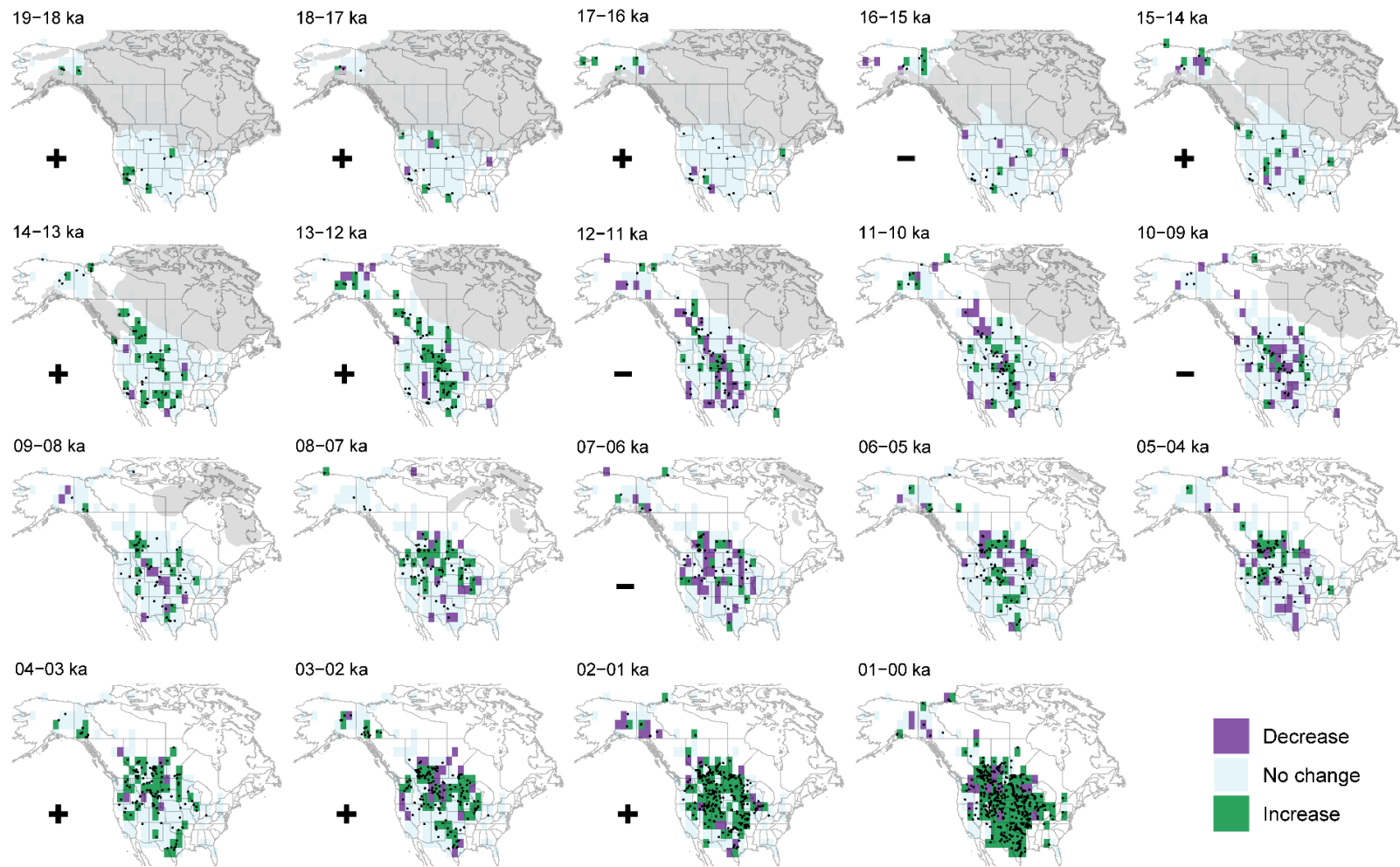


Figure. 2.2. Relative change in bison abundance based on raw bison site counts. The color of each $2.5^\circ \times 2.5^\circ$ grid cell indicates whether the number of bison sites (black dots) within the cell decreased (purple), did not change (light blue), or increased (green) relative to the preceding 1000-year interval. Ice sheet extent shown in gray (Gowan et al., 2016). Signs indicate directionality of agreement (positive: + or negative: -) between raw and corrected frequency datasets within each 1000-year interval.

Directionality of change: Bison sites

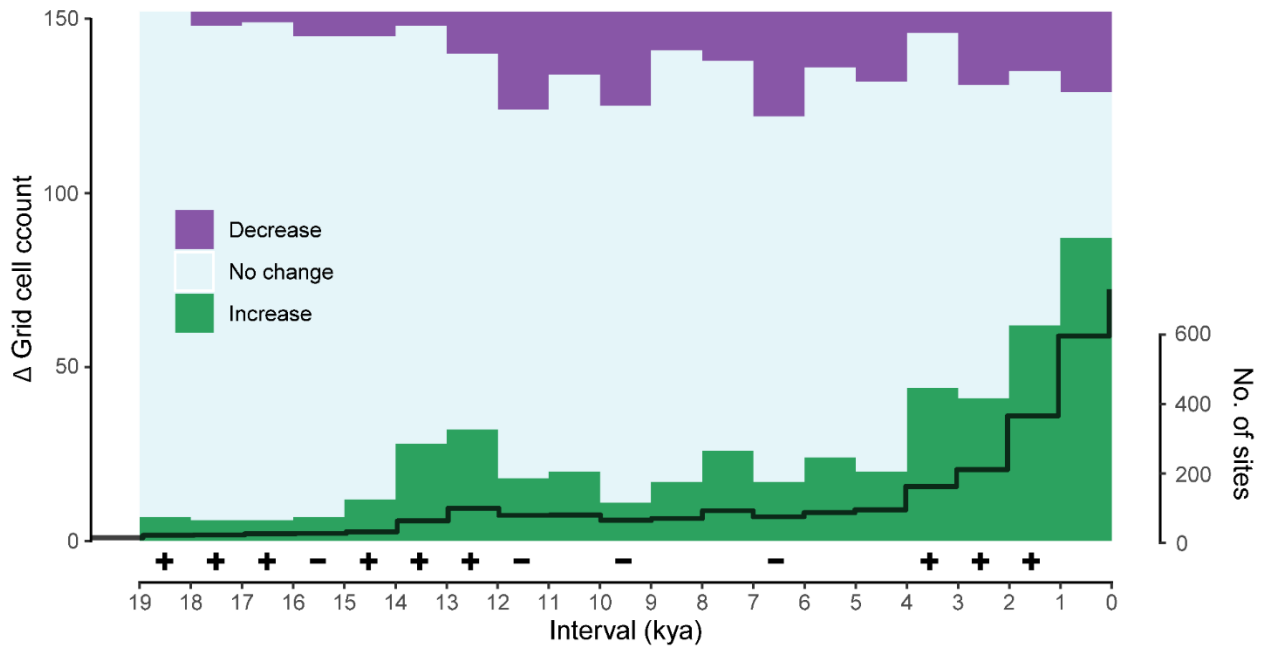


Figure. 2.3. Directionality of change in raw bison site counts (bars; left axis) and sums of site counts (black line; right axis) over the past 20,000 years. Cell count change reflects whether the number of bison sites within a given spatial grid cell ($2.5^\circ \times 2.5^\circ$) increased (green), did not change (gray), or decreased (purple) with respect to the prior 1000-year interval. Signs indicate directionality of agreement (positive: + or negative: -) between raw and corrected frequency datasets within each 1000-year interval.

Last Glacial Maximum (LGM): 20.0-14.7 ka

LGM bison localities are few in number but broadly distributed throughout much of ice-free NA. Precipitation seasonality best explains the 18-16 ka distribution of bison (percent contribution: 33-50%). Simulated precipitation seasonality across the bison range during this period exceeded the continental median and it ranks within the top three variables for the other LGM intervals. Between 19-14 ka simulated precipitation of the driest month was 0 cm and median precipitation of the warmest quarter ranged between 3-5 cm within the bison distribution. During the LGM, bison site turnover patterns were relatively minor and localized (Fig. 2.2). The absolute number of bison sites increased from 11 at 20-19 ka to 23 at 16-15 ka.

Bølling–Allerød Interstadial (BA): 14.7-12.9 ka

At 14 ka, mean temperature of the coldest quarter became the most important variable and maintained first or second importance rank among variables until present (percent contribution range: 17.0-66.5%). This shift in variable importance does not correspond to a substantial change in simulated mean temperature of the coldest quarter within the bison distribution. During the Bølling–Allerød Interstadial bison expanded northward into the ice-free corridor and additional bison observations appear in the southwestern United States and the western Great Plains. A substantial increase in sites and range extent took place at 14-13 ka. Predicted probabilities are highest in the southwestern United States, Idaho, and eastern Montana. At 14-13 ka, simulated median precipitation of the coldest quarter dropped to 3 cm and remained at or below this level to present.

Younger Dryas (YD): 12.9-11.7 ka

While portions of the North American ice-free land mass experienced a reversion to seasonally colder temperatures, simulated temperature changes within the reconstructed bison distribution varied by season. The simulated median mean temperature of the warmest quarter dropped from 33 °C to 31 °C, while the median mean temperature of the coldest quarter remained unchanged at 7 °C. At 13-12 ka, the modeled bison distribution spanned from northern Alberta to Mexico. Observations increased throughout a corridor that corresponds to the leeward side of the Rocky Mountains from Alaska to the Gulf of Mexico.

Early Holocene (EH): 11.7-8.0 ka

During the early Holocene, the predicted bison distribution area grew despite declining local abundances. Based on the TraCE-21ka simulation, early Holocene bison experienced warm summers and dry winters throughout their range. During this period, bison occurrences increased in west and central NA (Figs. 2.2 and 2.4). Increases primarily occurred within the Rocky Mountains and Great Plains regions. Widespread decreases in bison sites occurred at 12-11 ka and 10-9 ka, especially at the geographic perimeter of the bison distribution in southern, coastal, and low-elevation regions. Many sites in California, Nevada, Arizona, New Mexico, Utah, and Colorado cease recording bison presences during the early Holocene. A retraction of bison from the southwest during the early Holocene is also evident in the distribution models which predict the presence of bison in most of the southwest (excluding the Lower Colorado River Valley) until 9-8 ka, when bison became absent from the contemporary Mojave and Sonoran Deserts.

Mid-Holocene (MH): 8.0-4.0 ka

During the mid-Holocene, the predicted range of bison extended from northern British Columbia and Alberta to southern Texas and from the southern California coast to Iowa. This large mid-Holocene bison range coincides with low site counts (69 sites at 7-6 ka). These records suggest that continental population densities in the mid-Holocene were generally low relative to other time periods. Precipitation of the driest month is the second ranking variable between 9-6 ka (percent contribution: 18-20%) and precipitation of the coldest quarter ranks second in importance between 6-4 ka (percent contribution: 18-21%). Mid-Holocene bison distribution patterns are dynamic in the southern plains. At 5-4 ka, individual observations and the modeled bison distribution recede from Texas and significant portions of previously occupied areas of New Mexico, Oklahoma, Kansas, and Missouri.

Late Holocene (LH): 4.0-0.0 ka

Raw numbers of bison occurrences increased in the late Holocene more than any other period since the LGM. The number of bison sites rose dramatically from 160 to 722 between 4-0 ka (Table 2.1). Site increases between 4-1 ka likely reflect rising bison abundances, because the increases are detected after controlling for taphonomic effects on occurrences (Fig. 2.1). The predicted distribution area also reached its greatest extent at 4-3 ka (Appendix A Sup. Fig. 2.1). The predicted distribution of bison became more confined as the late Holocene progressed, but this change appears to be primarily driven by the increase of sites in the core of the distribution rather than site losses at the margins. Simulated temperatures in areas inhabited by bison rose throughout the late Holocene. The simulated median mean temperature of the coldest quarter in the bison distribution steadily increased and reached Holocene highs of 10 °C at 1-0 ka.

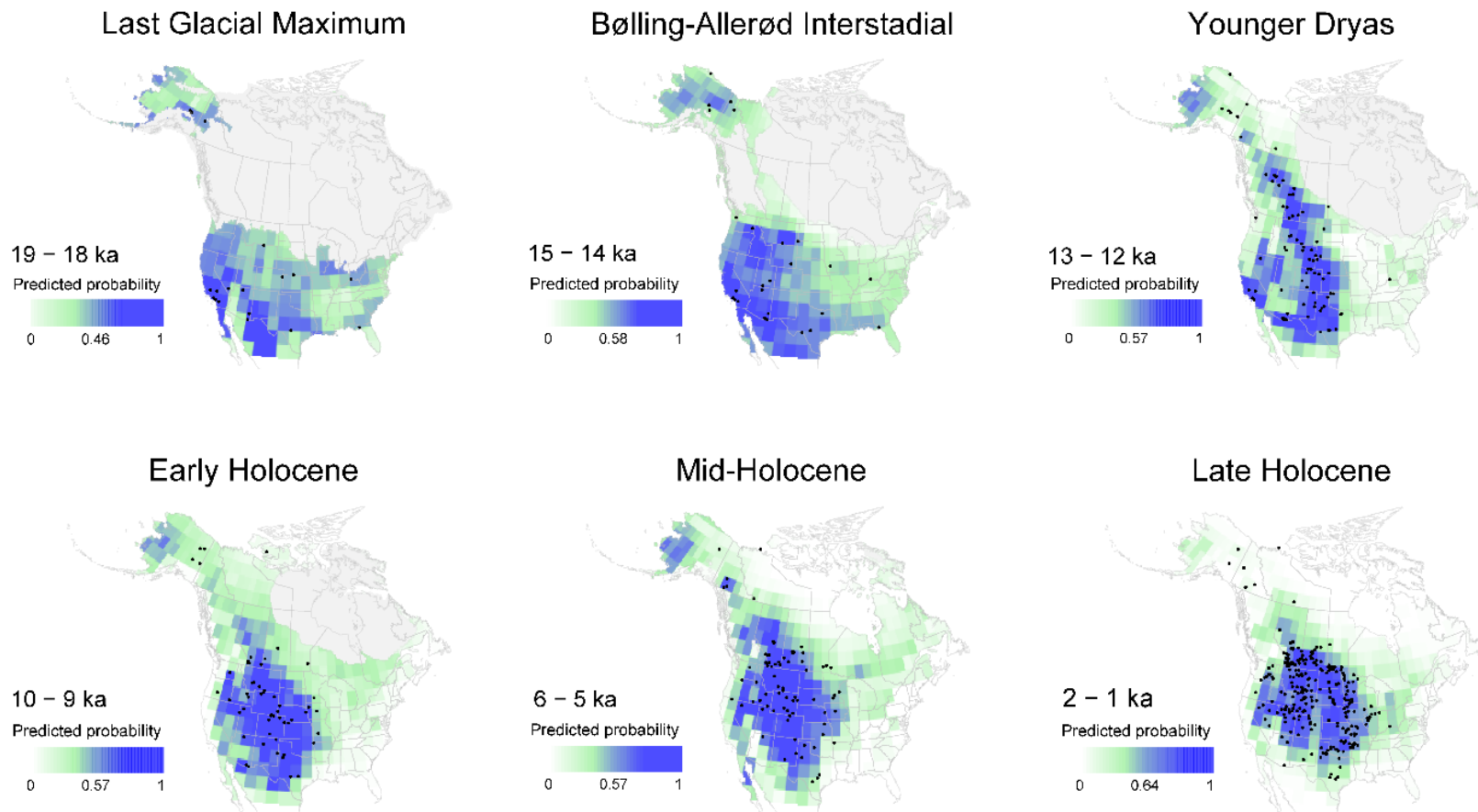


Figure. 2.4. Geographic representation of modeled bison distributions at key intervals between 20-0 ka. The middle number on each scale identifies the interval-specific predicted probability threshold for defining bison presences (blue) and absences (green and white). Observations (bison sites) shown as points (black). Ice sheet extent shown in gray (Gowan et al., 2016). All maps are available in the supplementary material.

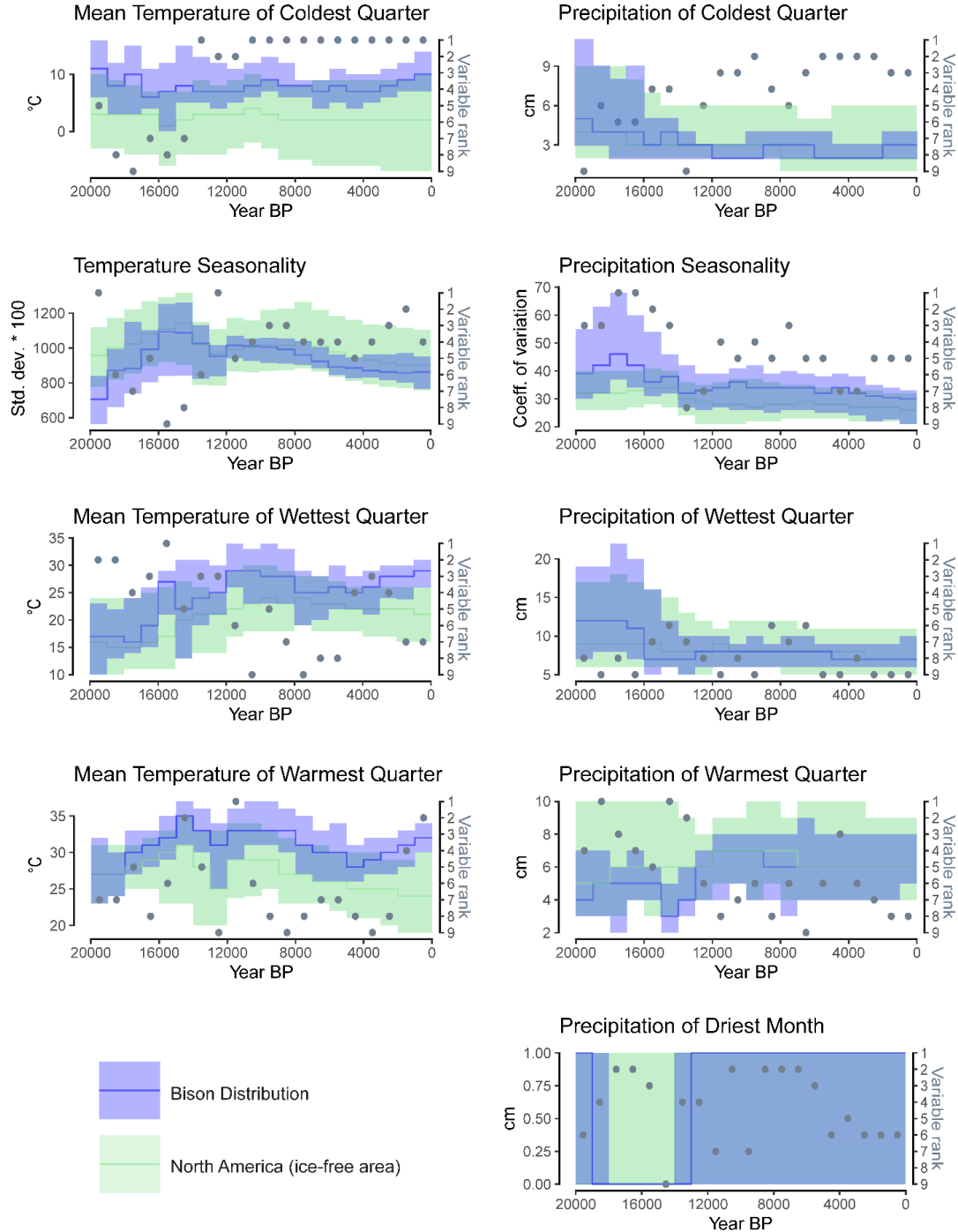


Figure. 2.5. Simulated evolution of climate conditions and variable rank for each 1000-year interval since 20 ka. The distributions of climate variables within the model-defined distribution of bison (blue) and North America minus ice-covered areas (green) are summarized with the median (line) and 1st and 3rd quartiles (IQR; shading). Variable rank (dots) reflects the ranking of the percent contribution score relative to the other climate variables (right axis) within a given interval.

Discussion

Our analysis of archaeological and paleontological bison assemblages reveals dynamic changes in bison distribution and abundance, and highlights linkages between these changes and environmental variability. Results suggest that late Quaternary changes in the distribution and abundance of bison were directly influenced by effects of large-scale climate and by biophysical and environmental changes (e.g., ice sheet recession, biome shifts including the expansion and contraction of grasslands, and changes in growing season length). Our results provide support for our hypotheses that: (H1) bison abundance in open habitats is positively correlated with moisture availability, and (H2) temperature changes and associated hydrothermal stress act as important controls on bison distribution.

Key Intervals of Change for Bison Populations

Pleistocene-Holocene Transition From the LGM to the beginning of the Holocene, the distribution of bison became increasingly widespread as populations dispersed from glacial refugia and expanded onto deglaciated lands. The Pleistocene-Holocene transition was a period of rapid climate change and dramatic ecological reorganization involving mass extinctions and drastic geographic range shifts. Despite the critical role that bison played as the most abundant large herbivore in NA since the LGM, changes in the abundance and distribution of bison and underlying climatic and environmental drivers are not well understood. Prior analyses of radiocarbon-dated bison fossils indicated that long-term bison abundance was relatively stable at the continental scale (McDonald, 1981; Scott, 2010). However, spatial patterns of bison occurrences reveal changes in abundance that reflect regional range shifts and extirpations. The first widespread decline in bison abundance occurred during the first millennium of the Holocene

(12-11 ka) when site losses are recorded throughout bison's entire distribution. Bison site turnover and regional distribution shifts indicate that bison were retreating from southern and southwestern NA and shifting to higher latitudes, especially to Alberta, Montana, and Wyoming. This elevated site turnover follows a genetic bottleneck observed ca. 15-13 ka (Heintzman et al., 2016). Between 16 ka and 8 ka the mean latitude of bison site observations increased from 43.9 °N to 46.7 °N and the mean elevation increased from 772 m to 1049 m (Fig. 2.6). This shift to higher latitudes and elevations coincides with the flattening of the latitudinal temperature gradient, rising summer insolation, recession of the Cordilleran and Laurentide Ice Sheets, and the expansion of grasslands across recently deglaciated landscapes (Grimm et al., 2011; Power et al., 2011; Williams et al., 2004).

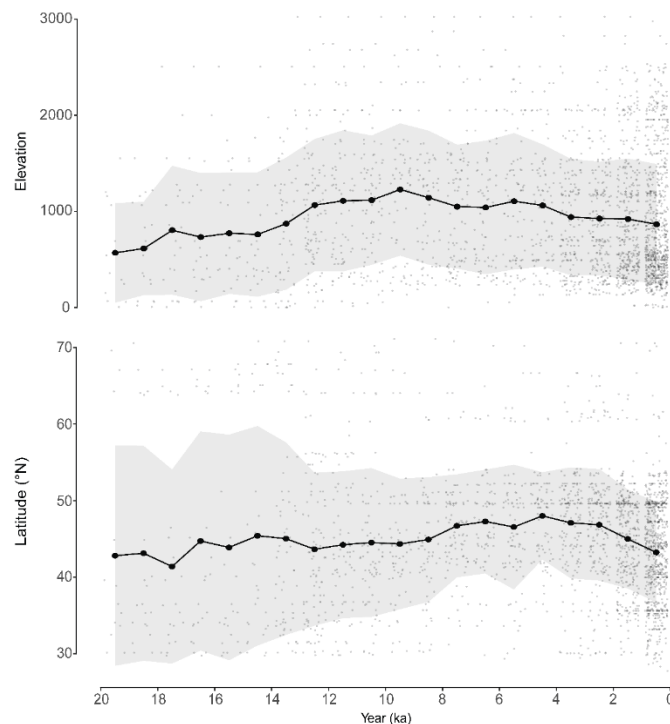


Figure. 2.6. Elevation (top) and latitude (bottom) of bison observations (small dots) across 1000-year intervals between 20-0 ka. Summarized by mean (large black dots) and standard deviation (gray shading).

Younger Dryas The long-term effects of Younger Dryas climate change on the distribution and abundance of bison were minor relative to the consequences of warming and drying trends that occurred through the Pleistocene-Holocene transition. Bison abundance generally increased throughout NA ca. 13-12 ka (Fig. 2.1) and bison observations increased substantially throughout portions of the western Great Plains and Rocky Mountains from Alaska to Texas (Fig. 2.2). The most notable YD distribution losses occurred along the Pacific Coast of northern California, Oregon, and Washington and in portions of the Intermountain West in Arizona, Utah, and Idaho (Fig. 2.4, Appendix A Sup. Fig. 2.1). Bison do not appear to have experienced a sustained, dramatic decline during the generally cooler YD. The median mean summer temperature in the bison distribution decreased by 2 °C, but model results show cooling temperatures explain only a small portion of changes in bison distribution at this time, suggesting climatic changes associated with the YD do not appear to have driven widespread bison declines.

Paleobiologists have remarked that it is not especially surprising that “Ice Age” bison survived a reversion to purportedly colder conditions during the YD (e.g., Fiedel and Haynes, 2004). However, paleoclimatic evidence suggests climatic conditions during the YD were spatially variable (Fastovich et al., 2020; Meltzer and Holliday, 2010). For example, multi-proxy temperature reconstructions reveal stable or warming temperature trends throughout the southeast United States (Fastovich et al., 2020) and northward advection of the warm southerly air masses combined with high summer insolation produced elevated summer temperatures in the continental interior (Shuman et al., 2002). Additionally, results from multiple climate simulations (including TraCE-21ka) show temperatures were warmer during the YD than the preceding Bølling-Allerød Interstadial in interior NA (Renssen, 2020). Our results provide little

evidence that bison experienced stress from declining temperatures during the YD, possibly because their geographic range was largely isolated from dramatic temperature drops that affected other regions. These findings have important implications for understanding organism response to current warming.

While bison persisted, other North American megafauna experienced extinctions between 14-11.5 ka (Broughton and Weitzel, 2018; Stewart et al., 2021; Widga et al., 2017). Indeed, in the late Pleistocene, several important changes took place: 1) multiple abrupt climate changes of different types impacted different portions of the continent (Fastovich et al., 2020; Meltzer and Holliday, 2010), 2) many animal species went extinct (Meltzer, 2020), and 3) Clovis hunters expanded across the continent which suggests changes in human use of ecosystems (Waters, 2019). The relationships among these changes are still unclear, but they mark a shift in the ecological context in which bison persisted for the remainder of the Pleistocene and Holocene. Consequently, the transient increase in bison abundance at this time (Fig. 2.1) could represent a release of bison from competition with other large grazers (e.g., horses, camels, mammoths, etc.) or a similar change in ecological dynamics after the extinction of other large herbivores.

Early and Mid-Holocene Through the early to mid-Holocene, bison experienced a series of regional declines in abundance, especially at range margins, resulting in the consolidation of bison presence toward the continental interior. The most substantial abundance declines took place 12-11 ka, 10-9 ka, and 7-6 ka (Fig. 2.1). Following the YD, continental climatic conditions were generally warm and dry (Fig. 2.5). Orbital changes that led to increasing summer insolation and recession of the Laurentide Ice Sheet resulted in increasingly warm and arid conditions throughout portions of the bison distribution as evidenced by dune and loess activity in the Great

Plains (Forman et al., 2008; Halfen and Johnson, 2013; Miao et al., 2007), increasingly open landscapes at grassland-forest ecotones in the Northern Rocky Mountains (Alt et al., 2018), grassland expansion at the eastern prairie peninsula (Nelson et al., 2006), and the continued recession of Great Basin pluvial lakes (Lyle et al., 2012; Reheis et al., 2014). Surface water was relatively scarce throughout the northern Great Plains. Many lakes in the region were significantly drawn down or completely desiccated (Donovan and Grimm, 2007; Filby et al., 2002; Schweger and Hickman, 1989; Smith et al., 2002). The timing of drying events varied by location (Liefert and Shuman, 2020), but by the mid-Holocene, bison had retracted from the southern, eastern, and western margins of their range (Fig. 2.4) towards higher latitudes and elevations (Fig. 2.6), which were presumably wetter and cooler. The number of sites recording bison during this interval increases in Rocky Mountains and portions of the Great Plains and decreases in southern and coastal NA. Early Holocene trends in bison skull morphology are indicative of a transition from “hook-and-roll” to “clash-and-release” dominance behavior (Widga, 2013). This behavioral shift possibly resulted from growing herd sizes and increasingly hierarchical social dominance hierarchies (Widga, 2013).

Late Holocene Through the late Holocene, bison abundances increased but bison distributions became more spatially confined to central NA. Over the course of the Holocene, changes in local to regional bison observations correspond closely with the timing and distribution of moisture availability. Rising lake levels coincide with increased bison observations throughout the Great Plains and Intermountain West between 4-1 ka (Fig. 2.2; Liefert and Shuman, 2020; Shuman and Serravezza, 2017). Bison abundances increase when winter precipitation increases during the late Holocene ca. 2-1 ka (Fig. 2.5). A trend towards

wetter conditions during the late Holocene would have resulted in reduced drought stress, more forage production, and improved water availability. The southward distribution shift between 4-0 ka may indicate that bison expanded south as northern latitudes experienced greater snowfall and drought eased in the south.

These results support the idea that late Holocene bison populations operated in a strong source-sink dynamic whereby bison source populations existed in the Great Plains and Intermountain West. We expect that hunting pressure would have exerted top-down pressure on bison abundance where climate conditions and habitat were marginal for bison. Although bison can persist in closed habitats, forest-dwelling populations were less numerous than those inhabiting open grasslands. Isotope and dental wear analysis suggest that during the late Holocene, forest-dwelling bison of the Ohio River Valley primarily consumed browse and occupied valley bottoms year-round (Widga, 2006). These behaviors may point to predator-avoidance strategies that have been observed in modern bison (Fortin et al., 2009; Widga, 2006). During the late Holocene, increasing Indigenous populations likely caused increased hunting pressure on bison, especially along the margins of the core bison distribution (Chaput et al., 2015; Chaput and Gajewski, 2016).

Regional Bison Abundance and Distribution Patterns

Northward Migration into the Ice-Free Corridor Bison distributions were disjunct before the opening of the ice-free corridor between the Laurentide and Cordilleran Ice Sheets. Bison expanded northward into the ice-free corridor by approximately 13.5 ka. The recession of the continental ice sheets and opening of the ice-free corridor facilitated the northward migration of the southern bison and subsequent genetic admixture of the Beringian and southern populations

(Heintzman et al., 2016). Phylogenetic evidence demonstrates that bison migrating into the ice-free corridor primarily originated from south of the ice sheets, as there was little southward gene flow from Beringian populations (Heintzman et al., 2016). In our study, distribution expansions associated with ice sheet recession are contiguous with the midcontinent bison distribution. The expanding midcontinent bison distribution reached its northern limit south of the Yukon. This northern limit is corroborated by evidence from mitochondrial DNA (Heintzman et al., 2016). Predicted probabilities of bison presence in the ice-free corridor are greatest between 13-12 ka, which agrees with the timing of gene flow between midcontinent and Beringian populations and inferred habitability of the corridor.

Bison Persistence in the Intermountain West The historical abundance and ecological role of large herds of herbivores in the Intermountain West has been a topic of interest among scientific and management communities for decades (Mack and Thompson, 1982; Perryman et al., 2021). According to Mack and Thompson (1982), the historical scarcity of large herbivores, and subsequent lack of evolutionary adaptation by grasses to grazing, has contributed to the apparent fragility of Great Basin ecosystems to domestic grazing. The results presented here demonstrate that while the late Quaternary distribution and abundance of bison did indeed fluctuate in response to changes in temperature and precipitation, bison herds were never completely absent from the Intermountain West during the last 20 thousand years. At millennial timescales, the climate-predicted distribution of bison consistently included most of the Intermountain West region. In agreement with previous studies, our results demonstrate that since the LGM, climate conditions throughout most of the region were suitable for bison. Declining bison observations in the Great Basin and southwestern United States between 14-8 ka

correspond to a major shift in regional hydroclimate. During this period, an intensifying moisture deficit, caused by rising summer insolation and northward migration of prevailing storm tracks, resulted in the widespread recession of intermountain pluvial lakes (Adams and Rhodes, 2019; Ibarra et al., 2014; Lyle et al., 2012; Reheis et al., 2014; Santi et al., 2019) and the expansion of semi-arid vegetation throughout the Intermountain West (Mensing et al., 2004; Nowak et al., 1994, 2017). Simultaneously, dominant open conifer woodland communities in southern New Mexico, Arizona, Nevada, and California were replaced by desert taxa (Thompson and Anderson, 2000). Bison became largely absent from much of the current extent of southwestern deserts by 8 ka, but they persisted in portions of the Great Basin and Colorado Plateau (Martin et al., 2017), and archaeological evidence points to bison reestablishment in the modern Chihuahuan Desert of northern Mexico and southern Texas, New Mexico, and Arizona ca. 2-0 ka (List et al., 2007).

Multiple sites record bison presences during periods when low abundances or absences have been previously inferred for the Great Basin. In fact, late Pleistocene bison site densities and predicted probabilities for the Great Basin are comparable to those of the Great Plains. The fossil record demonstrates that bison herds persisted during the late Quaternary throughout portions of the Great Basin (Grayson, 2006), Columbia Plateau (Chatters et al., 1995; Lyman, 2004; Lyman and Livingston, 1983), and Snake River Plain (Plew and Sundell, 2000). Grayson (2006) explored the distribution and abundance of bison in the Great Basin with a finer temporal resolution than our study and found that bison were most abundant in the northern and eastern portions of the Great Basin during the late Holocene. Similarly, several studies have demonstrated low artiodactyl abundances at Great Basin sites during the early and mid-Holocene

and increasing abundances beginning approximately 4 ka (Byers and Broughton, 2004; Durrant, 1970; Schmitt and Madsen, 2005). In a survey of dated bison specimens in eastern Washington, Lyman (2004) suggested that bison may have been completely extirpated from the region around 8 ka and scarce between 6-2.5 ka. However, extirpation seems unlikely since several bison fossils in eastern Washington date to this period. Additionally, in a review of the archaeological record of the Snake River Plain, Plew and Sundell (2000) demonstrated that bison herds were present and utilized by hunters throughout the Holocene. This evidence runs counter to claims that the Intermountain West historically lacked herds of large herbivores (e.g., Mack and Thompson, 1982).

Bison in Midcontinent North America Increasing bison observations and range expansions in central United States and south-central Canada coincide with well-documented eastward expansion of prairie assemblages at the grassland-forest ecotone beginning ca. 10 ka (McAndrews, 1966; Nelson et al., 2006; Williams et al., 2009; Wright et al., 1963). The fossil record documents the presence of resident bison herds that occupied habitats with varying degrees of openness across the grassland-forest gradient (Hill et al., 2014; Widga, 2014). Rapidly declining forest cover during the early Holocene is attributed to drying of the continental interior and associated fire-vegetation feedbacks (Williams et al., 2009). The persistence of grasslands in the prairie peninsula region after 6 ka, despite wetter conditions, highlights the role of disturbances such as fire in maintaining grassland systems (Anderson, 2006). While horning and rubbing can damage and kill a fraction of woody plants (Coppedge and Shaw, 1997), it is unlikely that these behaviors alone can prevent forest expansion.

A handful of additional records provide more detailed information on long-term local to regional trends in herbivore abundance and impacts in the North American continental interior (Fig. 2.7). Byers and Smith (2007) reconstructed Holocene trends in bison abundance from archaeological surveys of Wyoming Basin oil and gas fields. They quantified changes in large artiodactyl (bison and elk) fossil abundance in relation to the fossils of medium sized artiodactyls (deer, sheep, and pronghorn). The abundance of large artiodactyls was found to be positively correlated with moisture availability (Byers and Smith, 2007). Large artiodactyl abundance throughout the Wyoming Basin began to rise ca. 7 ka and reached a maximum at ca. 0.5 ka. Additionally, the Kettle Lake sedimentary record of *Selaginella densa*-type spores (a spikemoss) has been hypothesized to represent the impacts of herbivore populations on local vegetation in the paleoenvironmental record (Grimm et al., 2011). Today, *Selaginella densa* occurs throughout much of the northern Great Plains. In modern livestock grazing systems within the region, *S. densa* has responded positively to light grazing (Smoliak, 1965) and rotational grazing (Hubbard, 1951; Smoliak, 1960), but it can be reduced by high-intensity trampling (Coupland, 1950). A step-wise increase in *S. densa* at Kettle Lake ca. 0.9 ka corresponds to the initiation of a warm, dry episode (Shuman and Marsicek, 2016). Despite a return to cooler and wetter conditions regionally by 0.35 ka (Shuman and Marsicek, 2016), *S. densa* remained elevated, suggesting abundant bison (and other ungulates) may have facilitated the persistence of *S. densa* at Kettle Lake in spite of changing climatic conditions. *S. densa* then rose dramatically with the introduction of domestic livestock at 0.1 ka. The herbivore population changes shown by these independent records corroborate the coarse scale temporal patterns in our bison abundance dataset (Fig. 2.7).

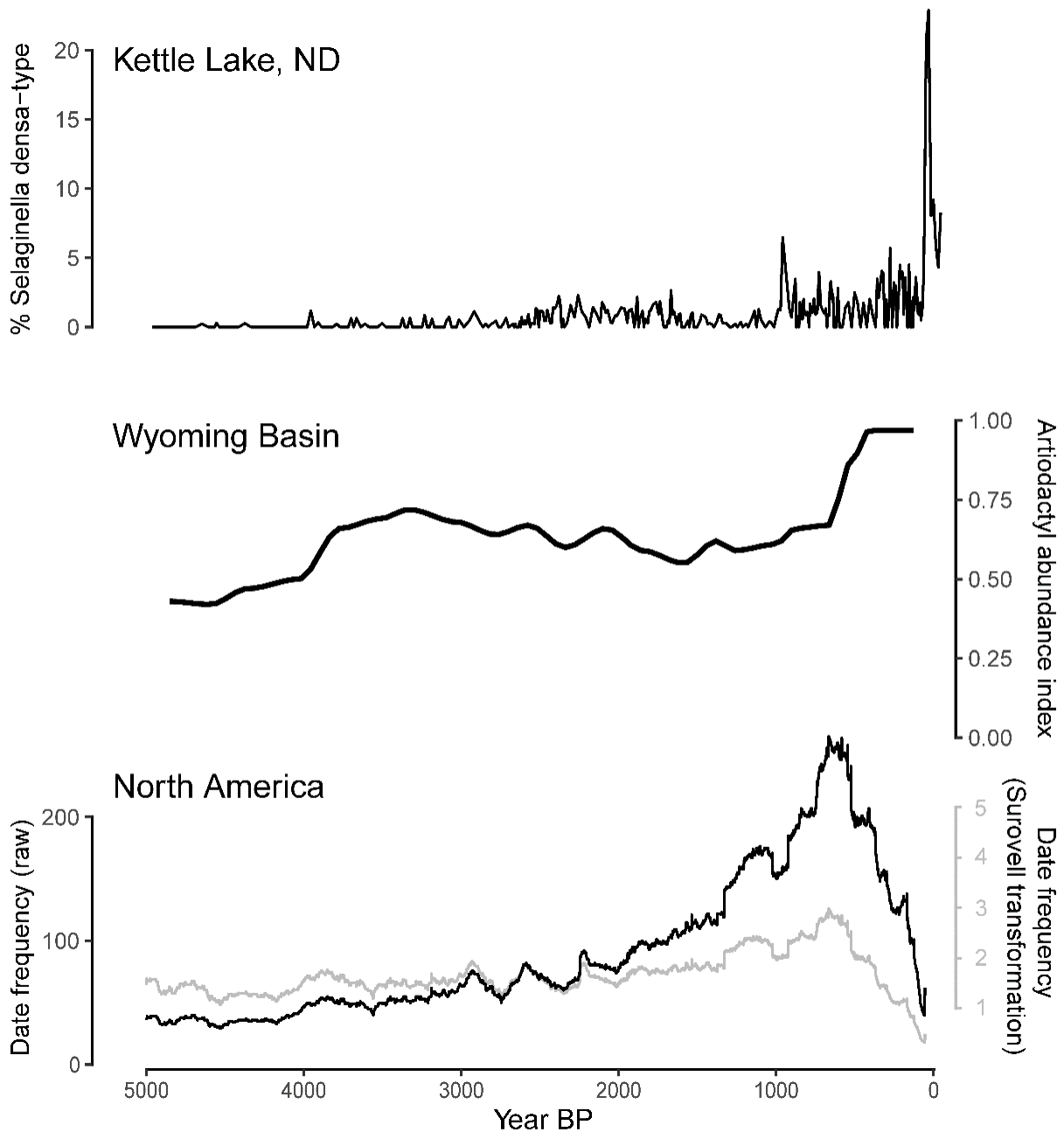


Figure. 2.7. Comparison of independent records of large herbivore abundance 5-0 ka. The abundance of *S. densa*-type spores (top) is expressed as a percentage relative to the terrestrial pollen sum of a given pollen subsample from Kettle Lake, ND (Grimm et al., 2011). The large artiodactyl index (center) represents the abundance of large artiodactyl fossils (elk or bison size) versus medium artiodactyls (deer, sheep, or pronghorn size) across archaeological surveys of Wyoming Basin oil & gas fields (Byers and Smith, 2007). Frequency of dated strata with bison fossils and directly dated fossils (bottom) from archaeological and paleontological studies throughout North America with raw (black) and transformed frequencies (gray).

Bison Adaptation: Evolution of the Bison Climate “Niche”

Since the Bølling–Allerød Interstadial, the modeled long-term distribution of bison was primarily controlled by the mean temperature of the coldest quarter (Fig. 2.5). The simulated median mean temperature of the wettest quarter and mean temperature of the warmest quarter within the bison distribution sharply diverged from the median continental temperatures ca. 18–17 ka (Fig. 2.5). From this point onward, bison continuously experienced temperatures exceeding the continental median. Hence, as temperatures rose, bison distributions shifted to higher latitudes and elevations (Fig. 2.6). These trends suggest that thermal stress applied considerable selective pressure, resulting in shifts in the distribution of late Quaternary bison populations.

Bison body mass has declined substantially since the LGM (Hill et al., 2008; Lyman, 2004; Martin et al., 2018). The most rapid body size loss occurred during the Pleistocene–Holocene transition when body size dropped by 26% over 3000 years (Martin et al., 2018). Researchers have debated the potential causes of this remarkable diminution. Proposed drivers have included human predation, forage quality and availability, predator avoidance, and thermal regulation. Together, sex, mean decadal temperature, and drought explain over 95% of decadal variance in body size of bison at Wind Cave National Park, South Dakota (Martin and Barboza, 2020b). Additionally, bison body size was found to be negatively correlated with global temperature anomalies derived from the GISP2 $\delta^{18}\text{O}$ ice core record at millennial timescales (Martin et al., 2018). The negative relationship between temperature and body size indicates that long-term diminution may be an evolutionary response to selective pressure exerted by rising temperatures throughout the late Pleistocene and early Holocene. The Heat Dissipation Limit (HDL) theory posits that the maximum energy expenditure of endothermic animals is limited by their ability to dissipate heat and avoid hyperthermia (Martin and Barboza, 2020a; Speakman and

Król, 2010). HDL theory thus predicts that when animals are limited by their capacity to dissipate heat, large-bodied individuals will be disadvantaged relative to smaller individuals, which possess a higher surface-to-volume ratio. Hence, warming temperatures, especially at the Pleistocene-Holocene transition, may have selected for smaller-bodied bison. We note that rapid bison diminution between 16-8 ka (Hill et al., 2008; Martin et al., 2018) coincides with the highest simulated summer temperatures within the bison distribution (Fig. 2.5).

Millennial-scale changes in bison abundance and distribution were also strongly influenced by hydroclimate dynamics. Elevated summer insolation drove pervasive drought conditions in midcontinent North America during the early to mid-Holocene (Shuman and Marsicek, 2016; Williams et al., 2010). The full severity of Holocene aridity in NA is not well captured by most climate models, including both the CCSM3 TraCE-21ka simulations used here (e.g., Befus et al., 2020) and updated generations of CMIP (Climate Model Intercomparison Project) mid-Holocene simulations (e.g., Morrill et al., 2019). Despite this bias in climate model output, patterns in bison occurrence frequencies (Figs. 2.1-2.3) parallel those in both time series (Shuman and Marsicek, 2016) and maps of NA hydroclimate (Liefert and Shuman, 2020). Between 12-6 ka, bison experienced multiple waves of abundance declines throughout much of their geographic distribution as reconstructed continental aridity intensified (Figs. 2.1-2.3). Subsequently, increasing moisture availability throughout midcontinent North America after 5 ka coincided with rising bison abundances throughout in the Great Plains and Intermountain West (Fig. 2.2). The observed relationship between hydroclimatic conditions favorable for increased abundance and availability of forage and growing bison populations aligns with archeological records that show an increased investment into the pursuit and procurement of bison and trade of

bison products by Indigenous populations in the late Holocene (Cooper, 2008; Roos et al., 2018; Zedeño et al., 2014). Sizable bison populations persisted until intensive harvest of bison in the 19th century led to steep declines. Historical documents describe vast herds throughout the continental interior in the 18th and 19th centuries. Scholarly estimates place Great Plains bison at ca. 30 million animals during this period (Flores, 1991; Isenberg, 2001; Lott and Greene, 2002).

From our distribution maps, modeled climate envelopes, and prior knowledge of past regional biome shifts, we conclude that bison populations persisted throughout a broad geographic range of NA since the LGM, and that the highest bison abundances were found in open temperate rangelands. Although historical distributions of biomes throughout most of western North America are poorly constrained, bison distribution shifts correspond to documented expansions and contractions of grassland and shrubland biomes, including, for example, the northward expansion of open rangelands into the previously glaciated ice-free corridor at 13-12 ka (bison range expansion), the aridification of the southwest through the early to mid-Holocene (bison range contraction), and the retreat of arboreal taxa at the forest-prairie ecotone along the northern and eastern margins of the Great Plains beginning at ca. 10 ka (bison range expansion). Additionally, hydroclimatic conditions appear to act as a strong control on bison abundance in open rangelands. While bison can incorporate woody vegetation into their diet and even subsist on browse, grassy habitats support the greatest bison populations and potential population growth. Perhaps the most striking evidence of bison abundance responding to climate-driven changes in forage production is found in the widespread increases in bison abundance throughout the rangelands of the Great Plains and Intermountain West during the

relatively wet late Holocene. This underscores the important influence of climate and climate-vegetation feedbacks on bison distributions at large spatiotemporal scales.

Conclusions

Over the past 20 thousand years, bison experienced dramatic environmental changes that shaped their distribution, morphology, behavior, and population dynamics. During the early deglacial period, bison were geographically widespread, yet fragmented into regional glacial refugia. Though large populations of most North American megafauna did not persist beyond the YD, bison survived and exhibited remarkable stability. As temperatures warmed and precipitation declined at the Pleistocene-Holocene transition, bison abundances declined in southern and low-lying regions, and populations shifted northward and upslope. With easing drought conditions in the late Holocene, increased forage production supported increasing bison populations throughout the continental interior. Late Holocene bison populations continued to increase until just recently, when 19th century market hunting led to the near extinction of bison from North America (Isenberg, 2001).

Our distribution modeling approach demonstrates that bison continuously inhabited significant portions of the Great Plains and Intermountain West since the LGM. Bison populations advanced and contracted in response to climate warming and cooling and changes in hydroclimatic conditions that influenced the quality and availability of forage. Our results highlight the remarkable adaptability of bison to a wide range of climatic and ecosystem conditions and support the premise that modern bison are unique in some ways from their Pleistocene ancestors. The climate envelope occupied by Pleistocene bison was different from the climate experienced by anatomically modern bison during the late Holocene.

Understanding the causes of past extinctions will require accurate reconstructions of the environmental conditions experienced by individual species. Our approach can be applied to other species of Pleistocene megafauna to characterize pre-extinction climate envelopes to understand the species-specific environmental conditions experienced before and during extinction.

A number of tribal entities are leading efforts to restore bison to North American landscapes to reinvigorate important cultural lifeways linked to bison. Results from this research provide important context for these efforts by identifying climatic conditions that pose opportunities and challenges for bison reintroduction. Today, bison face risks from constrained mobility, geographic isolation of herds, habitat loss, artificial selection for nonadaptive traits, inbreeding depression, reduced fitness from cattle introgression, competition with other herbivores, and other sources (Halbert and Derr, 2007; Hedrick, 2009; Martin et al., 2021). These risk factors may reduce bison capacity to adapt to rapid environmental changes in the future. Because the current distribution of bison has been greatly reduced from its historic extent and is highly influenced by human interventions, conservation planning for the establishment of new protected areas or identification of at-risk populations can leverage distribution models trained on bison occurrences in archaeological and paleontological records.

Acknowledgements

We thank Cathy Whitlock, Mio Alt, Buzz Nanavati, Christopher Schiller, and Wolfgang Traylor for their helpful input on early figures. We also thank Jeff Martin and an anonymous reviewer whose feedback substantially improved the manuscript. Data were obtained from the Neotoma Paleoecology Database (<http://www.neotomadb.org>), its constituent database

FAUNMAP, and the Canadian Archaeological Radiocarbon Database

(<https://www.canadianarchaeology.ca>). The work of data contributors, data stewards, and the Neotoma and CARD communities is gratefully acknowledged. This work was supported by a Joint Fire Science Program Graduate Research Innovation grant 19-1-01-30 to J.A.F.W. and D.B.M. and National Science Foundation grant BCS-1832486 to D.B.M.

CHAPTER THREE

PAST AND PRESENT BIOMASS CONSUMPTION BY HERBIVORES AND FIRE ACROSS
PRODUCTIVITY GRADIENTS IN NORTH AMERICA

Contributions of Authors and Co-Authors

Manuscript in Chapter 3

Author: John A.F. Wendt

Contribution: Conceptualization, data curation, formal analysis, funding acquisition, investigation, methodology, visualization, writing – original draft, and writing – review and editing.

Co-Author: David B. McWethy

Contribution: Conceptualization, funding acquisition, supervision, investigation, writing – original draft, and writing – review and editing.

Co-Author: Gareth P. Hempson

Contribution: Investigation, methodology, visualization, and writing – review and editing.

Co-Author: E.N. Jack Brookshire

Contribution: Investigation and writing – review and editing.

Co-Author: Samuel D. Fuhlendorf

Contribution: Investigation and writing – review and editing.

Manuscript Information

John A.F. Wendt, David B. McWethy, Gareth P. Hempson, E.N. Jack Brookshire, Samuel D. Fuhlendorf

Environmental Research Letters

Status of Manuscript

- Prepared for submission to a peer-reviewed journal
- Officially submitted to a peer-reviewed journal
- Accepted by a peer-reviewed journal
- Published in a peer-reviewed journal

Volume 18, IOP Publishing

<https://doi.org/10.1088/1748-9326/ad0ad0>

CHAPTER THREE

PAST AND PRESENT BIOMASS CONSUMPTION BY HERBIVORES AND FIRE ACROSS
PRODUCTIVITY GRADIENTS IN NORTH AMERICAAbstract

Herbivores and fire are important consumers of plant biomass that influence vegetation structure, nutrient cycling, and biodiversity globally. Departures from historic biomass consumption patterns due to wild herbivore losses, livestock proliferation, and altered fire regimes can have critical ecological consequences. We set out to (i) understand how consumer dominance and prevalence responded to spatial and temporal moisture gradients in Holocene North America and (ii) examine how past and present consumer dominance patterns in North America compare to less altered consumer regimes of modern Sub-Saharan Africa. We developed long-term records of bison abundance and biomass burning in Holocene midcontinent North America and compared these records to reconstructions of moisture availability and vegetation structure. We used these reconstructions to characterize bison and fire prevalence across associated moisture and vegetation gradients. We found that bison herbivory dominated biomass consumption in dry settings whereas fire dominated in wetter environments. Historical distributions of herbivory and burning in midcontinent North America resemble those of contemporary Sub-Saharan Africa, suggesting disturbance feedbacks and interactions regulate long-term consumer dynamics. Comparisons of consumer dynamics in contemporary North America with Holocene North America and Sub-Saharan Africa also reveal that fire is

functionally absent from regions where it was once common, with profound ecological implications.

Introduction

Biomass consumption by herbivores and fire has shaped vegetation structure and composition, and the distribution of terrestrial biomes on Earth for millions of years (Bond and Scott, 2010; Charles-Dominique et al., 2016). From the extinction of most Pleistocene megafauna to the introduction of Old World livestock, bison (*Bison spp.*) were the dominant large herbivore in many of North America's grasslands, woodlands, and savannas (Wendt et al., 2022). The activities of tens of millions of bison contributed to large-scale biomass consumption and turnover, nutrient redistribution, and direct disturbance of hundreds of millions of hectares (Knapp et al., 1999; Nickell et al., 2018). Bison abundance and distribution were influenced by climate, which shaped the quantity, quality, and type of forage as well as interspecific competition and predation dynamics (Wendt et al., 2022). Fire activity and fire regimes were similarly shaped by variations in climate, fuel type, availability and condition, as well as local edaphic and topographic features (Bond and Keeley, 2005; Schoennagel et al., 2004; Whitlock et al., 2010). Additionally, after arriving in the Americas over 21k years ago (Bennett et al., 2021; Pigati et al., 2023), humans played an important role in modifying the distribution of fire and herbivore 'consumer regimes', by regulating the frequency, timing, and extent of both fire, via intentional burning, and herbivory, via management of wild and domestic herbivores (Nowacki et al., 2012; Roos et al., 2018). Beginning with the introduction of cattle by Europeans in the 16th century (Delsol et al., 2023; Rouse, 1977), intensively managed and spatially constrained domestic livestock production systems have largely replaced free roaming herds of large

herbivores in North America. Acknowledgement of widespread ecological impacts caused by altered fire patterns and herbivore communities has prompted calls for and motivated initiatives aimed at restoring ancient consumer regimes (Fuhlendorf et al., 2009; Lorimer et al., 2015). Yet, the extent to which North American consumer regimes have been altered and the ecological consequences of these transitions remain surprisingly poorly understood, primarily due to the lack of long-term records of domestic and wild herbivore abundance and impacts.

Linking fossil-based reconstructions of past bison abundance with sediment charcoal records of burning provides new opportunities to evaluate past biomass consumption by large herbivores and fire (Wendt et al., 2022). However, understanding historical and current consumer dynamics in North America is challenging due to recent ecological transformations caused by the removal of large wild herbivore populations, the establishment of modern livestock production systems, fire suppression, and the replacement of native plant assemblages with cropland. In contrast to contemporary North America, Sub-Saharan Africa has retained large, extensive populations of wild herbivores and fire activity is relatively unconstrained by fire suppression. The distribution and drivers of African consumer regimes thus provide a valuable ecological model against which the changes and consequences of anthropogenic ecosystem transformation in North America can be assessed (Archibald and Hempson, 2016; Gill, 2015). Reconstructing historic consumer prevalence and comparing consumer dynamics with a more intact system is an important step toward revealing the processes that influenced the evolution and persistence of North American ecosystems, and for understanding the implications of human-modified consumer regimes for nutrient cycling, soil development, biodiversity, and ecosystem change.

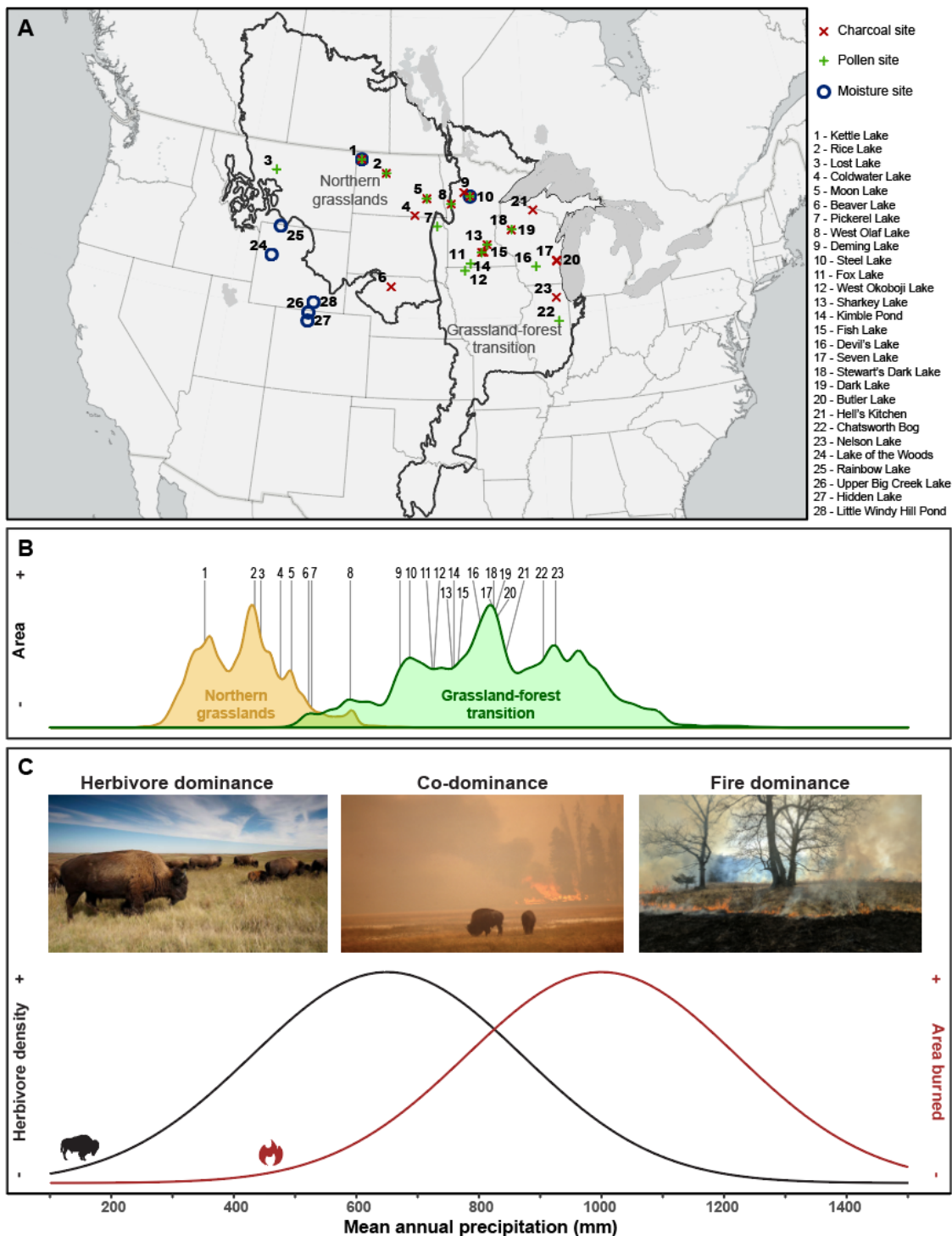


Figure 3.1. Map of study region and sites, with charcoal, pollen, and moisture records (panel A), distribution of study regions and paleoenvironmental sites across the midcontinent moisture gradient in North America (panel B), and conceptual diagram of predicted proportion of biomass consumed by herbivores (black line) or fire (red line) across a precipitation gradient (panel C). Panel B shows the current density distribution of area at a given moisture value for the northern

grasslands (NG; yellow) and the grassland-forest transition (GFT; green), with pollen and charcoal sites labeled. Dominant consumer modes are expected to vary across the moisture gradient (panel C). Herbivore density (black line), area burned (red line) curves in panel C represent hypothesized consumer dominance patterns in North America based on empirical data for Sub-Saharan Africa from Archibald and Hempson (2016).

The relative dominance of fire and herbivores as biomass consumers varies across abiotic and biotic gradients and is influenced by a set of interacting drivers that include climate, vegetation, soil, regional evolutionary histories, consumer interactions, and human activities. While the relative proportion of biomass consumption by herbivores and fire spans a continuum, data suggest there are three general consumer modes that occur in terrestrial ecosystems: herbivore dominance, fire dominance, and co-dominance (Archibald and Hempson 2016; Fig. 3.1 C). These modes reflect general outcomes of competition between herbivores and fire across moisture/vegetation production gradients at large spatiotemporal scales. Climate controls primary production by influencing precipitation, solar radiation, and temperature. While fire and/or herbivory are present in most systems, the relative dominance of either is strongly influenced by moisture availability and related vegetation/fuel characteristics (Archibald and Hempson, 2016; Hempson et al., 2019; Whitlock et al., 2010). In dry ecosystems, where forage is available, but fire spread is usually limited by discontinuous fuels, herbivores are expected to consume more biomass than fire (Archibald and Hempson 2016; see 'herbivore dominance' in Fig. 3.1 C). Conversely, fire is expected to consume more biomass than herbivores in wetter ecosystems where biomass is abundant but less palatable and/or less accessible to herbivores (Archibald and Hempson 2016, Hempson *et al* 2019; see 'fire dominance' in Fig. 3.1 C). At intermediate moisture levels both fire and herbivores can consume large quantities of vegetation (Archibald and Hempson 2016; see co-dominance in Fig. 3.1 C). These intermediate moisture

zones have the greatest potential for synergistic fire-herbivore interactions, exemplified by pyric herbivory (fire-driven grazing) and managed patch-burn grazing (Allred et al., 2011; Archibald et al., 2005; Fuhlendorf and Engle, 2004), as well as competitive exclusion via positive feedbacks with functionally distinct grass communities (Hempson et al., 2019). In addition, human activity can dramatically alter biomass consumption patterns resulting in more or less fire or herbivory than expected based on the influence of climate alone (Hempson et al., 2017; McWethy et al., 2013). Herbivory and fire are dynamic processes that vary across space and time. As a result, modes of biomass consumption are scale dependent (Spitz et al., 2018; Whitlock et al., 2010).

Our overarching hypothesis is, at large spatial (regional to continental) and temporal (centennial to millennial) scales, consumer dominance in temperate North America is primarily driven by the bottom-up effects of moisture availability on primary production, as well as the type, continuity, and structure of vegetation available for herbivores and fire. We predict that biomass consumption was mainly driven by herbivores in open arid and semi-arid environments, while fire dominated biomass consumption in closed mesic and humid environments of Holocene midcontinent North America. Although challenging to directly test, we evaluate this prediction by integrating paleoecological records of climate, vegetation, and fire with paleontological and archaeological records of bison from two regions that span the North American midcontinent moisture gradient (northern grasslands [NG] and grassland-forest transition [GFT]). This approach allows us to assess spatiotemporal changes in biomass consumption by fire and herbivores over the past 10k years, and to characterize likely historic consumer regimes in North America (see Fig. 3.1). We then compare modern herbivore and fire

patterns in Sub-Saharan Africa and North America to determine whether historic North American consumer regimes resemble consumer dynamics in a less altered continent. Contemporary data from Sub-Saharan Africa provide critical context for understanding general fire-herbivore interactions and biomass consumption patterns in other locations and time periods. Finally, we utilize continent-scale data on livestock populations and fire occurrences to identify differences between historic and modern consumer regimes in North America and consider the implications for ecosystem dynamics.

Methods

Reconstructing Modes of Herbivory and Fire

Improved understanding of long-term consumer interactions and impacts requires the integration of long-term records of burning and herbivore abundance. Recent advancements in laboratory and statistical charcoal analyses have improved our understanding of the role of fire in long-term ecological dynamics (Higuera et al., 2009; Whitlock and Larsen, 2001). However, methods for reconstructing herbivore abundance have lagged. As a result, it has been difficult to quantify abundances and subsequent ecological effects of ancient herbivores. We set out to address this problem by leveraging databases and new analytical techniques for radiocarbon dates to reconstruct regional-scale records of bison abundance. All following statistical and geospatial analyses were performed with R software (v. 4.1.3) in RStudio (Posit team, 2023; R Core Team, 2022). All ages presented in this paper are calibrated with the Intcal20 curve (Reimer et al., 2020) and are given as calendar years before present (cal yr BP).

Bison Abundance

Holocene reconstructions of regional bison abundance were developed using data and methods from Wendt et al. (2022). Bison observations are defined as archaeological or paleontological sites containing at least one bison fossil. Bison observations were extracted and classified by study region (NG or GFT). The frequency distributions of bison observations over time were transformed according to the transformation presented in Surovell *et al* (2009) to account for progressive site loss with time. The GFT frequency distribution was multiplied by the ratio of the area of the NG to the area of the GFT (1.31) to account for the area difference.

Charcoal

Charcoal data were accessed from the Global Paleofire Database (Appendix B Sup. Table 3.2). Age models were not modified from original database submissions. Charcoal data were converted from concentrations (particles cm^{-3}) to influx values (particles $\text{cm}^{-2} \text{yr}^{-1}$) and standardized using methods described in Power *et al* (2010).

Pollen

Pollen data were retrieved from the Neotoma Paleoecology Database (NPD; Appendix B Sup. Table 3.3). Updated chronologies were used, if available. Classification of arboreal and non-arboreal taxa was based on 'Ecological Group' classification in the NPD. Trees and shrubs were categorized as arboreal pollen (AP) and upland herbs were classified as non-arboreal pollen (NAP). AP:NAP ratios were calculated for each site and averaged to characterize the relative dominance of woody versus herbaceous species and provide information about vegetation structure and fuel characteristics.

Study Regions

Study regions definitions were based on ecoregion boundaries from WWF Terrestrial Ecoregions of the World (Olson *et al* 2001; Fig. 3.1 A). The Northern Grasslands (NG) region includes Canadian Aspen Forests and Parklands, Northern Mixed Grasslands, Northern Tall Grasslands, Northern Short Grasslands, Montana Valley and Foothill Grasslands, and Nebraska Sand Hills Mixed Grasslands. Small, forest-dominated areas within the geographic boundaries of the broader northern grassland ecoregion were included in the NG. These include Mid-Continental Canadian Forests and South-Central Rockies Forest. The Grassland-Forest Transition (GFT) region is defined as Western Great Lakes Forests, Upper Midwest Forest-Savanna Transition, Central Tall Grasslands, and Central Forest-Grasslands Transition.

Although midcontinent North America and Sub-Saharan Africa differ in terms of species composition and certain biophysical conditions (e.g., soils, geology, temperature, seasonality), these regions span similar precipitation gradients and manifest similar biomes including grasslands, woodlands, and dry forests. Midcontinent North America is generally characterized by high temperature seasonality, with freezing winter temperatures ($< 0\text{ }^{\circ}\text{C}$), while Sub-Saharan is very climatologically diverse, with warmer annual temperatures and growing season primarily driven by precipitation seasonality. The range of mean annual precipitation (MAP) in the NG (250-600 mm) corresponds to herbivore dominance in Sub-Saharan Africa (Fig. 3.1 C) and MAP in the GFT (350-1150 mm) spans the range from herbivore dominance to fire dominance in Sub-Saharan Africa (Fig 3.1 C).

Regional Composites

Bison, charcoal, and pollen records were interpolated to 1-year steps, and then binned and summarized at 50-year intervals. Bootstrapped mean estimates and 95% confidence intervals were calculated for each interval (1000 iterations with replacement). Proxy record means and confidence intervals were summarized (Fig. 3.2) by fitting local polynomial regressions (loess; window = 2925 yr).

Holocene Hydroclimatic Phases of Midcontinent North America

We used a multiproxy approach to describe general moisture trends and phases between 9-0.5k yr BP in midcontinent North America. The selected geophysical and geochemical records reflect long-term moisture availability trends with decadal- to millennial-scale variability and centennial- to decadal-resolutions (Appendix B Supplementary Fig. 3.2; Appendix B Sup. Table 3.1).

The mineral composition of Kettle Lake sediments reflects changes in local water availability. Aragonite is deposited via groundwater flow while other minerals (quartz, calcite, dolomite, and gypsum) are primarily aeolian dust (Grimm et al., 2011). High percent aragonite at Kettle Lake is interpreted as an indicator of elevated groundwater flows, while low aragonite indicates drought. Sand dune activity in the Nebraska Sand Hills is inferred from compiled luminescence dates (Appendix B Sup. Table 3.5). Luminescence dates reflect elevated upland dune activity and are interpreted as evidence for drought conditions. Luminescence dates indicate sediment burial, and thus constrain the timing of dune stabilization, meaning the timing of dune activation is less certain.

Declining lake levels in the Rocky Mountains, low groundwater flows at Kettle Lake, persistent dune activity, and high dust influx at Steel Lake indicate broadly dry conditions in midcontinent North America between 9-6k yr BP. Moisture availability generally increased between 6-4k yr BP, but two periods of low groundwater flows at Kettle Lake indicate some sub-regional variability during this period. Between 4-1.5k yr BP, most records suggest generally wet conditions, with few severe droughts, but multiple upland dune activations may reflect periods of sub-regional aridity. While lake levels remained stable or rose between 1.5-0.5k yr BP, other records show evidence of multiple severe droughts at lower elevations to the east.

Maximum aridity progressed across a longitudinal gradient, with peak dry conditions occurring earlier in the east and later in the west (Nelson and Hu, 2008; Wright et al., 2004). Dust influx at Steel Lake was greatest at ~8k yr BP, peak dune activity in the Nebraska Sand Hills occurred between 8.5-7.2k yr BP, Kettle Lake experienced repeated episodes of low groundwater flows between 8.2-7k yr BP, and Rocky Mountain lakes levels were lowest between 6.5-6k yr BP.

Spatial Analyses of Modern Fire and Herbivory

Data on fire and herbivory in North America were collected and processed following methods of Archibald and Hempson (2016) to facilitate inter-continent comparisons. Data on area burned, herbivore density, dry matter consumed, and proportion of dry matter consumed for Sub-Saharan Africa are from Archibald and Hempson (2016).

Fire and herbivory data for modern North America were collected and processed as follows. Precipitation data was extracted from the WorldClim2 gridded 30s mean monthly precipitation product for North America 1970-2000 (Fick and Hijmans, 2017). Monthly

precipitation rasters were summed to produce an average annual precipitation dataset. Monthly area burned and dry matter consumed by fire for 1997-2015 were extracted from Global Fire Emissions Data (GFEDv4; 50). This is a satellite-based product that includes but does not differentiate anthropogenic and natural wildfires and prescribed burns. Annual totals and medians for area burned and dry matter (biomass) consumed were then calculated.

All variables related to livestock consumption (dry matter consumed, livestock mass density) were derived from census-based livestock population data which include high-density feedlots, intensive pasture-based systems, and extensive rangeland-based systems. Spatial livestock population data were extracted from the Gridded Livestock of the World 3 (GLW 3) dasymetric products for cattle, goats, horses, sheep (Gilbert et al., 2018). GLW livestock population estimates were based on the most recent census result (all conducted in 2003 or later in North America). Biomass for each species was calculated by multiplying population by average mass estimates (Appendix B Sup. Table 3.4). Total herbivore biomass was calculated as the sum of all species biomass. Dry matter consumed by herbivores was calculated as a function of population, body weight, and net energy concentration of diet following standard IPCC methods outlined in Archibald and Hempson (2016).

Predicted proportion of dry matter consumed by herbivores versus fire in North America (Fig. 3.4 C) was modeled by fitting a generalized additive model to the data for the proportion of dry matter consumed by herbivores in Sub-Saharan Africa (Supplementary Fig. 3.3 B) and projecting to North America with the WorldClim2 precipitation data.

Wild herbivore populations of North America were not included in modern calculations because accurate continent-scale datasets are not available. We assume that biomass

consumption by wild herbivores in North America is negligible compared to that of domestic herbivores. Globally, the biomass of all wild mammals is 1-2 orders of magnitude less than that of livestock (Bar-On et al., 2018). We suspect this difference is even greater in North America, where there is substantial investment in high-density livestock production.

Results and Discussion

Paleoenvironmental reconstructions of regional hydroclimate, biomass burning, and bison abundance in midcontinent North America reveal how moisture availability once governed consumer dominance patterns at regional to continental scales. Over the past 10k years, the NG had more bison, less burning, and more open vegetation structure than the wetter GFT. These observations correspond with consumer dominance patterns in Sub-Saharan Africa, suggesting a level of generality among the biophysical constraints that shape consumer regimes on different continents. Yet current biomass consumption patterns in North America indicate that human activities have greatly expanded herbivore dominance and essentially eliminated the functional role of fire even in historically fire-dominated systems. This human-mediated shift in broad scale consumer dominance has important implications for biodiversity, nutrient cycling, carbon storage, and habitat structure.

Multiple hydroclimate records indicate that the period between 9-6k yr BP was the driest phase of the Holocene in midcontinent North America (Fig. 3.2; Appendix B Sup. Table 3.1; Appendix B Sup. Fig. 3.2). In the NG, woody plants were relatively sparse, biomass burning generally remained below the Holocene average, and bison populations were progressively declining (Fig. 3.2). To the east, the GFT experienced a substantial reduction in woody plant biomass between 10-8k yr BP. This transition to a more open landscape corresponds with rising

biomass burning and rising bison populations. A peak in GFT bison abundance just after 8k yr BP coincides with a low point in woody plant dominance.

Moisture availability began to increase between 6-4k yr BP (Appendix B Sup. Fig. 3.2.). The timing of the inflection point and the rate of change vary by region and record. Rocky Mountain lake levels began to rise rapidly at 6k yr BP. Two notable droughts are evident at Kettle Lake at ~5.4k yr BP and ~4.5k yr BP but limited dune activity in the Nebraska Sand Hills and dust deposition at Steel Lake suggest that the impacts of these droughts may have been geographically limited. The shift toward wetter conditions during the mid-Holocene corresponds with rising bison abundance and biomass burning in the NG. During this interval, NG biomass burning shifted from a record low at ~5.6k yr BP to a high at ~4.5 yr BP. Bison abundance followed a similar pattern with a low at ~6k yr BP followed by a peak at ~4k yr BP. GFT bison abundance briefly peaked at ~5.6k yr BP and then dropped to Holocene lows at ~4.5k yr BP, whereas GFT burning remained elevated and rose to Holocene highs by 4k yr BP.

Hydroclimate proxies indicate that the period between 4-0.5k yr BP was generally wet but punctuated by multiple severe droughts (Appendix B Sup. Fig. 3.2). Woody plant dominance in the NG rose continuously between 3-0.5k yr BP. NG biomass burning dropped to match early Holocene levels at ~3k yr BP, rose to the Holocene average by ~2k yr BP, and was elevated between 1.5-0.5k yr BP. NG bison abundance was elevated but stable 4-3k yr BP and then rapidly expanded to a Holocene maximum 1.5-0.5k yr BP. In the GFT, woody plants expanded from ~4k yr BP to ~1.5 yr BP. GFT biomass burning declined from a peak at 4k yr BP to its Holocene mean by 0.5 yr BP. Declining woody plant dominance beginning at ~2.5 yr BP is mirrored by increasing bison abundance. GFT bison abundance remained elevated to 0.5 yr BP.

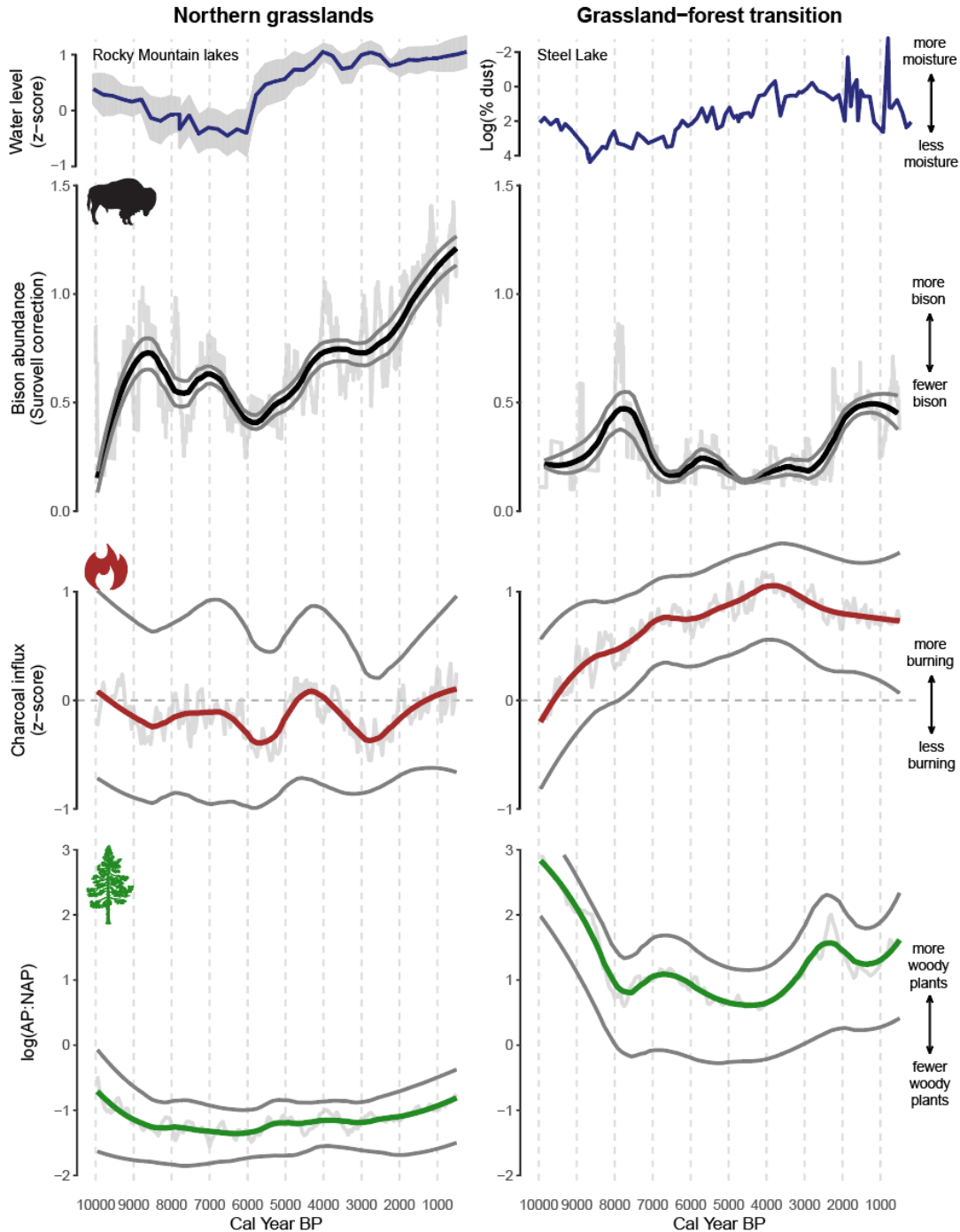


Figure 3.2. Regional comparison of reconstructed bison abundance (black line), biomass burning (red line), and woody plant dominance (green line) between 10-0.5k Cal yr BP in the northern grasslands and grassland-forest transition regions. Bootstrapped means (thick colored lines), 95% confidence intervals (dark gray lines), and unsmoothed composite means (light gray lines) are shown. Units for mean charcoal influx are particles $\text{cm}^{-2} \text{yr}^{-1}$. AP:NAP is the ratio of arboreal pollen to non-arboreal pollen; higher values reflect greater arboreal pollen abundance.

The observed shifts in consumer dominance through the Holocene (Fig. 3.3 E) correspond with modern patterns of consumer turnover in Sub-Saharan Africa (Archibald and Hempson 2016; Fig 3.1 C; Fig. 3.3 B & D), suggesting that biophysical constraints shape consumer regimes in similar ways on different continents. As in Sub-Saharan Africa, large herbivores dominated biomass consumption in dry, open environments and fire dominated in wetter, more wooded environments (Figs. 3.2 & 3.3 E). As moisture availability in the drier NG increased after 6k yr BP, bison abundance increased while fire activity remained relatively modest. Additionally, results from the GFT suggest that the region expressed a fire-dominated consumer regime when moisture availability was greatest between 4-3k yr BP. The following drop in moisture availability led to a transition towards herbivore/fire co-dominance as biomass burning declined and bison expanded 3-2k yr BP. These trends are consistent with Africa-based predictions (i) that as a dry systems become wetter, herbivore density will approach maximum potential, while potential biomass burning will increase modestly and (ii) wetter systems will shift from fire dominance toward consumer co-dominance as they dry. Temporal variation in fire and bison prevalence in relation to changing moisture availability broadly conform to expected grass palatability-flammability trade-offs established in African ecosystems (Archibald et al., 2019).

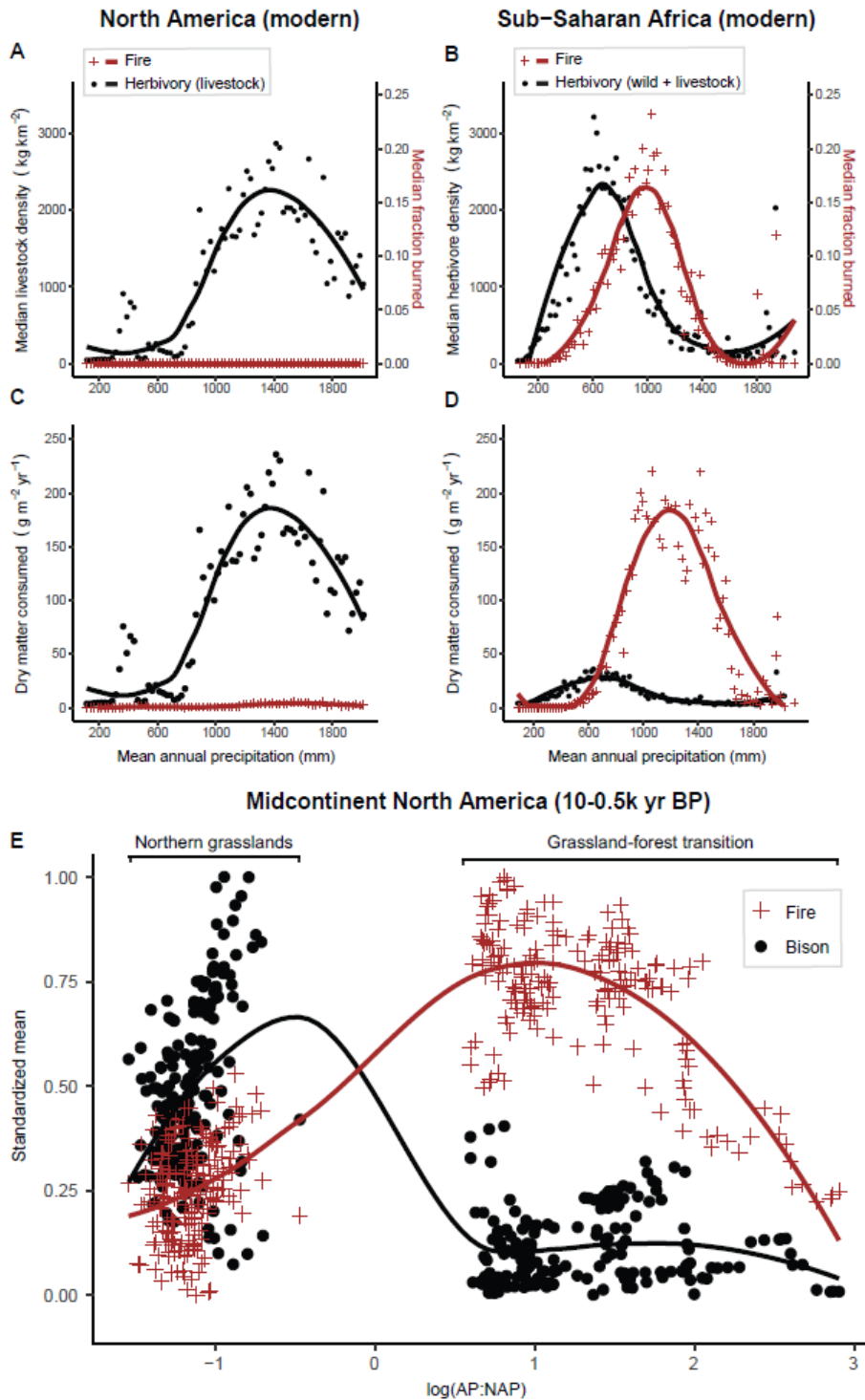


Figure 3.3. Fire and herbivory dynamics across moisture gradients in modern North America (left column), modern Sub-Saharan Africa (right column), and Holocene midcontinent North America (bottom panel). For modern data, points represent median values within each 25 mm mean annual precipitation band. Panels A & B compare herbivore biomass to area burned, and

panels C & D compare dry matter consumed. Panel E shows regional consumer dominance in Holocene midcontinent North America, points represent the mean of bison abundance or charcoal influx at a given level of woody plant dominance (arboreal pollen:non-arboreal pollen) for every 50 year interval between 10,000-250 Cal yr BP (bison abundance and charcoal influx were standardized at the population level). Lines are based on loess regressions through the points. Data for Sub-Saharan Africa are from Archibald and Hempson (2016).

Regional differences in vegetation structure and fuel type complicate interpretation of regional charcoal influx composites. Higher charcoal influx in the GFT may result from an increase in dominance of woody vegetation, which can result in greater charcoal production and preservation relative to finer, low-lignin grassland fuels (Feurdean, 2021; Yang et al., 2007). In this case, higher charcoal influx may reflect an increase in woody biomass and not necessarily an increase in fire frequency. However, it is unlikely that wood-fueled fires consumed less overall biomass than bison because GFT ecosystems burned regularly, and bison were relatively scarce.

Relatively high bison abundance and low fire prevalence in the Holocene NG suggests that the region predominantly functioned within an herbivore-dominated consumer regime. NG bison abundance trends broadly track changes in moisture availability, suggesting that forage quality is not limiting in this region, and accordingly, that moisture-driven variation in forage availability is directly linked to bison population trends. In contrast, bison abundance is lower in the wetter, more closed GFT. This may indicate that forage quality, which decreases as grasses become taller in wetter areas (Hempson et al., 2019), places a greater constraint on bison populations than forage availability does in that region. A high biomass and spatially continuous grass layer is, however, ideal fuel for spreading fire (Simpson et al., 2022).

The proxy measures we assess here are necessarily coarse, making it difficult to reveal the complex contingencies that would characterize a co-dominance consumer regime. Fire and bison were present in both regions throughout the last 10k years, and it is likely that both would

have experienced periods when fire and herbivory were co-dominant consumers at varying scales. One such instance occurred in the NG at 2-0.5k yr BP, when both fire and bison prevalence increased during a relatively mesic period. One interpretation for this is that conditions may have been wet enough to promote high availability of moderately palatable grasses, providing forage for bison and continuous fuels for fires. Pyric herbivory, with the potential to produce patches of high-quality forage, may have further bolstered bison populations. Archaeological evidence suggests that bison affinity for recently burned patches was exploited by Indigenous hunters in the NG (Roos et al., 2018).

Modern consumer regimes in North America have been greatly modified from the past (Fig. 3.3 A & C). The lack of any discernable peak in fire prevalence across the moisture gradient suggests that fires have been strongly suppressed in large parts of the continent. Indeed, mapping relative biomass consumption by livestock and fire shows that fire dominance is now largely restricted to sparsely inhabited boreal and mountain forests and rural areas with fire cultures (Fig. 3.4 A). The widespread lack of fire is likely a consequence of deliberate fire suppression policies as well as extensive land use change and landscape fragmentation that have altered fuel loads and fuel connectivity (Hessburg et al., 2019; Hessburg and Agee, 2003).

While anthropogenic influences have greatly distorted consumer regime distributions in contemporary North America, it is nonetheless intriguing that livestock biomass currently peaks at a much higher rainfall level than observed in Sub-Saharan Africa (1400 vs. 700 mm MAP; Fig. 3.3 A & B). This may indicate that the specific environmental drivers of palatability and flammability differ somewhat between North American and African ecosystems. Between 500-700 mm MAP, herbivore densities in North America are strikingly low compared to the same

range in Sub-Saharan Africa, as these regions are instead primarily used for intensive crop production systems (Massey et al., 2018). Crop agriculture may have displaced livestock production to wetter regions, where advanced animal husbandry practices such as land clearing, pasture fertilization, supplementary feed and water provision, and veterinary services help support animal densities that may far exceed those possible under natural environmental conditions. However, the herbivore density peak at higher precipitation may alternatively be due to ecological differences between temperate North American and tropical African ecosystems. Forage quantity-quality tradeoffs are linked to productivity and are underpinned by the need for grasses to grow taller to compete for light as productivity increases (Lane et al., 2000; Nelson and Moser, 1994). While productivity is largely determined by rainfall in tropical African ecosystems, temperature plays a much greater role in determining plant growing season duration and hence productivity in temperate North American ecosystems (Churkina and Running, 1998). As such, while total annual precipitation may appear adequate to produce a tall, unpalatable grass sward, a shorter, cooler growing season may limit this growth potential and thus enhance palatability, thereby shifting peak herbivore dominance up the precipitation gradient.

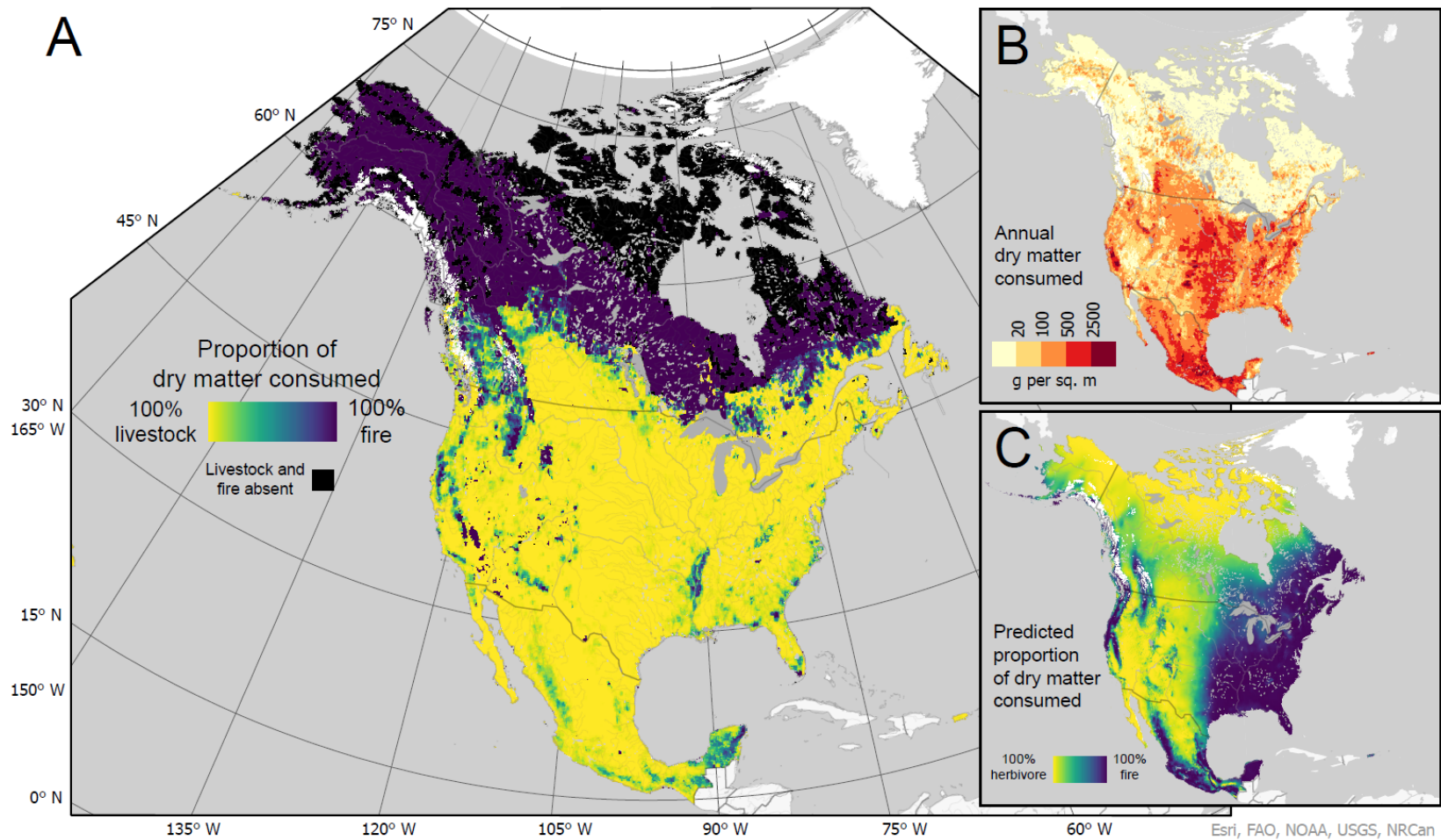


Figure 3.4. Map of relative proportion biomass consumed by herbivores and fire in contemporary North America (panel A); and annual total dry matter consumed by both livestock and fire in contemporary NA (panel B); and predicted relative proportion of dry matter consumed by herbivores and fire (panel C) are based on the observed precipitation-consumer dominance relationship for Sub-Saharan Africa (Archibald and Hempson 2016; Appendix B Sup. Fig. 3.3 B).

The precipitation-consumer dominance relationship for Sub-Saharan Africa can serve as a simplistic null model for biomass consumption patterns in pre-colonial North America (Fig. 3.4 C). This univariate model does not account for non-precipitation drivers of plant palatability and flammability including growing season length, temperature, and seasonality. Precipitation is likely a poor predictor of consumer dominance in high-latitude systems (e.g., boreal forests) with low potential evapotranspiration, low temperatures, and short growing seasons. In such low-energy settings (Veldhuis et al., 2019), large herbivores may struggle to balance thermoregulatory and food requirements, while fuel continuity and density are sufficient to promote rare, intense, and large fires during hot and dry summer conditions (Archibald et al., 2013). Therefore, the Africa-based precipitation-only model likely overpredicts herbivore dominance in cold regions. Despite these limitations, this null model is somewhat validated by observed similarities between the consumer distributions in contemporary Sub-Saharan Africa and Holocene Midcontinent North America. This model can facilitate further hypothesis generation and testing to identify influential constraints on consumer dominance for other North American regions and climates. Mapping hypothesized paleo-consumer dominance is an important step toward understanding the geographic distribution, relative dominance, and potential interactions of consumers that have long influenced ecosystem structure and biodiversity.

The dramatic distortion of North American consumer regimes by humans in the recent past likely holds major ecological consequences for the affected ecosystems. Among these are critical threats to biodiversity, as both fire and herbivores have structured niches and exerted considerable selective pressures on plant and animal assemblages across the globe (Bond, 2005;

Bond and Keeley, 2005; Lehmann et al., 2014; Staver et al., 2021). Removing one or both of these consumers potentiates biome transitions, particularly towards closed canopy ecosystems where environmental conditions allow (Fogarty et al., 2020; Holdo et al., 2009b). Herbivores and fire both influence a wide variety of ecological processes and functions, ranging from nutrient dispersal (Pellegrini et al., 2018; Wolf et al., 2013) and carbon storage (Kashian et al., 2006; Schmitz et al., 2023) to habitat structuring (Fuhlendorf and Engle, 2004; Staver et al., 2011) and biodiversity maintenance (Hartnett et al., 1996; Ratajczak et al., 2022). Rewilding for ecological restoration has gained considerable interest over the last 30 years. While rewilding initiatives promise to address some of the ecological dynamics missing from ecosystems, evidence from the past suggests that restoring natural fire regimes to North American landscapes is likely as important, and perhaps more readily achievable.

Acknowledgements

We acknowledge funding from the National Science Foundation (NSF) under BCS-1832486 (to D.B.M.), the Joint Fire Science Program (JFSP) award under Project JFSP 19-1-01-30 (to J.A.F.W. and D.B.M) and from the Biotechnology and Biological Sciences Research Council grant # BB/V004484/1 (to G.P.H.). Data were obtained from the Global Charcoal Database (<http://www.paleofire.org>), and the work of the data contributors and the Global Palaeofire Working Group is gratefully acknowledged. Data were obtained from the Neotoma Paleoecology Database (<http://www.neotomadb.org>). The work of data contributors, data stewards, and the Neotoma community is gratefully acknowledged. We thank Sally Archibald for helpful comments and three anonymous reviewers whose comments improved the

manuscript. Bison icon credit: Lukasiniho (license). Figure 3.1 photo credits: National Park Service (left and center) and Reid Brown (right).

CHAPTER FOUR

FECAL BIOMARKERS REVEAL UNPRECEDENTED 20TH CENTURY HERBIVORE
DENSITIES AND IMPACTS IN THE YELLOWSTONE NORTHERN RANGE

Contributions of Authors and Co-Authors

Manuscript in Chapter 4

Author: John A.F. Wendt

Contribution: Conceptualization, data curation, formal analysis, funding acquisition, investigation, methodology, visualization, writing – original draft, and writing – review and editing.

Co-Author: Elena Argiriadis

Contribution: Data curation, formal analysis, supervision, investigation, methodology, writing – original draft, and writing – review and editing.

Co-Author: Cathy Whitlock

Contribution: Conceptualization, supervision, project administration, formal analysis, investigation, and writing – review and editing.

Co-Author: Mara Bortolini

Contribution: Data curation, methodology, writing – original draft, and writing – review and editing.

Co-Author: Dario Battistel

Contribution: Methodology, project administration, supervision, and writing – review and editing.

Co-Author: David B. McWethy

Contribution: Conceptualization, supervision, funding acquisition, writing – original draft, and writing – review and editing.

Manuscript Information

John A.F. Wendt, Elena Argiriadis, Cathy Whitlock, Mara Bortolini, Dario Battistel, David B. McWethy

Status of Manuscript

- Prepared for submission to a peer-reviewed journal
- Officially submitted to a peer-reviewed journal
- Accepted by a peer-reviewed journal
- Published in a peer-reviewed journal

Abstract

Molecular biomarkers preserved in lake sediments are increasingly used to develop records of past organism occurrence. When linked with traditional paleoecological methods, analysis of molecular biomarkers can yield new insights into the ecology of herbivores and other animals and their role in past ecosystem dynamics. We sought to test the utility of fecal steroids in lake sediments for reconstructing past ungulate abundance and community composition in the Northern Range of Yellowstone National Park. To do so, we characterized the fecal steroid profiles of a selection of North American ungulates historically present in the Yellowstone region (bison, elk, moose, mule deer, and pronghorn) and compared the steroid profiles to those of lake sediments extracted from Buffalo Ford Lake, WY. Combined analysis of fecal steroids (Δ^5 -sterols, 5α -stanols, 5β -stanols, epi 5β -stanols, stanones, and bile acids) differentiated moose, pronghorn, and mule deer by the fecal steroid contents of their dung, whereas elk and bison were partially differentiated. Animal-specific compounds (5β -stanols and bile acids) were detected in the lake sediments, allowing for characterization of local ungulate density and community composition at decadal to millennial timescales. Our results show that bison and/or elk were the primary ungulates in the Buffalo Ford Lake watershed over the past *c.* 2300 years. According to fecal steroid influxes, local ungulate densities reached historically unprecedented levels during the early and middle 20th century, a conclusion that matches documentary evidence. Comparison of fecal steroid influxes and other paleoenvironmental proxies suggests that these elevated ungulate populations likely contributed to decreased forage taxa (*Poaceae*, *Artemisia*, and *Salix*), relative to long-term averages, and possibly increased lake production. Our results provide new long-term records of ungulate occurrence and suggest that recent (19th-20th century) human

activities had greater effects on local ungulate densities and their environmental impacts than climate, disturbance, disease, predation, or human management had during the two preceding millennia.

Introduction

The near extinction of bison (*Bison bison*) in North America in the 19th and 20th centuries ranks among the most dramatic ecological catastrophes in recent times, but little is known about herbivore-ecosystem dynamics prior to the event. Shortfalls in our knowledge are due to the limited temporal extent of the historical written record as well as the limited array of methods and proxies for reconstructing past herbivore populations and impacts. Because the historical record is limited to the past 200-300 years or less in most portions of western North America, alternative means are required to understand the pre-European ecology of these ungulates and their environment. Most of our information on past bison comes from fossil vertebrate remains largely recovered at archaeological sites. Bones and other remains provide valuable information on past animal presence, but these discontinuous snapshots of occurrences provide little information on past population size and community dynamics.

Molecular biomarkers are thermodynamically stable compounds with known environmental sources that can capture and preserve unique biological signatures. These qualities allow molecular biomarkers to provide continuous, high-resolution records of the occurrence and/or abundance of source organism and associated environmental conditions (Eglinton and Eglinton, 2008). Animal feces contains measurable quantities of steroids that can provide information about an animal's identity, diet, and intestinal flora (Prost et al., 2017). These steroids include Δ^5 -sterols, 5α -stanols, 5β -stanols, epi 5β -stanols, stanones, and bile acids. Of

particular interest are 5 β -stanols and bile acids for characterizing past herbivore presence and density because animals are their primary environmental source (Bull et al., 2002). 5 β -stanols are derived from the microbial alteration of precursor sterols (e.g., cholesterol and β -sitosterol) in the intestinal tracts of higher animals. Similarly, primary bile acids (e.g., cholic acid and chenodeoxycholic acid) are modified by gut bacteria into secondary bile acids (e.g., deoxycholic acid and lithocholic acid). Environmental anaerobic microbial activity may contribute to small background levels of 5 β -stanols (Gaskell and Eglinton, 1975; Taylor et al., 1981). However, bile acids provide a high degree of source specificity because vertebrates are the only known natural producers (Haslewood, 1967; Hofmann and Hagey, 2008). 5 β -stanols and secondary bile acids may be directly deposited or transported to lake or wetland sediments, where they can persist for millennia due to their generally high affinity for particulate organic matter (Lloyd et al., 2012). When analyzed together, 5 β -stanols and bile acids provide information about the identity and abundance of animal sources.

Interspecies variability in the relative abundance of 5 β -stanols can facilitate identification of the principal contributors of fecal steroids in sediments so long as prior species distributions are known (Harrault et al., 2019). Incorporating bile acids into this analysis can further differentiate animal sources because some compounds may be exclusively produced by a single locally present species (Prost et al., 2017). Variability among fecal steroid profiles has been leveraged to investigate sources of sewage contamination (Carreira et al., 2004; Chan et al., 1998; Daughton, 2012; Grimalt et al., 1990; Reeves and Patton, 2005; Saeed et al., 2015; Speranza et al., 2018; Writer et al., 1995) and to characterize past agricultural practices in archaeological contexts (Bull et al., 2001, 1999a, 1999b; Harrault et al., 2019; Pescini et al.,

2023; Prost et al., 2017; Simpson et al., 1999; White et al., 2018), yet 5 β -stanols and bile acids have not been extensively used in continuous lake and wetland sediment cores to reconstruct changes in paleoherbivore density, community composition, and impacts over time (but see Davies et al., 2022; Guillemot et al., 2015).

The Yellowstone Northern Range (Fig. 4.1) refers to the 300,000+ ha landscape of the Lamar, Gardiner, and Yellowstone River valleys in northern Yellowstone National Park and adjoining private and public lands where large free-roaming herds of elk and bison winter (Keigley, 2019; Meagher, 1989, 1973; Rush, 1933). The vegetation of the region is primarily grassland and sagebrush steppe, with conifer forests on steep slopes of mountains and canyon walls, and patches of aspen and willow in moist lowlands. The Yellowstone Northern Range provides an ideal setting to test the utility of fecal steroid biomarkers for reconstructing past herbivore community composition, abundance, and environmental impacts. Today, elk and bison are by far the most abundant ungulates in the Yellowstone Northern Range (Appendix C Sup. Table 4.1). Population estimates and wildlife management records from the last 100+ years allow for independent validation of fecal steroids as proxies for past herbivores. Bison and elk populations in the Yellowstone Northern Range varied greatly during this period. The bison population consisted of just over 20 individuals at the turn of the 19th century and numbered over 4000 in 2022. Elk population estimates exceeded 30,000 between 1911-1915, while the northern Yellowstone herd numbered 5800 in 2019.

Since the establishment of Yellowstone National Park in 1872, managers have struggled to balance protection for elk and bison herds with other resource management goals, including maintenance of habitat integrity (Beschta et al., 2020; Leopold et al., 1963; National Research

Council et al., 2002; Research Division, 1992). The long-running debate over the management of large ungulates in Yellowstone National Park has generated interest in the historic origins, occupancy, abundance, and impacts of bison and elk (Eberhardt et al., 2007; Engstrom et al., 1991; Forgacs et al., 2016; Hamilton, 1994; Meagher, 1973; Research Division, 1992; Whittlesey et al., 2018). Current understanding of long-term abundance and community composition of ungulates in the Yellowstone Northern Range is largely based on limited fossil evidence from paleontological and archaeological sites, which confirm the presence of bison and elk in the region and locally (Barnosky, 1996; Cannon, 2001; Wendt et al., 2022). Engstrom et al. (1991) sought to identify herbivore impacts on vegetation and soil stability via analysis of recent lake sediments (past *c.* 100-200 years), but they lacked a way to quantify local herbivore density. Analysis of fecal steroid biomarkers in lake sediments may provide additional information about the historic composition, abundance, and impacts of ungulates in the Yellowstone Northern Range and elsewhere.

Our objectives are to 1) validate the utility of fecal steroids for reconstructing past herbivore abundance and community composition; 2) characterize decadal- to millennial-scale changes in herbivore abundance and community composition in the Yellowstone Northern Range; and 3) evaluate multi-proxy paleoenvironmental data to better understand how large herbivores in the Yellowstone Northern Range shaped, responded to, and interacted with their changing environment. To address these objectives, we developed a multi-proxy dataset from Buffalo Ford Lake that builds on previous research described in Engstrom et al. (1991) based on an examination of changes in local herbivores, vegetation, and fire history over the last *c.* 2300 years.

Site Description

Buffalo Ford Lake (44.934, -110.383; 1921 m elevation) is a small (4.3 ha) glacial kettle located in the lower Lamar Valley of Yellowstone National Park (YNP), 1.4 km northeast of the confluence of the Yellowstone and Lamar rivers (Fig. 4.1). The Buffalo Ford Lake catchment (427 ha) and surrounding area is the current and historic home to a variety of large ungulates including bison (*Bison bison*), elk (*Cervus canadensis*), moose (*Alces alces*), pronghorn (*Antilocapra americana*), bighorn sheep (*Ovis canadensis*), and mule deer (*Odocoileus hemionus*). The Buffalo Ford Lake area provides critical resources including water, food, and shelter for ungulates throughout the year.

Vegetation

The vegetation in the Buffalo Ford Lake catchment is primarily steppe composed of big sagebrush (*Artemisia tridentata*), rabbitbrush (*Ericameria nauseosa*), Idaho fescue (*Festuca idahoensis*), and Great Basin wild rye (*Leymus cinereus*). Patches of Rocky Mountain juniper (*Juniperus scopulorum*) and Douglas-fir (*Pseudotsuga menziesii*) are found on rocky outcrops and hillslopes around the lake. Lodgepole pine (*Pinus contorta*) grows on rocky outcrops and areas of exposed rhyolite, and Engelmann spruce (*Picea engelmannii*) and subalpine fir (*Abies lasiocarpa*) are present in cool settings and at higher elevation. Small stands of quaking aspen (*Populus tremuloides*) grow in nearby drainages. Willows (*Salix* spp.) are present in riparian areas. Sedges (*Cyperaceae*) are found along the wetland margins of Buffalo Ford Lake and in the surrounding uplands.

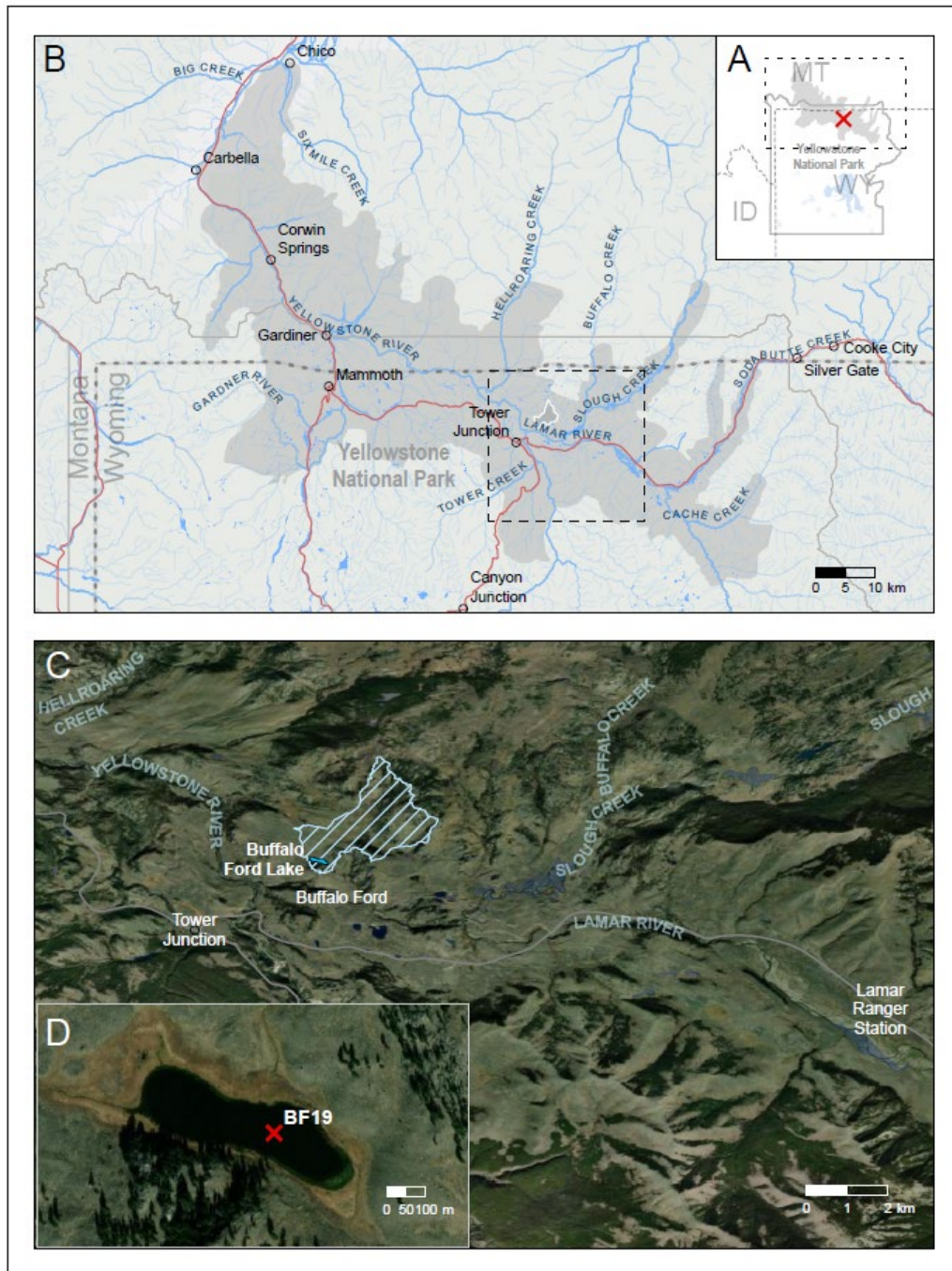


Figure 4.1. Maps of (panel A) Yellowstone National Park showing extent of the Yellowstone Northern Range (gray shading), location of Buffalo Ford Lake (red X), and extent indicator for panel B (black dashed line); (panel B) the Yellowstone Northern Range (gray shading) with the Buffalo Ford Lake catchment area (white outline), roads (red), rivers and streams (blue), and extent indicator for panel C (dashed black line); (panel C) the Lower Lamar Valley showing Buffalo Ford Lake and its catchment (hatched area); and (panel D) Buffalo Ford Lake showing location of BF19 core (red X).

Climate

During the period from 1948 to 2005, the Tower Falls weather station (4.5 km south of Buffalo Ford Lake) recorded an average maximum temperature of 11.4° C, an average minimum temperature of -7.1° C, and an average annual precipitation of 42.16 cm (<https://wrcc.dri.edu/cgi-bin/cliMAIN.pl?wy9025>). Convective summer storm systems drive summer-wet precipitation patterns in the Yellowstone Northern Range. The wettest three months (May, June, and July) account for 33% of total annual precipitation at Tower Falls. On average, snow begins to accumulate in early November, snow depth peaks in early March, and melt-off ends by early May.

Materials and Methods

Sediment Core Collection

One 1.6 m-long sediment core (BF19) was retrieved in August 2019 from Buffalo Ford Lake from a raft at a water depth of 5.1 m with a 7.5-cm diameter polycarbonate tube. The core was extracted near the location of a core collected in 1987 (BF87; Engstrom et al., 1991). The BF19 core was stabilized with Zorbitol, sealed, and transported to the Paleoecology Lab at Montana State University where it was split longitudinally and placed in refrigerated storage.

Sediment Core Chronology

All statistical analyses were performed in R version 4.1.3 (R Core Team, 2022) with RStudio (Posit team, 2023), unless stated otherwise. The chronology of the BF19 sediment record is based on a Bayesian age-depth model calculated with the Intcal20 calibration curve using the rbacon R package (Appendix C Sup. Fig. 4.1; Blaauw and Christen, 2011). The

chronology was constructed with two ^{14}C samples from BF19, twelve ^{210}Pb ages from BF87 (Engstrom et al., 1991), and a charcoal layer from the 1988 Yellowstone fires. The BF87 ^{210}Pb series was anchored to BF19 by assigning the top of BF87 1 cm below the charcoal peak from the 1988 Yellowstone fire season. All ages presented in this paper are calibrated with the Intcal20 curve (Reimer et al., 2020) and are given as calendar years before present (cal yr BP), or alternatively converted to the Gregorian calendar (BCE/CE).

Table 4.2 Calendar ages, AMS radiocarbon dates, and ^{210}Pb dates from Buffalo Ford Lake, WY, US.

Age control/Lab no.	Depth (cm)	$^{14}\text{C}/^{210}\text{Pb}$ age \pm 2σ error	Cal yr BP (2σ range)	Material dated
Surface	0	-	-69	-
1988 fire	5	-	-38	Charcoal
210pb-1 ^a	6	2 ± 1	-34 (-37, -21)	Bulk sediment
210pb-2 ^a	9	7 ± 1	-27 (-30, -15)	Bulk sediment
210pb-3 ^a	11	15 ± 1	-22 (-25, -11)	Bulk sediment
210pb-4 ^a	15	24 ± 1	-13 (-15, -2)	Bulk sediment
210pb-5 ^a	18	35 ± 2	0 (-4, 9)	Bulk sediment
210pb-6 ^a	22	52 ± 2	15 (11, 25)	Bulk sediment
210pb-7 ^a	25	62 ± 2	27 (21, 36)	Bulk sediment
210pb-8 ^a	28	71 ± 3	32 (27, 41)	Bulk sediment
210pb-9 ^a	32	86 ± 8	51 (41, 62)	Bulk sediment
210pb-10 ^a	35	105 ± 14	65 (46, 89)	Bulk sediment
210pb-11 ^a	38	127 ± 27	91 (64, 129)	Bulk sediment
210pb-12 ^a	40	144 ± 49	107 (68, 170)	Bulk sediment
210pb-13 ^a	43	174 ± 123	148 (91, 246)	Bulk sediment
OS-156938 ^b	75	785 ± 25	696 (632, 765)	Wood
OS-158769 ^b	148	2210 ± 20	2188 (2065, 2296)	Wood

^a ^{210}Pb ages originally reported in (Engstrom et al., 1991)

^b Samples measured at NOSAMS Laboratory at Woods Hole Oceanographic Institution

To characterize long-term fire trends and to identify the charcoal layer produced by the 1988 Yellowstone fires, samples of 2 cm³ of sediment were taken at contiguous 0.5 cm intervals for the top 11 cm of the core, and at contiguous 1 cm intervals for the remainder of the core for

charcoal analysis. Samples were soaked for 24 hours in a 50:50 solution of bleach and 5% sodium hexametaphosphate (NaPO_3)₆ to leach color from organic material and deflocculate the sediment. Samples were screened through a 125 μm -mesh sieve. Particles larger than 125 μm were counted under a stereomicroscope on the assumption that particles of this large size typically originate from local fire events (Whitlock and Larsen, 2001).

Biomarker Sample Preparation

Forty dung samples from five ungulate species (bison, elk, moose, mule deer, and pronghorn) were identified (Halfpenny, 2019) and collected from the Bison Range, MT and near the YNP boundary in Cooke City, MT and Silver Gate, MT (Appendix C Sup. Table 4.2). Dung samples were frozen for storage, air dried, and then freeze-dried. Dung samples were air dried by placing samples in a running fume hood for 48 hours. Twenty-seven subsamples from BF19 were taken at 2-10 cm intervals, resulting in a mean temporal resolution of 85 years (min: 3 years; max: 209 years; Appendix C Sup. Table 4.3). All dung and sediment samples were freeze-dried for 24 hours and then hand-milled and homogenized with a ceramic mortar and pestle. Samples were stored at room temperature in aluminum-foil packets until extraction.

Extraction of Dung Samples

Dung samples were spiked with known quantities of ^{13}C -cholesterol (cholesterol-25,26,27- $^{13}\text{C}_3$) and ^{13}C -deoxycholic acid (deoxycholic acid-24- ^{13}C). Dung samples were extracted twice with 20 mL of a 2:1 DCM:MeOH solution in an ultrasonic bath for 15 minutes. Anhydrous Na_2SO_4 was added to the extract and a 1 mL aliquot was purified via flash chromatography with florisil.

Biomarker Extraction of Lake-Sediment Samples

Extraction of biomarkers from lake sediment samples was performed with an ASE 350 (Accelerated Solvent Extractor, *Dionex Thermo Fisher Scientific*) equipped with 22 mL stainless steel extraction cells. Each sample was mixed with diatomaceous earth and a spike with a known quantity of the ^{13}C -labeled internal standards. Extraction was performed twice with a 9:1 DCM:MeOH solution at 100 °C and 1500 psi.

Cleanup and fractionation of dung and sediment samples were performed according to (Birk et al., 2012), with minor modifications. Extracts were dried under a nitrogen flow and saponified with 3.5 mL of 0.7 M KOH in MeOH (10-14 hours at room temperature), then 10 mL of ultrapure water were added. The neutral fraction (containing sterols, stanols, and stanones) was extracted three times with 15 mL of chloroform, then the sample was acidified with 6 M HCl until $\text{pH} \leq 2$. An acidic fraction (containing bile acids) was obtained by extracting three times with 15 mL of chloroform.

The neutral fraction was then concentrated and purified on neutral silica following the methods described in Battistel et al. (2015), dried, remobilized with 100 μL of DCM and derivatized with 100 μL of BSTFA + 1% TCMS, transferred to GC vials and heated to 70 °C for 1 hour, cooled to room temperature, and analyzed with GC-MS after 24 hours.

The acidic fraction was dried and methylated with 2 mL of 1.25 M HCl in methanol at 80 °C for 2 hours, purified following Birk et al. (2012), dried and redissolved in 50 μL of toluene, then derivatized with 100 μL of BSTFA + 1% TMCS, transferred to GC vials and heated to 80 °C for 1 hour, cooled to room temperature, and analyzed with GC-MS.

GC-MS Analysis

All analyses were performed using an Agilent Technologies 7890 GC system coupled to a 5975C MSD and equipped with a HP-5ms 60 m capillary column (0.25 mm I.D.; 0.25 μm film thickness; Agilent Technologies).

Sterols were separated using the following chromatographic run: 150 °C (1 min), 30 °C min^{-1} to 220 °C (0 min), 0.7 °C min^{-1} to 275 °C (0 min), 10 °C min^{-1} to 300 °C (5 min), 10 min at 315 °C (post run); helium flow 1 mL min^{-1} . Injector and transfer line temperatures were 290 °C and 300 °C, respectively.

For bile acids, the following chromatographic method was used: 40 °C (1 min), 20 °C min^{-1} to 230 °C (0 min), 2 °C min^{-1} to 300 °C (20 min), 10 min at 315 °C (post run); helium flow 1 mL min^{-1} . Injector: 280 °C; transfer line: 300 °C. For both methods: source temperature 230 °C and quadrupole temperature 150 °C.

Fecal Steroid Nomenclature

The fecal stanols measured were coprostanol (5 β -cholestan-3 β -ol), epicoprostanol (5 β -cholestan-3 α -ol), cholesterol (cholest-5-en-3 β -ol), cholestanol (5 α -cholestan-3 β -ol), cholestanone (5 α -cholestane-3-one), 24-ethylcoprostanol (24-ethyl 5 β -cholestan-3 β -ol), 24-ethylepicoprostanol (24-ethyl 5 β -cholestan-3 α -ol), campesterol (campest-5-en-3 β -ol), stigmasterol (stigmasta-5,22-dien-3 β -ol), β -sitosterol (stigmast-5-en-3 β -ol), ergosterol (3 β -ergosta-5,7,22-trien-3-ol), and stigmastanol (5 α -stigmastan-3 β -ol). Bile acids analyzed were chenodeoxycholic acid, deoxycholic acid, hyodeoxycholic acid, lithocholic acid, and ursodeoxycholic acid. Refer to Appendix C Sup. Table 4.4 for additional compound information.

Statistical Analysis of Biomarker Profiles

Statistical analysis of fecal stanols followed Harrault et al. (2019). Steroid values of dung and lake sediment samples were transformed from absolute concentrations to relative abundances of (i) sterols, stanols, and stanones and (ii) bile acids to account for variability among samples (Fig. 4.2 A & B). Principal component analysis (PCA) was performed on the relative abundances of each compound in dung samples (Fig. 4.2 C & D). Chenodeoxycholic acid and ursodeoxycholic acid were excluded because they were absent from nearly all dung samples.

This was followed by analysis of the relative proportions of 5β -stanols, which are predominantly produced in the digestive tract of animals, while other fecal steroids have other environmental sources. We used hierarchical clustering on principal components (HCPC) based on all 4 principal components, with Euclidean distance and Ward's method (Fig. 4.3). Lake-sediment samples were added to the PCA as supplementary individuals to assess the similarity of lake-sediment 5β -stanol profiles to those of historically present species. These analyses were performed using the PCA and HCPC functions from the FactoMineR R package (Lê et al., 2008).

Herbivore Population and Biomass

Population records for bison (1877-2015 CE) and elk (1911-2015 CE) in the Yellowstone Northern Range were compiled from multiple literature sources (Evans, 1939; Fuller, 2006; Geremia et al., 2015; MacNulty et al., 2016; Meagher, 1973; Rush, 1933). Elk population estimates from before the start of aerial surveys in 1952 are less reliable but included here as

general estimates. Populations were converted to biomass based on average body masses of 665 kg for bison (Martin et al., 2018) and 235 kg for elk (Cook et al., 2004).

Pollen Analysis

Samples of 1 cm³ of sediment were taken at 4-8 cm intervals for pollen analysis resulting in a mean temporal resolution of 101 years (min: 9 years, max: 168 years). The samples were processed according to the methods outlined in Bennett and Willis (2001). Each sample was spiked with a tablet containing a known quantity of *Lycopodium* spores to calculate pollen concentration (grains cm⁻³) and pollen accumulation rate (grains cm⁻² yr⁻¹). Pollen residues were mounted in silicone oil and examined at 400-1000x magnification. A minimum of 300 terrestrial pollen grains and spores were identified to the lowest taxonomic level possible on each slide and tallied. Terrestrial taxa were converted to percentages based on the sum of terrestrial pollen and spores. Aquatic pollen counts were converted to percentages relative to the sum of all pollen and spores. *Cyperaceae* was classified as an aquatic taxon.

Pinus pollen grains with intact distal membranes were identified to subgenus. *Pinus* subg. *Strobus* (haploxyton type, verrucate distal membrane) includes *P. albicaulis* and *P. flexilis*, which both grow in northern Yellowstone National Park. *Pinus* subg. *Pinus* (diploxyton type, psilate distal membrane) primarily represents *P. contorta* in the area. Grains of *Cupressaceae* are attributed to *Juniperus*-type because only *J. scopulorum*, *J. horizontalis*, and *J. communis* occur within the region.

The relative abundance of dominant functional groups (evergreen conifers versus shrubs and grasses) was calculated with pollen percentages as $(Pinus + Pseudotsuga) / (Artemisia +$

Poaceae). The pollen diagram (Appendix C Sup. Fig. 4.2) was created with the rioja R package (Juggins, 2020).

Statistical Charcoal Analysis

Statistical analysis of the Buffalo Ford Lake charcoal record was performed with CharAnalysis software (<https://sites.google.com/site/charanalysis>) for MatLab following the methods of Higuera et al. (2009). Charcoal counts were converted to charcoal accumulation rates (CHAR; particles $\text{cm}^{-2} \text{yr}^{-1}$), which were interpreted as an indicator of fire activity or biomass burned. A 500-yr loess smoother, robust to outliers, was used to characterize long-term background charcoal accumulation rates (BCHAR; Higuera et al., 2010). Charcoal peaks were identified as significant fire episodes (a single or sequence of local fires within the time span of the sample) if they exceeded the 99th percentile of the local CHAR noise distribution as defined by a Gaussian mixture model.

Results

Chronology

The extrapolated age-depth model gives a basal core age of 2289 cal yr BP. Before YNP was established in the late 19th century, the median sediment accumulation rate was stable at 0.05 cm yr^{-1} over the preceding *c.* 2200 years. Sediment accumulation rate sharply increased in the late 19th century and subsequently peaked with an increase to 0.33-0.50 cm yr^{-1} in the 1920s, stabilized at 0.25 cm yr^{-1} between *c.* 1930-1960 CE, and then rose to 0.50 cm yr^{-1} again from the 1960s to the mid-1980s. The most recent sediment accumulation rate of 0.17 cm yr^{-1} is lower than the 20th century average but remains elevated relative to the long-term average.

Lithology

The BF19 sediment core consisted entirely of brown, organic-rich mud, similar to the description in Engstrom et al. (1991) that noted that the BF87 core consisted of 44% organic content, 39% inorganic components, and 17% carbonates by dry mass. That study also determined that the sediments became more organic (from 40 to 50%) from *c.* 1600 CE to 1850 CE (Engstrom et al., 1991).

Fecal Steroids

Deoxycholic acid was the most prevalent secondary bile acid in all species analyzed (bison [58%], elk [51%], moose [74%], mule deer [86%], and pronghorn [78%]). Elk dung also contained lithocholic acid (49%), moose feces also contained lithocholic acid (21%) and hyodeoxycholic acid (4%), and mule deer feces also contained lithocholic acid (14%). Elk and mule deer dung did not contain detectable levels of hyodeoxycholic acid. Bison dung was distinguished from other species by relatively high concentrations of hyodeoxycholic acid (11%), while chenodeoxycholic acid was only detected in a single bison dung sample. We did not detect ursodeoxycholic acid in any analyzed ungulate feces.

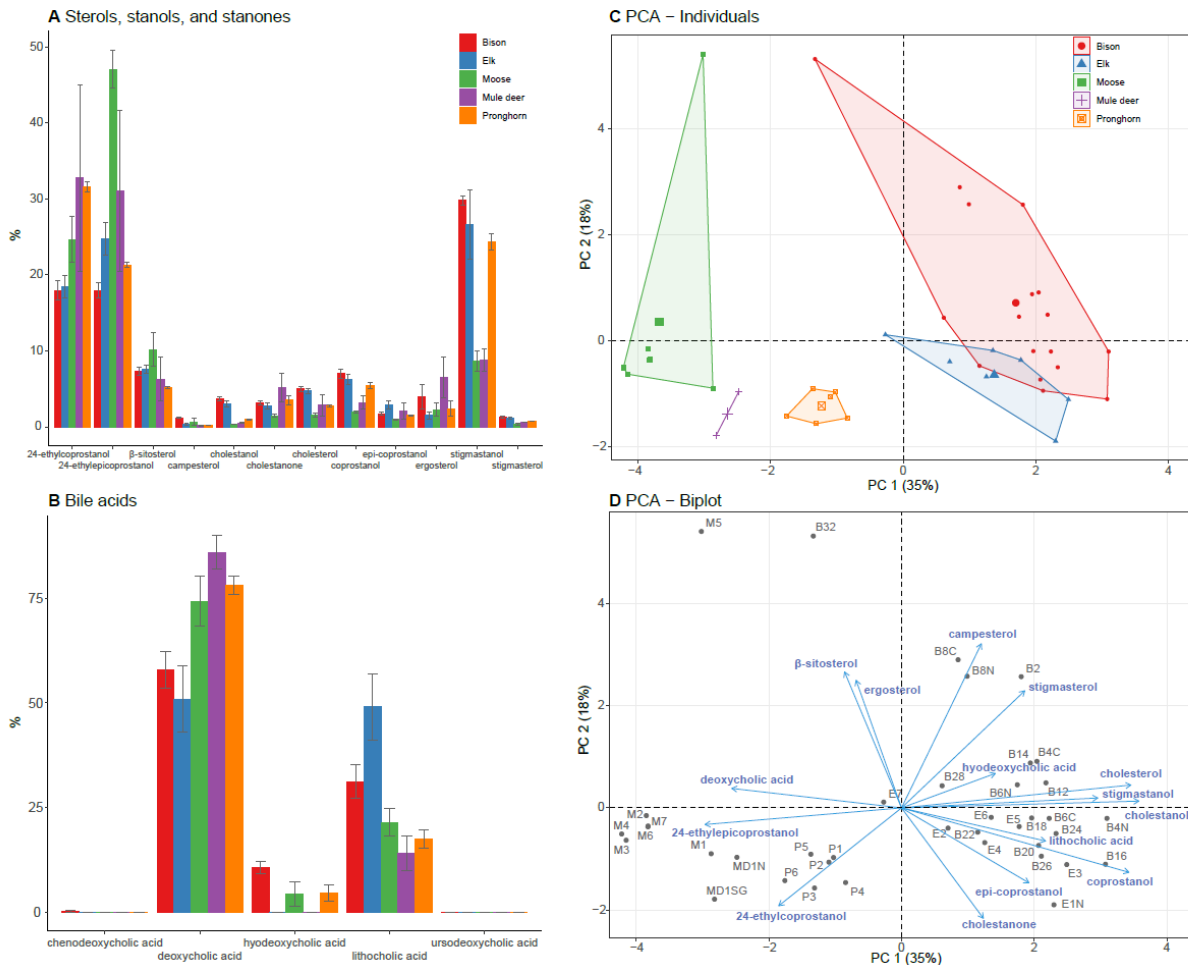


Figure 4.2. Characterization of fecal steroid profiles bison (red), elk (blue), moose (green), mule deer (purple), and pronghorn (orange) based on the relative abundances of sterols, stanols, and stanones and bile acids in individual dung samples. Distributions of (A) sterols, stanols, and stanones and (B) bile acids (mean \pm SE). (C) Score plot and (D) biplot showing the first two principal components of the fecal steroid profile PCA. Chenodeoxycholic acid, and ursodeoxycholic acid were excluded from principal components analysis. Number of individuals: bison: 17, elk: 7, moose: 7, mule deer: 2, pronghorn: 6. See Appendix C Sup. Table 4.4 for compound information. See Appendix C Sup. Table 4.2 for individual sample information and fecal steroid distributions.

Our results indicate that fecal steroid profiles of bison, elk, moose, mule deer, and pronghorn are distinctive (Fig. 4.2), and allowed complete differentiation of moose, mule deer, and pronghorn and partial differentiation of elk and bison when multivariate analysis using a considered a broad suite of fecal sterols (Fig. 4.2 C). However, many fecal sterols have

significant non-animal environmental sources, so it is not appropriate to use this broad-spectrum approach to identify ungulate contributors to mixed sediments like soils or lake sediments (Harrault et al., 2019). For this reason, our lake sediment analysis focuses on 5β -stanols (i.e., zoostanols), which are strong indicators of fecal input.

Hierarchical clustering on principal components, based on the relative abundances of four 5β -stanols (coprostanol, epi-coprostanol, 24-ethylcoprostanol, and 24-ethylepicoprostanol) in dung, differentiated three ungulate groups typified by moose (Fig. 4.3, cluster 1), pronghorn (Fig. 4.3, cluster 2), and elk and bison (Fig. 4.3, cluster 3). Bison and elk were not differentiated by their 5β -stanol profiles alone. The 5β -stanol profiles of ungulates form a gradient defined by the proportion of 24-ethylcoprostanol and 24-ethylepicoprostanol versus coprostanol and epi-coprostanol. Moose dung contained the greatest proportions of 24-ethylepicoprostanol. Mule deer and pronghorn dung had relatively high levels of 24-ethylcoprostanol. The dung of elk and bison was higher in coprostanol than mule deer and moose, and elk dung contained relatively high quantities of epi-coprostanol.

The 5β -stanol signature of the lake-sediment samples most closely resembles that of elk and bison throughout the record (Fig. 4.3 D, cluster 3). These two genera, however, could not be distinguished. Pronghorn and mule deer likely contributed modestly to the 5β -stanol composition of the sediment, with greatest relative contributions around *c.* 2000 CE (Fig. 4.3 D, cluster 2). Moose were not well represented by the lake sediment 5β -stanol signature, indicating little to no local presence in the Buffalo Ford catchment over the past two millennia (Fig. 4.3 D, cluster 1).

Influxes of zoostanols and bile acids were generally low and stable throughout the sediment record (BF19; Fig. 4.4) until the mid to late 19th century, when influxes increased

dramatically and peaked in the early 20th century (Appendix C Sup. Fig. 4.2). Fecal steroid influxes remained variable but generally decreased, approaching long-term averages into the 21st century (Fig. 4.5).

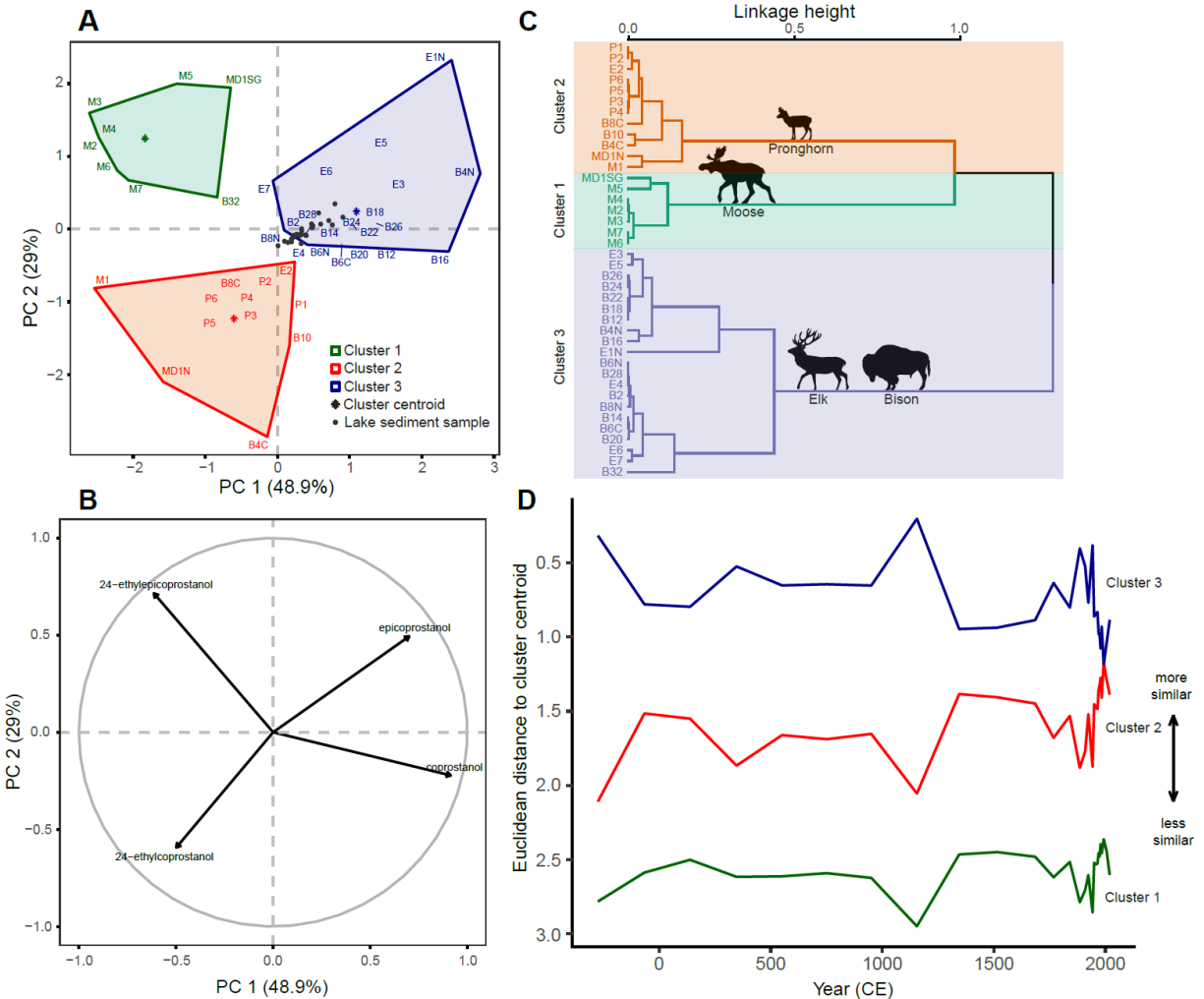


Figure 4.3. Characterization of 5 β -stanol profiles of sediments from Buffalo Ford Lake, YNP, Wyoming in relation to the dung profiles of local ungulates. (A) PCA score plot of 5 β -stanols in dung, with lake sediment samples as supplementary observations. Clusters are defined by HCPC (panel C). (B) PCA correlation circle depicting correlation between the first two principal components the relative abundance of 5 β -stanols. (C) HCPC dendrogram of 5 β -stanol distributions for individual ungulate dung samples. (D) Euclidean distance of lake-sediment samples to cluster centroids (from panel A). Shorter distance indicates greater similarity (note the y-axis reversal).

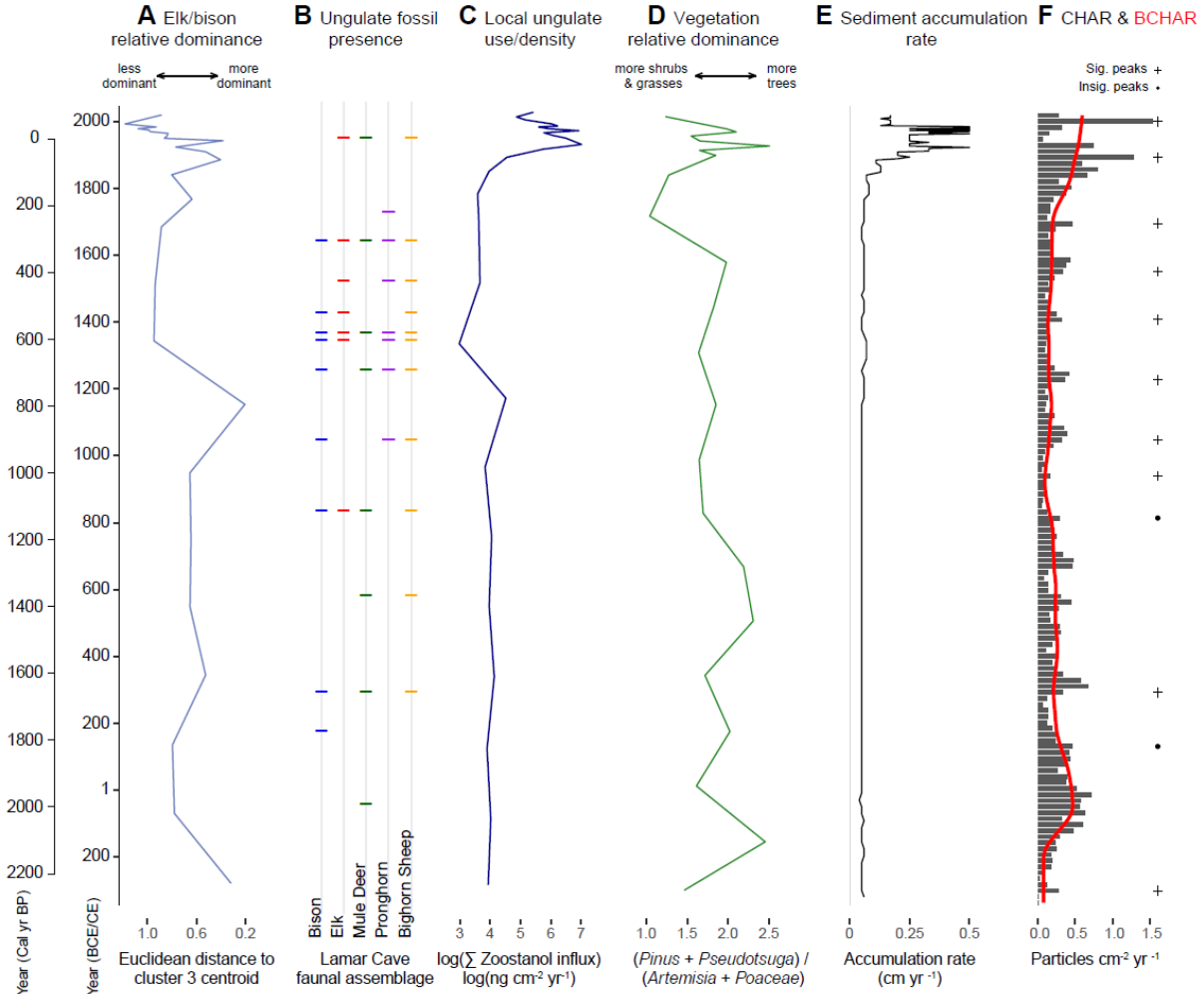


Figure 4.4. Evolution of (A) relative elk/bison dominance at Buffalo Ford Lake, (B) ungulate fossil presence at Lamar Cave, (C) local ungulate use/density at Buffalo Ford Lake, (D) pollen-inferred vegetation dominance, (E) sediment accumulation rate, and (F) charcoal accumulation rates and long-term CHAR trends (red line; loess smoother; window = 500). Significant (+) and insignificant (•) charcoal peaks throughout the last 2300 years identify past fire-episodes.

Pollen

The pollen record indicates that the vegetation around Buffalo Ford Lake experienced only minor fluctuations in relative dominance and limited species turnover during the past *c.* 2300 years (Appendix C Sup. Fig. 4.2). *Pinus* and *Pseudotsuga* were the dominant conifers throughout the record. *Poaceae* and *Artemisia* were well represented in the pollen record (10–30%) but their relative abundance was inversely correlated among samples. *Populus* only

appears sporadically in the BF19 pollen record. *Salix* percentages fluctuated over time, with a general decline towards present.

Conifer (*Pinus* and *Pseudotsuga*) percentages relative to those of shrubs (*Artemisia*) and grasses (*Poaceae*) peaked above the long-term average twice during the 20th century (Fig. 4.5). The first peak occurred at *c.* 1930 and the second at *c.* 1970. *Salix* percentages remained below the long-term average throughout the 20th century and slightly declined toward the present (Fig. 4.5).

Charcoal

The charcoal record indicates variable fire activity over the last 2300 years at Buffalo Ford Lake. Background charcoal (BCHAR), which indicates extra-local biomass burning trends, was relatively high *c.* 2000 cal yr BP. BCHAR then declined to a record minimum *c.* 1000 cal yr BP, and gradually increased over the next 800 years until charcoal accumulation rapidly increased from 200 cal yr BP to present. Local fires, indicated by significant peaks, were infrequent between 2200-1000 cal yr BP, with only two significant peaks occurring during this period. Local fires then become more frequent from 1000 cal yr BP to present with a mean fire return interval of <100 years (Fig. 4.4).

Discussion

Analyses of fecal steroid signatures of ungulate species provide new information on herbivore-ecosystem dynamics over two millennia in the Yellowstone Northern Range. Comparison of 5 β -stanol signatures of lake sediments and ungulates shows long-term variations in ungulate dominance. Results suggest that elk and/or bison were the dominant herbivores in the

Buffalo Ford Lake area over the past *c.* 2300 years (Fig. 4.3 A & D). The initial low zoostanols influxes indicate that local elk/bison densities were relatively low and stable before the establishment of Yellowstone National Park in the late 19th century (Fig 4.4).

The ungulate fossil assemblage of nearby Lamar Cave (2.5 km from Buffalo Ford Lake on the rocky banks of the Lamar River) covers the same time span as BF19 (dated to *c.* 1200 BCE, 3200 cal yr BP), includes bison, elk, mule deer, pronghorn, and bighorn sheep (Hadly, 1996). The ungulate composition of Lamar Cave may be biased by the behavior of carnivores and scavengers that transported bones to the cave but nonetheless, the site indicates that elk may have become more abundant in the last *c.* 300 years (levels 1-3). Low quantities of bison specimens (1-2) occur in most stratigraphic levels of Lamar Cave, but none were detected within modern-dated levels. In contrast, white-tailed deer and moose are not locally abundant at present (Appendix C Sup. Table 4.1) and not detected in the Lamar Cave faunal record. Bighorn sheep were locally present at Lamar Cave and likely occupied the rocky cliffs along the Lamar River or at higher elevations instead of the forest, steppe, and wetlands around Buffalo Ford Lake.

By comparing 5 β -stanols with historical and paleoenvironmental proxy data, we detect in the sedimentary record some of the probable environmental impacts of herbivores in the Yellowstone Northern Range. Two 20th century peaks in 5 β -stanol influx correspond to documented periods of high ungulate density in the lower Lamar Valley. The first and largest 20th century 5 β -stanol peak at 1923 (2 σ 1914, 1929 CE) coincides with record high elk populations that peaked in 1915 with an estimated 37,000+ individuals (Evans, 1939). Historical documents indicate that predator suppression and hunting bans led to irruptive elk population growth (Fig. 4.5; Evans, 1939; Rush, 1933), although it should be noted that population trends

before this time are poorly documented. High fecal steroid influxes, rapid sediment accumulation, elevated biogenic silica, and near-record low pollen abundances of forage taxa (e.g., *Poaceae* and *Salix*) at Buffalo Ford Lake are consistent with rapid elk population growth between the 1880s and the 1920s (Fig. 4.5). High ungulate densities were also associated with a ten-fold increase in sediment accumulation rate and elevated biogenic silica, a sign of increased lake production (Fig. 4.5; Engstrom et al., 1991). Engstrom et al. (1991) observed that this phase of increased sediment accumulation likely resulted from in-lake sediment redistribution or increased algal production, and not only increased erosion, because it was not accompanied by a change in sediment composition. Thus, high fecal steroid influxes and regional elk population trends suggest intensive elk use of the watershed in the early 20th century.

The early 20th century fecal steroid peak also coincides with low *Artemisia* and *Poaceae* pollen percentages relative to *Pinus* and *Pseudotsuga* (Fig 4.5). Vegetation monitoring data from this time are insufficient to quantify the effects of ungulate population growth on vegetation composition and structure. However, an official report in 1933 expressed concern about the effects of high ungulate populations on the condition of Yellowstone Northern Range soils and grassland, noting top soil erosion, severe overgrazing, and proliferation of grazing-adapted plants (Rush, 1933).

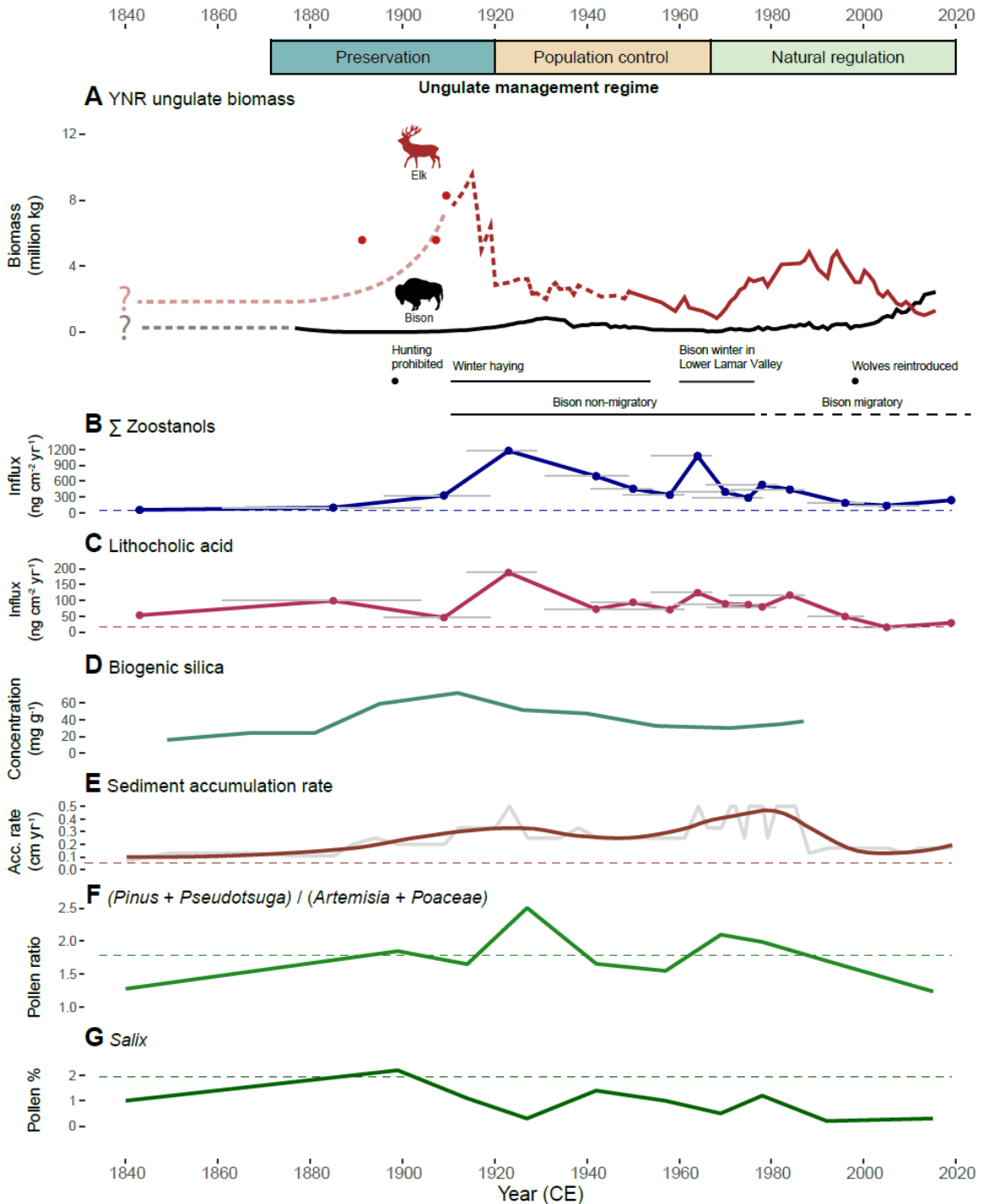


Figure 4.5. Summary of historical Yellowstone Northern Range (YNR) bison and elk management regimes and biomass trends in relation to fecal steroids and associated records of environmental change at Buffalo Ford Lake, YNP, WY. (A) YNR elk (red) and bison (black) biomass trends, based on survey records, with key events noted below. Elk counts before aerial surveys began in 1952 are considered less reliable (dashed line). Hypothetical pre-survey trends are indicated with question marks (transparent dashed lines). (B) Influx of total zoostanols (sum

of 24-ethylcoprostanol, 24-ethylepicoprostanol, coprostanol, and epicoprostanol). (C) Influx of lithocholic acid. Horizontal gray lines in panels B and C indicate age uncertainty (95% confidence range) associated with sample depths. (D) Biogenic silica concentration from BF87 (Engstrom et al., 1991) show changes in algal production. (E) Sediment accumulation rates based on BF19 & BF87 composite age-depth model (gray line), with loess smoother (light brown), marking periods of increased lake productivity and/or sediment redeposition. (F) Ratio of pollen percentage of locally dominant trees (*Pinus* & *Pseudotsuga*) to sagebrush and grasses (*Artemisia* & *Poaceae*). (G) *Salix* pollen percentage. The dashed horizontal lines in all plots indicate long-term means from 340 BCE to 1850 CE.

The harsh winter of 1919-20 reduced the elk population by approximately 60% to ~11,000 individuals (Rush, 1933). Subsequent concerns over ungulate overpopulation and habitat degradation led to a culling program, which resulted in progressive reductions in elk and bison populations between 1931-1967 (Fig. 4.5; Eberhardt et al., 2007; National Research Council et al., 2002). Fecal steroid influxes generally show a negative trend during the culling period, with the notable exception of a peak in stanols in 1964 (2 σ 1954, 1967 CE) that mark a temporary increase in local ungulate use (Fig. 4.5).

After winter haying at the Lamar Buffalo Ranch ceased in 1952, the primary bison winter range shifted to the lower Lamar Valley, where Buffalo Ford Lake is located (Fig. 4.1; Meagher, 1973). This area served as the herd's wintering grounds through the 1960s and early 1970s, until the winter of 1975-1976 when harsh winter conditions drove bison migration to lower elevation (Meagher, 1989, 1973). This period of high local bison use in the Buffalo Ford area from the late 1950s-early 1970s may account for the second 20th century decline in *Poaceae* and *Artemisia* pollen abundance (Fig. 4.5). It seems likely that high local herbivore densities reduced grass and sagebrush dominance and erosion or nutrient deposition may have increased sediment accumulation rates on multiple occasions during the 20th century.

After the 1940s, the lake-sediment 5β -stanol signatures shift away from the bison and elk cluster (Fig. 4.3), indicating that local bison and elk dominance slightly declined in recent decades. This change corresponds with declines in fecal steroid influxes and sediment accumulation rates (Fig. 4.5). The cessation of winter haying in 1952, the resumption of bison migration in 1975, and the reintroduction of wolves in 1995 may have contributed to reduced local bison and elk use (see Table 4.2 for a timeline of key historical events).

Table 4.2. Timeline of events relating to elk and bison in Yellowstone National Park, adapted from National Research Council et al. (2002).

Year/Period	Event
1860s	Bison in Paradise Valley exterminated (Meagher, 1989)
1872	Yellowstone National Park established by Organic Act
1869-1883	Extensive market hunting reduced populations of ungulates and carnivores (Yellowstone National Park, 1997)
1884	Public hunting within YNP prohibited by Lacey Act
1886	U.S. Calvary assigned to protect park; beginning of effective control of hunting (Yellowstone National Park, 1997)
1890s	Bison absent from Northern Range (Meagher, 1989)
1900-1935	Intensive predator control; wolves extirpated (Yellowstone National Park, 1997)
1902	Few bison remained in YNP; population supplemented with domestic herds (Meagher, 1973)
1907-1915	Bison day-herded and fenced at Lamar Ranger Station Buffalo Ranch (Meagher, 1973)
1907-1951	Winter haying in Lamar Valley (Meagher, 1989)
1918	U.S. National Park Services assumed control of Yellowstone National Park
1920s	Increasing concern about overgrazing; active management to control elk population
1920-1960	Intensive ungulate population control (Yellowstone National Park, 1997)
1923-1929	Elk removed primarily by hunting outside park boundaries
1930s-present	Limited recruitment of aspen in Northern Range
1952	Beginning of aerial elk surveys (National Research Council et al., 2002)
1960s-1970s	Bison winter in Lower Lamar Valley (Meagher, 1989, 1973)
1968	YNP adopts “natural regulation” policy; intensive management of elk and bison ends (Cole, 1971)
1975-1976	Bison migrations begin again resulting in range expansion (Meagher, 1989)
1988	Extensive fires in Yellowstone National Park
1995	Reintroduction of wolves

The shifts in fecal steroid influx in response to ungulate population size and behavior are illustrative of the applications and limitations of fecal steroid biomarkers. Although landscape-level population size is an important driver of local ungulate use, ungulates generally use landscapes unevenly. Large herbivores may concentrate in or avoid specific areas in response to predator pressure, forage availability and quality, water distribution, thermal regulation needs, or other factors (Anderson et al., 2005; Mao et al., 2005; Payne et al., 2020). Additionally, shifting seasonal migration patterns over time can change spatial occupancy and local densities. For example, the Lamar River valley was a primary wintering area for Yellowstone elk in the 1960s, yet no wintering elk were observed there in 2007-2008 (White et al., 2010). Fecal steroids in lake sediments within small catchments are unlikely to match landscape-scale population dynamics and should be primarily interpreted as indicators of local ungulate abundance and use.

Although we assume that most fecal steroids found in the lake sediments were leached from dung and transported from uplands via overland flow or originated in dung deposited directly along the lake margins, there are other potential sources to consider. In the Yellowstone Northern Range, ungulates often expire on the frozen lake surface during winter, fall through ice, or become mired in floating vegetation mats along lake margins. These decomposing carcasses release substantial quantities of fecal steroids (von der Lühne et al., 2018). Further study is needed to quantify the relative fecal steroid contributions of dung and carcasses to lake sediments.

To our knowledge, the fecal steroid profiles of bison, elk, pronghorn, and mule deer have not been previously characterized. Our results show that the dung of many North American ungulate species can be identified by broad-spectrum fecal-steroid characterization. Multivariate

analysis of sterols, stanones, and stanols with secondary bile acids resulted in complete differentiation of sampled species, except elk and bison (Fig. 4.2). Although this approach is not suitable for fecal source identification of mixed sediments (e.g., soils and lake sediments) due to the inclusion of compounds that have significant non-animal environmental sources, it would be useful for discerning sources of materials with unmixed fecal components, such as coprolites. Our fecal steroid analysis shows that, like Eurasian moose, North American moose dung is characterized by exceptionally high relative levels of 24-ethylcoprostanol and 24-ethylepicoprostanol (Harrault et al., 2019).

Knowledge of past ecological conditions is an important reference for restoration efforts, natural resource management, and scientific inquiry, yet pre-20th century animal populations and their dynamics are poorly understood. Population data from protected areas are often used to establish historical baselines because human impacts in such places are considered low (e.g., Pachzelt et al., 2013; Pedersen et al., 2023). However, our results demonstrate how contemporary animal population densities within protected areas, especially those lacking predators, like Yellowstone National Park before the reintroduction of wolves, can differ dramatically from long-term averages. Further development of sedimentary fecal biomarker records can shed light on prehistoric herbivore communities and thereby inform ecological conservation and restoration initiatives.

Conclusions

Fecal steroid biomarkers in lake sediments are promising tools to help managers and conservationists understand native ungulate population dynamics through time. While written records in the Americas are limited to the past several hundred years, sediments containing fecal

steroids extend to the Pleistocene and beyond. Analysis of the Buffalo Ford Lake record demonstrates how such records can be used to identify variability in species dominance, local abundance, and environmental impacts at sub-decadal to millennial timescales. The Buffalo Ford Lake record provides important context for understanding local ungulate population responses to evolving land uses and management approaches since the arrival of Euro-Americans. Specifically, our results point to two millennia of continuous presence of elk and bison and exceptionally high densities of these ungulates in the 20th century at a small catchment in the Yellowstone Northern Range.

This study establishes proof of concept for the application of fecal steroids for lake-sediment reconstructions of wild paleoherbivore identity and abundance. Additional calibration studies are needed to evaluate the sensitivity of fecal steroids to fluctuations in herbivore use. Further development of biomarker reference databases will help characterize intra- and interspecies variability and thereby improve differentiation. Future research comparing new records of past ungulate populations from fecal steroid biomarkers with changes in a host of ecosystem properties and conditions can provide key insights into how dominant paleoherbivores shaped and interacted with ecosystems, and how changes to herbivore communities and densities have impacted ecosystem dynamics. Because herds of large herbivores operate at landscape to regional scales, multi-site networks are needed to fully characterize past herbivore dynamics. Continued development of fecal steroid records can address critical questions about the historic role of bison, elk, and other ungulates in the Yellowstone Northern Range and beyond.

CHAPTER FIVE

CONCLUSION TO DISSERTATION

Summary

Methodological advancements are opening new horizons in the study of paleoherbivores. In this dissertation I leverage recent advances in the analysis of dated fossil bone deposits and molecular biomarkers to develop new paleoherbivore records. As I have shown, such records can help address key questions about herbivore ecology and help tell the stories of ecologically and culturally significant species like bison.

As shown in Chapters 2 & 3, radiocarbon dates associated with fossil bones provide critical information about the geographic distribution and relative abundance of common animals at regional to continental scales. When linked with environmental datasets, such reconstructions can be used to understand how species responded to changing environmental conditions in the long term (Chapter 2) and how species interact with and actively shape ecosystems (Chapter 3). Paleoenvironmental data repositories facilitate advances in paleo-informatics and paleo-analytics and promise to generate further insights from the fossil record.

In general, analysis of molecular biomarkers in lake sediments is in its early stages and many questions remain about applications and limitations. Chapter 4 demonstrates how molecular biomarkers can document the local presence of large herbivores and provide information about their ecosystem impacts. In the Yellowstone Northern Range, variability in fecal steroid signatures of different species allows for characterization of dominant species within a small watershed. When compared with other paleoenvironmental proxies (pollen,

charcoal, geochemistry, and diatoms), the data showed the changes in ungulate abundance altered the vegetation and possibly the lake. Further work is needed to develop comprehensive fecal steroid databases that include more species and more samples to better characterize intraspecies variability. Development of more lake sediment records in the Yellowstone Northern Range will expand inference from watershed to regional scales. Additionally, better interpretation of sedimentary fecal biomarkers requires improved understanding of their dispersal pathways and taphonomy.

Significance

This dissertation highlights the role of herbivores in North America broadly, and in rangeland and forest transition ecosystems in particular, prior to Euro-American modification. Large herbivores drive critical trophic and non-trophic processes that shaped subsequent ecological interactions and dynamics across a range of timescales. Without reliable paleoherbivore reconstructions, long-term herbivore-environment interactions have been largely left to speculation. This can have unintended and sometimes unfortunate consequences for rangeland management.

Information on the role of large herbivores in past ecosystems shapes our understanding of how those ecosystems once functioned and influence decisions as to how they should be managed today. For example, the view espoused by Mack and Thompson (1982), that large herbivores were absent from the Intermountain West, and therefore native plant communities were not adapted to grazing, is widely held among scientists, managers, and conservationists. This claim is used to argue for the reduction or elimination of populations of domestic, feral, and wild ungulates that currently inhabit the steppes west of the Rocky Mountains. Yet, a

comprehensive survey of the postglacial bison fossil record demonstrates that bison herds were more common in western US ecosystems than previously thought (Chapter 2). This calls into question widely held assumptions about the historic role of large grazing animals in sagebrush and salt desert scrub systems in the Intermountain West (Perryman et al., 2021), and raises a new compelling question: How did these apparently fragile systems persist in spite of herbivore disturbance?

The notion that bison were historically abundant in eastern forests and woodlands is also popular among some scientists, managers, and conservationists, yet it too appears to be similarly mistaken, based on the fossil record. This view of abundant eastern bison is advanced by proponents of alternative grazing systems, who claim that conventional grazing practices produce poor ecological outcomes because such systems fail to emulate the way bison would have grazed (Green Cover Seed, 2022). Instead, they argue, adaptive multi-paddock grazing, a high-density, short-duration rotational grazing scheme, produces more desirable ecological outcomes because it creates intense temporary disturbances that are then permitted sufficient time to recover. Although this grazing strategy may replicate historical bison behavior in some settings, this approach is being promoted in systems, such as eastern hardwood forests (Apfelbaum et al., 2022; Mosier et al., 2021), where the fossil record suggests that bison likely did not have persistent populations during most of the Holocene (Chapter 2). Furthermore, habitat reconstructions of fossil bison in the Ohio River valley indicate that bison there likely did not congregate in large herds to graze open patches of grassy forage. Instead, they kept to valley bottoms and fed primarily on browse (Widga, 2006). In addition, focusing on grazing to restore disturbance patterns to ecosystems in eastern North America overlooks the historical importance

of fire, which dominated biomass consumption throughout the region during the Holocene (Chapter 3).

There is perhaps no better example of efforts to preserve the native fauna observed by Lewis and Clark on their 1804 journey than Yellowstone National Park. Yet even there, predator extirpation and supplemental feeding in the early and middle 20th century, based on a naïve understanding of herbivore population ecology, resulted in spectacular population instability and threatened the integrity of the forage base (Rush, 1933). Given the paucity of fossil bone deposits, scientists and managers have only inferred the nature of long-term ungulate population dynamics in the Yellowstone Northern Range (National Research Council et al., 2002), and left understanding of the historical abundance and relative dominance of ungulates to speculation. However, fecal steroid biomarkers in lake sediments now provide a means to reconstruct temporal changes in herbivore dominance and density within a specific catchment (Chapter 4). With this discovery and recent innovations in isotope analysis, the stage is set to reconstruct past ungulate abundance, community dynamics, migrations, and ecological impacts in the entire Yellowstone Northern Range through time.

REFERENCES CITED

- Adams, K.D., Rhodes, E.J., 2019. Late Pleistocene to present lake-level fluctuations at Pyramid and Winnemucca lakes, Nevada, USA. *Quaternary Research* 92, 146–164.
<https://doi.org/10.1017/qua.2018.134>
- Agrawal, A.A., 2000. Overcompensation of plants in response to herbivory and the by-product benefits of mutualism. *Trends in Plant Science* 5, 309–313.
[https://doi.org/10.1016/S1360-1385\(00\)01679-4](https://doi.org/10.1016/S1360-1385(00)01679-4)
- Allred, B.W., Fuhlendorf, S.D., Engle, D.M., Elmore, R.D., 2011. Ungulate preference for burned patches reveals strength of fire–grazing interaction. *Ecol Evol* 1, 132–144.
<https://doi.org/10.1002/ece3.12>
- Alt, M., McWethy, D.B., Everett, R., Whitlock, C., 2018. Millennial scale climate–fire–vegetation interactions in a mid-elevation mixed coniferous forest, Mission Range, northwestern Montana, USA. *Quaternary Research* 90, 66–82.
<https://doi.org/10.1017/qua.2018.25>
- Anderson, D.P., Forester, J.D., Turner, M.G., Frair, J.L., Merrill, E.H., Fortin, D., Mao, J.S., Boyce, M.S., 2005. Factors influencing female home range sizes in elk (*Cervus elaphus*) in North American landscapes. *Landscape Ecology* 20, 257–271.
<https://doi.org/10.1007/s10980-005-0062-8>
- Anderson, R.C., 2006. Evolution and origin of the Central Grassland of North America: climate, fire, and mammalian grazers. *The Journal of the Torrey Botanical Society* 133, 626–647.
[https://doi.org/10.3159/1095-5674\(2006\)133\[626:EAOOTC\]2.0.CO;2](https://doi.org/10.3159/1095-5674(2006)133[626:EAOOTC]2.0.CO;2)
- Apfelbaum, S.I., Thompson, R., Wang, F., Mosier, S., Teague, R., Byck, P., 2022. Vegetation, water infiltration, and soil carbon response to Adaptive Multi-Paddock and Conventional grazing in Southeastern USA ranches. *Journal of Environmental Management* 308, 114576. <https://doi.org/10.1016/j.jenvman.2022.114576>
- Archibald, S., Bond, W.J., Stock, W.D., Fairbanks, D.H.K., 2005. Shaping the Landscape: Fire–Grazer Interactions in an African Savanna. *Ecological Applications* 15, 96–109.
<https://doi.org/10.1890/03-5210>
- Archibald, S., Hempson, G.P., 2016. Competing consumers: contrasting the patterns and impacts of fire and mammalian herbivory in Africa. *Philosophical Transactions of the Royal Society B: Biological Sciences* 371, 20150309. <https://doi.org/10.1098/rstb.2015.0309>
- Archibald, S., Hempson, G.P., Lehmann, C., 2019. A unified framework for plant life-history strategies shaped by fire and herbivory. *New Phytologist* 224, 1490–1503.
<https://doi.org/10.1111/nph.15986>
- Archibald, S., Lehmann, C.E.R., Gómez-Dans, J.L., Bradstock, R.A., 2013. Defining pyromes and global syndromes of fire regimes. *PNAS* 110, 6442–6447.
<https://doi.org/10.1073/pnas.1211466110>

- Argiriadis, E., Battistel, D., McWethy, D.B., Vecchiato, M., Kirchgeorg, T., Kehrwald, N.M., Whitlock, C., Wilmschurst, J.M., Barbante, C., 2018. Lake sediment fecal and biomass burning biomarkers provide direct evidence for prehistoric human-lit fires in New Zealand. *Scientific Reports* 8. <https://doi.org/10.1038/s41598-018-30606-3>
- Augustine, D.J., Derner, J.D., Milchunas, D.G., 2010. Prescribed Fire, Grazing, and Herbaceous Plant Production in Shortgrass Steppe. *rama* 63, 317–323. <https://doi.org/10.2111/REM-D-09-00044.1>
- Baker, A.G., Bhagwat, S.A., Willis, K.J., 2013. Do dung fungal spores make a good proxy for past distribution of large herbivores? *Quaternary Science Reviews* 62, 21–31. <https://doi.org/10.1016/j.quascirev.2012.11.018>
- Bårdsen, B.-J., Tveraa, T., 2012. Density-dependence vs. density-independence – linking reproductive allocation to population abundance and vegetation greenness. *Journal of Animal Ecology* 81, 364–376. <https://doi.org/10.1111/j.1365-2656.2011.01913.x>
- Barnosky, C.W., 1989. Postglacial vegetation and climate in the northwestern Great Plains of Montana. *Quaternary Research* 31, 57–73. [https://doi.org/10.1016/0033-5894\(89\)90085-9](https://doi.org/10.1016/0033-5894(89)90085-9)
- Barnosky, E.H., 1996. Late Holocene Mammalian Fauna of Lamar Cave and its Implications for Ecosystem Dynamics in Yellowstone National Park (Technical Report No. NPS/NRYELL/NRTR/96-01), Effects of Grazing by Wild Ungulates in Yellowstone National Park. National Park Service, Denver, Colorado.
- Bar-On, Y.M., Phillips, R., Milo, R., 2018. The biomass distribution on Earth. *Proceedings of the National Academy of Sciences* 115, 6506–6511. <https://doi.org/10.1073/pnas.1711842115>
- Battistel, D., Piazza, R., Argiriadis, E., Marchiori, E., Radaelli, M., Barbante, C., 2015. GC-MS method for determining faecal sterols as biomarkers of human and pastoral animal presence in freshwater sediments. *Anal Bioanal Chem* 407, 8505–8514. <https://doi.org/10.1007/s00216-015-8998-2>
- Befus, K.M., Darhower, S., Liefert, D.T., Shuman, B.N., 2020. Reconstructing the groundwater recharge history for the Plymouth-Carver Aquifer Massachusetts, USA. *Quaternary International, Groundwater and global paleoclimate signals* 547, 101–112. <https://doi.org/10.1016/j.quaint.2019.06.026>
- Bennett, K.D., Willis, K.J., 2001. Pollen, in: Smol, J.P., Birks, H.J.B., Last, W.M., Bradley, R.S., Alverson, K. (Eds.), *Tracking Environmental Change Using Lake Sediments: Terrestrial, Algal, and Siliceous Indicators, Developments in Paleoenvironmental Research*. Springer Netherlands, Dordrecht, pp. 5–32. https://doi.org/10.1007/0-306-47668-1_2
- Bennett, M.R., Bustos, D., Pigati, J.S., Springer, K.B., Urban, T.M., Holliday, V.T., Reynolds, S.C., Budka, M., Honke, J.S., Hudson, A.M., Fenerty, B., Connelly, C., Martinez, P.J.,

- Santucci, V.L., Odess, D., 2021. Evidence of humans in North America during the Last Glacial Maximum. *Science* 373, 1528–1531. <https://doi.org/10.1126/science.abg7586>
- Beschta, R.L., Ripple, W.J., Kauffman, J.B., Painter, L.E., 2020. Bison limit ecosystem recovery in northern Yellowstone. *Food Webs* 23, e00142. <https://doi.org/10.1016/j.fooweb.2020.e00142>
- Beumer, L.T., Pohle, J., Schmidt, N.M., Chimienti, M., Desforges, J.-P., Hansen, L.H., Langrock, R., Pedersen, S.H., Stelvig, M., van Beest, F.M., 2020. An application of upscaled optimal foraging theory using hidden Markov modelling: year-round behavioural variation in a large arctic herbivore. *Movement Ecology* 8, 25. <https://doi.org/10.1186/s40462-020-00213-x>
- Bevan, A., Crema, E.R., 2018. rcarbon: Methods for calibrating and analysing radiocarbon dates.
- Birk, J.J., Dippold, M., Wiesenberg, G.L.B., Glaser, B., 2012. Combined quantification of faecal sterols, stanols, stanones and bile acids in soils and terrestrial sediments by gas chromatography–mass spectrometry. *Journal of Chromatography A* 1242, 1–10. <https://doi.org/10.1016/j.chroma.2012.04.027>
- Blaauw, M., Christen, J.A., 2011. Flexible paleoclimate age-depth models using an autoregressive gamma process. *Bayesian Anal.* 6, 457–474. <https://doi.org/10.1214/11-BA618>
- Bond, W.J., 2005. Large parts of the world are brown or black: A different view on the ‘Green World’ hypothesis. *Journal of Vegetation Science* 16, 261–266. <https://doi.org/10.1111/j.1654-1103.2005.tb02364.x>
- Bond, W.J., Keeley, J.E., 2005. Fire as a global ‘herbivore’: the ecology and evolution of flammable ecosystems. *Trends in Ecology & Evolution* 20, 387–394. <https://doi.org/10.1016/j.tree.2005.04.025>
- Bond, W.J., Scott, A.C., 2010. Fire and the spread of flowering plants in the Cretaceous. *New Phytologist* 188, 1137–1150. <https://doi.org/10.1111/j.1469-8137.2010.03418.x>
- Broughton, J.M., Weitzel, E.M., 2018. Population reconstructions for humans and megafauna suggest mixed causes for North American Pleistocene extinctions. *Nature Communications* 9, 5441. <https://doi.org/10.1038/s41467-018-07897-1>
- Bruegger, R.A., Varelas, L.A., Howery, L.D., Torell, L.A., Stephenson, M.B., Bailey, D.W., 2016. Targeted Grazing in Southern Arizona: Using Cattle to Reduce Fine Fuel Loads. *Rangeland Ecology & Management* 69, 43–51. <https://doi.org/10.1016/j.rama.2015.10.011>
- Bull, I.D., Betancourt, P.P., Evershed, R.P., 1999a. Chemical evidence for a structured agricultural manuring regime on the island of Pseira, Crete during the Minoan period.

Meletemata: Studies in Aegean Archaeology (AEGAEUM 20 Annales d'archeologie egeene de l'Universite de Liege et UT-PASP 69–72.

- Bull, I.D., Evershed, R.P., Betancourt, P.P., 2001. An organic geochemical investigation of the practice of manuring at a Minoan site on Pseira Island, Crete. *Geoarchaeology* 16, 223–242. [https://doi.org/10.1002/1520-6548\(200102\)16:2<223::AID-GEA1002>3.0.CO;2-7](https://doi.org/10.1002/1520-6548(200102)16:2<223::AID-GEA1002>3.0.CO;2-7)
- Bull, I.D., Lockheart, M.J., Elhmmali, M.M., Roberts, D.J., Evershed, R.P., 2002. The origin of faeces by means of biomarker detection. *Environment International* 27, 647–654. [https://doi.org/10.1016/S0160-4120\(01\)00124-6](https://doi.org/10.1016/S0160-4120(01)00124-6)
- Bull, I.D., Simpson, I.A., van Bergen, P.F., Evershed, R.P., 1999b. Muck 'n' molecules: organic geochemical methods for detecting ancient manuring. *Antiquity* 73, 86–96. <https://doi.org/10.1017/S0003598X0008786X>
- Busby, W.H., Brecheisen, W.R., 1997. Chorusing Phenology and Habitat Associations of the Crawfish Frog, *Rana areolata* (Anura: Ranidae), in Kansas. *The Southwestern Naturalist* 42, 210–217.
- Bush, M.B., Conrad, S., Restrepo, A., Thompson, D.M., Lofverstrom, M., Conroy, J.L., 2022. Human-induced ecological cascades: Extinction, restoration, and rewilding in the Galápagos highlands. *Proceedings of the National Academy of Sciences* 119, e2203752119. <https://doi.org/10.1073/pnas.2203752119>
- Byers, D.A., Broughton, J.M., 2004. Holocene Environmental Change, Artiodactyl Abundances, and Human Hunting Strategies in the Great Basin. *American Antiquity* 69, 235–255. <https://doi.org/10.2307/4128418>
- Byers, D.A., Smith, C.S., 2007. Ecosystem controls and the archaeofaunal record: an example from the Wyoming Basin, USA. *The Holocene* 17, 1171–1183. <https://doi.org/10.1177/0959683607085122>
- Camill, P., Umbanhowar, C.E., Teed, R., Geiss, C.E., Aldinger, J., Dvorak, L., Kenning, J., Limmer, J., Walkup, K., 2003. Late-glacial and Holocene climatic effects on fire and vegetation dynamics at the prairie–forest ecotone in south-central Minnesota. *Journal of Ecology* 91, 822–836. <https://doi.org/10.1046/j.1365-2745.2003.00812.x>
- Campos, P.F., Willerslev, E., Sher, A., Orlando, L., Axelsson, E., Tikhonov, A., Aaris-Sørensen, K., Greenwood, A.D., Kahlke, R.-D., Kosintsev, P., Krakhmalnaya, T., Kuznetsova, T., Lemey, P., MacPhee, R., Norris, C.A., Shepherd, K., Suchard, M.A., Zazula, G.D., Shapiro, B., Gilbert, M.T.P., 2010. Ancient DNA analyses exclude humans as the driving force behind late Pleistocene musk ox (*Ovibos moschatus*) population dynamics. *PNAS* 107, 5675–5680. <https://doi.org/10.1073/pnas.0907189107>
- Cannon, K., 2001. What the Past Can Provide: Contribution of Prehistoric Bison Studies to Modern Bison Management. *Great Plains Research* 11.

- Carreira, R.S., Wagener, A.L.R., Readman, J.W., 2004. Sterols as markers of sewage contamination in a tropical urban estuary (Guanabara Bay, Brazil): space–time variations. *Estuarine, Coastal and Shelf Science* 60, 587–598. <https://doi.org/10.1016/j.ecss.2004.02.014>
- Chan, K.-H., Lam, M.H.W., Poon, K.-F., Yeung, H.-Y., Chiu, T.K.T., 1998. APPLICATION OF SEDIMENTARY FECAL STANOLS AND STEROLS IN TRACING SEWAGE POLLUTION IN COASTAL WATERS. *Water Research* 32, 225–235. [https://doi.org/10.1016/S0043-1354\(97\)00175-9](https://doi.org/10.1016/S0043-1354(97)00175-9)
- Chaput, M.A., Gajewski, K., 2016. Radiocarbon dates as estimates of ancient human population size. *Anthropocene* 15, 3–12. <https://doi.org/10.1016/j.ancene.2015.10.002>
- Chaput, M.A., Kriesche, B., Betts, M., Martindale, A., Kulik, R., Schmidt, V., Gajewski, K., 2015. Spatiotemporal distribution of Holocene populations in North America. *PNAS* 112, 12127–12132. <https://doi.org/10.1073/pnas.1505657112>
- Charles-Dominique, T., Davies, T.J., Hempson, G.P., Bezeng, B.S., Daru, B.H., Kabongo, R.M., Maurin, O., Muasya, A.M., van der Bank, M., Bond, W.J., 2016. Spiny plants, mammal browsers, and the origin of African savannas. *Proceedings of the National Academy of Sciences* 113, E5572–E5579. <https://doi.org/10.1073/pnas.1607493113>
- Chatters, J.C., Campbell, S.K., Smith, G.D., Minthorn, P.E., 1995. Bison Procurement in the Far West: A 2,100-Year-Old Kill Site on the Columbia Plateau. *American Antiquity* 60, 751–763. <https://doi.org/10.2307/282056>
- Churkina, G., Running, S.W., 1998. Contrasting Climatic Controls on the Estimated Productivity of Global Terrestrial Biomes. *Ecosystems* 1, 206–215. <https://doi.org/10.1007/s100219900016>
- Clark, J.S., Hussey, T.C., 1996. Estimating the mass flux of charcoal from sedimentary records: effects of particle size, morphology, and orientation. *The Holocene* 6, 129–144. <https://doi.org/10.1177/095968369600600201>
- Clark, J.S., Royall, P.D., 1996. Local and Regional Sediment Charcoal Evidence for Fire Regimes in Presettlement North-Eastern North America. *Journal of Ecology* 84, 365–382. <https://doi.org/10.2307/2261199>
- Clark, J.S., Stocks, B.J., Richard, P.J. h., 1996. Climate implications of biomass burning since the 19th century in eastern North America. *Global Change Biology* 2, 433–442. <https://doi.org/10.1111/j.1365-2486.1996.tb00093.x>
- Clauss, M., Steuer, P., Müller, D.W.H., Codron, D., Hummel, J., 2013. Herbivory and Body Size: Allometries of Diet Quality and Gastrointestinal Physiology, and Implications for Herbivore Ecology and Dinosaur Gigantism. *PLoS One* 8. <https://doi.org/10.1371/journal.pone.0068714>

- Clayton, L., 1975. Bison trails and their geologic significance. *Geology* 3, 498–500. [https://doi.org/10.1130/0091-7613\(1975\)3<498:BTATGS>2.0.CO;2](https://doi.org/10.1130/0091-7613(1975)3<498:BTATGS>2.0.CO;2)
- Coe, M.J., Cumming, D.H., Phillipson, J., 1976. Biomass and Production of Large African Herbivores in Relation to Rainfall and Primary Production. *Oecologia* 22, 341–354.
- Cole, G., 1971. An Ecological Rationale for the Natural or Artificial Regulation of Native Ungulates in Parks. U.S. National Park Service Publications and Papers.
- Commerford, J.L., Leys, B., Mueller, J.R., McLauchlan, K.K., 2016. Great Plains vegetation dynamics in response to fire and climatic fluctuations during the Holocene at Fox Lake, Minnesota (USA). *Holocene* 26, 302–313. <https://doi.org/10.1177/0959683615608691>
- Cook, R.C., Cook, J.G., Mech, L.D., 2004. Nutritional Condition of Northern Yellowstone Elk. *Journal of Mammalogy* 85, 714–722. <https://doi.org/10.1644/BRG-131>
- Cooper, J.R., 2008. Bison hunting and Late Prehistoric human subsistence economies in the Great Plains (Ph.D.). Southern Methodist University, United States -- Texas.
- Coppedge, B.R., Shaw, J.H., 1997. Effects of Horning and Rubbing Behavior by Bison (Bison bison) on Woody Vegetation in a Tallgrass Prairie Landscape. *The American Midland Naturalist* 138, 189–196. <https://doi.org/10.2307/2426665>
- Coppock, D.L., Detling, J.K., Ellis, J.E., Dyer, M.I., 1983. Plant-Herbivore Interactions in a North American Mixed-Grass Prairie. I. Effects of Black-Tailed Prairie Dogs on Intra-seasonal Aboveground Plant Biomass and Nutrient Dynamics and Plants Species Diversity. *Oecologia* 56, 1–9.
- Coupland, R.T., 1950. Ecology of Mixed Prairie in Canada. *Ecological Monographs* 20, 271–315. <https://doi.org/10.2307/1943568>
- Cromsigt, J.P.G.M., Olff, H., 2008. Dynamics of grazing lawn formation: an experimental test of the role of scale-dependent processes. *Oikos* 117, 1444–1452. <https://doi.org/10.1111/j.0030-1299.2008.16651.x>
- Daughton, C.G., 2012. Real-time estimation of small-area populations with human biomarkers in sewage. *Sci. Total Environ.* 414, 6–21. <https://doi.org/10.1016/j.scitotenv.2011.11.015>
- Davies, A.L., Harrault, L., Milek, K., McClymont, E.L., Dallimer, M., Hamilton, A., Warburton, J., 2022. A multiproxy approach to long-term herbivore grazing dynamics in peatlands based on pollen, coprophilous fungi and faecal biomarkers. *Palaeogeography, Palaeoclimatology, Palaeoecology* 598, 111032. <https://doi.org/10.1016/j.palaeo.2022.111032>

- Davies, K., Boyd, C., Bates, J., Hulet, A., 2015. Dormant season grazing may decrease wildfire probability by increasing fuel moisture and reducing fuel amount and continuity. <https://doi.org/10.1071/WF14209>
- Delsol, N., Stucky, B.J., Oswald, J.A., Cobb, C.R., Emery, K.F., Guralnick, R., 2023. Ancient DNA confirms diverse origins of early post-Columbian cattle in the Americas. *Sci Rep* 13, 12444. <https://doi.org/10.1038/s41598-023-39518-3>
- Donaldson, J.E., Archibald, S., Govender, N., Pollard, D., Luhdo, Z., Parr, C.L., 2018. Ecological engineering through fire-herbivory feedbacks drives the formation of savanna grazing lawns. *Journal of Applied Ecology* 55, 225–235. <https://doi.org/10.1111/1365-2664.12956>
- Donovan, J.J., Grimm, E.C., 2007. Episodic struvite deposits in a Northern Great Plains flyway lake: indicators of mid-Holocene drought? *The Holocene*. <https://doi.org/10.1177/0959683607082556>
- Durrant, S.D., 1970. Faunal remains as indicators of neothermal climates at Hogup Cave: [Appendix II], in: *Hogup Cave*, [by] C. Melvin Aikens, *Anthropological Papers* (Salt Lake City, Utah). University of Utah Press, pp. 241–245.
- Eberhardt, L.L., White, P.J., Garrott, R.A., Houston, D.B., 2007. A Seventy-Year History of Trends in Yellowstone's Northern Elk Herd. *The Journal of Wildlife Management* 71, 594–602.
- Eglinton, T.I., Eglinton, G., 2008. Molecular proxies for paleoclimatology. *Earth and Planetary Science Letters* 275, 1–16. <https://doi.org/10.1016/j.epsl.2008.07.012>
- Elith, J., Phillips, S.J., Hastie, T., Dudík, M., Chee, Y.E., Yates, C.J., 2011. A statistical explanation of MaxEnt for ecologists: Statistical explanation of MaxEnt. *Diversity and Distributions* 17, 43–57. <https://doi.org/10.1111/j.1472-4642.2010.00725.x>
- Engstrom, D.R., Whitlock, C., Fritz, S.C., Wright, H.E., Jr., 1991. Recent environmental changes inferred from the sediments of small lakes in Yellowstone's northern range. *Journal of Palaeolimnology* 5, 139. <https://doi.org/10.1007/BF00176875>
- Eskelinen, A., Harpole, W.S., Jessen, M.-T., Virtanen, R., Hautier, Y., 2022. Light competition drives herbivore and nutrient effects on plant diversity. *Nature* 611, 301–305. <https://doi.org/10.1038/s41586-022-05383-9>
- Evans, L., 1939. A summary of the history of the Yellowstone elk herd. *Yellowstone Nature Notes* 16, 3–13.
- Fastovich, D., Russell, J.M., Jackson, S.T., Krause, T.R., Marcott, S.A., Williams, J.W., 2020. Spatial Fingerprint of Younger Dryas Cooling and Warming in Eastern North America.

- Geophysical Research Letters 47, e2020GL090031.
<https://doi.org/10.1029/2020GL090031>
- Feurdean, A., 2021. Experimental production of charcoal morphologies to discriminate fuel source and fire type: an example from Siberian taiga. *Biogeosciences* 18, 3805–3821.
<https://doi.org/10.5194/bg-18-3805-2021>
- Fick, S.E., Hijmans, R.J., 2017. WorldClim 2: new 1-km spatial resolution climate surfaces for global land areas. *International Journal of Climatology* 37, 4302–4315.
<https://doi.org/10.1002/joc.5086>
- Fiedel, S., Haynes, G., 2004. A premature burial: Comments on Grayson and Meltzer’s “Requiem for overkill.” *Journal of Archaeological Science - J ARCHAEOLOGICAL SCI* 31.
<https://doi.org/10.1016/j.jas.2003.06.004>
- Filby, S.K., Locke, S.M., Person, M.A., Winter, T.C., Rosenberry, D.O., Nieber, J.L., Gutowski, W.J., Ito, E., 2002. Mid-Holocene Hydrologic Model of the Shingobee Watershed, Minnesota. *Quaternary Research* 58, 246–254. <https://doi.org/10.1006/qres.2002.2377>
- Flores, D., 1991. Bison Ecology and Bison Diplomacy: The Southern Plains from 1800 to 1850. *The Journal of American History* 78, 465. <https://doi.org/10.2307/2079530>
- Fogarty, D.T., Roberts, C.P., Uden, D.R., Donovan, V.M., Allen, C.R., Naugle, D.E., Jones, M.O., Allred, B.W., Twidwell, D., 2020. Woody Plant Encroachment and the Sustainability of Priority Conservation Areas. *Sustainability* 12, 8321.
<https://doi.org/10.3390/su12208321>
- Fordham, D.A., Saltré, F., Haythorne, S., Wigley, T.M.L., Otto-Bliesner, B.L., Chan, K.C., Brook, B.W., 2017. PaleoView: a tool for generating continuous climate projections spanning the last 21 000 years at regional and global scales. *Ecography* 40, 1348–1358.
<https://doi.org/10.1111/ecog.03031>
- Forgacs, D., Wallen, R.L., Dobson, L.K., Derr, J.N., 2016. Mitochondrial Genome Analysis Reveals Historical Lineages in Yellowstone Bison. *PLOS ONE* 11, e0166081.
<https://doi.org/10.1371/journal.pone.0166081>
- Forman, S.L., Marín, L., Gomez, J., Pierson, J., 2008. Late Quaternary eolian sand depositional record for southwestern Kansas: Landscape sensitivity to droughts. *Palaeogeography, Palaeoclimatology, Palaeoecology* 265, 107–120.
<https://doi.org/10.1016/j.palaeo.2008.04.028>
- Forman, S.L., Marin, L., Pierson, J., Gomez, J., Miller, G.H., Webb, R.S., 2005. Aeolian sand depositional records from western Nebraska: landscape response to droughts in the past 1500 years. *The Holocene* 15, 973–981. <https://doi.org/10.1191/0959683605hl871ra>

- Fortin, D., Fortin, M.-E., Beyer, H.L., Duchesne, T., Courant, S., Dancose, K., 2009. Group-size-mediated habitat selection and group fusion–fission dynamics of bison under predation risk. *Ecology* 90, 2480–2490. <https://doi.org/10.1890/08-0345.1>
- Froese, D., Stiller, M., Heintzman, P.D., Reyes, A.V., Zazula, G.D., Soares, A.E.R., Meyer, M., Hall, E., Jensen, B.J.L., Arnold, L.J., MacPhee, R.D.E., Shapiro, B., 2017. Fossil and genomic evidence constrains the timing of bison arrival in North America. *PNAS* 114, 3457–3462. <https://doi.org/10.1073/pnas.1620754114>
- Fuhlendorf, S.D., Engle, D.M., 2004. Application of the fire–grazing interaction to restore a shifting mosaic on tallgrass prairie. *Journal of Applied Ecology* 41, 604–614. <https://doi.org/10.1111/j.0021-8901.2004.00937.x>
- Fuhlendorf, S.D., Engle, D.M., Kerby, J., Hamilton, R., 2009. Pyric Herbivory: Rewilding Landscapes through the Recoupling of Fire and Grazing. *Conservation Biology* 23, 588–598. <https://doi.org/10.1111/j.1523-1739.2008.01139.x>
- Fuller, J.A., 2006. Population demography of the Yellowstone National Park bison herds. Montana State University, Bozeman, MT.
- Gaillard, J.-M., Festa-Bianchet, M., Yoccoz, N.G., Loison, A., Toïgo, C., 2000. Temporal Variation in Fitness Components and Population Dynamics of Large Herbivores. *Annual Review of Ecology and Systematics* 31, 367–393. <https://doi.org/10.1146/annurev.ecolsys.31.1.367>
- Gaines, S.M., Eglinton, G., Rullkotter, J., 2008. *Echoes of Life: What Fossil Molecules Reveal about Earth History*, 1 edition. ed. Oxford University Press, Oxford ; New York.
- Gaskell, S.J., Eglinton, G., 1975. Rapid hydrogenation of sterols in a contemporary lacustrine sediment. *Nature* 254, 209–211. <https://doi.org/10.1038/254209b0>
- Geiss, C., Umbanhowar, C., Camill, P., Banerjee, S., 2003. Sediment magnetic properties reveal Holocene climate change along the Minnesota prairie-forest ecotone. *Journal of Paleolimnology* 30, 151–166. <https://doi.org/10.1023/A:1025574100319>
- Geremia, C., Merkle, J.A., Eacker, D.R., Wallen, R.L., White, P.J., Hebblewhite, M., Kauffman, M.J., 2019. Migrating bison engineer the green wave. *PNAS*. <https://doi.org/10.1073/pnas.1913783116>
- Geremia, C., Wallen, R., White, P.J., 2015. Population Dynamics and Adaptive Management of Yellowstone Bison.
- Giglio, L., Randerson, J.T., Werf, G.R. van der, 2013. Analysis of daily, monthly, and annual burned area using the fourth-generation global fire emissions database (GFED4). *Journal of Geophysical Research: Biogeosciences* 118, 317–328. <https://doi.org/10.1002/jgrg.20042>

- Giguet-Covex, C., Ficetola, G.F., Walsh, K., Poulénard, J., Bajard, M., Fouinat, L., Sabatier, P., Gielly, L., Messenger, E., Develle, A.L., David, F., Taberlet, P., Brisset, E., Guiter, F., Sinet, R., Arnaud, F., 2019. New insights on lake sediment DNA from the catchment: importance of taphonomic and analytical issues on the record quality. *Sci Rep* 9, 14676. <https://doi.org/10.1038/s41598-019-50339-1>
- Giguet-Covex, C., Pansu, J., Arnaud, F., Rey, P.-J., Griggo, C., Gielly, L., Domaizon, I., Coissac, E., David, F., Choler, P., Poulénard, J., Taberlet, P., 2014. Long livestock farming history and human landscape shaping revealed by lake sediment DNA. *Nat Commun* 5, 3211. <https://doi.org/10.1038/ncomms4211>
- Gilbert, M., Nicolas, G., Cinardi, G., Van Boeckel, T.P., Vanwambeke, S.O., Wint, G.R.W., Robinson, T.P., 2018. Global distribution data for cattle, buffaloes, horses, sheep, goats, pigs, chickens and ducks in 2010. *Scientific Data* 5, 180227. <https://doi.org/10.1038/sdata.2018.227>
- Gill, J.L., 2015. Learning from Africa's herbivores. *Science* 350, 1036–1037. <https://doi.org/10.1126/science.aad6760>
- Gill, J.L., Williams, J.W., Jackson, S.T., Lininger, K.B., Robinson, G.S., 2009. Pleistocene megafaunal collapse, novel plant communities, and enhanced fire regimes in North America. *Science* 326, 1100–1103. <https://doi.org/10.1126/science.1179504>
- Goble, R.J., Mason, J.A., Loope, D.B., Swinehart, J.B., 2004. Optical and radiocarbon ages of stacked paleosols and dune sands in the Nebraska Sand Hills, USA. *Quaternary Science Reviews* 23, 1173–1182. <https://doi.org/10.1016/j.quascirev.2003.09.009>
- Goring, S., Dawson, A., Simpson, G., Ram, K., Graham, R., Grimm, E., Williams, J., 2015. neotoma: A Programmatic Interface to the Neotoma Paleoecological Database. *Open Quaternary* 1, Art. 2. <https://doi.org/10.5334/oq.ab>
- Gowan, E.J., Tregoning, P., Purcell, A., Montillet, J.-P., McClusky, S., 2016. A model of the western Laurentide Ice Sheet, using observations of glacial isostatic adjustment. *Quaternary Science Reviews* 139, 1–16. <https://doi.org/10.1016/j.quascirev.2016.03.003>
- Grayson, D.K., 2006. Holocene bison in the Great Basin, western USA. *The Holocene* 16, 913–925. <https://doi.org/10.1191/0959683606hol982fa>
- Green Cover Seed, 2022. Adaptive Multi-Paddock (AMP) Grazing in a Nutshell. NM Healthy Soil Working Group. URL <https://www.nmhealthysoil.org/2022/03/13/adaptive-multi-paddock-amp-grazing-in-a-nutshell/> (accessed 10.23.23).
- Grimalt, J.O., Fernandez, P., Bayona, J.M., Albaiges, J., 1990. Assessment of fecal sterols and ketones as indicators of urban sewage inputs to coastal waters. *Environ. Sci. Technol.* 24, 357–363. <https://doi.org/10.1021/es00073a011>

- Grimm, E.C., Donovan, J.J., Brown, K.J., 2011. A high-resolution record of climate variability and landscape response from Kettle Lake, northern Great Plains, North America. *Quaternary Science Reviews* 30, 2626–2650. <https://doi.org/10.1016/j.quascirev.2011.05.015>
- Groenen, M.A.M., 2016. A decade of pig genome sequencing: a window on pig domestication and evolution. *Genetics Selection Evolution* 48, 23. <https://doi.org/10.1186/s12711-016-0204-2>
- Guillemot, T., Zocatelli, R., Bichet, V., Jacob, J., Massa, C., Le Milbeau, C., Richard, H., Gauthier, E., 2015. Evolution of pastoralism in Southern Greenland during the last two millennia reconstructed from bile acids and coprophilous fungal spores in lacustrine sediments. *Organic Geochemistry* 81, 40–44. <https://doi.org/10.1016/j.orggeochem.2015.01.012>
- Hadly, E.A., 1996. Influence of Late-Holocene Climate on Northern Rocky Mountain Mammals. *Quaternary Research* 46, 298–310. <https://doi.org/10.1006/qres.1996.0068>
- Hairston, N.G., Smith, F.E., Slobodkin, L.B., 1960. Community Structure, Population Control, and Competition. *The American Naturalist* 94, 421–425. <https://doi.org/10.1086/282146>
- Halbert, N.D., Derr, J.N., 2007. A Comprehensive Evaluation of Cattle Introgression into US Federal Bison Herds. *Journal of Heredity* 98, 1–12. <https://doi.org/10.1093/jhered/esl051>
- Halfen, A.F., Johnson, W.C., 2013. A review of Great Plains dune field chronologies. *Aeolian Research* 10, 135–160. <https://doi.org/10.1016/j.aeolia.2013.03.001>
- Halfpenny, J., 2019. *Scats and Tracks of North America: A Field Guide To The Signs Of Nearly 150 Wildlife Species*, Second edition. ed. Falcon Guides, Lanham, MD.
- Hamilton, W.L., 1994. Comment: Recent environmental changes inferred from the sediments of small lakes in Yellowstone's northern range (Engstrom et al., 1991). *J Paleolimnol* 10, 153–157. <https://doi.org/10.1007/BF00682512>
- Harrault, L., Milek, K., Jardé, E., Jeanneau, L., Derrien, M., Anderson, D.G., 2019. Faecal biomarkers can distinguish specific mammalian species in modern and past environments. *PLOS ONE* 14, e0211119. <https://doi.org/10.1371/journal.pone.0211119>
- Hartnett, D.C., Hickman, K.R., Walter, L.E.F., 1996. Effects of Bison Grazing, Fire, and Topography on Floristic Diversity in Tallgrass Prairie. *Journal of Range Management* 49, 413. <https://doi.org/10.2307/4002922>
- Haslewood, G.A.D., 1967. Bile salt evolution. *J. Lipid Res.* 8, 535–550.

- He, F., Shakun, J.D., Clark, P.U., Carlson, A.E., Liu, Z., Otto-Bliesner, B.L., Kutzbach, J.E., 2013. Northern Hemisphere forcing of Southern Hemisphere climate during the last deglaciation. *Nature* 494, 81–85. <https://doi.org/10.1038/nature11822>
- Hedrick, P.W., 2009. Conservation Genetics and North American Bison (*Bison bison*). *Journal of Heredity* 100, 411–420. <https://doi.org/10.1093/jhered/esp024>
- Heide, K., 1984. Holocene pollen stratigraphy from a lake and small hollow in north-central Wisconsin, USA. *Palynology* 8, 3–19. <https://doi.org/10.1080/01916122.1984.9989268>
- Heintzman, P.D., Froese, D., Ives, J.W., Soares, A.E.R., Zazula, G.D., Letts, B., Andrews, T.D., Driver, J.C., Hall, E., Hare, P.G., Jass, C.N., MacKay, G., Southon, J.R., Stiller, M., Woywitka, R., Suchard, M.A., Shapiro, B., 2016. Bison phylogeography constrains dispersal and viability of the Ice Free Corridor in western Canada. *PNAS* 113, 8057–8063. <https://doi.org/10.1073/pnas.1601077113>
- Hempson, G.P., Archibald, S., Bond, W.J., 2017. The consequences of replacing wildlife with livestock in Africa. *Scientific Reports* 7, 17196. <https://doi.org/10.1038/s41598-017-17348-4>
- Hempson, G.P., Archibald, S., Donaldson, J.E., Lehmann, C.E.R., 2019. Alternate Grassy Ecosystem States Are Determined by Palatability–Flammability Trade-Offs. *Trends in Ecology & Evolution*. <https://doi.org/10.1016/j.tree.2019.01.007>
- Hessburg, P.F., Agee, J.K., 2003. An environmental narrative of Inland Northwest United States forests, 1800–2000. *Forest Ecology and Management, The Effect of Wildland Fire on Aquatic Ecosystems in the Western USA*. 178, 23–59. [https://doi.org/10.1016/S0378-1127\(03\)00052-5](https://doi.org/10.1016/S0378-1127(03)00052-5)
- Hessburg, P.F., Miller, C.L., Parks, S.A., Povak, N.A., Taylor, A.H., Higuera, P.E., Prichard, S.J., North, M.P., Collins, B.M., Hurteau, M.D., Larson, A.J., Allen, C.D., Stephens, S.L., Rivera-Huerta, H., Stevens-Rumann, C.S., Daniels, L.D., Gedalof, Z., Gray, R.W., Kane, V.R., Churchill, D.J., Hagmann, R.K., Spies, T.A., Cansler, C.A., Belote, R.T., Veblen, T.T., Battaglia, M.A., Hoffman, C., Skinner, C.N., Safford, H.D., Salter, R.B., 2019. Climate, Environment, and Disturbance History Govern Resilience of Western North American Forests. *Front. Ecol. Evol.* 7. <https://doi.org/10.3389/fevo.2019.00239>
- Higuera, P.E., Brubaker, L.B., Anderson, P.M., Hu, F.S., Brown, T.A., 2009. Vegetation mediated the impacts of postglacial climate change on fire regimes in the south-central Brooks Range, Alaska. *Ecological Monographs* 79, 201–219. <https://doi.org/10.1890/07-2019.1>
- Higuera, P.E., Gavin, D.G., Bartlein, P.J., Hallett, D.J., 2010. Peak detection in sediment-charcoal records: impacts of alternative data analysis methods on fire-history interpretations. *International journal of wildland fire*.

- Hijmans, R.J., Phillips, S., Elith, J.L. and J., 2017. *dismo: Species Distribution Modeling*.
- Hill, M., Hawley, M., Widga, C., Monahan, L., Wanamaker, A., 2014. The Nye Site, Wisconsin: The Search for Early Man in the Upper Midwest, Investigative Incursions, and Paleozoology. *The Wisconsin Archeologist* 95, 200–238.
- Hill, M.E., 2007. A Moveable Feast: Variation in Faunal Resource Use among Central and Western North American Paleoindian Sites. *American Antiquity* 72, 417–438.
<https://doi.org/10.2307/40035854>
- Hill, M.E., Hill, M.G., Widga, C.C., 2008. Late Quaternary Bison diminution on the Great Plains of North America: evaluating the role of human hunting versus climate change. *Quaternary Science Reviews* 27, 1752–1771.
<https://doi.org/10.1016/j.quascirev.2008.07.002>
- Hobbs, N.T., Schimel, D.S., Owensby, C.E., Ojima, D.S., 1991. Fire and Grazing in the Tallgrass Prairie: Contingent Effects on Nitrogen Budgets. *Ecology* 72, 1374–1382.
<https://doi.org/10.2307/1941109>
- Hofmann, A.F., Hagey, L.R., 2008. Bile Acids: Chemistry, Pathochemistry, Biology, Pathobiology, and Therapeutics. *Cell. Mol. Life Sci.* 65, 2461–2483.
<https://doi.org/10.1007/s00018-008-7568-6>
- Holdo, R.M., Holt, R.D., Fryxell, J.M., 2009a. Grazers, browsers, and fire influence the extent and spatial pattern of tree cover in the Serengeti. *Ecological Applications* 19, 95–109.
<https://doi.org/10.1890/07-1954.1>
- Holdo, R.M., Sinclair, A.R.E., Dobson, A.P., Metzger, K.L., Bolker, B.M., Ritchie, M.E., Holt, R.D., 2009b. A Disease-Mediated Trophic Cascade in the Serengeti and its Implications for Ecosystem C. *PLOS Biology* 7, e1000210.
<https://doi.org/10.1371/journal.pbio.1000210>
- Horne, J.S., Hurley, M.A., White, C.G., Rachael, J., 2019. Effects of wolf pack size and winter conditions on elk mortality. *The Journal of Wildlife Management* 83, 1103–1116.
<https://doi.org/10.1002/jwmg.21689>
- Huang, S., Eronen, J.T., Janis, C.M., Saarinen, J.J., Silvestro, D., Fritz, S.A., 2017. Mammal body size evolution in North America and Europe over 20 Myr: similar trends generated by different processes. *Proceedings of the Royal Society B: Biological Sciences* 284, 20162361. <https://doi.org/10.1098/rspb.2016.2361>
- Hubbard, W.A., 1951. Rotational Grazing Studies in Western Canada. *Rangeland Ecology & Management / Journal of Range Management Archives* 4, 25–29.

- Huerta, M.A., Whitlock, C., Yale, J., 2009. Holocene vegetation–fire–climate linkages in northern Yellowstone National Park, USA. *Palaeogeography, Palaeoclimatology, Palaeoecology* 271, 170–181. <https://doi.org/10.1016/j.palaeo.2008.10.015>
- Ibarra, D.E., Egger, A.E., Weaver, K.L., Harris, C.R., Maher, K., 2014. Rise and fall of late Pleistocene pluvial lakes in response to reduced evaporation and precipitation: Evidence from Lake Surprise, California. *GSA Bulletin* 126, 1387–1415. <https://doi.org/10.1130/B31014.1>
- Isenberg, A.C., 2001. *The Destruction of the Bison: An Environmental History, 1750-1920*. Cambridge University Press, Cambridge New York Melbourne Madrid Cape Town Singapore Sao Paulo.
- Jackson, N.J., Stewart, K.M., Wisdom, M.J., Clark, D.A., Rowland, M.M., 2021. Demographic performance of a large herbivore: effects of winter nutrition and weather. *Ecosphere* 12, e03328. <https://doi.org/10.1002/ecs2.3328>
- Janis, C.M., Damuth, J., Theodor, J.M., 2002. The origins and evolution of the North American grassland biome: the story from the hoofed mammals. *Palaeogeography, Palaeoclimatology, Palaeoecology* 177, 183–198. [https://doi.org/10.1016/S0031-0182\(01\)00359-5](https://doi.org/10.1016/S0031-0182(01)00359-5)
- Jardine, P.E., Janis, C.M., Sahney, S., Benton, M.J., 2012. Grit not grass: Concordant patterns of early origin of hypsodonty in Great Plains ungulates and Glires. *Palaeogeography, Palaeoclimatology, Palaeoecology* 365–366, 1–10. <https://doi.org/10.1016/j.palaeo.2012.09.001>
- Juggins, S., 2020. rioja: Analysis of Quaternary Science Data.
- Karp, A.T., Faith, J.T., Marlon, J.R., Staver, A.C., 2021. Global response of fire activity to late Quaternary grazer extinctions. *Science* 374, 1145–1148. <https://doi.org/10.1126/science.abj1580>
- Karpinski, E., Hackenberger, D., Zazula, G., Widga, C., Duggan, A.T., Golding, G.B., Kuch, M., Klunk, J., Jass, C.N., Groves, P., Druckenmiller, P., Schubert, B.W., Arroyo-Cabrales, J., Simpson, W.F., Hoganson, J.W., Fisher, D.C., Ho, S.Y.W., MacPhee, R.D.E., Poinar, H.N., 2020. American mastodon mitochondrial genomes suggest multiple dispersal events in response to Pleistocene climate oscillations. *Nature Communications* 11, 4048. <https://doi.org/10.1038/s41467-020-17893-z>
- Kashian, D.M., Romme, W.H., Tinker, D.B., Turner, M.G., Ryan, M.G., 2006. Carbon Storage on Landscapes with Stand-replacing Fires. *BioScience* 56, 598–606. [https://doi.org/10.1641/0006-3568\(2006\)56\[598:CSOLWS\]2.0.CO;2](https://doi.org/10.1641/0006-3568(2006)56[598:CSOLWS]2.0.CO;2)
- Keigley, R.B., 2019. The Prehistoric Bison of Yellowstone National Park. *Rangelands* 41, 107–120. <https://doi.org/10.1016/j.rala.2018.11.004>

- King, J.E., 1981. Late Quaternary Vegetational History of Illinois. *Ecological Monographs* 51, 43–62. <https://doi.org/10.2307/2937306>
- Knapp, A.K., Blair, J.M., Briggs, J.M., Collins, S.L., Hartnett, D.C., Johnson, L.C., Towne, E.G., 1999. The Keystone Role of Bison in North American Tallgrass Prairie: Bison increase habitat heterogeneity and alter a broad array of plant, community, and ecosystem processes. *BioScience* 49, 39–50. <https://doi.org/10.1525/bisi.1999.49.1.39>
- Kruys, A., Wedin, M., 2009. Phylogenetic relationships and an assessment of traditionally used taxonomic characters in the Sporormiaceae (Pleosporales, Dothideomycetes, Ascomycota), utilising multi-gene phylogenies. *Systematics and Biodiversity* 7, 465–478. <https://doi.org/10.1017/S1477200009990119>
- Laird, K.R., Fritz, S.C., Grimm, E.C., Mueller, P.G., 1996. Century scale paleoclimatic reconstruction from Moon Lake, a closed-basin lake in the northern Great Plains. *Limnology and Oceanography* 41, 890–902. <https://doi.org/10.4319/lo.1996.41.5.0890>
- Lane, D.R., Coffin, D.P., Lauenroth, W.K., 2000. Changes in grassland canopy structure across a precipitation gradient. *Journal of Vegetation Science* 11, 359–368. <https://doi.org/10.2307/3236628>
- Lê, S., Josse, J., Husson, F., 2008. FactoMineR: A Package for Multivariate Analysis. *Journal of Statistical Software* 25, 1–18. <https://doi.org/10.18637/jss.v025.i01>
- Lehmann, C.E.R., Anderson, T.M., Sankaran, M., Higgins, S.I., Archibald, S., Hoffmann, W.A., Hanan, N.P., Williams, R.J., Fensham, R.J., Felfili, J., Hutley, L.B., Ratnam, J., Jose, J.S., Montes, R., Franklin, D., Russell-Smith, J., Ryan, C.M., Durigan, G., Hiernaux, P., Haidar, R., Bowman, D.M.J.S., Bond, W.J., 2014. Savanna Vegetation-Fire-Climatic Relationships Differ Among Continents. *Science* 343, 548–552. <https://doi.org/10.1126/science.1247355>
- Leopold, A.S., Cain, S.A., Cottam, C.M., Gabrielson, I.N., Kimball, T.L., 1963. *Wildlife Management in the National Parks*.
- Liefert, D.T., Shuman, B.N., 2020. Pervasive Desiccation of North American Lakes During the Late Quaternary. *Geophysical Research Letters* 47, e2019GL086412. <https://doi.org/10.1029/2019GL086412>
- List, R., Ceballos, G., Curtin, C., Gogan, P.J.P., Pacheco, J., Truett, J., 2007. Historic Distribution and Challenges to Bison Recovery in the Northern Chihuahuan Desert. *Conservation Biology* 21, 1487–1494. <https://doi.org/10.1111/j.1523-1739.2007.00810.x>
- Liu, Z., Lu, Z., Wen, X., Otto-Bliesner, B.L., Timmermann, A., Cobb, K.M., 2014. Evolution and forcing mechanisms of El Niño over the past 21,000 years. *Nature* 515, 550–553. <https://doi.org/10.1038/nature13963>

- Lloyd, C.E.M., Michaelides, K., Chadwick, D.R., Dungait, J.A.J., Evershed, R.P., 2012. Tracing the flow-driven vertical transport of livestock-derived organic matter through soil using biomarkers. *Organic Geochemistry* 43, 56–66. <https://doi.org/10.1016/j.orggeochem.2011.11.001>
- Lohse, J.C., Madsen, D.B., Culleton, B.J., Kennett, D.J., 2014. Isotope paleoecology of episodic mid-to-late Holocene bison population expansions in the Southern Plains, U.S.A. *Quaternary Science Reviews* 102, 14–26. <https://doi.org/10.1016/j.quascirev.2014.07.021>
- Long, C.J., Power, M.J., McDonald, B., 2011. Millennial-scale fire and vegetation history from a mesic hardwood forest of southeastern Wisconsin, USA. *Journal of Quaternary Science* 26, 318–325. <https://doi.org/10.1002/jqs.1456>
- Lora, J.M., Mitchell, J.L., Tripathi, A.E., 2016. Abrupt reorganization of North Pacific and western North American climate during the last deglaciation. *Geophysical Research Letters* 43, 11,796–11,804. <https://doi.org/10.1002/2016GL071244>
- Lorimer, J., Sandom, C., Jepson, P., Doughty, C., Barua, M., Kirby, K.J., 2015. Rewilding: Science, Practice, and Politics. *Annual Review of Environment and Resources* 40, 39–62. <https://doi.org/10.1146/annurev-environ-102014-021406>
- Lott, D.F., Greene, H.W., 2002. Bison Numbers Before the Great Slaughter, in: *American Bison, A Natural History*. University of California Press, pp. 167–169.
- Lupo, K.D., Schmitt, D.N., 1997. On Late Holocene Variability in Bison Populations in the Northeastern Great Basin. *Journal of California and Great Basin Anthropology* 19, 21.
- Lyle, M., Heusser, L., Ravelo, C., Yamamoto, M., Barron, J., Diffenbaugh, N.S., Herbert, T., Andreasen, D., 2012. Out of the Tropics: The Pacific, Great Basin Lakes, and Late Pleistocene Water Cycle in the Western United States. *Science* 337, 1629–1633. <https://doi.org/10.1126/science.1218390>
- Lyman, R.L., 2004. Late-Quaternary diminution and abundance of prehistoric bison (*Bison* sp.) in eastern Washington State, USA. *Quaternary Research* 62, 76–85. <https://doi.org/10.1016/j.yqres.2004.04.001>
- Lyman, R.L., Livingston, S.D., 1983. Late Quaternary mammalian zoogeography of eastern Washington. *Quaternary Research* 20, 360–373. [https://doi.org/10.1016/0033-5894\(83\)90018-2](https://doi.org/10.1016/0033-5894(83)90018-2)
- Mack, R.N., Thompson, J.N., 1982. Evolution in Steppe with Few Large, Hooved Mammals. *The American Naturalist* 119, 757–773. <https://doi.org/10.1086/283953>
- MacNulty, D.R., Stahler, D.R., Wyman, C.T., Ruprecht, J., Smith, D.W., 2016. The Challenge of Understanding Northern Yellowstone Elk Dynamics after Wolf Reintroduction (No. Ys 24-1). Yellowstone National Park.

- Maher Jr., L.J., 1982. The palynology of Devils Lake, Sauk County, Wisconsin, in: Quaternary History of the Driftless Area. Field Trip Guide Book 5. University of Wisconsin-Extension, Geological and Natural History Survey, Madison, Wisconsin, USA, pp. 119–135.
- Mao, J.S., Boyce, M.S., Smith, D.W., Singer, F.J., Vales, D.J., Vore, J.M., Merrill, E.H., 2005. Habitat Selection by Elk Before and After Wolf Reintroduction in Yellowstone National Park. *The Journal of Wildlife Management* 69, 1691–1707. [https://doi.org/10.2193/0022-541X\(2005\)69\[1691:HSBEBA\]2.0.CO;2](https://doi.org/10.2193/0022-541X(2005)69[1691:HSBEBA]2.0.CO;2)
- Marai, I.F.M., Haezeb, A.A.M., 2010. Buffalo's biological functions as affected by heat stress — A review. *Livestock Science* 127, 89–109. <https://doi.org/10.1016/j.livsci.2009.08.001>
- Martin, J.M., Barboza, P.S., 2020a. Thermal biology and growth of bison (*Bison bison*) along the Great Plains: examining four theories of endotherm body size. *Ecosphere* 11, e03176. <https://doi.org/10.1002/ecs2.3176>
- Martin, J.M., Barboza, P.S., 2020b. Decadal heat and drought drive body size of North American bison (*Bison bison*) along the Great Plains. *Ecology and Evolution* 10, 336–349. <https://doi.org/10.1002/ece3.5898>
- Martin, J.M., Martin, R.A., Mead, J.I., 2017. Late Pleistocene and Holocene Bison of the Colorado Plateau. *swna* 62, 14–28. <https://doi.org/10.1894/0038-4909-62.1.14>
- Martin, J.M., Mead, J.I., Barboza, P.S., 2018. Bison body size and climate change. *Ecol Evol* 8, 4564–4574. <https://doi.org/10.1002/ece3.4019>
- Martin, J.M., Zarestky, J., Briske, D.D., Barboza, P.S., 2021. Vulnerability assessment of the multi-sector North American bison *Bison bison* management system to climate change. *People and Nature* 3, 711–722. <https://doi.org/10.1002/pan3.10209>
- Martindale, A., Morlan, R., Betts, M., Blake, M., Gajewski, K., Chaput, M., Mason, A., Vermeersch, P., 2015. Canadian Archaeological Radiocarbon Database.
- Mason, J.A., Jacobs, P.M., Hanson, P.R., Miao, X., Goble, R.J., 2003. Sources and paleoclimatic significance of Holocene Bignell Loess, central Great Plains, USA. *Quat. res.* 60, 330–339. <https://doi.org/10.1016/j.yqres.2003.07.005>
- Mason, J.A., Miao, X., Hanson, P.R., Johnson, W.C., Jacobs, P.M., Goble, R.J., 2008. Loess record of the Pleistocene–Holocene transition on the northern and central Great Plains, USA. *Quaternary Science Reviews* 27, 1772–1783. <https://doi.org/10.1016/j.quascirev.2008.07.004>
- Mason, J.A., Swinehart, J.B., Hanson, P.R., Loope, D.B., Goble, R.J., Miao, X., Schmeisser, R.L., 2011. Late Pleistocene dune activity in the central Great Plains, USA. *Quaternary Science Reviews* 30, 3858–3870. <https://doi.org/10.1016/j.quascirev.2011.10.005>

- Massey, R., Sankey, T.T., Yadav, K., Congalton, R.G., Tilton, J.C., 2018. Integrating cloud-based workflows in continental-scale cropland extent classification. *Remote Sensing of Environment* 219, 162–179. <https://doi.org/10.1016/j.rse.2018.10.013>
- McAndrews, J.H., 1966. Postglacial History of Prairie, Savanna, and Forest in Northwestern Minnesota. *Memoirs of the Torrey Botanical Club* 22, 1–72.
- McCann, N.P., Moen, R.A., Harris, T.R., 2013. Warm-season heat stress in moose (*Alces alces*). *Can. J. Zool.* 91, 893–898. <https://doi.org/10.1139/cjz-2013-0175>
- McDonald, J.N., 1981. *North American Bison: Their Classification and Evolution*. The McDonald & Woodward Publishing Company.
- McHugh, T., 1979. *The Time of the Buffalo*, First Thus edition. ed. Bison Books, Lincoln.
- McWethy, D.B., Alt, M., Argiriadis, E., Battistel, D., Everett, R., Pederson, G.T., 2020. Millennial-Scale Climate and Human Drivers of Environmental Change and Fire Activity in a Dry, Mixed-Conifer Forest of Northwestern Montana. *Frontiers in Forests and Global Change* 3.
- McWethy, D.B., Higuera, P.E., Whitlock, C., Veblen, T.T., Bowman, D.M.J.S., Cary, G.J., Haberle, S.G., Keane, R.E., Maxwell, B.D., McGlone, M.S., Perry, G.L.W., Wilmschurst, J.M., Holz, A., Tepley, A.J., 2013. A conceptual framework for predicting temperate ecosystem sensitivity to human impacts on fire regimes. *Global Ecology and Biogeography* 22, 900–912. <https://doi.org/10.1111/geb.12038>
- Meagher, M., 1989. Range Expansion by Bison of Yellowstone National Park. *Journal of Mammalogy* 70, 670–675. <https://doi.org/10.2307/1381449>
- Meagher, M.M., 1973. *The bison of Yellowstone National Park*. U.S. Dept. of the Interior, National Park Service, Washington, D.C.
- Meltzer, D.J., 2020. Overkill, glacial history, and the extinction of North America's Ice Age megafauna. *PNAS* 117, 28555–28563. <https://doi.org/10.1073/pnas.2015032117>
- Meltzer, D.J., Holliday, V.T., 2010. Would North American Paleoindians have Noticed Younger Dryas Age Climate Changes? *J World Prehist* 23, 1–41. <https://doi.org/10.1007/s10963-009-9032-4>
- Mensing, S.A., Benson, L.V., Kashgarian, M., Lund, S., 2004. A Holocene pollen record of persistent droughts from Pyramid Lake, Nevada, USA. *Quat. res.* 62, 29–38. <https://doi.org/10.1016/j.yqres.2004.04.002>
- Miao, X., Mason, J., Goblet, R.J., Hanson, P.R., 2005. Loess record of dry climate and aeolian activity in the early-to mid-Holocene, central Great Plains, North America. *The Holocene* 15, 339–346. <https://doi.org/10.1191/0959683605h1805rp>

- Miao, X., Mason, J.A., Swinehart, J.B., Loope, D.B., Hanson, P.R., Goble, R.J., Liu, X., 2007. A 10,000 year record of dune activity, dust storms, and severe drought in the central Great Plains. *Geology* 35, 119–122. <https://doi.org/10.1130/G23133A.1>
- Minckley, T.A., Shriver, R.K., Shuman, B., 2012. Resilience and regime change in a southern Rocky Mountain ecosystem during the past 17 000 years. *Ecological Monographs* 82, 49–68. <https://doi.org/10.1890/11-0283.1>
- Morrill, C., Meador, E., Livneh, B., Liefert, D.T., Shuman, B.N., 2019. Quantitative model-data comparison of mid-Holocene lake-level change in the central Rocky Mountains. *Clim Dyn* 53, 1077–1094. <https://doi.org/10.1007/s00382-019-04633-3>
- Morrison, T.A., Holdo, R.M., Anderson, T.M., 2016. Elephant damage, not fire or rainfall, explains mortality of overstorey trees in Serengeti. *Journal of Ecology* 104, 409–418. <https://doi.org/10.1111/1365-2745.12517>
- Mosier, S., Apfelbaum, S., Byck, P., Calderon, F., Teague, R., Thompson, R., Cotrufo, M.F., 2021. Adaptive multi-paddock grazing enhances soil carbon and nitrogen stocks and stabilization through mineral association in southeastern U.S. grazing lands. *Journal of Environmental Management* 288, 112409. <https://doi.org/10.1016/j.jenvman.2021.112409>
- Myrbo, A., Wright, H.E., Jr., 2008. An introduction to Livingstone and Bolivia coring equipment.
- National Research Council, Division on Earth and Life Studies, Board on Environmental Studies and Toxicology, Committee on Ungulate Management in Yellowstone National Park, 2002. *Ecological Dynamics on Yellowstone's Northern Range*. National Academies Press.
- Nelson, C.J., Moser, L.E., 1994. Plant Factors Affecting Forage Quality, in: *Forage Quality, Evaluation, and Utilization*. John Wiley & Sons, Ltd, pp. 115–154. <https://doi.org/10.2134/1994.foragequality.c3>
- Nelson, D.M., Hu, F.S., 2008. Patterns and drivers of Holocene vegetational change near the prairie-forest ecotone in Minnesota: revisiting McAndrews' transect. *New Phytol* 179, 449–459. <https://doi.org/10.1111/j.1469-8137.2008.02482.x>
- Nelson, D.M., Hu, F.S., Grimm, E.C., Curry, B.B., Slate, J.E., 2006. The Influence of Aridity and Fire on Holocene Prairie Communities in the Eastern Prairie Peninsula. *Ecology* 87, 2523–2536. [https://doi.org/10.1890/0012-9658\(2006\)87\[2523:TIOAAF\]2.0.CO;2](https://doi.org/10.1890/0012-9658(2006)87[2523:TIOAAF]2.0.CO;2)
- Nelson, D.M., Hu, F.S., Tian, J., Stefanova, I., Brown, T.A., 2004. Response of C3 and C4 plants to middle-Holocene climatic variation near the prairie-forest ecotone of Minnesota. *Proceedings of the National Academy of Sciences* 101, 562–567. <https://doi.org/10.1073/pnas.0307450100>

- Nickell, Z., Varriano, S., Plemmons, E., Moran, M.D., 2018. Ecosystem engineering by bison (*Bison bison*) wallowing increases arthropod community heterogeneity in space and time. *Ecosphere* 9, e02436. <https://doi.org/10.1002/ecs2.2436>
- Nowacki, G.J., MacCleery, D.W., Lake, F.K., 2012. Native Americans, Ecosystem Development, and Historical Range of Variation, in: *Historical Environmental Variation in Conservation and Natural Resource Management*. John Wiley & Sons, Ltd, pp. 76–91. <https://doi.org/10.1002/9781118329726.ch6>
- Nowak, C.L., Nowak, R.S., Tausch, R.J., Wigand, P.E., 1994. Tree and Shrub Dynamics in Northwestern Great Basin Woodland and Shrub Steppe During the Late-Pleistocene and Holocene. *American Journal of Botany* 81, 265–277. <https://doi.org/10.2307/2445452>
- Nowak, R.S., Nowak, C.L., Tausch, R.J., 2017. Vegetation dynamics during last 35,000 years at a cold desert locale: preferential loss of forbs with increased aridity. *Ecosphere* 8, e01873. <https://doi.org/10.1002/ecs2.1873>
- O’Keefe, F.R., Dunn, R.E., Weitzel, E.M., Waters, M.R., Martinez, L.N., Binder, W.J., Southon, J.R., Cohen, J.E., Meachen, J.A., DeSantis, L.R.G., Kirby, M.E., Ghezze, E., Coltrain, J.B., Fuller, B.T., Farrell, A.B., Takeuchi, G.T., MacDonald, G., Davis, E.B., Lindsey, E.L., 2023. Pre–Younger Dryas megafaunal extirpation at Rancho La Brea linked to fire-driven state shift. *Science* 381, eabo3594. <https://doi.org/10.1126/science.abo3594>
- Olf, H., Ritchie, M.E., Prins, H.H.T., 2002. Global environmental controls of diversity in large herbivores. *Nature* 415, 901–904. <https://doi.org/10.1038/415901a>
- Olson, D.M., Dinerstein, E., Wikramanayake, E.D., Burgess, N.D., Powell, G.V.N., Underwood, E.C., D’amico, J.A., Itoua, I., Strand, H.E., Morrison, J.C., Loucks, C.J., Allnutt, T.F., Ricketts, T.H., Kura, Y., Lamoreux, J.F., Wettengel, W.W., Hedao, P., Kassem, K.R., 2001. Terrestrial Ecoregions of the World: A New Map of Life on Earth. *BioScience* 51, 933–938. [https://doi.org/10.1641/0006-3568\(2001\)051\[0933:TEOTWA\]2.0.CO;2](https://doi.org/10.1641/0006-3568(2001)051[0933:TEOTWA]2.0.CO;2)
- Pachzelt, A., Forrest, M., Rammig, A., Higgins, S.I., Hickler, T., 2015. Potential impact of large ungulate grazers on African vegetation, carbon storage and fire regimes. *Global Ecology and Biogeography* 24, 991–1002. <https://doi.org/10.1111/geb.12313>
- Pachzelt, A., Rammig, A., Higgins, S., Hickler, T., 2013. Coupling a physiological grazer population model with a generalized model for vegetation dynamics. *Ecological Modelling* 263, 92–102. <https://doi.org/10.1016/j.ecolmodel.2013.04.025>
- Paine, R.T., 1969. A Note on Trophic Complexity and Community Stability. *The American Naturalist* 103, 91–93. <https://doi.org/10.1086/282586>
- Payne, B.L., Bro-Jørgensen, J., 2016. Disproportionate Climate-Induced Range Loss Forecast for the Most Threatened African Antelopes. *Current Biology* 26, 1200–1205. <https://doi.org/10.1016/j.cub.2016.02.067>

- Payne, J.C., Buuveibaatar, B., Bowler, D.E., Olson, K.A., Walzer, C., Kaczensky, P., 2020. Hidden treasure of the Gobi: understanding how water limits range use of khulan in the Mongolian Gobi. *Sci Rep* 10, 2989. <https://doi.org/10.1038/s41598-020-59969-2>
- Pedersen, M.W., Ginolhac, A., Orlando, L., Olsen, J., Andersen, K., Holm, J., Funder, S., Willerslev, E., Kjær, K.H., 2013. A comparative study of ancient environmental DNA to pollen and macrofossils from lake sediments reveals taxonomic overlap and additional plant taxa. *Quaternary Science Reviews* 75, 161–168. <https://doi.org/10.1016/j.quascirev.2013.06.006>
- Pedersen, R.Ø., Faurby, S., Svenning, J.-C., 2023. Late-Quaternary megafauna extinctions have strongly reduced mammalian vegetation consumption. *Global Ecology and Biogeography* 32, 1814–1826. <https://doi.org/10.1111/geb.13723>
- Pejchar, L., Medrano, L., Niemiec, R.M., Barfield, J.P., Davidson, A., Hartway, C., 2021. Challenges and opportunities for cross-jurisdictional bison conservation in North America. *Biological Conservation* 256, 109029. <https://doi.org/10.1016/j.biocon.2021.109029>
- Pellegrini, A.F.A., Ahlström, A., Hobbie, S.E., Reich, P.B., Nieradzik, L.P., Staver, A.C., Scharenbroch, B.C., Jumpponen, A., Anderegg, W.R.L., Randerson, J.T., Jackson, R.B., 2018. Fire frequency drives decadal changes in soil carbon and nitrogen and ecosystem productivity. *Nature* 553, 194–198. <https://doi.org/10.1038/nature24668>
- Perrotti, A.G., Kiahtipes, C.A., Russell, J.M., Jackson, S.T., Gill, J.L., Robinson, G.S., Krause, T., Williams, J.W., 2022. Diverse responses of vegetation and fire after pleistocene megaherbivore extinction across the eastern US. *Quaternary Science Reviews* 294, 107696. <https://doi.org/10.1016/j.quascirev.2022.107696>
- Perrotti, A.G., van Asperen, E., 2019. Dung fungi as a proxy for megaherbivores: opportunities and limitations for archaeological applications. *Veget Hist Archaeobot* 28, 93–104. <https://doi.org/10.1007/s00334-018-0686-7>
- Perryman, B., Schultz, B., Meiman, P., 2021. Forum: A Change in the Ecological Understanding of Rangelands in the Great Basin and Intermountain West and Implications for Management: Revisiting Mack and Thompson (1982). *Rangeland Ecology & Management* 76, 1–11. <https://doi.org/10.1016/j.rama.2021.01.003>
- Pescini, V., Carbonell, A., Colominas, L., Égüez, N., Mayoral, A., Palet, J.M., 2023. Neolithic livestock practices in high mountain areas: A multi-proxy study of pastoral enclosures of Molleres II (Eastern Pyrenees). *Quaternary International*. <https://doi.org/10.1016/j.quaint.2023.04.008>
- Phillips, S.J., Anderson, R.P., Schapire, R.E., 2006. Maximum entropy modeling of species geographic distributions. *Ecological Modelling* 190, 231–259. <https://doi.org/10.1016/j.ecolmodel.2005.03.026>

- Phillips, S.J., Dudík, M., Schapire, R.E., 2016. Maxent software for modeling species niches and distributions.
- Pigati, J.S., Springer, K.B., Honke, J.S., Wahl, D., Champagne, M.R., Zimmerman, S.R.H., Gray, H.J., Santucci, V.L., Odess, D., Bustos, D., Bennett, M.R., 2023. Independent age estimates resolve the controversy of ancient human footprints at White Sands. *Science* 382, 73–75. <https://doi.org/10.1126/science.adh5007>
- Plew, M.G., Sundell, T., 2000. The Archaeological Occurrence of Bison on the Snake River Plain. *North American Archaeologist* 21, 119–137. <https://doi.org/10.2190/Y9XE-YTA4-RP20-XC3W>
- Polley, H.W., Wallace, L.L., 1986. The Relationship of Plant Species Heterogeneity to Soil Variation in Buffalo Wallows. *The Southwestern Naturalist* 31, 493–501. <https://doi.org/10.2307/3671703>
- Posit team, 2023. RStudio: Integrated Development for R.
- Power, M.J., Marlon, J.R., Bartlein, P.J., Harrison, S.P., 2010. Fire history and the Global Charcoal Database: A new tool for hypothesis testing and data exploration. *Palaeogeography, Palaeoclimatology, Palaeoecology, Charcoal and its use in palaeoenvironmental analysis* 291, 52–59. <https://doi.org/10.1016/j.palaeo.2009.09.014>
- Power, M.J., Whitlock, C., Bartlein, P.J., 2011. Postglacial fire, vegetation, and climate history across an elevational gradient in the Northern Rocky Mountains, USA and Canada. *Quaternary Science Reviews* 30, 2520–2533. <https://doi.org/10.1016/j.quascirev.2011.04.012>
- Pribyl, P., Shuman, B.N., 2014. A computational approach to Quaternary lake-level reconstruction applied in the central Rocky Mountains, Wyoming, USA. *Quaternary Research* 82, 249–259. <https://doi.org/10.1016/j.yqres.2014.01.012>
- Prost, K., Birk, J.J., Lehndorff, E., Gerlach, R., Amelung, W., 2017. Steroid Biomarkers Revisited – Improved Source Identification of Faecal Remains in Archaeological Soil Material. *PLOS ONE* 12, e0164882. <https://doi.org/10.1371/journal.pone.0164882>
- R Core Team, 2022. R: A Language and Environment for Statistical Computing.
- Rasmussen, S., Allentoft, M.E., Nielsen, K., Orlando, L., Sikora, M., Sjögren, K.-G., Pedersen, A.G., Schubert, M., Van Dam, A., Kapel, C.M.O., Nielsen, H.B., Brunak, S., Avetisyan, P., Epimakhov, A., Khalyapin, M.V., Gnuni, A., Kriiska, A., Lasak, I., Metspalu, M., Moiseyev, V., Gromov, A., Pokutta, D., Saag, L., Varul, L., Yepiskoposyan, L., Sicheritz-Pontén, T., Foley, R.A., Lahr, M.M., Nielsen, R., Kristiansen, K., Willerslev, E., 2015. Early Divergent Strains of *Yersinia pestis* in Eurasia 5,000 Years Ago. *Cell* 163, 571–582. <https://doi.org/10.1016/j.cell.2015.10.009>

- Ratajczak, Z., Collins, S., Blair, J., Koerner, S., Louthan, A., Smith, M., Taylor, J., Nippert, J., 2022. Reintroducing bison results in long-running and resilient increases in grassland diversity. *Proceedings of the National Academy of Sciences* 119, e2210433119. <https://doi.org/10.1073/pnas.2210433119>
- Raynor, E.J., Derner, J.D., Hoover, D.L., Parton, W.J., Augustine, D.J., 2020. Large-scale and local climatic controls on large herbivore productivity: implications for adaptive rangeland management. *Ecological Applications* 30, e02053. <https://doi.org/10.1002/eap.2053>
- Reeves, A.D., Patton, D., 2005. Faecal sterols as indicators of sewage contamination in estuarine sediments of the Tay Estuary, Scotland: an extended baseline survey. *Hydrology and Earth System Sciences* 9, 81–94. <https://doi.org/10.5194/hess-9-81-2005>
- Reheis, M.C., Adams, K.D., Oviatt, C.G., Bacon, S.N., 2014. Pluvial lakes in the Great Basin of the western United States—a view from the outcrop. *Quaternary Science Reviews* 97, 33–57. <https://doi.org/10.1016/j.quascirev.2014.04.012>
- Reimer, P.J., Austin, W.E.N., Bard, E., Bayliss, A., Blackwell, P.G., Ramsey, C.B., Butzin, M., Cheng, H., Edwards, R.L., Friedrich, M., Grootes, P.M., Guilderson, T.P., Hajdas, I., Heaton, T.J., Hogg, A.G., Hughen, K.A., Kromer, B., Manning, S.W., Muscheler, R., Palmer, J.G., Pearson, C., Plicht, J. van der, Reimer, R.W., Richards, D.A., Scott, E.M., Southon, J.R., Turney, C.S.M., Wacker, L., Adolphi, F., Büntgen, U., Capano, M., Fahrni, S.M., Fogtmann-Schulz, A., Friedrich, R., Köhler, P., Kudsk, S., Miyake, F., Olsen, J., Reinig, F., Sakamoto, M., Sookdeo, A., Talamo, S., 2020. The IntCal20 Northern Hemisphere Radiocarbon Age Calibration Curve (0–55 cal kBP). *Radiocarbon* 62, 725–757. <https://doi.org/10.1017/RDC.2020.41>
- Renssen, H., 2020. Comparison of Climate Model Simulations of the Younger Dryas Cold Event. *Quaternary* 3, 29. <https://doi.org/10.3390/quat3040029>
- Research Division, 1992. Interim Report Yellowstone National Park Northern Range Research.
- Rivals, F., Solounias, N., Mithlacher, M.C., 2007. Evidence for geographic variation in the diets of late Pleistocene and early Holocene Bison in North America, and differences from the diets of recent Bison. *Quaternary Research* 68, 338–346. <https://doi.org/10.1016/j.yqres.2007.07.012>
- Roos, C.I., Zedeño, M.N., Hollenback, K.L., Erlick, M.M.H., 2018. Indigenous impacts on North American Great Plains fire regimes of the past millennium. *PNAS* 115, 8143–8148. <https://doi.org/10.1073/pnas.1805259115>
- Rouet-Leduc, J., Pe'er, G., Moreira, F., Bonn, A., Helmer, W., Shahsavani Zadeh, S.A.A., Zizka, A., van der Plas, F., 2021. Effects of large herbivores on fire regimes and wildfire mitigation. *Journal of Applied Ecology* 58, 2690–2702. <https://doi.org/10.1111/1365-2664.13972>

- Rouse, J., 1977. *The Criollo: Spanish Cattle in the Americas*. University of Oklahoma Press.
- Rush, W.M., 1933. Northern Yellowstone elk study. Montana Fish and Game Commission, Helena, MT.
- Saeed, T., Al-Shimmari, F., Al-Mutairi, A., Abdullah, H., 2015. Spatial assessment of the sewage contamination of Kuwait's marine areas. *Marine Pollution Bulletin* 94, 307–317. <https://doi.org/10.1016/j.marpolbul.2015.01.030>
- Sanderson, E.W., Redford, K.H., Weber, B., Aune, K., Baldes, D., Berger, J., Carter, D., Curtin, C., Derr, J., Dobrott, S., Fearn, E., Fleener, C., Forrest, S., Gerlach, C., Cormack Gates, C., Gross, J.E., Gogan, P., Grassel, S., Hilty, J.A., Jensen, M., Kunkel, K., Lammers, D., List, R., Minkowski, K., Olson, T., Pague, C., Robertson, P.B., Stephenson, B., 2008. The Ecological Future of the North American Bison: Conceiving Long-Term, Large-Scale Conservation of Wildlife. *Conservation Biology* 22, 252–266. <https://doi.org/10.1111/j.1523-1739.2008.00899.x>
- Sánchez, J., Froehner, S., Hansel, F., Parron, L., Knapik, H., Fernandes, C., Rizzi, J., 2017. Bile acids combined with fecal sterols: a multiple biomarker approach for deciphering fecal pollution using river sediments. *J Soils Sediments* 17, 861–872. <https://doi.org/10.1007/s11368-016-1592-1>
- Sankaran, M., Hanan, N.P., Scholes, R.J., Ratnam, J., Augustine, D.J., Cade, B.S., Gignoux, J., Higgins, S.I., Le Roux, X., Ludwig, F., Ardo, J., Banyikwa, F., Bronn, A., Bucini, G., Caylor, K.K., Coughenour, M.B., Diouf, A., Ekaya, W., Feral, C.J., February, E.C., Frost, P.G.H., Hiernaux, P., Hrabar, H., Metzger, K.L., Prins, H.H.T., Ringrose, S., Sea, W., Tews, J., Worden, J., Zambatis, N., 2005. Determinants of woody cover in African savannas. *Nature* 438, 846–849. <https://doi.org/10.1038/nature04070>
- Santi, L., Ibarra, D., Mering, J., Arnold, A., Tripathi, A., Whicker, C., Oviatt, C., 2019. Lake Level Fluctuations in the Northern Great Basin for the Last 25,000 years (preprint). *Physical Sciences and Mathematics*. <https://doi.org/10.31223/OSF.IO/6AS7T>
- Schmeisser McKean, R.L., Goble, R.J., Mason, J.B., Swinehart, J.B., Loope, D.B., 2015. Temporal and spatial variability in dune reactivation across the Nebraska Sand Hills, USA. *The Holocene* 25, 523–535. <https://doi.org/10.1177/0959683614561889>
- Schmieder, J., Fritz, S.C., Grimm, E.C., Jacobs, K.C., Brown, K.J., Swinehart, J.B., Porter, S.C., 2013. Holocene variability in hydrology, vegetation, fire, and eolian activity in the Nebraska Sand Hills, USA. *The Holocene* 23, 515–527. <https://doi.org/10.1177/0959683612463100>
- Schmitt, D.N., Madsen, D.B., 2005. *Camels Back Cave: Anthropological Paper 125*, 1st edition. ed. University of Utah Press, Salt Lake City.

- Schmitz, O.J., Sylvén, M., Atwood, T.B., Bakker, E.S., Berzaghi, F., Brodie, J.F., Croomsigt, J.P.G.M., Davies, A.B., Leroux, S.J., Schepers, F.J., Smith, F.A., Stark, S., Svenning, J.-C., Tilker, A., Ylänne, H., 2023. Trophic rewilding can expand natural climate solutions. *Nat. Clim. Chang.* 13, 324–333. <https://doi.org/10.1038/s41558-023-01631-6>
- Schoennagel, T., Veblen, T.T., Romme, W.H., 2004. The Interaction of Fire, Fuels, and Climate across Rocky Mountain Forests. *BioScience* 54, 661–676. [https://doi.org/10.1641/0006-3568\(2004\)054\[0661:TIOFFA\]2.0.CO;2](https://doi.org/10.1641/0006-3568(2004)054[0661:TIOFFA]2.0.CO;2)
- Scholtz, R., Fuhlendorf, S.D., Archer, S.R., 2018. Climate–fire interactions constrain potential woody plant cover and stature in North American Great Plains grasslands. *Global Ecology and Biogeography* 27, 936–945. <https://doi.org/10.1111/geb.12752>
- Schweger, C., Hickman, M., 1989. Holocene paleohydrology of central Alberta: testing the general-circulation-model climate simulations. *Canadian Journal of Earth Sciences* 26, 1826–1833. <https://doi.org/10.1139/e89-155>
- Scott, E., 2010. Extinctions, scenarios, and assumptions: Changes in latest Pleistocene large herbivore abundance and distribution in western North America. *Quaternary International, Faunal Dynamics and Extinction in the Quaternary: Studies in Honor of Ernest L. Lundelius, Jr.* 217, 225–239. <https://doi.org/10.1016/j.quaint.2009.11.003>
- Seersholm, F.V., Werndly, D.J., Greal, A., Johnson, T., Keenan Early, E.M., Lundelius, E.L., Winsborough, B., Farr, G.E., Toomey, R., Hansen, A.J., Shapiro, B., Waters, M.R., McDonald, G., Linderholm, A., Stafford, T.W., Bunce, M., 2020. Rapid range shifts and megafaunal extinctions associated with late Pleistocene climate change. *Nature Communications* 11, 2770. <https://doi.org/10.1038/s41467-020-16502-3>
- Seton, E.T., 1929. *The lives of game animals*. Doubleday, Doran & Company, New York.
- Shakun, J.D., Clark, P.U., He, F., Marcott, S.A., Mix, A.C., Liu, Z., Otto-Bliesner, B., Schmittner, A., Bard, E., 2012. Global warming preceded by increasing carbon dioxide concentrations during the last deglaciation. *Nature* 484, 49–54. <https://doi.org/10.1038/nature10915>
- Shamon, H., Cosby, O.G., Andersen, C.L., Augare, H., BearCub Stiffarm, J., Bresnan, C.E., Brock, B.L., Carlson, E., Deichmann, J.L., Epps, A., Guernsey, N., Hartway, C., Jørgensen, D., Kipp, W., Kinsey, D., Komatsu, K.J., Kunkel, K., Magnan, R., Martin, J.M., Maxwell, B.D., McShea, W.J., Mormorunni, C., Olimb, S., Rattling Hawk, M., Ready, R., Smith, R., Songer, M., Speakthunder, B., Stafne, G., Weatherwax, M., Akre, T.S., 2022. The Potential of Bison Restoration as an Ecological Approach to Future Tribal Food Sovereignty on the Northern Great Plains. *Frontiers in Ecology and Evolution* 10.
- Shapiro, B., Drummond, A.J., Rambaut, A., Wilson, M.C., Matheus, P.E., Sher, A.V., Pybus, O.G., Gilbert, M.T.P., Barnes, I., Binladen, J., Willerslev, E., Hansen, A.J., Baryshnikov,

- G.F., Burns, J.A., Davydov, S., Driver, J.C., Froese, D.G., Harington, C.R., Keddie, G., Kosintsev, P., Kunz, M.L., Martin, L.D., Stephenson, R.O., Storer, J., Tedford, R., Zimov, S., Cooper, A., 2004. Rise and Fall of the Beringian Steppe Bison. *Science* 306, 1561–1565. <https://doi.org/10.1126/science.1101074>
- Shaw, H., 1995. How Many Bison Originally Populated Western Rangelands? *Rangelands* 5.
- Sheppard, A.H.C., Hecker, L.J., Edwards, M.A., Nielsen, S.E., 2021. Determining the influence of snow and temperature on the movement rates of wood bison (*Bison bison athabasca*). *Can. J. Zool.* 99, 489–496. <https://doi.org/10.1139/cjz-2020-0280>
- Shuman, B., Henderson, A.K., Colman, S.M., Stone, J.R., Fritz, S.C., Stevens, L.R., Power, M.J., Whitlock, C., 2009. Holocene lake-level trends in the Rocky Mountains, U.S.A. *Quaternary Science Reviews* 28, 1861–1879. <https://doi.org/10.1016/j.quascirev.2009.03.003>
- Shuman, B., Webb III, T., Bartlein, P., Williams, J.W., 2002. The anatomy of a climatic oscillation: vegetation change in eastern North America during the Younger Dryas chronozone. *Quaternary Science Reviews* 21, 1777–1791. [https://doi.org/10.1016/S0277-3791\(02\)00030-6](https://doi.org/10.1016/S0277-3791(02)00030-6)
- Shuman, B.N., Marsicek, J., 2016. The structure of Holocene climate change in mid-latitude North America. *Quaternary Science Reviews* 141, 38–51. <https://doi.org/10.1016/j.quascirev.2016.03.009>
- Shuman, B.N., Pribyl, P., Buettner, J., 2015. Hydrologic changes in Colorado during the mid-Holocene and Younger Dryas. *Quaternary Research* 84, 187–199. <https://doi.org/10.1016/j.yqres.2015.07.004>
- Shuman, B.N., Serravezza, M., 2017. Patterns of hydroclimatic change in the Rocky Mountains and surrounding regions since the last glacial maximum. *Quaternary Science Reviews* 173, 58–77. <https://doi.org/10.1016/j.quascirev.2017.08.012>
- Simpson, I.A., van Bergen, P.F., Perret, V., Elhmmali, M.M., Roberts, D.J., Evershed, R.P., 1999. Lipid biomarkers of manuring practice in relict anthropogenic soils. *The Holocene* 9, 223–229. <https://doi.org/10.1191/095968399666898333>
- Simpson, K.J., Archibald, S., Osborne, C.P., 2022. Savanna fire regimes depend on grass trait diversity. *Trends in Ecology & Evolution* 37, 749–758. <https://doi.org/10.1016/j.tree.2022.04.010>
- Singer, F.J., Harting, A., Symonds, K.K., Coughenour, M.B., 1997. Density Dependence, Compensation, and Environmental Effects on Elk Calf Mortality in Yellowstone National Park. *The Journal of Wildlife Management* 61, 12–25. <https://doi.org/10.2307/3802410>

- Smith, A.J., Donovan, J.J., Ito, E., Engstrom, D.R., Panek, V.A., 2002. Climate-driven hydrologic transients in lake sediment records: multiproxy record of mid-Holocene drought. *Quaternary Science Reviews* 21, 625–646. [https://doi.org/10.1016/S0277-3791\(01\)00041-5](https://doi.org/10.1016/S0277-3791(01)00041-5)
- Smith, B.L., Anderson, S.H., 1998. Juvenile Survival and Population Regulation of the Jackson Elk Herd. *The Journal of Wildlife Management* 62, 1036–1045. <https://doi.org/10.2307/3802556>
- Smoliak, S., 1965. A Comparison of Ungrazed and Lightly Grazed Stipa–Bouteloua Prairie in Southeastern Alberta. *Can. J. Plant Sci.* 45, 270–275. <https://doi.org/10.4141/cjps65-050>
- Smoliak, S., 1960. Effects of Deferred-Rotation and Continuous Grazing on Yearling Steer Gains and Shortgrass Prairie Vegetation of Southeastern Alberta. *Rangeland Ecology & Management / Journal of Range Management Archives* 13, 239–243.
- Speakman, J.R., Król, E., 2010. Maximal heat dissipation capacity and hyperthermia risk: neglected key factors in the ecology of endotherms. *Journal of Animal Ecology* 79, 726–746. <https://doi.org/10.1111/j.1365-2656.2010.01689.x>
- Speranza, E.D., Colombo, M., Skorupka, C.N., Colombo, J.C., 2018. Early diagenetic alterations of sterol biomarkers during particle settling and burial in polluted and pristine areas of the Rio de la Plata Basin. *Organic Geochemistry* 117, 1–11. <https://doi.org/10.1016/j.orggeochem.2017.11.013>
- Spiers, D.E., Spain, J.N., Sampson, J.D., Rhoads, R.P., 2004. Use of physiological parameters to predict milk yield and feed intake in heat-stressed dairy cows. *Journal of Thermal Biology, International Thermal Physiology Symposium: Physiology and Pharmacology of Temperature Regulation* 29, 759–764. <https://doi.org/10.1016/j.jtherbio.2004.08.051>
- Spitz, D.B., Clark, D.A., Wisdom, M.J., Rowland, M.M., Johnson, B.K., Long, R.A., Levi, T., 2018. Fire history influences large-herbivore behavior at circadian, seasonal, and successional scales. *Ecological Applications* 28, 2082–2091. <https://doi.org/10.1002/eap.1797>
- Starns, H.D., Fuhlendorf, S.D., Elmore, R.D., Twidwell, D., Thacker, E.T., Hovick, T.J., Luttbeg, B., 2019. Recoupling fire and grazing reduces wildland fuel loads on rangelands. *Ecosphere* 10, e02578. <https://doi.org/10.1002/ecs2.2578>
- Staver, A.C., Abraham, J.O., Hempson, G.P., Karp, A.T., Faith, J.T., 2021. The past, present, and future of herbivore impacts on savanna vegetation. *Journal of Ecology* 109, 2804–2822. <https://doi.org/10.1111/1365-2745.13685>
- Staver, A.C., Archibald, S., Levin, S.A., 2011. The Global Extent and Determinants of Savanna and Forest as Alternative Biome States. *Science* 334, 230–232. <https://doi.org/10.1126/science.1210465>

- Steenweg, R., Hebblewhite, M., Gummer, D., Low, B., Hunt, B., 2016. Assessing Potential Habitat and Carrying Capacity for Reintroduction of Plains Bison (*Bison bison bison*) in Banff National Park. *PLOS ONE* 11, e0150065. <https://doi.org/10.1371/journal.pone.0150065>
- Stewart, M., Carleton, W.C., Groucutt, H.S., 2021. Climate change, not human population growth, correlates with Late Quaternary megafauna declines in North America. *Nature Communications* 12, 965. <https://doi.org/10.1038/s41467-021-21201-8>
- Strömberg, C.A.E., 2011. Evolution of Grasses and Grassland Ecosystems. *Annu. Rev. Earth Planet. Sci.* 39, 517–544. <https://doi.org/10.1146/annurev-earth-040809-152402>
- Sun, W., Wang, B., Zhang, Q., Pausata, F.S.R., Chen, D., Lu, G., Yan, M., Ning, L., Liu, J., 2019. Northern Hemisphere Land Monsoon Precipitation Increased by the Green Sahara During Middle Holocene. *Geophysical Research Letters* 46, 9870–9879. <https://doi.org/10.1029/2019GL082116>
- Surovell, T.A., Byrd Finley, J., Smith, G.M., Brantingham, P.J., Kelly, R., 2009. Correcting temporal frequency distributions for taphonomic bias. *Journal of Archaeological Science* 36, 1715–1724. <https://doi.org/10.1016/j.jas.2009.03.029>
- Taylor, C.D., Smith, S.O., Gagosian, R.B., 1981. Use of microbial enrichments for the study of the anaerobic degradation of cholesterol. *Geochimica et Cosmochimica Acta* 45, 2161–2168. [https://doi.org/10.1016/0016-7037\(81\)90068-5](https://doi.org/10.1016/0016-7037(81)90068-5)
- Thompson, R.S., Anderson, K.H., 2000. Biomes of western North America at 18,000, 6000 and 0 14C yr bp reconstructed from pollen and packrat midden data. *Journal of Biogeography* 27, 555–584. <https://doi.org/10.1046/j.1365-2699.2000.00427.x>
- Tian, J., Brown, T.A., Hul, F.S., 2005. Comparison of varve and 14C chronologies from Steel Lake, Minnesota, USA. *The Holocene* 15, 510–517. <https://doi.org/10.1191/0959683605hl828rp>
- Torbit, S.C., LaRose, L., 2001. A Commentary on Bison and Cultural Restoration: Partnership Between the National Wildlife Federation and the Intertribal Bison Cooperative. *Great Plains Research* 11, 175–182.
- Tyagi, P., Edwards, D.R., Coyne, M.S., 2008. Use of Sterol and Bile Acid Biomarkers to Identify Domesticated Animal Sources of Fecal Pollution. *Water Air Soil Pollut* 187, 263–274. <https://doi.org/10.1007/s11270-007-9514-x>
- Ulrich, B.C., 2020. Understanding the Coprophilous fungus *Sporormiella* as a proxy for megaherbivores (Thesis). Montana State University - Bozeman, College of Letters & Science.

- Umbanhowar, C.E., 2004. Interactions of climate and fire at two sites in the northern Great Plains, USA. *Palaeogeography, Palaeoclimatology, Palaeoecology* 208, 141–152. <https://doi.org/10.1016/j.palaeo.2004.03.001>
- van Asperen, E.N., Kirby, J.R., Shaw, H.E., 2020. Relating dung fungal spore influx rates to animal density in a temperate environment: Implications for palaeoecological studies. *The Holocene* 30, 218–232. <https://doi.org/10.1177/0959683619875804>
- Van Zant, K., 1979. Late glacial and postglacial pollen and plant macrofossils from Lake West Okoboji, Northwestern Iowa. *Quaternary Research* 12, 358–380. [https://doi.org/10.1016/0033-5894\(79\)90034-6](https://doi.org/10.1016/0033-5894(79)90034-6)
- Veldhuis, M.P., Kihwele, E.S., Cromsigt, J.P.G.M., Ogutu, J.O., Hopcraft, J.G.C., Owen-Smith, N., Olff, H., 2019. Large herbivore assemblages in a changing climate: incorporating water dependence and thermoregulation. *Ecology Letters* 22, 1536–1546. <https://doi.org/10.1111/ele.13350>
- Vermeire, L.T., Mitchell, R.B., Fuhlendorf, S.D., Gillen, R.L., 2004. Patch burning effects on grazing distribution. *rama.1* 57, 248–252. [https://doi.org/10.2111/1551-5028\(2004\)057\[0248:PBEOGD\]2.0.CO;2](https://doi.org/10.2111/1551-5028(2004)057[0248:PBEOGD]2.0.CO;2)
- von der Lühe, B., Birk, J.J., Dawson, L., Mayes, R.W., Fiedler, S., 2018. Steroid fingerprints: Efficient biomarkers of human decomposition fluids in soil. *Organic Geochemistry* 124, 228–237. <https://doi.org/10.1016/j.orggeochem.2018.07.016>
- Waters, M.R., 2019. Late Pleistocene exploration and settlement of the Americas by modern humans. *Science* 365. <https://doi.org/10.1126/science.aat5447>
- Watts, W.A., Bright, R.C., 1968. Pollen, Seed, and Mollusk Analysis of a Sediment Core from Pickerel Lake, Northeastern South Dakota. *GSA Bulletin* 79, 855–876. [https://doi.org/10.1130/0016-7606\(1968\)79\[855:PSAMAO\]2.0.CO;2](https://doi.org/10.1130/0016-7606(1968)79[855:PSAMAO]2.0.CO;2)
- Wendt, J.A.F., McWethy, D.B., Hempson, G.P., Brookshire, E.N.J., Fuhlendorf, S.D., 2023. Past and present biomass consumption by herbivores and fire across productivity gradients in North America. *Environ. Res. Lett.* <https://doi.org/10.1088/1748-9326/ad0ad0>
- Wendt, J.A.F., McWethy, D.B., Widga, C., Shuman, B.N., 2022. Large-scale climatic drivers of bison distribution and abundance in North America since the Last Glacial Maximum. *Quaternary Science Reviews* 284, 107472. <https://doi.org/10.1016/j.quascirev.2022.107472>
- Whicker, A.D., Detling, J.K., 1988. Ecological Consequences of Prairie Dog Disturbances. *BioScience* 38, 778–785. <https://doi.org/10.2307/1310787>

- White, A.J., Stevens, L.R., Lorenzi, V., Munoz, S.E., Lipo, C.P., Schroeder, S., 2018. An evaluation of fecal stanols as indicators of population change at Cahokia, Illinois. *Journal of Archaeological Science* 93, 129–134. <https://doi.org/10.1016/j.jas.2018.03.009>
- White, P.J., Proffitt, K.M., Mech, L.D., Evans, S.B., Cunningham, J.A., Hamlin, K.L., 2010. Migration of northern Yellowstone elk: implications of spatial structuring. *Journal of Mammalogy* 91, 827–837. <https://doi.org/10.1644/08-MAMM-A-252.1>
- Whitlock, C., Bartlein, P.J., 1993. Spatial Variations of Holocene Climatic Change in the Yellowstone Region. *Quaternary Research* 39, 231–238. <https://doi.org/10.1006/qres.1993.1026>
- Whitlock, C., Higuera, P., Mcwethy, D., Briles, C., 2010. Paleoecological Perspectives on Fire Ecology: Revisiting the Fire-Regime Concept. *The Open Ecology Journal* 3, 6–23. <https://doi.org/10.2174/1874213001003020006>
- Whitlock, C., Larsen, C., 2001. Charcoal as a Fire Proxy, in: Smol, J.P., Birks, H.J.B., Last, W.M., Bradley, R.S., Alverson, K. (Eds.), *Tracking Environmental Change Using Lake Sediments*. Kluwer Academic Publishers, Dordrecht, pp. 75–97. https://doi.org/10.1007/0-306-47668-1_5
- Whittlesey, L.H., Schullery, P.D., Bone, S., Klein, A., White, P.J., Rodman, A.W., Hallac, D.E., 2018. Using Historical Accounts (1796–1881) to Inform Contemporary Wildlife Management in the Yellowstone Area. *naar* 38, 99–107. <https://doi.org/10.3375/043.038.0110>
- Widga, C., 2014. Middle Holocene Taphonomy and Paleozoology at the Prairie-Forest Border, the Itasca Bison Site, MN. *Midcontinental Journal of Archaeology* 39, 251–279. <https://doi.org/10.1179/2327427114Y.0000000014>
- Widga, C., 2013. Evolution of the High Plains Paleoindian Landscape: The Paleoecology of Great Plains Faunal Assemblages, in: *Paleoindian Lifeways of the Cody Complex*. pp. 69–92.
- Widga, C., 2006. Niche variability in late Holocene bison: a perspective from Big Bone Lick, KY. *Journal of Archaeological Science* 33, 1237–1255. <https://doi.org/10.1016/j.jas.2005.12.011>
- Widga, C., Lengyel, S.N., Saunders, J., Hodgins, G., Walker, J.D., D. Wanamaker, A., 2017. Late Pleistocene proboscidean population dynamics in the North American Midcontinent. *Boreas* 46, 772–782. <https://doi.org/10.1111/bor.12235>
- Wilkins, K., Pejchar, L., Garvoille, R., 2019. Ecological and social consequences of bison reintroduction in Colorado. *Conservation Science and Practice* 1, e9. <https://doi.org/10.1111/csp2.9>

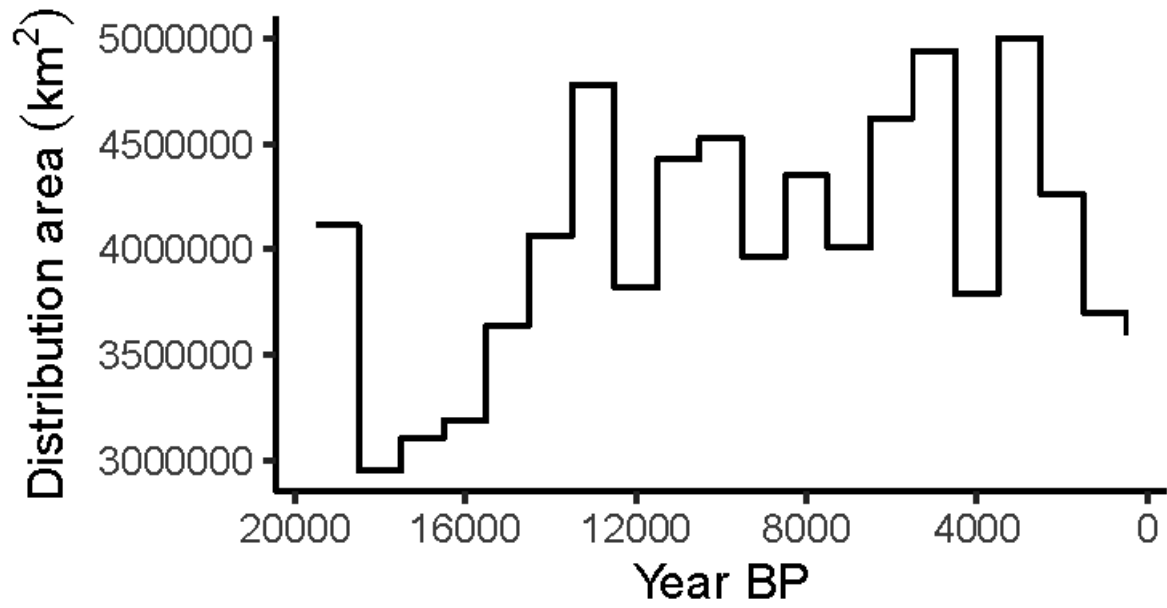
- Williams, J.W., Grimm, E.C., Blois, J.L., Charles, D.F., Davis, E.B., Goring, S.J., Graham, R.W., Smith, A.J., Anderson, M., Arroyo-Cabral, J., Ashworth, A.C., Betancourt, J.L., Bills, B.W., Booth, R.K., Buckland, P.I., Curry, B.B., Giesecke, T., Jackson, S.T., Latorre, C., Nichols, J., Purdum, T., Roth, R.E., Stryker, M., Takahara, H., 2018. The Neotoma Paleoecology Database, a multiproxy, international, community-curated data resource. *Quaternary Research* 89, 156–177. <https://doi.org/10.1017/qua.2017.105>
- Williams, J.W., Shuman, B., Bartlein, P.J., 2009. Rapid responses of the prairie-forest ecotone to early Holocene aridity in mid-continental North America. *Global and Planetary Change* 66, 195–207. <https://doi.org/10.1016/j.gloplacha.2008.10.012>
- Williams, J.W., Shuman, B., Bartlein, P.J., Diffenbaugh, N.S., Webb, T., III, 2010. Rapid, time-transgressive, and variable responses to early Holocene midcontinental drying in North America. *Geology* 38, 135–138. <https://doi.org/10.1130/G30413.1>
- Williams, J.W., Shuman, B.N., Webb, T., Bartlein, P.J., Leduc, P.L., 2004. Late-Quaternary Vegetation Dynamics in North America: Scaling from Taxa to Biomes. *Ecological Monographs* 74, 309–334. <https://doi.org/10.1890/02-4045>
- Wolf, A., Doughty, C.E., Malhi, Y., 2013. Lateral Diffusion of Nutrients by Mammalian Herbivores in Terrestrial Ecosystems. *PLOS ONE* 8, e71352. <https://doi.org/10.1371/journal.pone.0071352>
- Wright, H.E., Jr., Winter, T.C., Patten, H.L., 1963. Two Pollen Diagrams from Southeastern Minnesota: Problems in the Regional Late-Glacial and Postglacial Vegetational History. *GSA Bulletin* 74, 1371–1396. [https://doi.org/10.1130/0016-7606\(1963\)74\[1371:TPDFSM\]2.0.CO;2](https://doi.org/10.1130/0016-7606(1963)74[1371:TPDFSM]2.0.CO;2)
- Wright, H.E., Stefanova, I., Tian, J., Brown, T.A., Hu, F.S., 2004. A chronological framework for the Holocene vegetational history of central Minnesota: the Steel Lake pollen record. *Quaternary Science Reviews* 23, 611–626. <https://doi.org/10.1016/j.quascirev.2003.09.003>
- Writer, J.H., Leenheer, J.A., Barber, L.B., Amy, G.L., Chapra, S.C., 1995. Sewage contamination in the upper Mississippi River as measured by the fecal sterol, coprostanol. *Water Research* 29, 1427–1436. [https://doi.org/10.1016/0043-1354\(94\)00304-P](https://doi.org/10.1016/0043-1354(94)00304-P)
- Yang, H., Yan, R., Chen, H., Lee, D.H., Zheng, C., 2007. Characteristics of hemicellulose, cellulose and lignin pyrolysis. *Fuel* 86, 1781–1788. <https://doi.org/10.1016/j.fuel.2006.12.013>
- Yellowstone National Park, 2022a. Yellowstone Bison - Yellowstone National Park (U.S. National Park Service) [WWW Document]. URL <https://www.nps.gov/yell/learn/nature/bison.htm> (accessed 9.15.23).

- Yellowstone National Park, 2022b. Mule Deer - Yellowstone National Park [WWW Document]. URL <https://www.nps.gov/yell/learn/nature/mule-deer.htm> (accessed 9.15.23).
- Yellowstone National Park, 2022c. Moose - Yellowstone National Park [WWW Document]. URL <https://www.nps.gov/yell/learn/nature/moose.htm> (accessed 9.15.23).
- Yellowstone National Park, 2022d. Pronghorn - Yellowstone National Park (U.S. National Park Service) [WWW Document]. URL <https://www.nps.gov/yell/learn/nature/pronghorn.htm> (accessed 9.15.23).
- Yellowstone National Park, 2022e. White-tailed Deer - Yellowstone National Park [WWW Document]. URL <https://www.nps.gov/yell/learn/nature/white-tailed-deer.htm> (accessed 9.15.23).
- Yellowstone National Park, 2019. 2019 late winter survey of northern Yellowstone elk [WWW Document]. URL <https://www.nps.gov/yell/learn/news/2019-late-winter-survey-of-northern-yellowstone-elk.htm> (accessed 9.15.23).
- Yellowstone National Park, 1997. Yellowstone's Northern Range: Complexity & Change in a Wildland Ecosystem. Yellowstone National Park, National Park Service, Mammoth Hot Springs, Wyo. <https://doi.org/10.5962/bhl.title.69442>
- Zedeño, M.N., Ballenger, J.A.M., Murray, J.R., 2014. Landscape Engineering and Organizational Complexity among Late Prehistoric Bison Hunters of the Northwestern Plains. *Current Anthropology* 55, 23–58. <https://doi.org/10.1086/674535>
- Zocatelli, R., Lavrieux, M., Guillemot, T., Chassiot, L., Le Milbeau, C., Jacob, J., 2017. Fecal biomarker imprints as indicators of past human land uses: Source distinction and preservation potential in archaeological and natural archives. *Journal of Archaeological Science* 81, 79–89. <https://doi.org/10.1016/j.jas.2017.03.010>
- Zver, L., Toškan, B., Bužan, E., 2021. Phylogeny of Late Pleistocene and Holocene Bison species in Europe and North America. *Quaternary International* 595, 30–38. <https://doi.org/10.1016/j.quaint.2021.04.022>

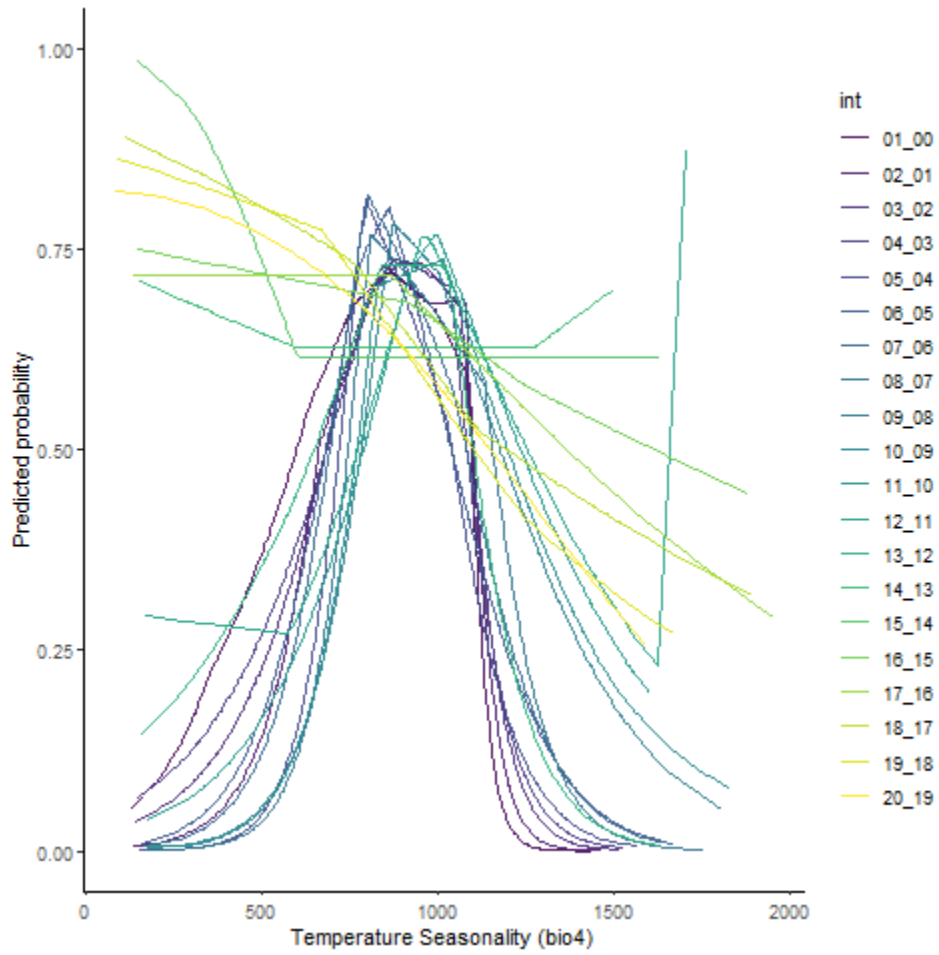
APPENDICES

APPENDIX A

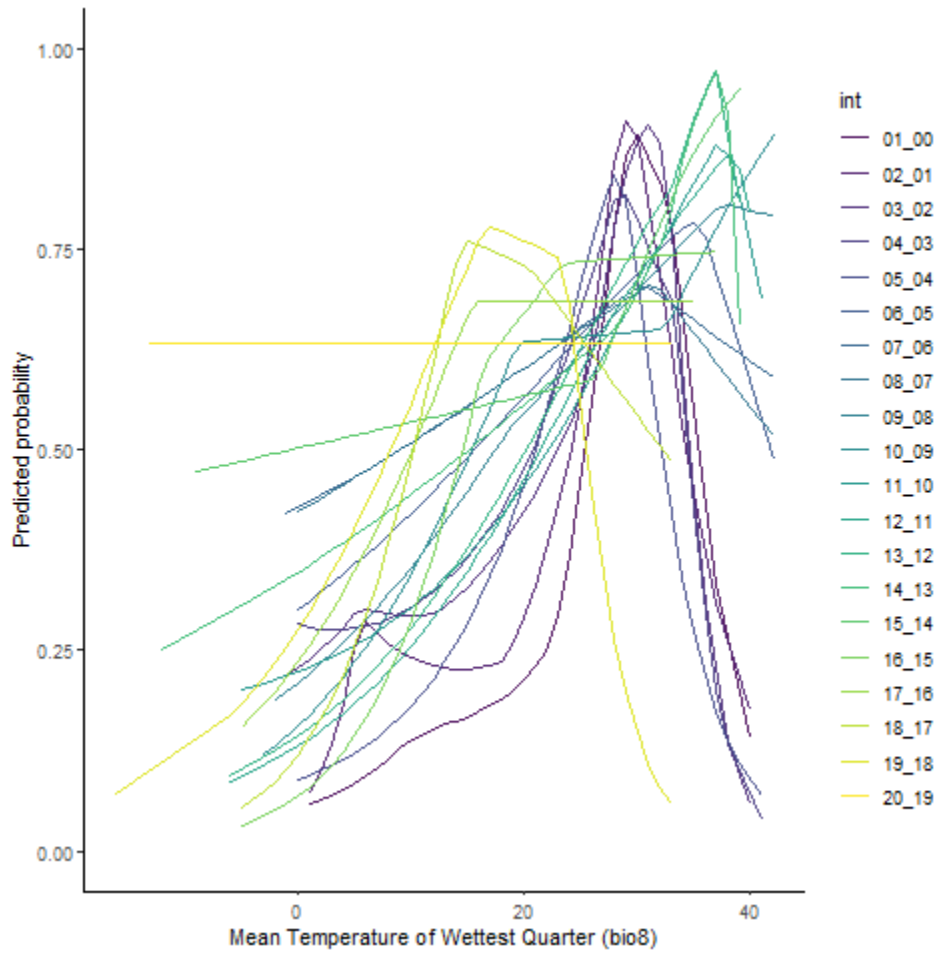
SUPPLEMENTARY INFORMATION FOR CHAPTER TWO



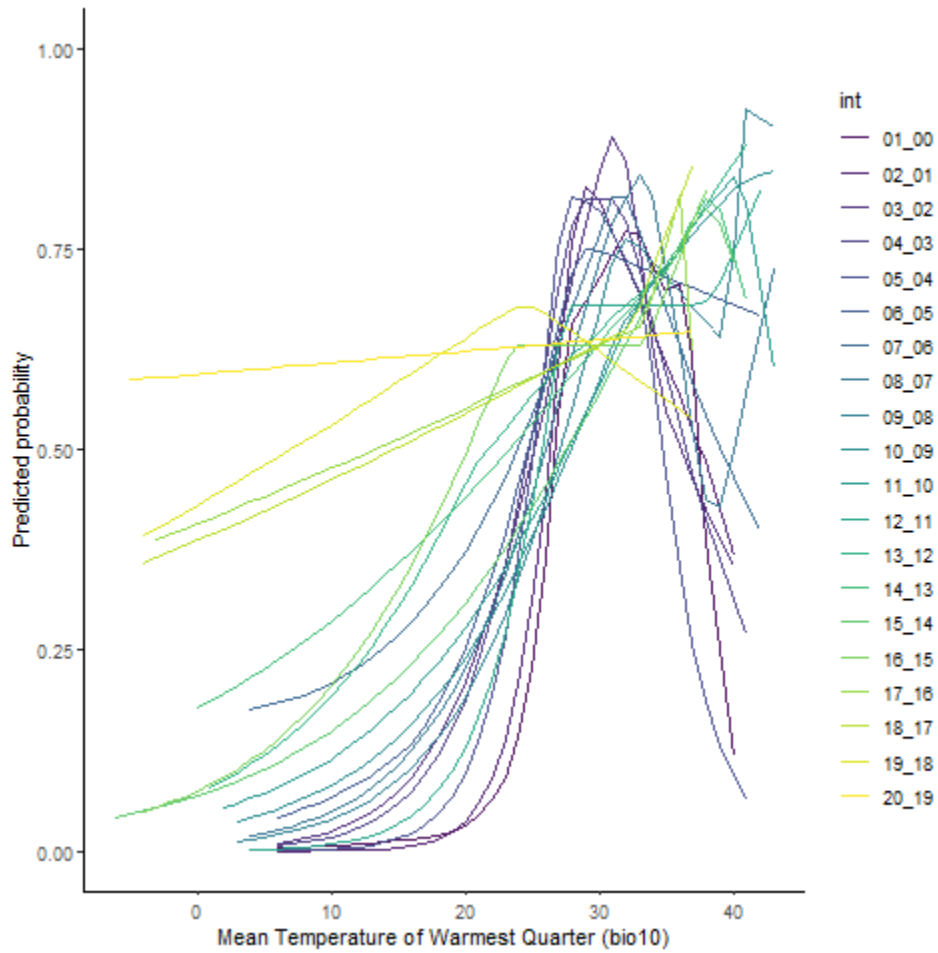
Supplementary Figure 2.1. Area of modeled bison distribution across 1000-year intervals between 20-0 ka.



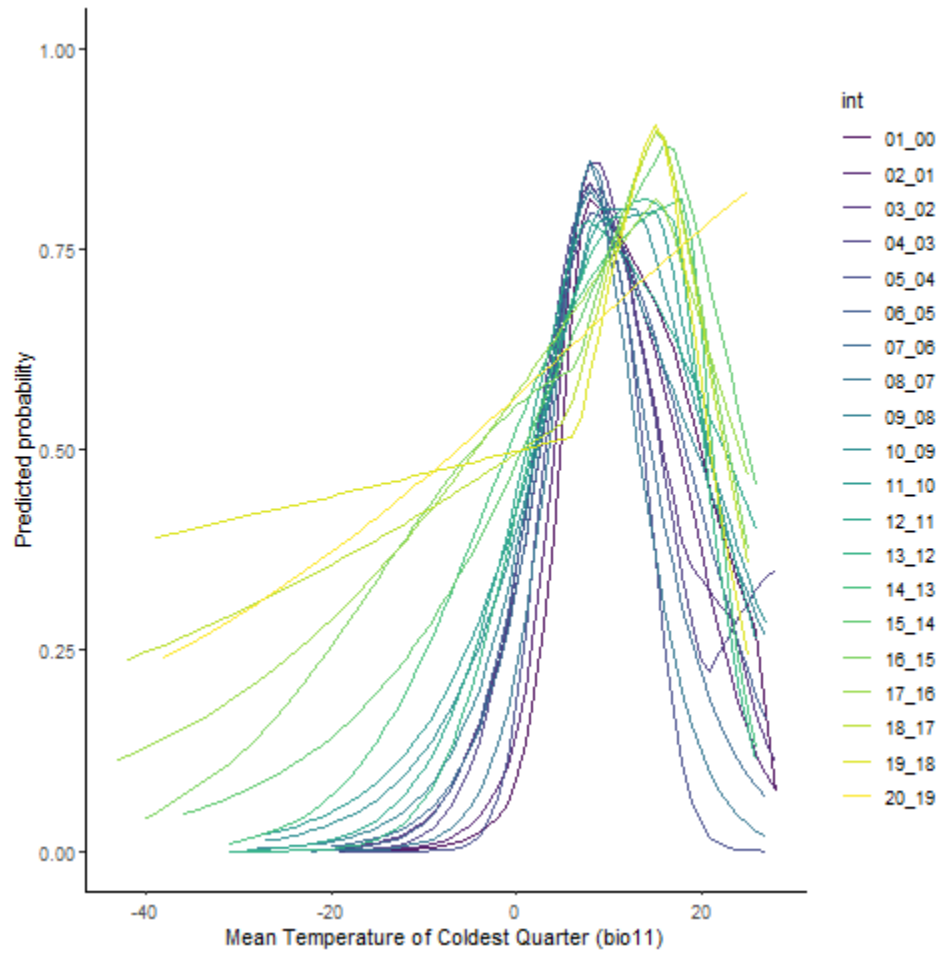
Supplementary Figure 2.2. Response curves for Temperature Seasonality (bio4) in 1000-year intervals between 20-0 ka.



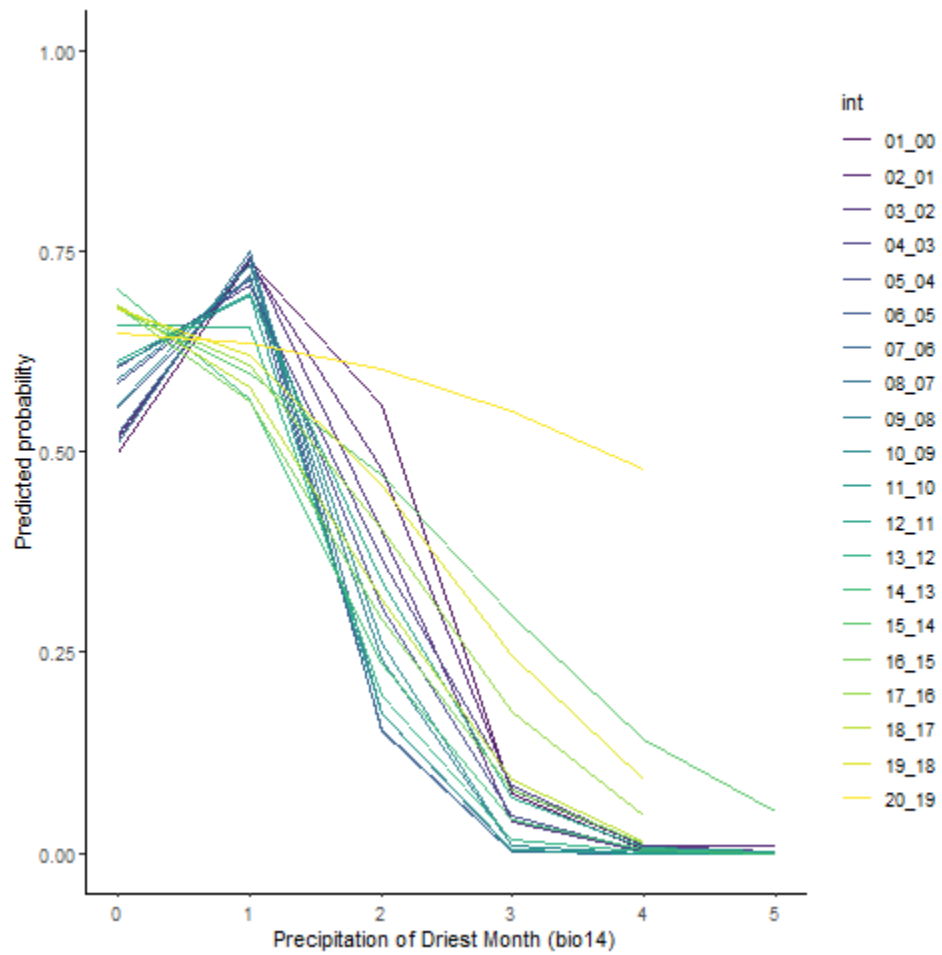
Supplementary Figure 2.3. Response curves for Mean Temperature of the Wettest Quarter (bio8) in 1000-year intervals between 20-0 ka.



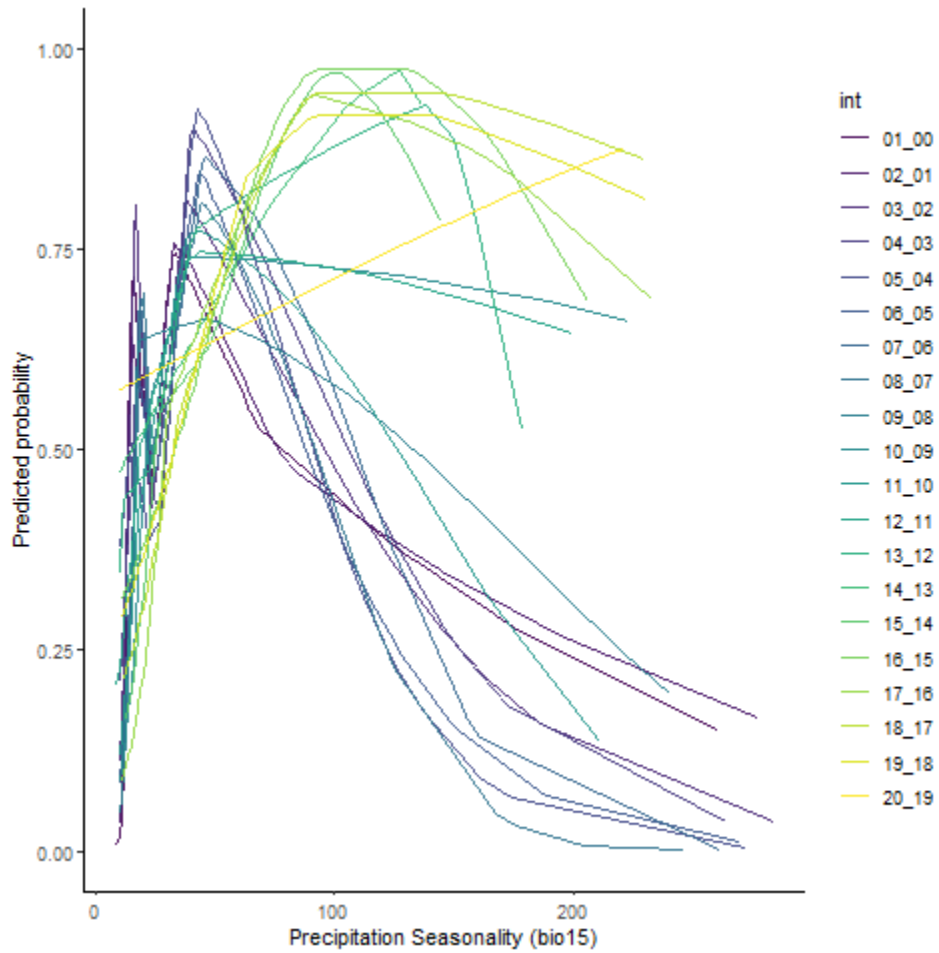
Supplementary Figure 2.4. Response curves for Mean Temperature of the Warmest Quarter (bio10) in 1000-year intervals between 20-0 ka.



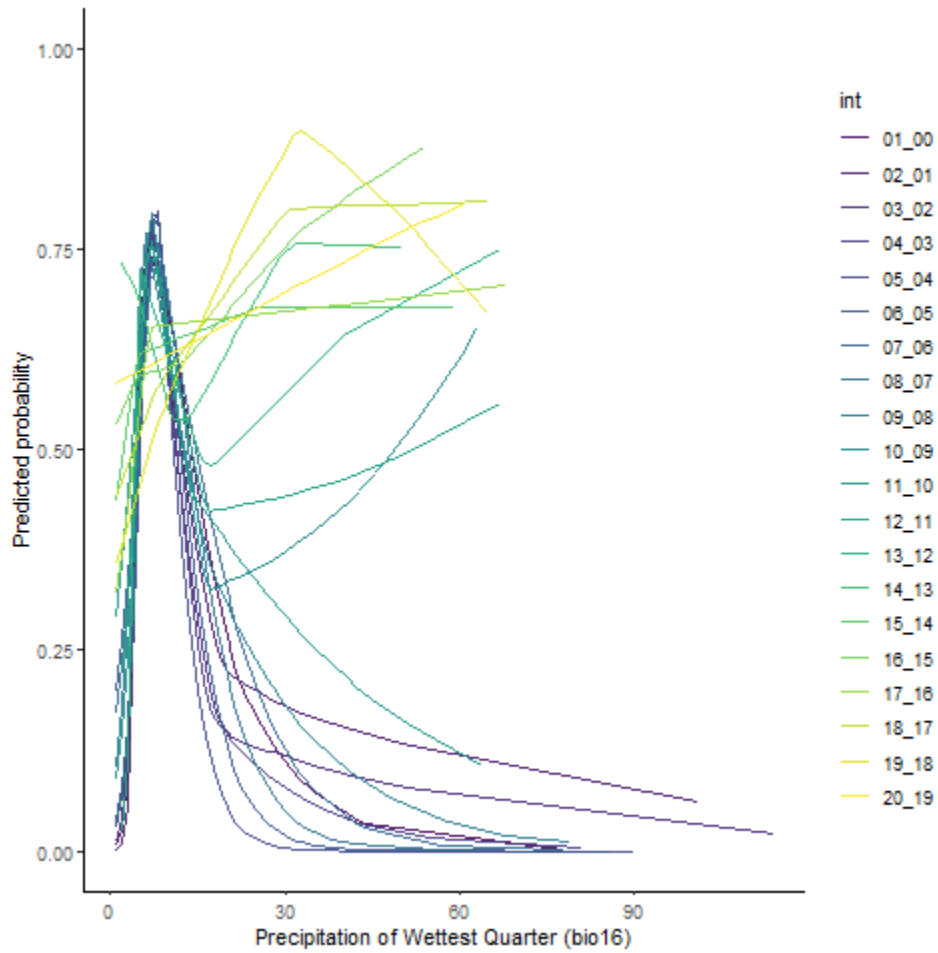
Supplementary Figure 2.5. Response curves for Mean Temperature of the Coldest Quarter (bio11) in 1000-year intervals between 20-0 ka.



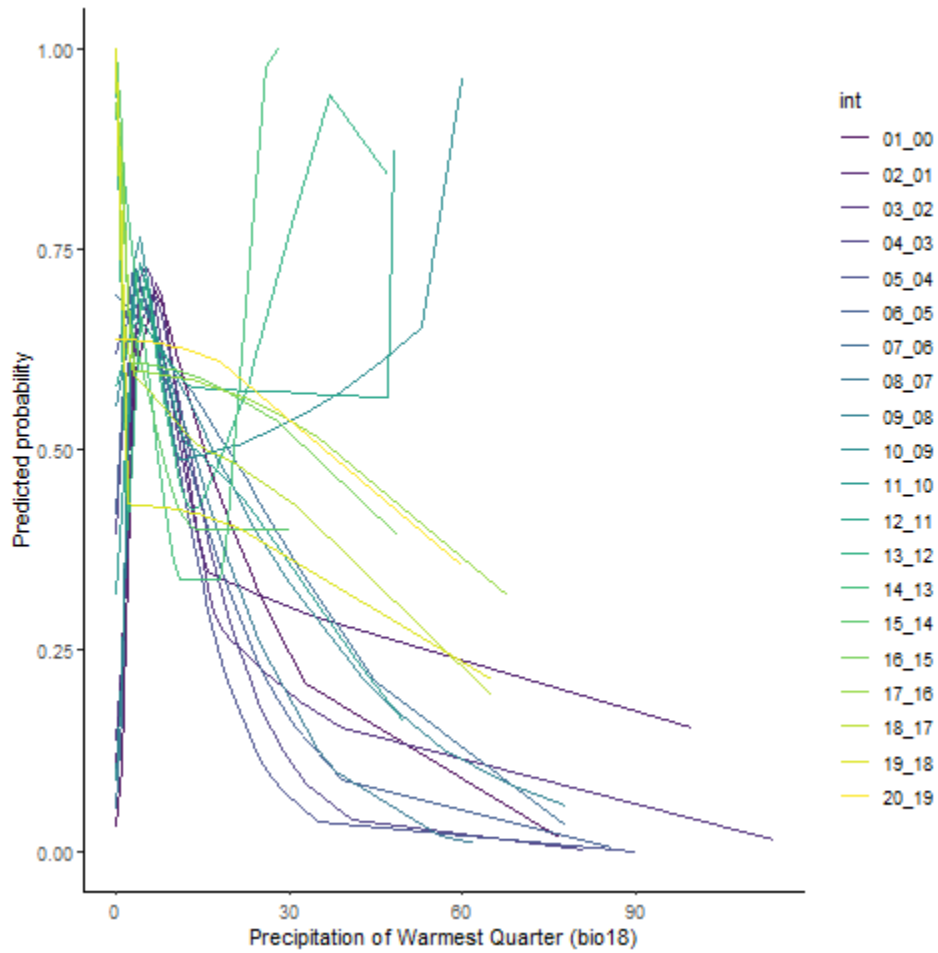
Supplementary Figure 2.6. Response curves for Precipitation of the Driest Month (bio14) in 1000-year intervals between 20-0 ka.



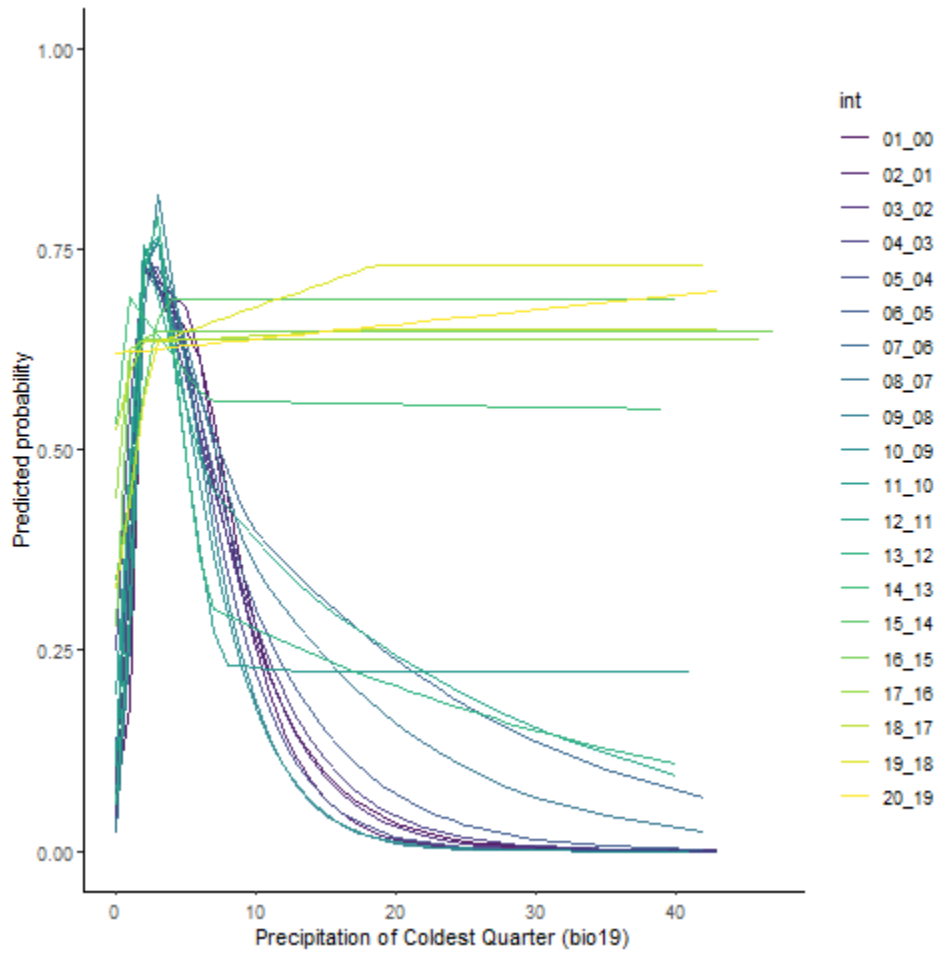
Supplementary Figure 2.7. Response curves for Precipitation Seasonality (bio15) in 1000-year intervals between 20-0 ka.



Supplementary Figure 2.8. Response curves for Precipitation of the Wettest Quarter (bio16) in 1000-year intervals between 20-0 ka.

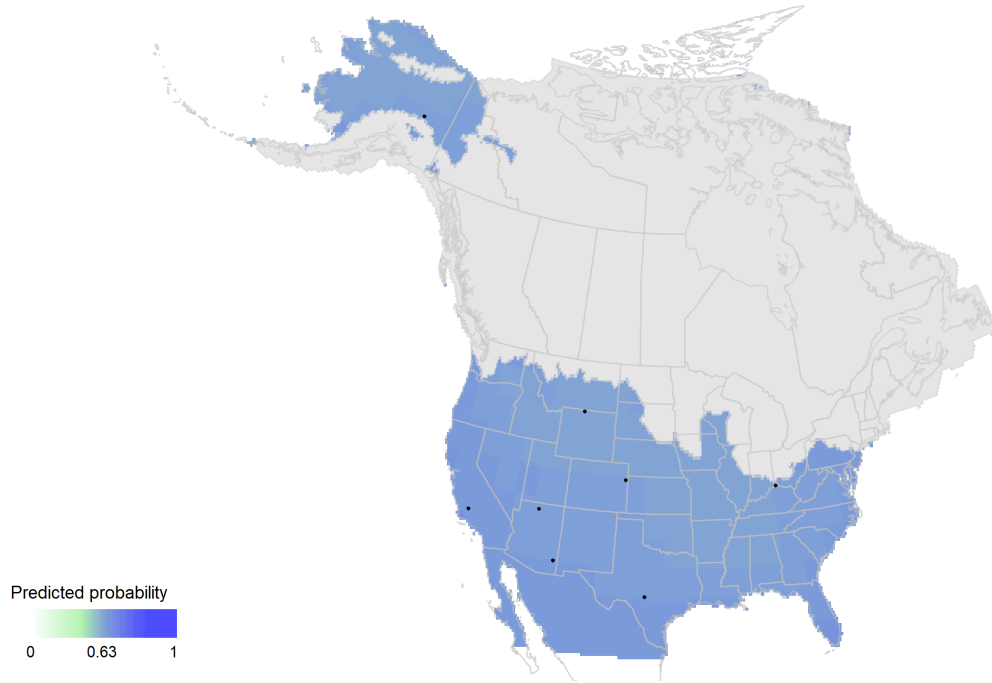


Supplementary Figure 2.9. Response curves for Precipitation of the Warmest Quarter (bio18) in 1000-year intervals between 20-0 ka.



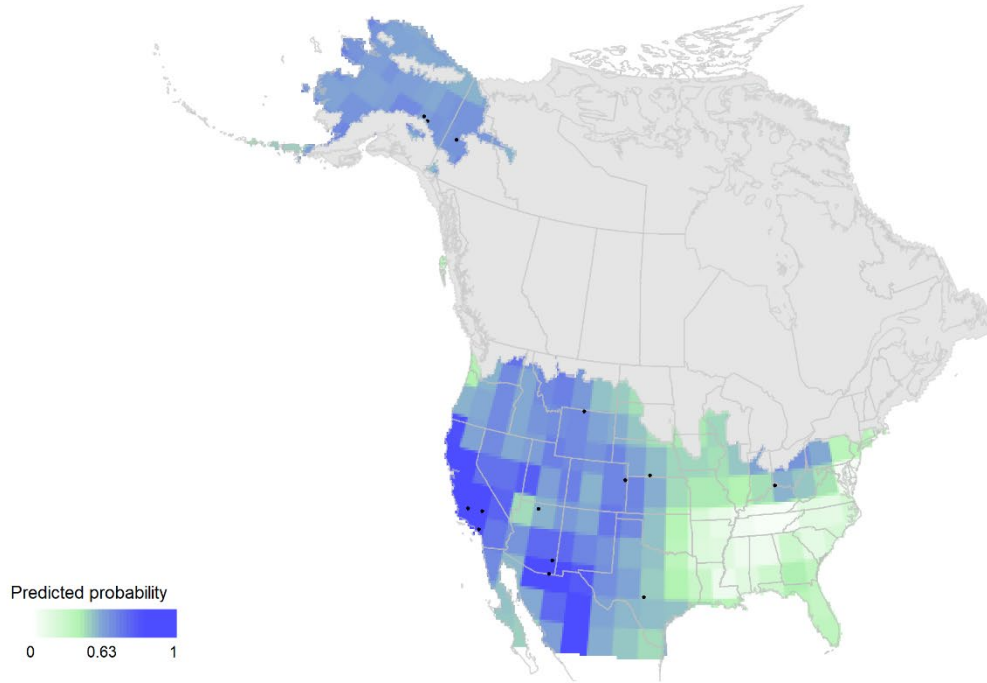
Supplementary Figure 2.10. Response curves for Precipitation of the Coldest Quarter (bio19) in 1000-year intervals between 20-0 ka.

20 - 19 ka



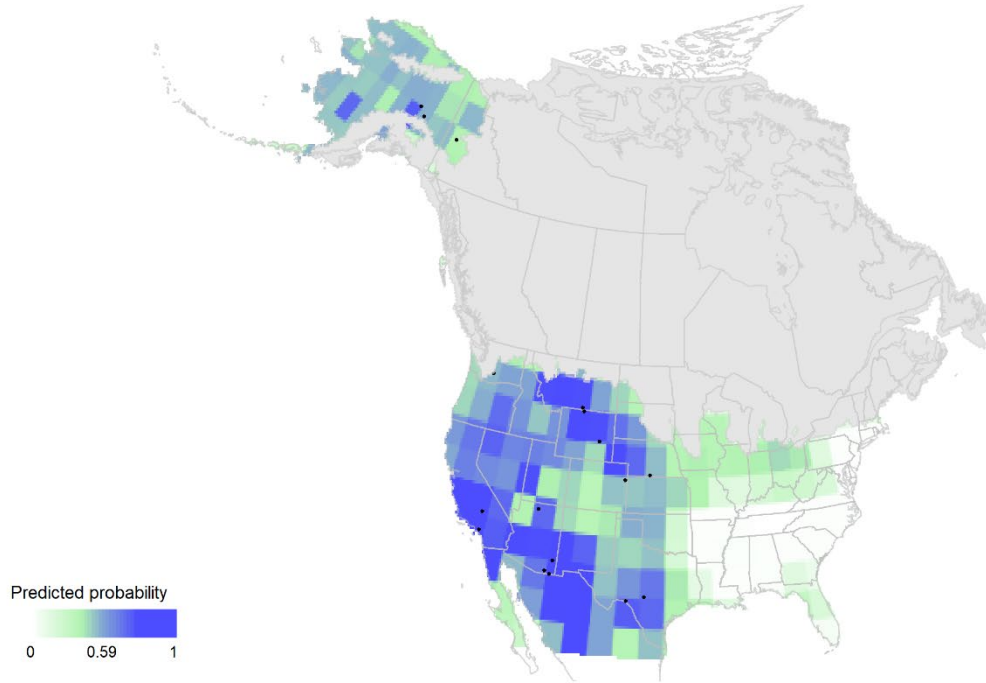
Supplementary Figure 2.11. Bison distribution map 20-19 ka.

19 - 18 ka



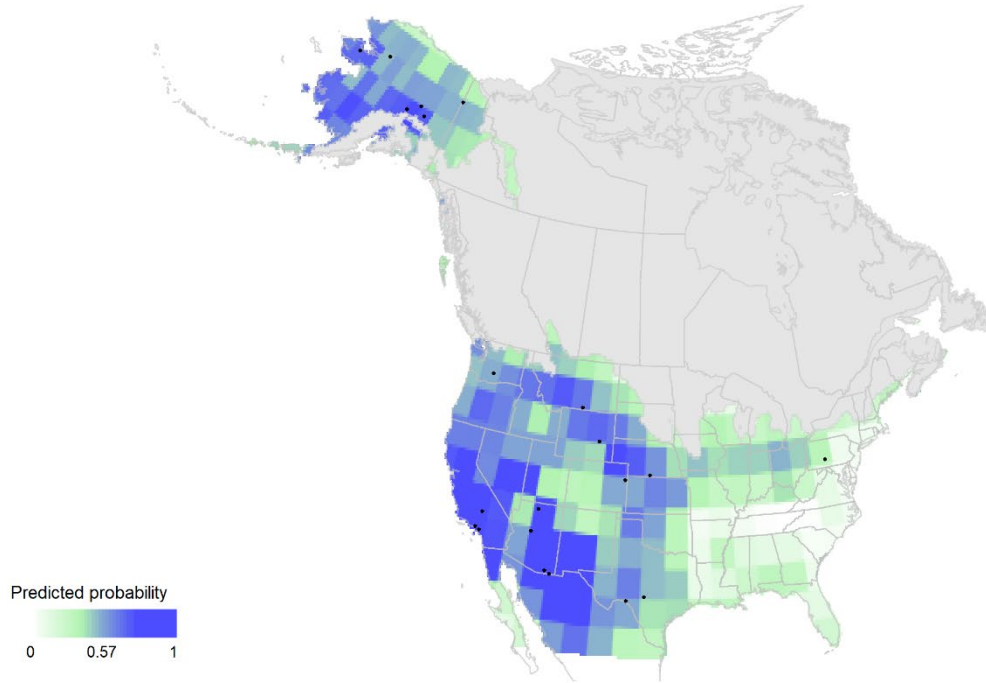
Supplementary Figure 2.12. Bison distribution map 19-19 ka.

18 - 17 ka



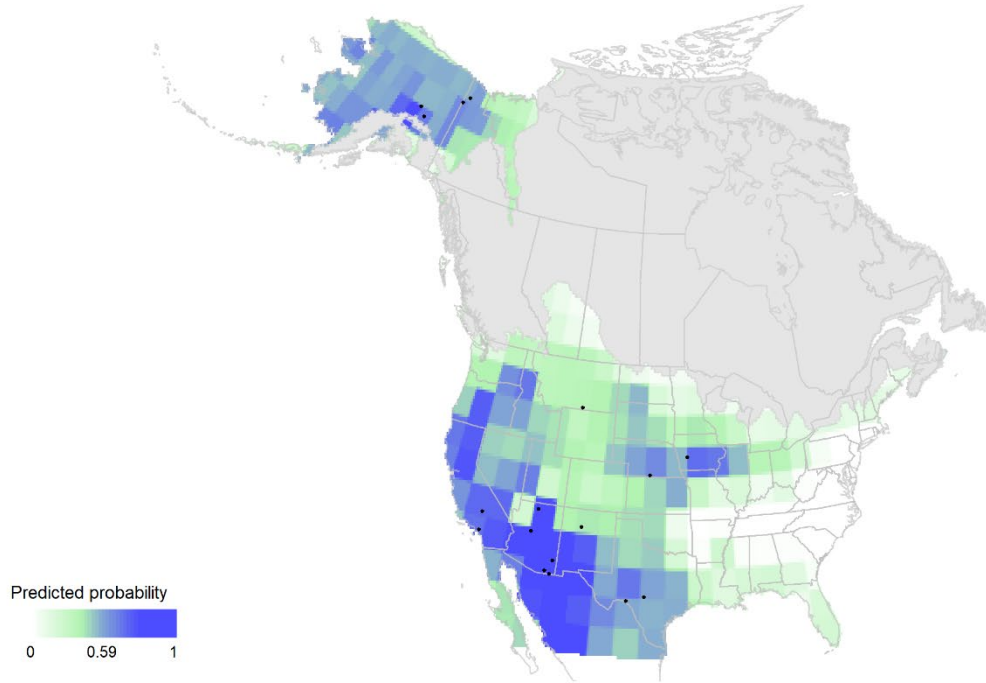
Supplementary Figure 2.13. Bison distribution map 18-17 ka.

17 - 16 ka



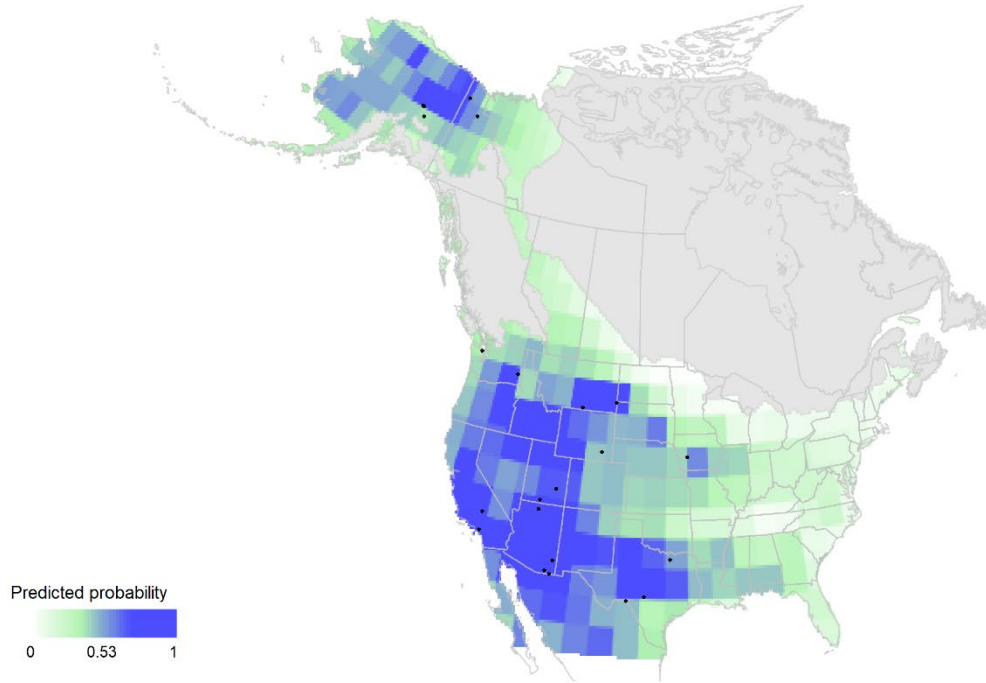
Supplementary Figure 2.14. Bison distribution map 17-16 ka.

16 - 15 ka



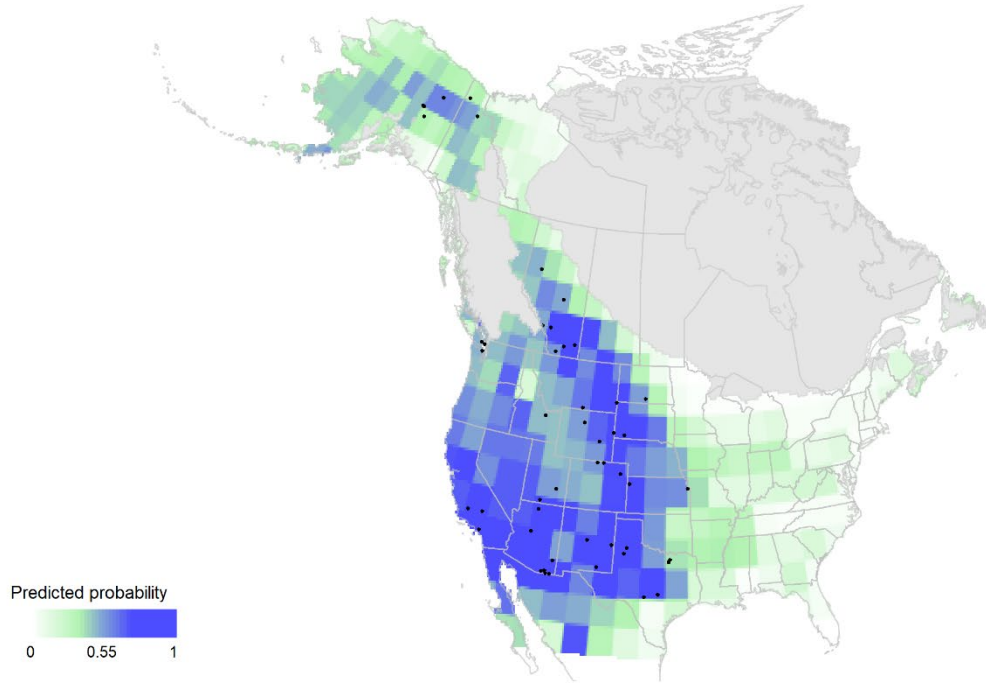
Supplementary Figure 2.15. Bison distribution map 16-15 ka.

15 - 14 ka



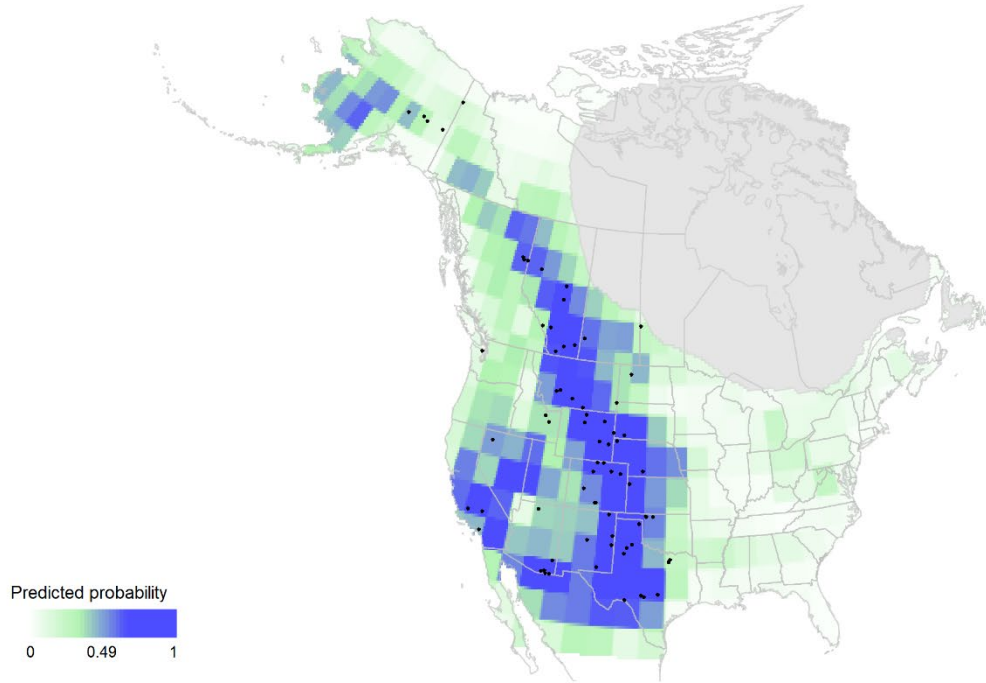
Supplementary Figure 2.16. Bison distribution map 15-14 ka.

14 - 13 ka



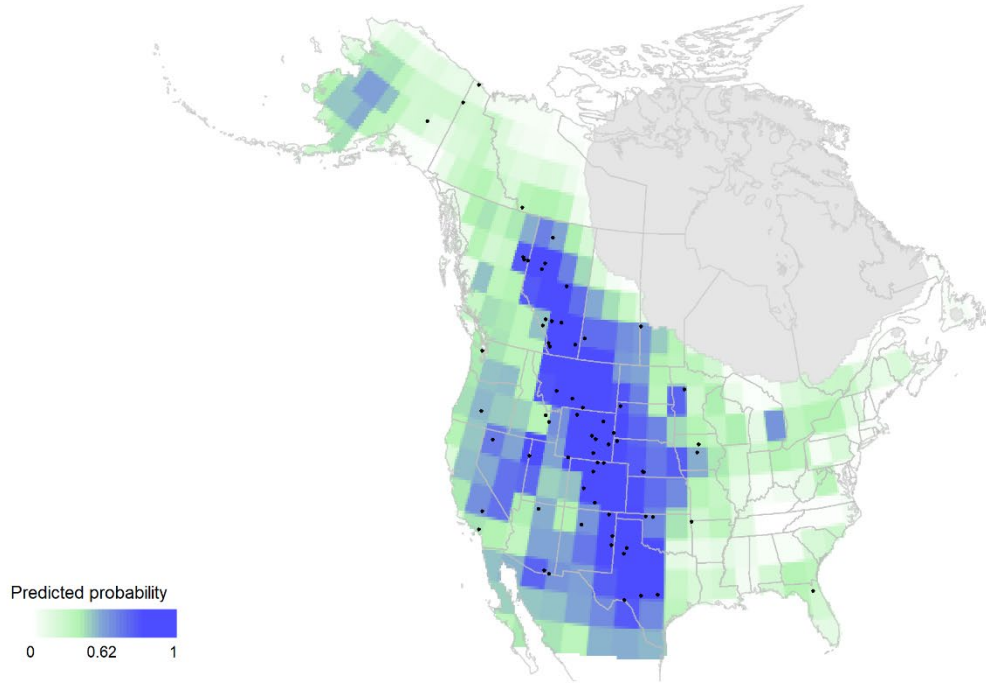
Supplementary Figure 2.17. Bison distribution map 14-13 ka.

13 - 12 ka



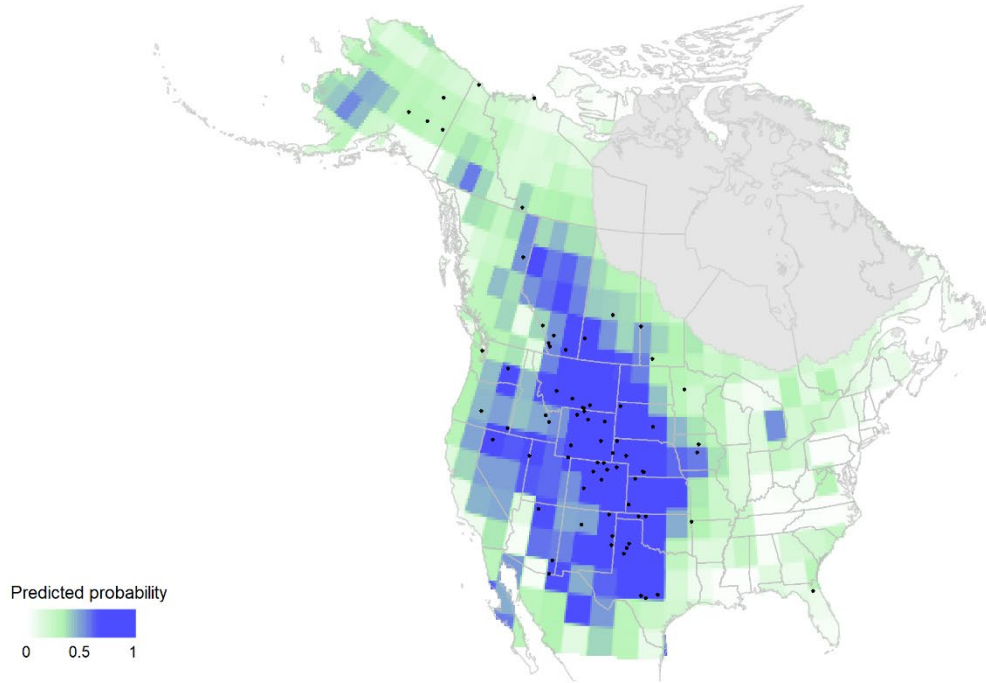
Supplementary Figure 2.18. Bison distribution map 13-12 ka.

12 - 11 ka



Supplementary Figure 2.19. Bison distribution map 12-11 ka.

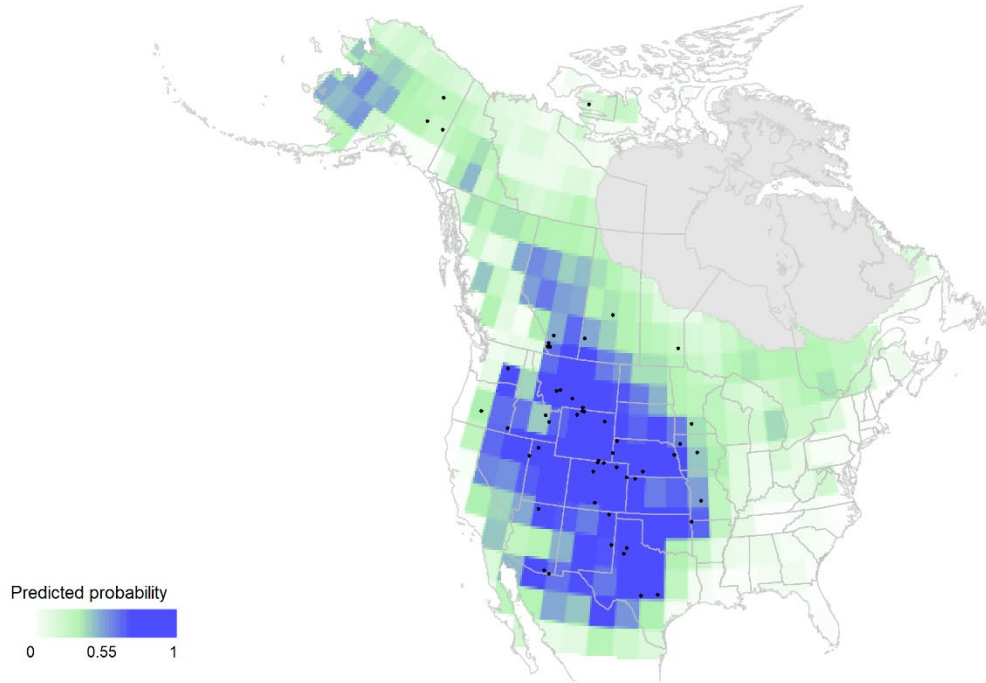
11 - 10 ka



Supplementary Figure 2.20. Bison distribution map 11-10 ka.

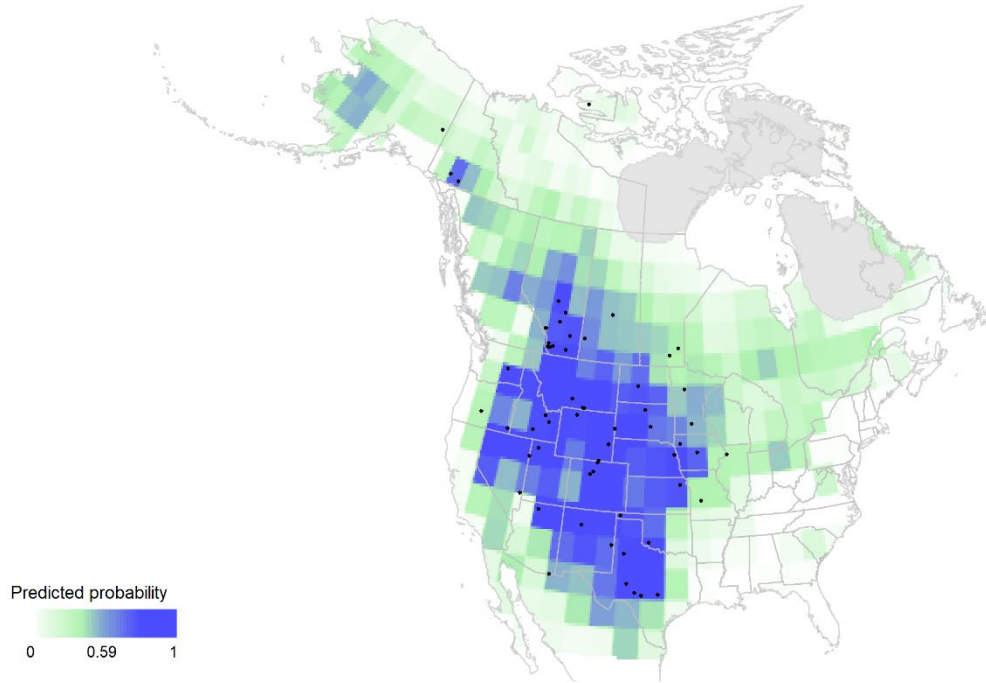
176

10 - 9 ka



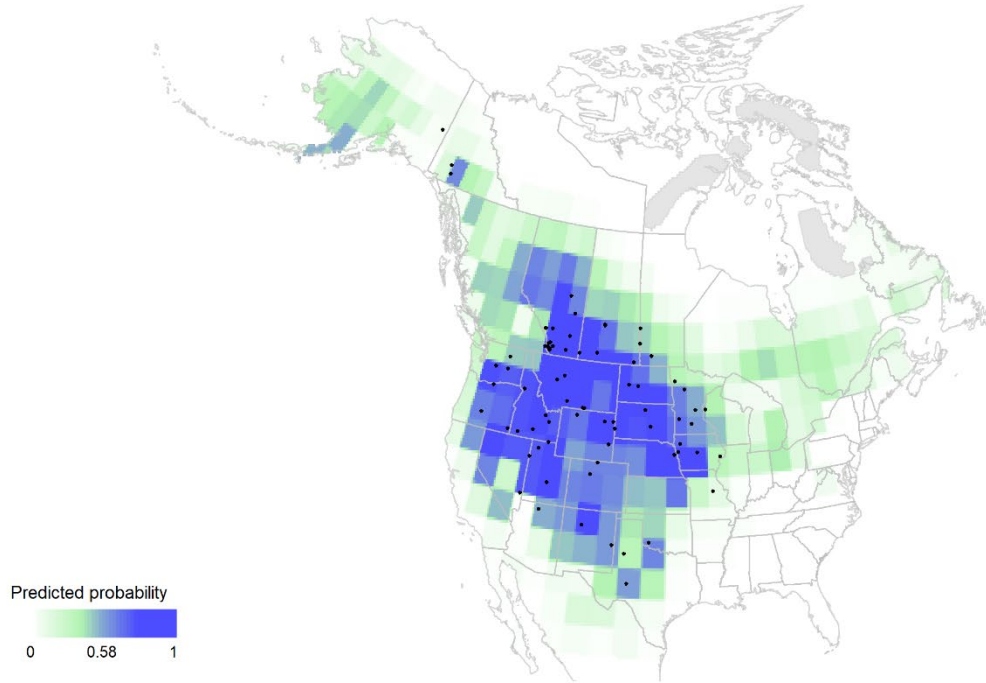
Supplementary Figure 2.21. Bison distribution map 10-9 ka.

9 - 8 ka



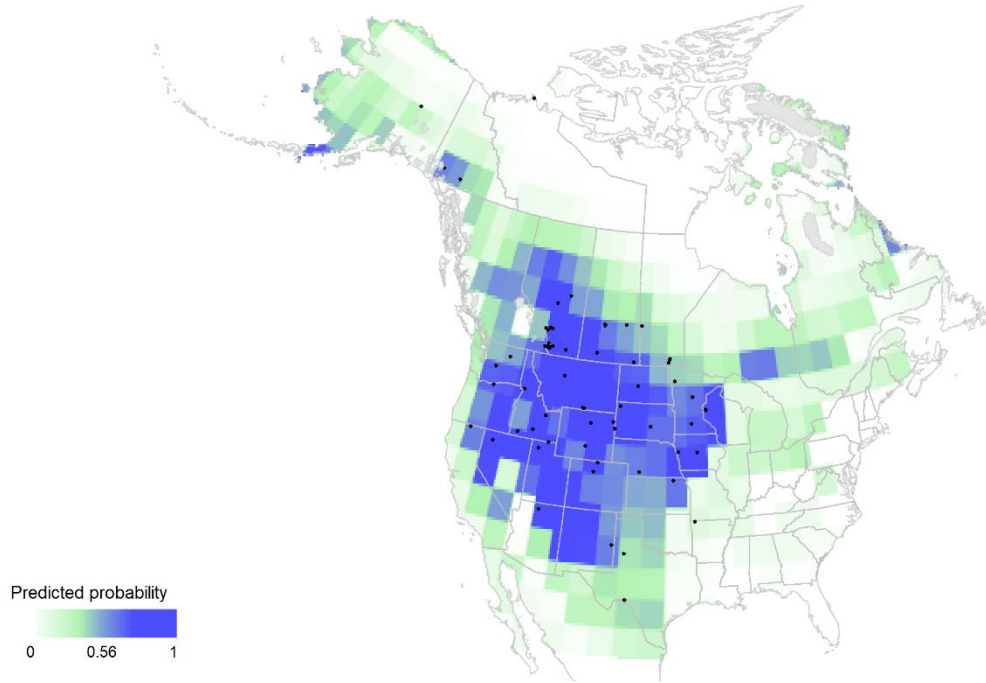
Supplementary Figure 2.22. Bison distribution map 9-8 ka.

8 - 7 ka



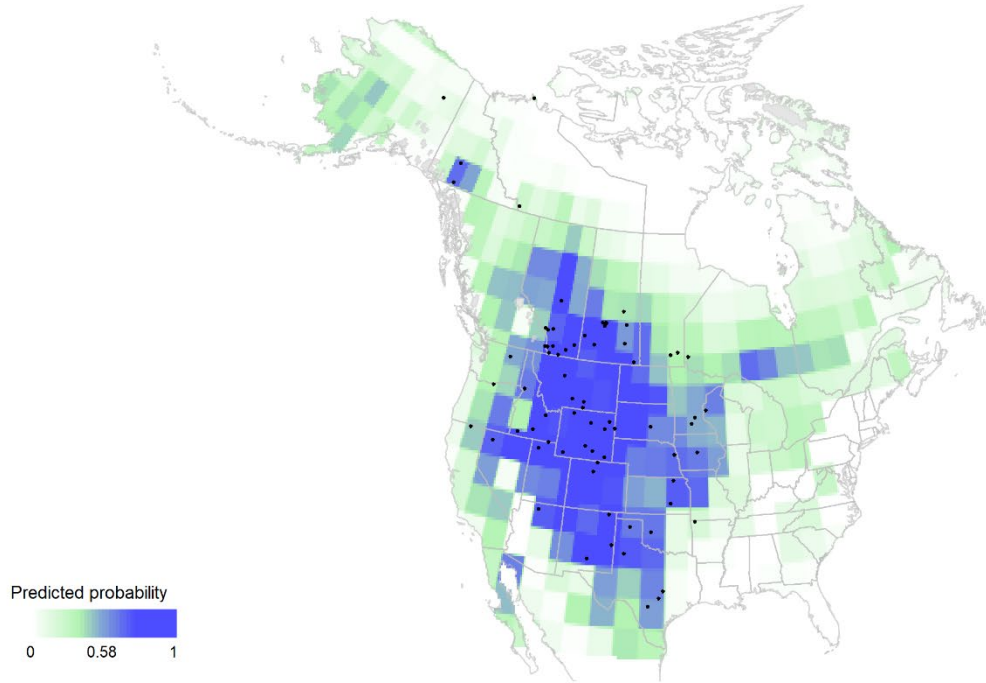
Supplementary Figure 2.23. Bison distribution map 8-7 ka.

7 - 6 ka



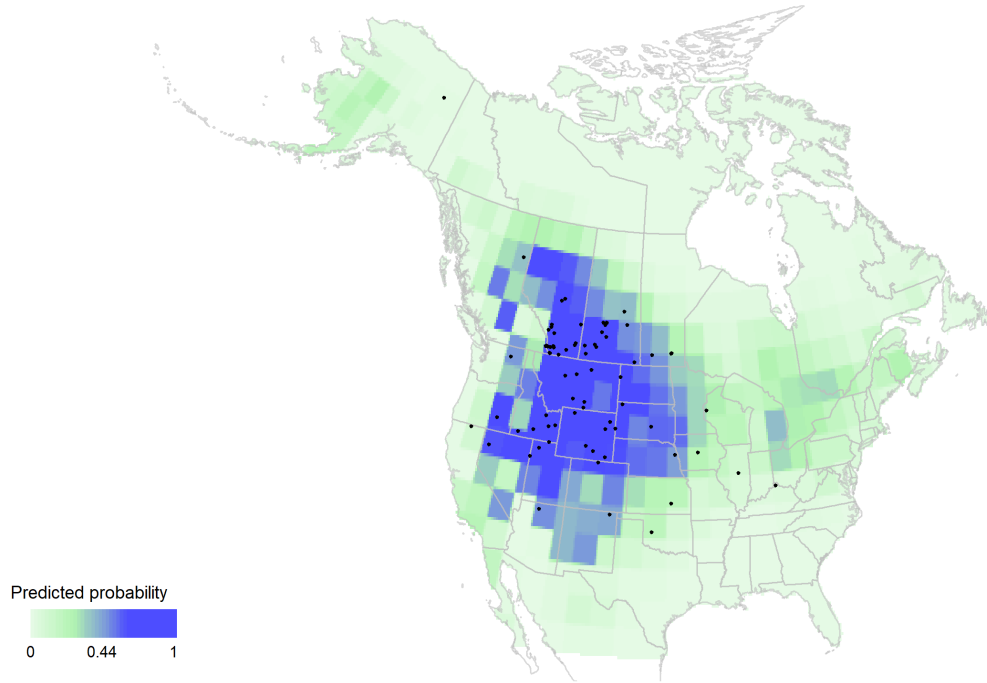
Supplementary Figure 2.24. Bison distribution map 7-6 ka.

6 - 5 ka



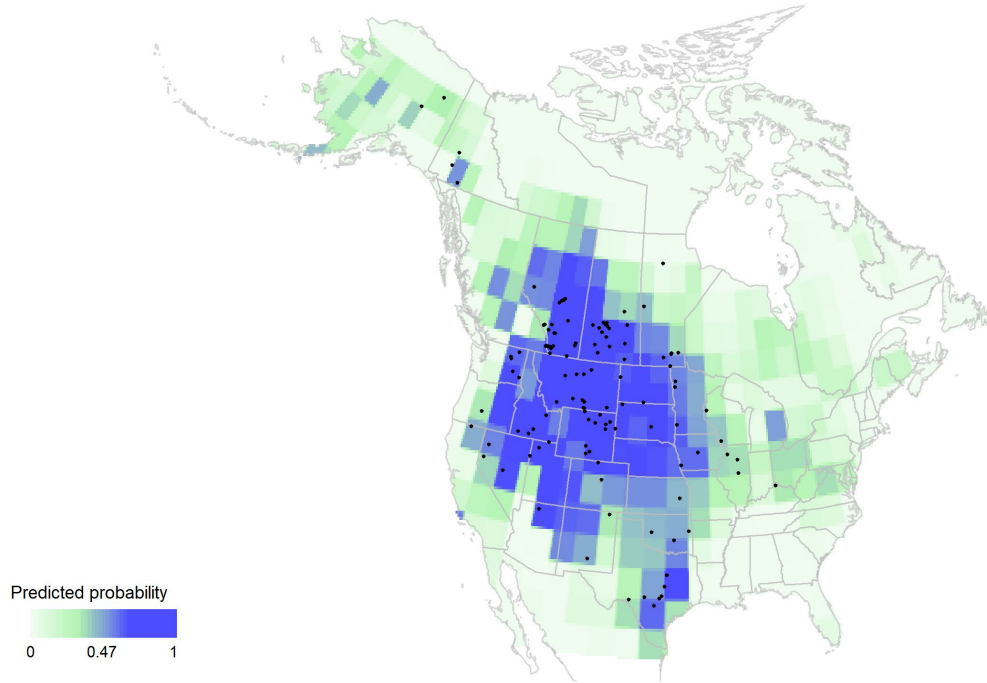
Supplementary Figure 2.25. Bison distribution map 6-5 ka.

5 - 4 ka



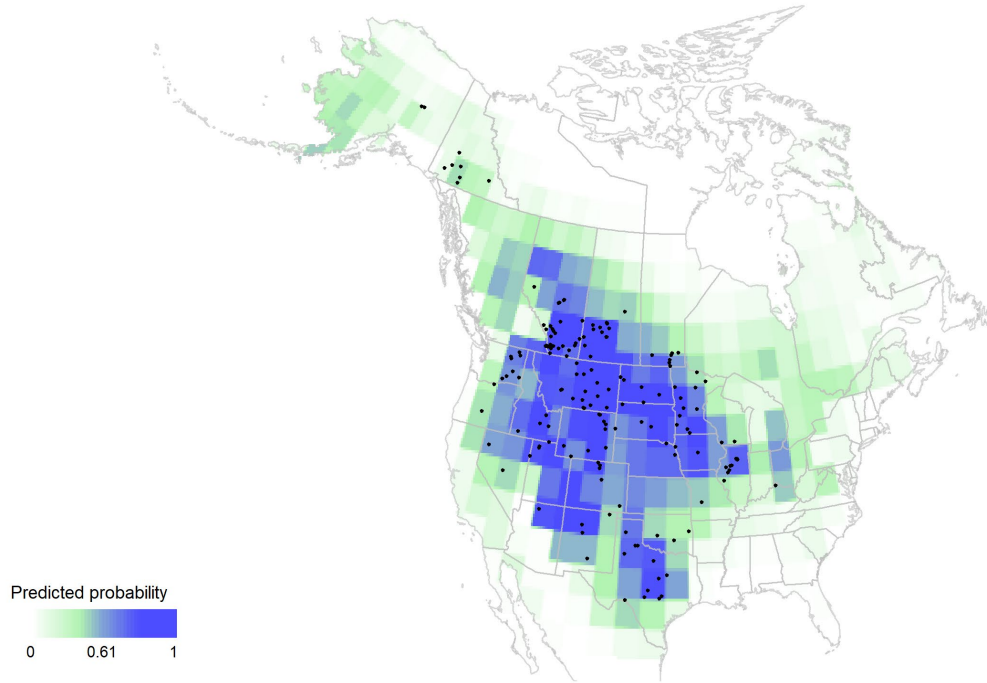
Supplementary Figure 2.26. Bison distribution map 5-4 ka.

4 - 3 ka



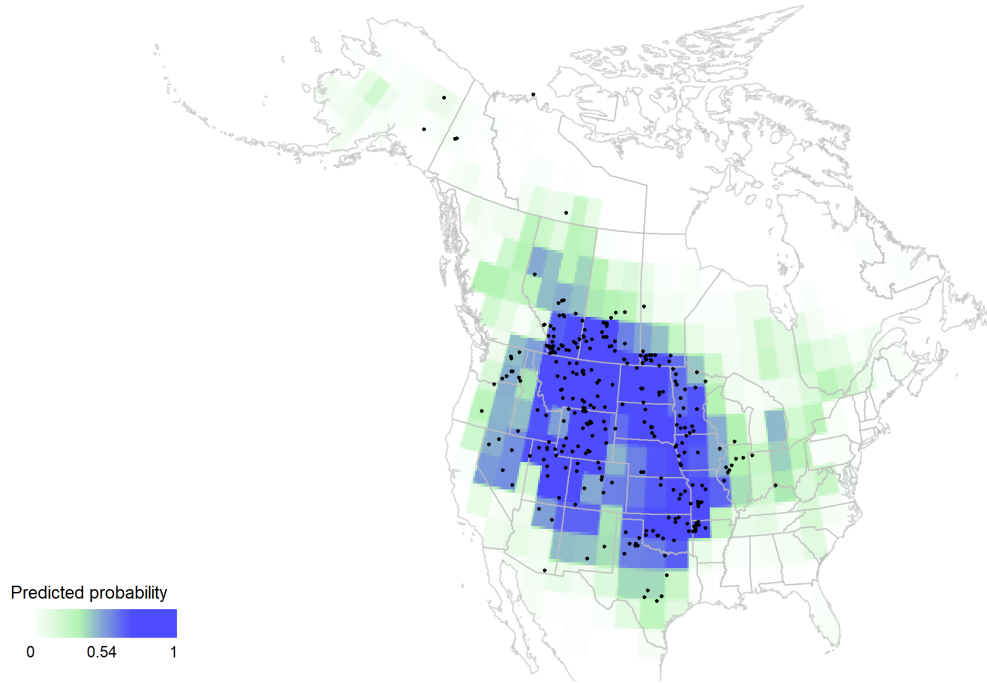
Supplementary Figure 2.27. Bison distribution map 4-3 ka.

3 - 2 ka



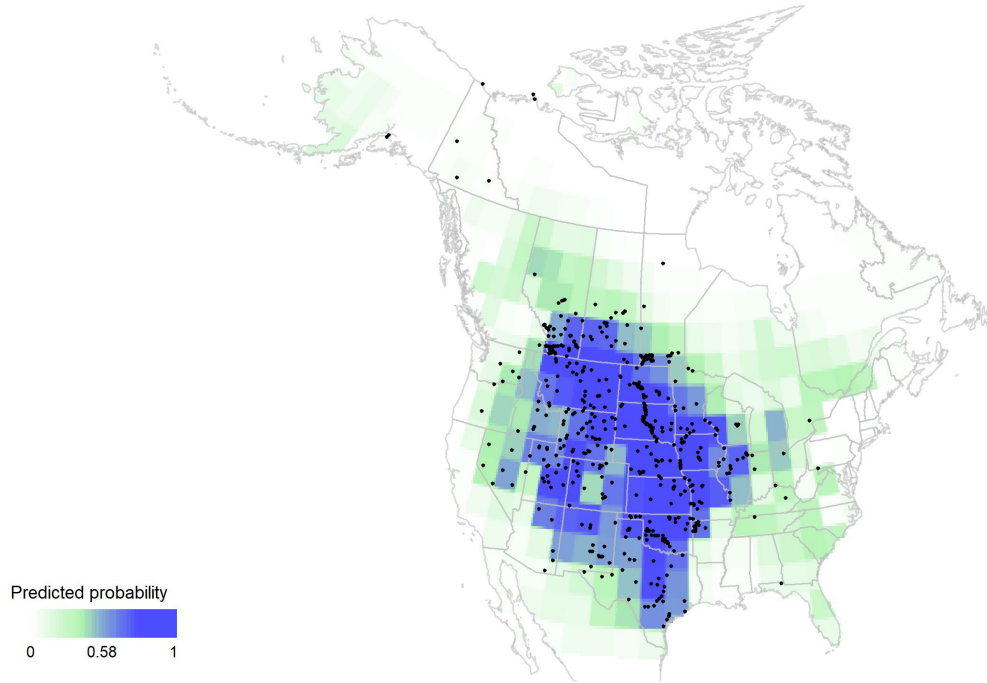
Supplementary Figure 2.28. Bison distribution map 3-2 ka.

2 - 1 ka



Supplementary Figure 2.29. Bison distribution map 2-1 ka.

1 - 0 ka



Supplementary Figure 2.28. Bison distribution map 1-0 ka.

Supplementary Table 2.1. Fossil bison observations used in this study (file available at <https://doi.org/10.1016/j.quascirev.2022.107472>).

APPENDIX B

SUPPLEMENTARY INFORMATION FOR CHAPTER THREE

Supplementary Table 3.3. Moisture availability site metadata. Sites listed from west to east.

Site	Latitude (°N), longitude (°W)	Record start, end (Cal yr BP)	Type	Method	References
Lake of the Woods	43.48, -109.89	17750, 250	Lake level	GPR	(Pribyl and Shuman, 2014)
Rainbow Lake	44.94, -109.50	17750, 250	Lake level	GPR	(Shuman and Serravezza, 2017)
Upper Big Creek Lake	40.91, -106.62	17750, 250	Lake level	GPR	(Shuman et al., 2015)
Hidden Lake	40.50, -106.61	7750, 250	Lake level	GPR	(Shuman et al., 2009)
Little Windy Hill Pond	41.43, -106.33	17750, 250	Lake level	GPR	(Minckley et al., 2012)
Kettle Lake	48.61, -103.62	12972, -45	Geochemistry	XRD	(Grimm et al., 2011)
Nebraska Sand Hills	42.23, -101.40	33390, -67	Dune activity	OSL dates	(Forman et al., 2005; Goble et al., 2004; Mason et al., 2011, 2008, 2003; Miao et al., 2007, 2005; Schmeisser McKean et al., 2015)
Steel Lake	46.97, -94.68	10751, 123	Geochemistry	XRD	(Nelson et al., 2006; Shuman and Marsicek, 2016)

Supplementary Table 3.4. Charcoal site metadata. Sites ordered from driest to wettest.

Site	Mean annual precipitation (mm)	Latitude (°N), longitude (°W)	Elevation (m)	Record start, end (Cal yr BP)	Average sample resolution (cm/yr)	Region	References
Kettle Lake, ND	355	48.61, -103.62	610	12730, -46	6	NG	(Grimm et al., 2011)
Rice Lake, ND	434	48.01, -101.53	631	10424, -9	28	NG	(Umbanhowar, 2004)
Coldwater Lake, ND	476	46.01, -99.07	593	11670, -48	25	NG	(Umbanhowar, 2004)
Moon Lake, ND	494	46.85, -98.16	457	13570, -34	72	NG	(Clark et al., 1996)
Beaver Lake, NE	522	42.47, -100.67	913	6265, 36	168	NG	(Schmieder et al., 2013)
West Olaf Lake, MN	590	46.60, -96.19	400	8888, 42	52	GFT	(Nelson et al., 2004)
Deming Lake, MN	671	47.17, -95.17	485	9148, 740	93	GFT	(Clark and Royall, 1996)
Steel Lake, MN	679	45.97, -94.68	429	9604, 298	81	GFT	(Nelson et al., 2004)
Sharkey Lake, MN	756	44.59, -93.41	309	13037, -34	50	GFT	(Camill et al., 2003)
Kimble Pond, MN	759	44.22, -93.84	308	12340, -47	65	GFT	(Camill et al., 2003)
Fish Lake, MN	766	44.23, -93.67	321	14588, -43	151	GFT	Jim Clark, unpub.
Seven Lake, WI	822	43.61, -88.14	311	11049, -55	17	GFT	(Long et al., 2011)
Dark Lake, WI	827	45.28, -91.48	348	8558, -42	151	GFT	(Clark and Hussey, 1996)
Butler Lake, WI	830	43.66, -88.13	317	14861, -50	18	GFT	(Long et al., 2011)
Hell's Kitchen, WI	844	46.19, -89.70	517	11263, 1200	174	GFT	(Clark and Royall, 1996)
Nelson Lake, IL	925	41.84, -88.38	216	18038, 114	105	GFT	(Nelson et al., 2006)

Supplementary Table 3.5. Pollen site metadata. Sites ordered from driest to wettest.

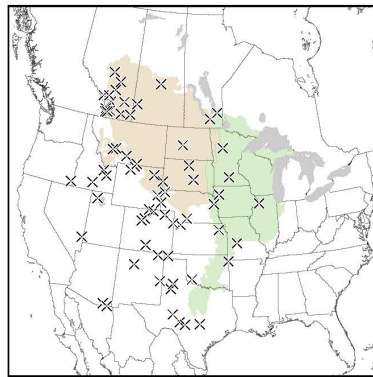
Site	Mean annual precipitation (mm)	Latitude (°N), longitude (°W)	Elevation (m)	Record start, end (Cal yr BP)	Average sample resolution (cm/yr)	Region	References
Kettle Lake, ND	355	48.61, -103.62	610	12830, -45	551	NG	(Grimm et al., 2011)
Rice Lake, ND	434	48.01, -101.53	631	9693, -30	88	NG	Eric Grimm, unpub.
Lost Lake, MT	444	47.64, -110.48	1098	9420, -35	43	NG	(Barnosky, 1989)
Moon Lake, ND	494	46.85, -98.16	457	13969, -35	170	NG	(Laird et al., 1996)
Pickerel Lake, SD	527	45.50, -97.28	563	11138, 0	86	NG	(Watts and Bright, 1968)
West Olaf Lake, MN	590	46.60, -96.19	400	8905, -110	78	GFT	(Nelson et al., 2004; Nelson and Hu, 2008)
Steel Lake, MN	689	45.97, -94.68	365	12070, -50	125	GFT	(Nelson et al., 2004; Tian et al., 2005; Wright et al., 2004)
Fox Lake, IA	724	43.68, -94.70	380	9315, -9	99	GFT	(Commerford et al., 2016)
West Okoboji Lake, IA	726	43.34, -95.13	439	15231, -18	110	GFT	(Van Zant, 1979)
Sharkey Lake, MN	756	44.59, -93.41	309	12034, 61	165	GFT	(Camill et al., 2003; Geiss et al., 2003)
Kimble Pond, MN	759	44.22, -93.84	308	12254, -48	236	GFT	(Camill et al., 2003; Geiss et al., 2003)
Devil's Lake	802	43.42, -89.73	306	14342, -4	122	GFT	(Maher Jr., 1982)
Stewart's Dark Lake, WI	824	45.30, -91.45	334	10649, 482	192	GFT	(Heide, 1984)
Chatsworth Bog, IL	905	40.68, -88.32	228	13260, 800	64	GFT	(King, 1981)

Supplementary Table 3.4. Herbivore mass estimates, based on average values from scientific publications.

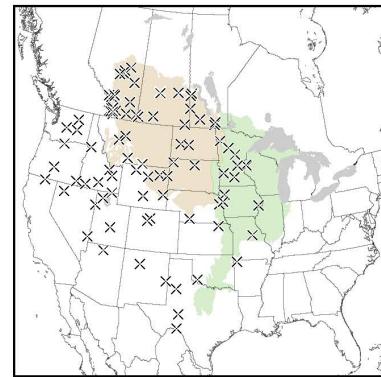
Herbivore	Mass (kg)
Horse	540
Cattle	450
Goat	70
Sheep	50

Bison observations 10,000 - 0 Cal yr BP

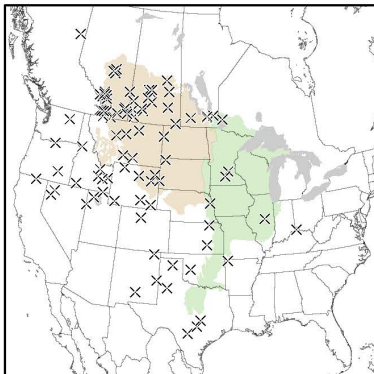
- Grassland-forest transition
- Northern grasslands



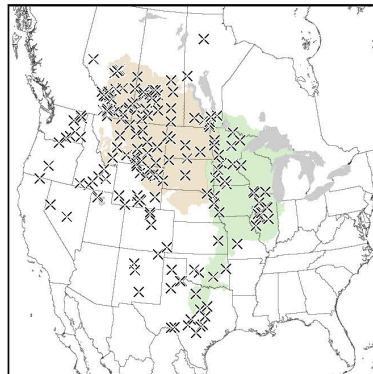
10000-8000 Cal yr BP



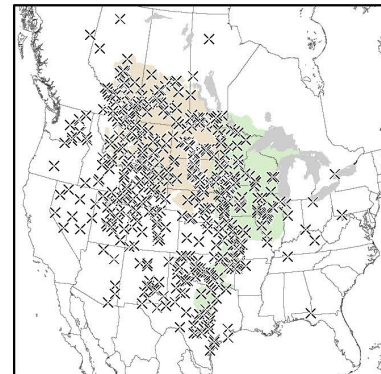
8000-6000 Cal yr BP



6000-4000 Cal yr BP

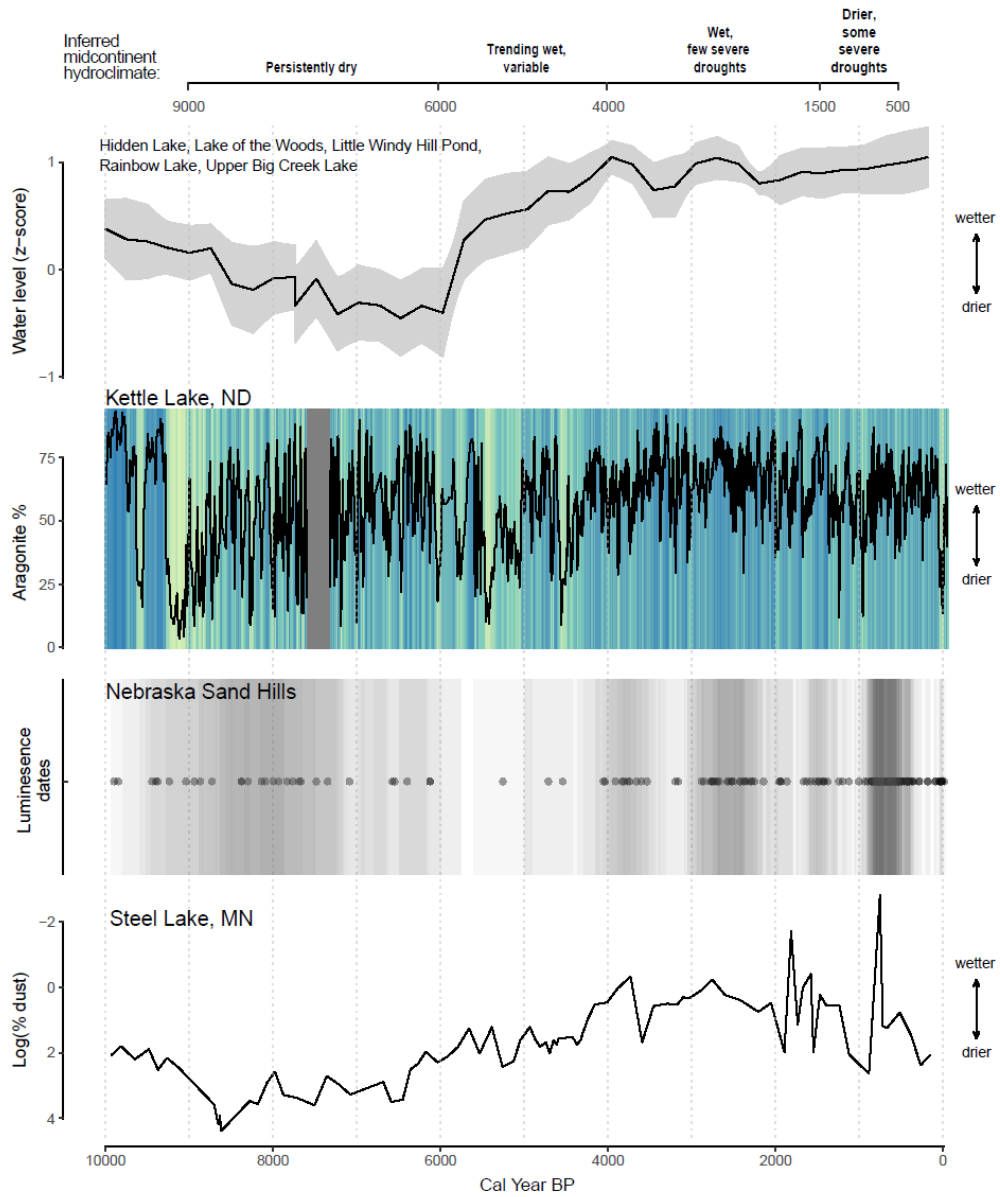


4000-2000 Cal yr BP

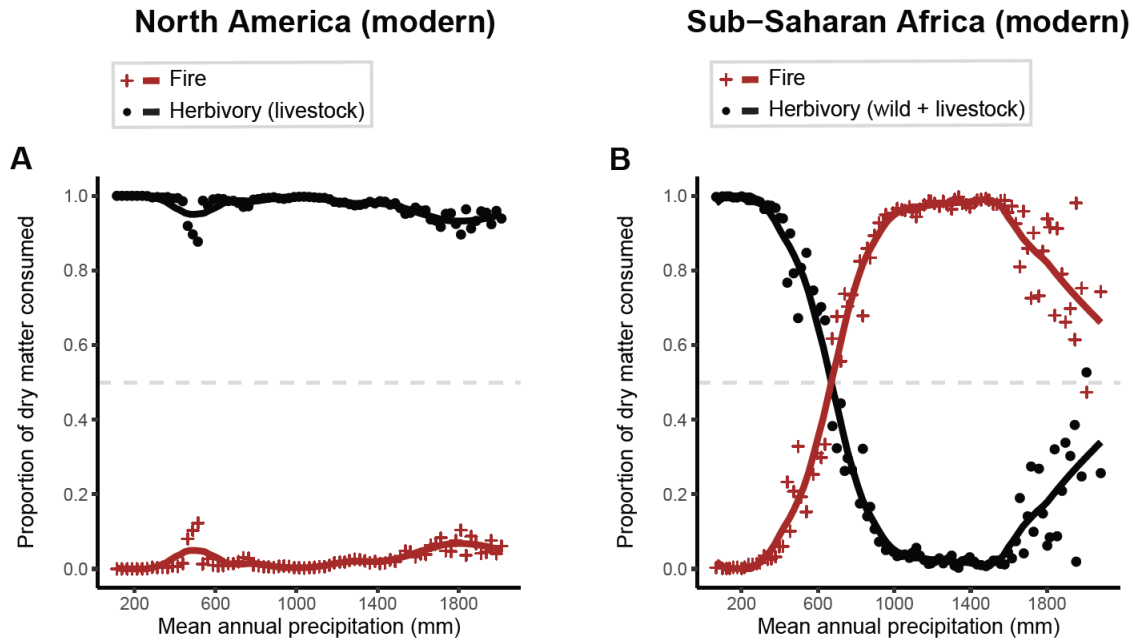


2000-0 Cal yr BP

Supplementary Figure 3.1. Fossil bison observations in North America 10,000-0 Cal yr BP. Observations the grassland-forest transition (green) and northern grasslands (tan) ecoregions were used to create regional bison abundance curves. Data from Wendt et al. (2022).



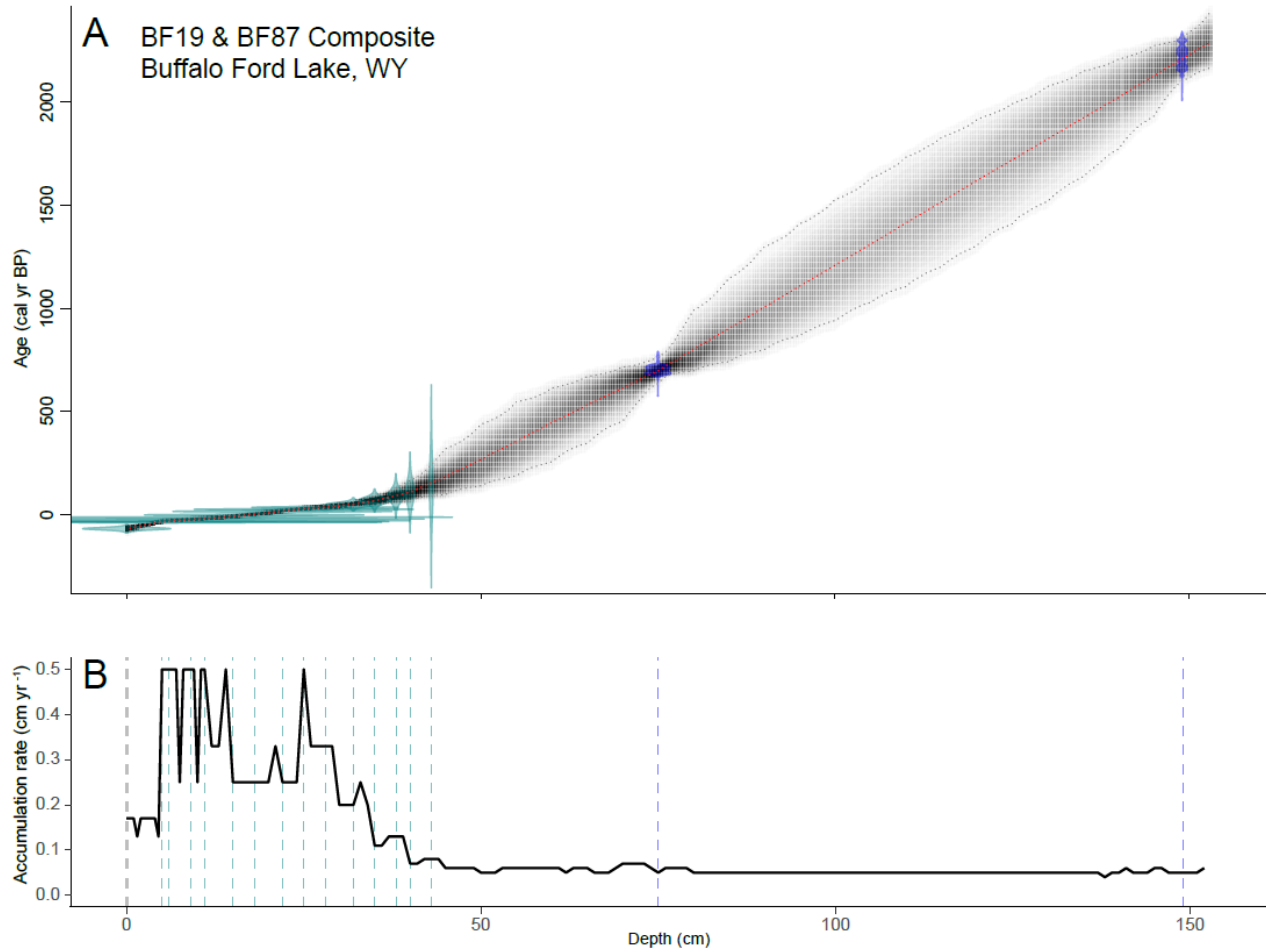
Supplementary Figure 3.2. Moisture availability proxy records of midcontinent North America 10-0k Cal yr BP, with summarized hydroclimate phases (top). See Supplementary Table 3.1 for site and record metadata.



Supplementary Figure 3.3. Comparison of proportion of biomass consumed by herbivores and fire across precipitation gradients in modern North America (panel A) and Sub-Saharan Africa (panel B). Lines are based on loess regressions through the points. Data for Sub-Saharan Africa are from Archibald and Hempson (2016).

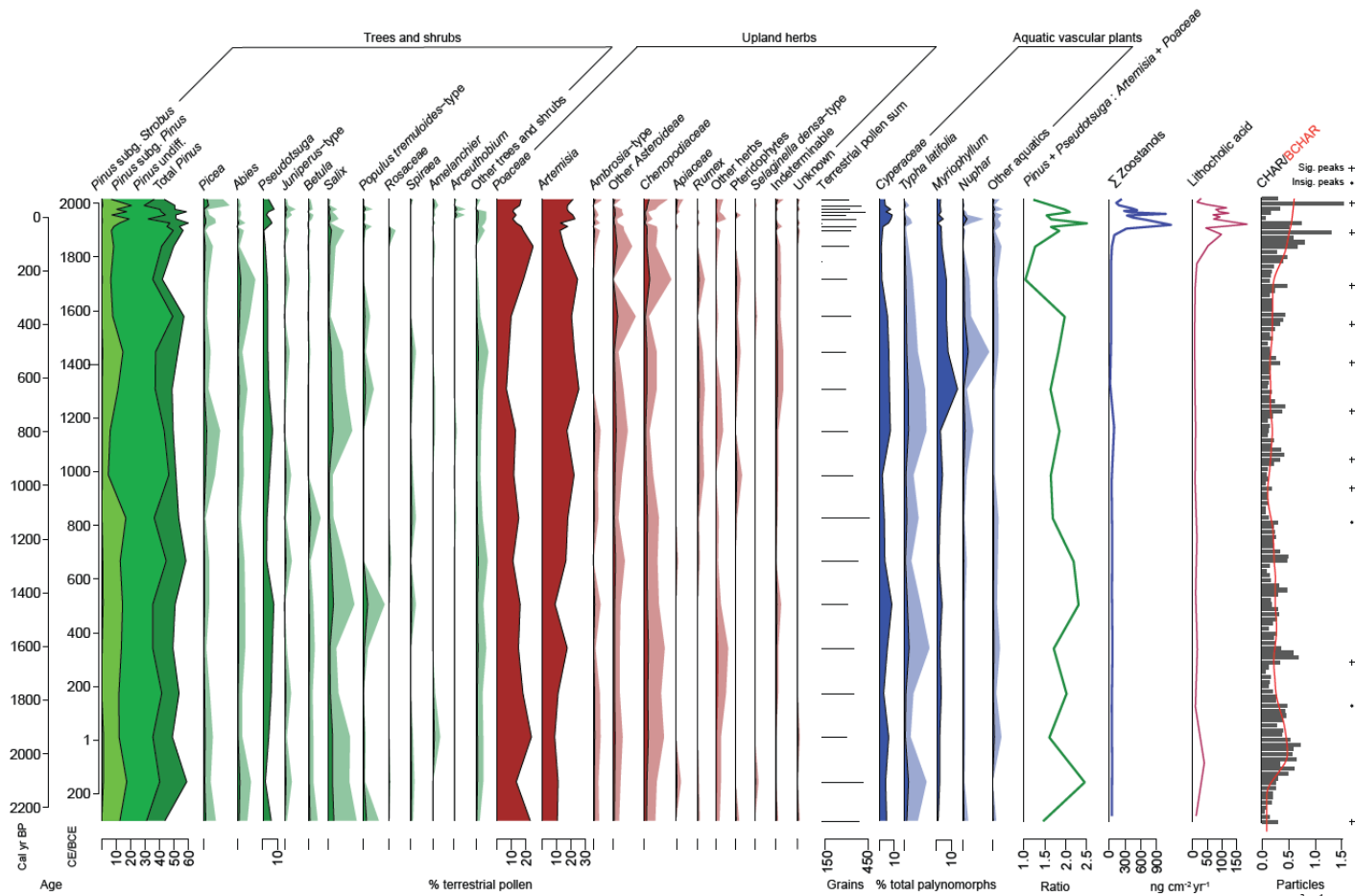
APPENDIX C

SUPPLEMENTARY INFORMATION FOR CHAPTER FOUR



Supplementary Figure 4.1. Composite age-depth model and sediment accumulation rate for BF19 & BF87. (A) Composite age-depth model for Buffalo Ford Lake based on ^{14}C dates from BF19 (blue density curves), ^{210}Pb dates from BF87 (green density curves), and the charcoal lens from the 1988 Yellowstone fires using rbacon version 2.5.7 (Blaauw and Christen, 2011). (B) Sediment accumulation rate over core depth. The dotted red line represents the weighted mean age at a given depth, gray shading and the dotted gray lines represent the distribution of the most likely age-depth model and 95% posterior density intervals.

Buffalo Ford Lake, Yellowstone National Park



Supplementary Figure 4.2. Percentage diagrams of major pollen types and spores, total sum of terrestrial pollen, the ratio *Pinus* and *Pseudotsuga* to *Artemisia* and *Poaceae* pollen, local density of ungulates based on fecal steroid biomarkers (total zoostanols: sum of 24-ethylcoprostanol, 24-ethylepicoprostanol, coprostanol, and epicoprostanol), and charcoal data (CHAR and BCHAR) with significant and insignificant peaks from Buffalo Ford Lake 2019 sediment core. Curve exaggeration is represented by light shading.

Supplementary Table 4.1. Recent population estimates for ungulates in Yellowstone's Northern Range.

Species	Estimated population	Year	Citation
Elk	5800	2019	(Yellowstone National Park, 2019)
Bison	4460	2022	(Yellowstone National Park, 2022a)
Mule deer	1850-1900	2022	(Yellowstone National Park, 2022b)
Bighorn sheep	345	2018	(Yellowstone National Park, 2022c)
Pronghorn	500-600	2022	(Yellowstone National Park, 2022d)
Moose	<200	1996	(Yellowstone National Park, 2022c)
White-tailed deer	Negligible	2022	(Yellowstone National Park, 2022e)

Supplementary Table 4.2. Concentrations ($\mu\text{g/g}$) of fecal steroids from dung samples. <LOD = Below limit of detection.

Sample ID	Common name	Scientific name	Site	coprostanol	epi-coprostanol	cholesterol	cholestanol	cholestanone	24-ethylcoprostanol	24-ethylepicoprostanol	campesterol	stigmasterol	ergosterol	beta-sitosterol	stigmastanol	lithocholic_acid	deoxycholic acid	hydoxycholic acid	ursodeoxycholic acid	chenodeoxycholic acid
B12	Bison	B. bison	Bison Range, MT	104.56	28.55	59.45	56.03	40.72	224.19	223.80	17.47	12.86	22.45	90.96	358.80	0.26	0.75	0.23	< LOD	< LOD
B14	Bison	B. bison	Bison Range, MT	91.88	21.49	66.59	54.42	55.91	199.49	230.14	19.56	18.91	39.67	93.55	414.57	0.25	0.76	0.11	< LOD	< LOD
B16	Bison	B. bison	Bison Range, MT	212.43	44.46	114.20	81.65	59.28	326.05	326.62	14.24	8.78	18.04	81.97	518.79	0.66	0.93	0.23	< LOD	< LOD
B18	Bison	B. bison	Bison Range, MT	117.29	34.20	60.37	77.35	50.68	250.54	293.66	16.00	10.97	20.64	80.32	473.49	0.17	0.52	0.13	< LOD	< LOD
B2	Bison	B. bison	Bison Range, MT	63.11	12.93	48.52	40.77	18.61	154.40	221.63	12.55	28.01	87.16	69.46	256.21	0.29	0.59	0.19	< LOD	< LOD
B20	Bison	B. bison	Bison Range, MT	123.55	30.18	68.91	60.04	67.72	299.70	326.12	15.90	12.26	34.45	83.84	538.84	1.81	1.29	0.24	< LOD	< LOD
B22	Bison	B. bison	Bison Range, MT	117.23	32.51	67.60	62.75	55.00	242.06	285.64	13.87	11.19	15.49	80.33	448.29	0.09	0.62	< LOD	< LOD	< LOD
B24	Bison	B. bison	Bison Range, MT	123.51	27.48	72.68	55.93	58.26	248.15	322.91	15.87	10.28	18.98	79.02	463.11	0.27	0.25	0.09	< LOD	< LOD
B26	Bison	B. bison	Bison Range, MT	128.16	31.33	61.93	53.28	69.71	244.63	319.46	12.98	9.95	21.45	72.68	448.69	0.36	0.45	0.14	< LOD	< LOD
B28	Bison	B. bison	Bison Range, MT	84.72	22.93	65.90	51.87	58.22	252.26	291.82	18.01	14.42	33.40	100.13	463.75	0.33	2.78	0.15	< LOD	< LOD
B32	Bison	B. bison	Bison Range, MT	4.76	2.86	16.91	9.72	3.00	35.68	88.51	8.76	8.50	136.90	41.09	119.24	0.29	2.52	0.07	< LOD	< LOD
B4N	Bison	B. bison	Bison Range, MT	128.99	48.69	55.78	81.07	46.19	178.71	236.26	14.81	16.52	16.55	88.68	365.22	0.47	1.05	0.17	< LOD	< LOD
B4C	Bison	B. bison	Cooke City, MT	129.79	5.79	99.75	43.51	34.05	648.10	62.35	27.46	21.74	15.83	222.55	611.72	2.63	0.68	0.35	< LOD	< LOD
B6C	Bison	B. bison	Cooke City, MT	91.63	22.34	70.00	57.21	59.10	210.91	227.33	15.56	11.57	24.21	83.65	444.35	7.73	9.52	0.35	< LOD	0.77
B6N	Bison	B. bison	Bison Range, MT	76.41	18.94	71.79	46.38	40.13	213.93	249.05	11.87	12.22	15.37	93.22	403.32	0.21	0.47	0.13	< LOD	< LOD
B8C	Bison	B. bison	Cooke City, MT	38.55	11.99	48.68	24.91	18.38	290.94	186.63	14.63	37.01	44.50	155.58	319.80	0.91	0.92	0.22	< LOD	< LOD
B8N	Bison	B. bison	Bison Range, MT	25.93	6.77	20.96	17.73	10.60	80.96	105.90	8.83	10.01	45.43	40.45	153.86	0.11	0.34	0.09	< LOD	< LOD
E1N	Elk	C. canadensis	Bison Range, MT	111.39	72.78	78.84	68.16	62.83	267.57	473.45	0.00	23.53	5.12	116.06	0.00	0.49	0.40	< LOD	< LOD	< LOD
E2	Elk	C. canadensis	Bison Range, MT	123.25	46.17	84.53	56.79	41.78	566.23	425.32	5.93	23.72	23.63	216.59	594.10	0.24	0.16	< LOD	< LOD	< LOD
E3	Elk	C. canadensis	Bison Range, MT	140.92	50.13	70.30	58.23	45.60	305.42	397.80	14.16	14.37	18.03	94.51	487.96	2.31	0.57	< LOD	< LOD	< LOD
E4	Elk	C. canadensis	Bison Range, MT	121.77	28.08	107.41	42.22	39.13	347.68	392.25	0.00	13.34	19.32	138.21	646.58	0.69	0.56	< LOD	< LOD	< LOD

Supplementary Table 4.2 Continued. Concentrations ($\mu\text{g/g}$) of fecal steroids from dung samples. <LOD = Below limit of detection.

Sample ID	Common name	Scientific name	Site	coprostanol	epi-coprostanol	cholesterol	cholestanol	cholestanone	24-ethylcoprostanol	24-ethylpicoprostanol	campesterol	stigmasterol	ergosterol	beta-sitosterol	stigmasterol	lithocholic_acid	deoxycholic acid	hyodeoxycholic acid	ursodeoxycholic acid	chenodeoxycholic acid
E5	Elk	<i>C. canadensis</i>	Bison Range, MT	78.86	43.42	50.23	37.75	38.59	194.00	305.44	7.00	20.68	20.40	94.28	418.29	1.01	0.72	< LOD	< LOD	< LOD
E6	Elk	<i>C. canadensis</i>	Bison Range, MT	95.57	35.36	86.10	40.82	48.16	238.48	425.09	10.21	20.01	22.23	107.02	563.75	0.61	0.61	< LOD	< LOD	< LOD
E7	Elk	<i>C. canadensis</i>	Bison Range, MT	65.99	43.08	84.92	48.73	36.09	332.96	476.65	0.00	19.64	80.86	149.48	621.97	0.88	2.60	< LOD	< LOD	< LOD
M1	Moose	<i>A. alces</i>	Silver Gate, MT	49.52	12.07	19.13	6.93	20.84	831.83	786.87	0.00	2.06	24.96	157.26	305.07	0.97	1.18	0.56	< LOD	< LOD
M2	Moose	<i>A. alces</i>	Silver Gate, MT	41.43	24.41	22.23	6.33	44.72	616.04	1307.35	5.61	7.26	143.32	183.75	143.13	0.82	2.08	0.30	< LOD	< LOD
M3	Moose	<i>A. alces</i>	Silver Gate, MT	27.96	19.84	15.26	4.66	38.82	444.55	1039.49	6.26	6.09	32.66	128.38	96.80	0.74	1.95	< LOD	< LOD	< LOD
M4	Moose	<i>A. alces</i>	Silver Gate, MT	49.89	31.28	48.76	8.06	52.66	743.19	1545.21	8.27	4.56	21.69	234.92	255.03	0.30	2.04	< LOD	< LOD	< LOD
M5	Moose	<i>A. alces</i>	Silver Gate, MT	27.68	20.30	49.07	6.36	10.28	160.31	704.38	52.14	18.20	82.42	364.11	80.58	0.29	2.13	< LOD	< LOD	< LOD
M6	Moose	<i>A. alces</i>	Silver Gate, MT	67.30	27.93	53.64	8.81	61.89	772.92	1391.23	7.72	3.97	13.95	316.61	272.35	0.65	2.50	< LOD	< LOD	< LOD
M7	Moose	<i>A. alces</i>	Silver Gate, MT	50.48	21.49	33.55	6.23	19.54	546.71	914.54	4.66	3.56	18.57	173.07	272.56	0.63	3.46	< LOD	< LOD	< LOD
MDISG	Mule deer	<i>O. hemionus</i>	Silver Gate, MT	54.89	75.85	33.68	10.85	168.08	490.74	997.46	3.23	13.79	221.24	81.49	244.49	0.69	11.05	< LOD	< LOD	< LOD
MDIN	Mule deer	<i>O. hemionus</i>	Silver Gate, MT	61.12	15.92	64.49	9.44	49.78	676.94	306.75	3.62	8.37	57.80	137.53	110.09	0.19	0.92	< LOD	< LOD	< LOD
P1	Pronghorn	<i>A. americana</i>	Bison Range, MT	148.52	34.57	58.60	22.04	34.54	633.88	462.85	3.67	13.96	59.90	99.75	595.62	1.64	6.14	0.29	< LOD	< LOD
P2	Pronghorn	<i>A. americana</i>	Bison Range, MT	140.02	34.62	60.05	21.81	42.14	629.71	480.62	3.90	16.96	31.79	111.45	549.49	1.84	6.27	< LOD	< LOD	< LOD
P3	Pronghorn	<i>A. americana</i>	Bison Range, MT	119.52	35.27	65.73	26.33	94.21	739.19	476.73	4.81	18.76	0.00	122.62	548.33	1.59	9.55	< LOD	< LOD	< LOD
P4	Pronghorn	<i>A. americana</i>	Bison Range, MT	112.89	33.43	69.36	25.89	94.46	719.17	478.05	5.36	18.75	0.00	125.14	578.33	1.92	5.98	0.42	< LOD	< LOD
P5	Pronghorn	<i>A. americana</i>	Bison Range, MT	109.11	32.18	68.11	20.20	101.34	814.42	501.30	5.57	16.11	134.26	136.29	549.04	0.31	1.75	0.31	< LOD	< LOD
P6	Pronghorn	<i>A. americana</i>	Bison Range, MT	121.12	39.09	62.14	21.37	136.57	897.56	581.29	4.86	19.29	130.93	132.93	560.26	1.07	7.95	0.48	< LOD	< LOD

Supplementary Table 4.3. Concentrations (ng/g) of fecal steroids from Buffalo Ford Lake, Yellowstone National Park, WY, USA.
 <LOD = below limit of detection.

Depth (cm)	Age (cal yr BP)	coprostanol	epi-coprostanol	cholesterol	cholestanol	cholestanone	24-ethylcoprostanol	24-ethylcoprostanol	campesterol	stigmasterol	beta-sitosterol	stigmasterol	lithocholic_acid	deoxycholic_acid	hyodeoxycholic acid	ursodeoxycholic acid	chenodeoxycholic acid
0	-69	278	160	1781	1321	96	724	245	872	1746	5641	3156	170	< LOD	72	42	< LOD
2	-55	116	87	1175	707	35	431	172	518	978	3243	2045	88	< LOD	108	34	< LOD
4	-46	147	107	1549	1054	39	595	244	969	1634	5761	3227	288	7410	79	142	< LOD
6	-34	147	114	1222	895	28	413	210	659	1025	4291	2732	233	< LOD	< LOD	84	< LOD
8	-28	157	123	1720	1084	49	549	237	877	1296	5703	3284	159	5342	< LOD	63	< LOD
10	-25	205	132	1935	1173	56	567	233	807	1407	5202	3678	346	< LOD	73	93	< LOD
12	-20	199	148	1881	1203	61	588	258	821	1598	5609	3948	270	< LOD	75	81	< LOD
14	-14	408	294	3445	2015	84	964	485	1411	2545	9872	6703	248	< LOD	< LOD	146	< LOD
16	-8	248	177	2145	1212	61	628	301	800	1296	5786	4104	282	5421	56	134	< LOD
18	0	302	225	2024	1393	61	884	411	947	1600	7105	5747	375	7861	57	193	< LOD
20	8	555	423	3138	2287	89	1317	478	1081	2296	7251	6020	289	4792	< LOD	176	< LOD
25	27	426	325	3422	2159	86	1198	397	931	2323	8351	7439	375	8287	< LOD	332	< LOD
30	41	470	338	4725	3063	75	553	287	1182	2946	7158	5935	228	9909	72	60	< LOD
35	65	259	194	2358	1148	55	312	146	615	1306	3870	3286	898	< LOD	117	764	< LOD
40	107	194	151	2513	1629	57	295	150	659	1515	4174	4126	759	3945	112	587	< LOD
45	174	161	120	2063	868	31	222	130	469	1022	2725	2479	235	< LOD	105	130	< LOD
50	259	176	126	2516	1088	40	317	171	690	1617	4309	3092	174	10457	44	60	< LOD
60	439	131	97	1822	676	36	296	159	549	925	3815	2460	105	1534	31	26	< LOD

Supplementary Table 4.3 Continued. Concentrations (ng/g) of fecal steroids from Buffalo Ford Lake, Yellowstone National Park, WY, USA. <LOD = below limit of detection.

Depth (cm)	Age (cal yr BP)	coprostanol	epi-coprostanol	cholesterol	cholestanol	cholestanone	24-ethylcoprostanol	24-ethylepicoprostanol	campesterol	stigmasterol	beta-sitosterol	stigmastanol	lithocholic_acid	deoxycholic acid	hyodeoxycholic acid	ursodeoxycholic acid	chenodeoxycholic acid
70	620	48	39	589	270	14	149	59	177	354	1334	937	107	145	36	< LOD	< LOD
80	782	434	337	2973	1185	55	819	335	942	1750	5710	3847	197	< LOD	39	40	< LOD
90	987	268	191	3313	1635	29	337	173	788	2082	5493	2850	167	14331	< LOD	21	< LOD
100	1194	261	253	2817	1616	66	497	195	939	2271	6743	4241	288	6166	90	55	< LOD
110	1401	258	208	2268	1269	35	443	203	892	1785	6007	3846	204	< LOD	11	17	< LOD
120	1611	260	322	4693	945	58	473	259	994	2674	7125	3666	317	12626	34	33	< LOD
130	1825	233	224	3979	1631	36	426	153	1007	2580	7321	3842	186	< LOD	76	90	< LOD
140	2034	284	195	2852	1404	62	523	168	818	1882	7069	3842	796	40085	< LOD	409	< LOD
150	2231	299	315	3651	1125	64	221	241	749	1461	6800	3918	236	43211	49	44	< LOD

Supplementary Table 4.4. Compound information for analyzed fecal steroids.

Trivial name	IUPAC nomenclature	CAS number	Mass-to-charge ratio (m/z)
24-ethylcoprostanol	24-ethyl 5 β -cholestan-3 β -ol	CAS 4736-91-8	215, 398
24-ethylepicoprostanol	24-ethyl 5 β -cholestan-3 α -ol	CAS 5060-24-2	215, 398
β-sitosterol	stigmast-5-en-3 β -ol	CAS 83-46-5	396, 357
campesterol	campest-5-en-3 β -ol	CAS 474-62-4	343, 382
cholestanol	5 α -cholestan-3 β -ol	CAS 80-97-7	215, 445
cholestanone	5 α -cholestane-3-one	CAS 566-88-1	316, 386
cholesterol	cholest-5-en-3 β -ol	CAS 57-88-5	329, 368
coprostanol	5 β -cholestan-3 β -ol	CAS 360-68-9	215, 370
epicoprostanol	5 β -cholestan-3 α -ol	CAS 516-92-7	215, 370
ergosterol	3 β -Ergosta-5,7,22-trien-3-ol	CAS 57-87-4	363, 253
stigmastanol	5 α -stigmastan-3 β -ol	CAS 19466-47-8	215, 473
stigmasterol	stigmasta-5,22-dien-3 β -ol	CAS 83-48-7	484, 394
chenodeoxycholic acid	(3 α ,5 β ,7 α ,8 ξ)-3,7-dihydroxycholan-24-oic acid	CAS 474-25-9	370, 355
deoxycholic acid	(3 α ,5 β ,12 α)-3,12-dihydroxycholan-24-oic acid	CAS 83-44-3	370, 208
hyodeoxycholic acid	(3 α ,5 β ,6 α)-3,6-dihydroxycholan-24-oic acid	CAS 83-49-8	370, 255
lithocholic acid	(3 α ,5 β)-3-hydroxycholan-24-oic acid	CAS 434-13-9	215, 372
ursodeoxycholic acid	(3 α ,5 β ,7 β)-3,7-dihydroxycholan-24-oic acid	CAS 128-13-2	370, 255